



# Multi-Stage Aqueous Two-Phase Extraction

Brown Group  
Author: Emma Chandler

PhD Thesis

A thesis submitted in partial fulfilment of the requirements for the degree of  
Doctor of Philosophy

Department of Chemical & Biological Engineering  
University of Sheffield  
United Kingdom  
July, 2021



# Declaration

I, the author, confirm that the Thesis is my own work. I am aware of the University's guidance on the Use of Unfair means (<https://www.sheffield.ac.uk/ssid/unfair-means>). This work has not been previously presented for an award at this, or any other, university. Part of this work is published in the following conference paper and paper:

Chandler, E. Cordiner, J., & Brown, S. (2021). Accounting for interface behaviour in multi-stage aqueous two-phase extraction. *Chemical Engineering Science*, 230.

Chandler, E., Falconer, R., & Brown, S. (2019). Optimisation of Aqueous Two-Phase Systems. *Proceedings of the 29th European Symposium on Computer Aided Process Engineering*, 631–636.



# Abstract

[Aqueous Two-Phase Extraction \(ATPE\)](#) is an alternative, cheap and continuous protein purification technique which can handle large and varying material types as well as achieve high purities and yields. It could be used to shift protein manufacturing from a batch to a continuous process. The implementation of continuous processing would be beneficial to the biopharmaceutical industry as it increases the product quality, decreases costs, and increases throughput. However, [ATPE](#) is associated with a low resolution and reliability which has led to a lack of wide acceptance within an industrial setting. This thesis uses [Multi-stage Extraction \(MSE\)](#) and the McCabe Thiele method to better understand [ATPE](#) and improve resolution.

This work experimentally evaluated [MSE](#) using model pigmented proteins. The yield and purities demonstrated there were differences between the separation methods tested. The gravity settled systems (to a distinct horizontal interface formation) had a lower resolution than centrifuge settled systems despite literature suggesting they were comparable. To understand the differences, settling of [ATPE](#) was evaluated using traditional dispersion height measurements, turbidity measurements, microscopic observation, and changes in protein concentration in each of the phases. It was found protein precipitated and settled from the bulk liquid phases into the horizontal interface after its formation. Single-stage protein partitioning data was experimentally determined and used in a modified McCabe Thiele method to predict multi-stage behaviour; this was compared to [MSE](#) experimental systems. Previous literature only considered two bulk liquid phases in the partitioning data. This work found that horizontal interface partitioning data was required to accurately describe multi-stage [ATPE](#). Deming regression was used to show uncertainty in horizontal interface partitioning data did not impact the stage-wise modelling. This thesis has shown considering partitioning into the horizontal interface of a system is required to model multi-stage [ATPE](#). Accurate understanding and modelling of multi-stage [ATPE](#) will aid in more reliable and successful process design.

---

**Keywords:** [ATPS](#), multi-stage extraction, McCabe Thiele method, horizontal interface partitioning



# Acknowledgements

First of all, I would like to thank my supervisors Dr Solomon Brown and Professor Robert Falconer for their invaluable support and guidance throughout my PhD, I very much enjoyed my time as your student. I'd like to thank Dr Robert Milton for his input with the uncertainty modelling in data chapter 3. I'd also like to thank the very long list of proof readers, who I'm sure did not enjoy the task of reading chapters of my thesis: Adam Canner, Hannah Lefley, Alice Kirvin, Dr Richard Archer, Matt Wilkes, Peter Bugryniec, Dr Robert Milton, Aaron Yeardley, Alex Chandler, and my poor Mum and Dad. I feel very fortunate that I had as many 'volunteers' as I did.

On a more personal note I'd like to thank two people, without whom I do not think I'd have made it to the end of my write up. Firstly and most importantly, my best friend and partner Adam who gave me more support (both personally and professionally) than I could have had any right to receive despite also undertaking a PhD. I hope we have many more years together in the future and that none of them involve anything like this PhD process. And lastly, to Tink. I truly do not know how to thank you for the kindness and compassion you showed me. It has not only got me to this particular milestone, but I feel certain I will feel its impact for the rest of my life.



# Contents

<b>Declaration</b>	<b>iii</b>
<b>Abstract</b>	<b>v</b>
<b>Acknowledgements</b>	<b>vii</b>
<b>Contents</b>	<b>xii</b>
<b>List of Figures</b>	<b>xvi</b>
<b>List of Tables</b>	<b>xviii</b>
<b>Glossary</b>	<b>xix</b>
<b>Notation</b>	<b>xxiii</b>
<b>1 Introduction, Aims and Objectives</b>	<b>1</b>
1.1 Aqueous Two-Phase Extraction (ATPE) as a process . . . . .	1
1.2 Background . . . . .	2
1.3 Industry and ATPE . . . . .	4
1.4 Research aims and objectives . . . . .	5
<b>2 Literature Review</b>	<b>7</b>
2.1 Introduction . . . . .	7
2.1.1 Applications of ATPE . . . . .	7
2.1.2 Competing Technologies . . . . .	8
2.1.3 Advantages of ATPE . . . . .	11
2.1.4 Challenges Establishing ATPE as an Industrial Process . . . . .	14
2.1.5 System Representation . . . . .	15
2.1.6 ATPE Process Operation . . . . .	17
2.1.7 Equipment Design . . . . .	18
2.2 Aqueous Two-Phase Systems (ATPS) Behaviour . . . . .	20

---

2.2.1	Overview . . . . .	20
2.2.2	Comparison to Traditional Liquid-Liquid Extraction (LLE) . . . . .	21
2.2.3	Phase Separation . . . . .	23
2.2.4	Protein Behaviour . . . . .	24
2.2.5	System Variables . . . . .	26
2.3	Kinetics of Phase Separation . . . . .	27
2.3.1	Overview . . . . .	27
2.3.2	Mechanism . . . . .	30
2.3.3	Phase Continuity . . . . .	31
2.3.4	System Properties and Phase Separation . . . . .	33
2.3.5	Effect of Protein . . . . .	33
2.4	Modelling Approaches . . . . .	34
2.4.1	Overview . . . . .	34
2.4.2	Modelling Partitioning . . . . .	35
2.4.3	Phase Equilibrium Modelling . . . . .	35
2.4.4	Mixing Modelling . . . . .	37
2.4.5	Kinetics Modelling . . . . .	38
2.4.6	Multi-stage Modelling . . . . .	40
2.5	Conclusion . . . . .	42
<b>3</b>	<b>Materials and Methods</b>	<b>45</b>
3.1	Introduction . . . . .	45
3.2	Experimental Materials and Methods . . . . .	46
3.2.1	Materials . . . . .	46
3.2.2	Model protein . . . . .	46
3.2.3	Stock and System Preparation . . . . .	47
3.2.4	Binodal Curve Determination . . . . .	48
3.2.5	Treatment of Phases . . . . .	50
3.2.6	Single Protein Analysis . . . . .	50
3.2.7	Phycocyanin Data Analysis . . . . .	51
3.2.8	Screening . . . . .	53
3.2.9	Selection of Single Model Contaminant . . . . .	54
3.2.10	Equilibrium Curves . . . . .	54
3.2.11	Volume Curves . . . . .	55
3.2.12	Single-stage ATPE . . . . .	55
3.2.13	Multi-stage ATPE . . . . .	56
3.2.14	Conventional Dispersion Height Diagrams . . . . .	59
3.2.15	Ultraviolet-visible (UV-vis) Analysis at 555 nm . . . . .	59

---

3.2.16	Microscopic Observation . . . . .	60
3.2.17	Protein Kinetics . . . . .	61
3.2.18	Error Calculations . . . . .	61
3.3	Computational Methods . . . . .	62
3.3.1	Liquid-Liquid (LL) Distribution . . . . .	64
3.3.2	Liquid-Interface-Liquid (LIL) Distribution . . . . .	65
3.3.3	Optimisation . . . . .	66
3.3.4	Deming Regression . . . . .	67
<b>4</b>	<b>Experimental Investigations of Multi-stage Aqueous Two-Phase Extraction</b>	<b>71</b>
4.1	Introduction . . . . .	71
4.2	Results and Discussion . . . . .	76
4.2.1	System Selection . . . . .	76
4.2.2	Feed and System Characterisation . . . . .	80
4.2.3	Single-stage Extraction . . . . .	82
4.2.4	C-phycocyanin Stock 1 Multi-stage Extraction (MSE) . . . . .	84
4.2.5	C-phycocyanin Stock 2 MSE . . . . .	88
4.2.6	C-phycocyanin Stock 3 MSE . . . . .	91
4.2.7	Overview of MSEs . . . . .	94
4.3	Conclusions . . . . .	97
<b>5</b>	<b>Equilibrium Modelling of Multi-stage Aqueous Two-Phase Extraction</b>	<b>99</b>
5.1	Introduction . . . . .	99
5.2	Results and Discussion . . . . .	103
5.2.1	Model Development . . . . .	103
5.2.2	Model Validation . . . . .	109
5.2.3	Process Design Using the Model . . . . .	115
5.2.4	Overview . . . . .	118
5.3	Conclusions . . . . .	120
<b>6</b>	<b>Variables Effecting Multi-Stage Aqueous Two-Phase Extraction</b>	<b>123</b>
6.1	Introduction . . . . .	123
6.2	Results and Discussion . . . . .	126
6.2.1	The Kinetics of the Phase Separation . . . . .	126
6.2.2	C-phycocyanin System Study . . . . .	129
6.2.3	Horizontal Interface Variation . . . . .	140
6.3	Conclusions . . . . .	148

---

<b>7</b>	<b>Conclusions and Future Work</b>	<b>149</b>
7.1	Conclusions . . . . .	150
7.2	Future Work . . . . .	154
	<b>References</b>	<b>159</b>
	<b>Appendix A</b>	<b>177</b>

# List of Figures

1.1	A schematic of an Aqueous Two-Phase Extraction (ATPE) . . . . .	2
2.1	A typical representation of a binodal curve which shows the critical point, tie lines and the points at which the system shifts from forming a single to a two-phase system. . . . .	16
2.2	A schematic of an Aqueous Two-Phase Systems (ATPS) with a continuous bottom phase undergoing separation. . . . .	30
2.3	A typical representation of a binodal curve which shows the phase inversion point. . . . .	32
2.4	A typical representation of a dispersion height graph of a ATPS. . .	39
2.5	A schematic to illustrate a five stage counter-current ATPE with a feed at stage three . . . . .	40
3.1	A schematic to illustrate the top, bottom, extract and waste phases in an ATPE . . . . .	50
3.2	A schematic to illustrate a three stage counter-current ATPE with a feed at stage one . . . . .	58
3.3	A schematic to illustrate a four stage counter-current ATPE with a feed at stage one . . . . .	58
3.4	A schematic to illustrate a five stage counter-current ATPE with a feed at stage three . . . . .	59
4.1	Structures of phycoerythrin, C-phycoyanin and allophycoyanin as depicted by Sonani (2016). . . . .	73
4.2	A schematic of a binodal curve (represented by the solid black line) illustrating regions which have robust ATPS. . . . .	75
4.3	Binodal curve of a Polyethylene Glycol (PEG) 6000 - ammonium phosphate at a pH of 7.4 ATPS. The black dots represent the point at which the system shifts from a single phase to a two-phase system. The red cross represents the system chosen for further case study. . .	78

4.4	The partitioning of C-phycoerythrin into the top, bottom, and horizontal interface in the C-phycoerythrin case study system. . . . .	79
4.5	ATPS in which material, including protein, has partitioned heavily into the horizontal interface of the system. . . . .	79
4.6	Amount of C-phycoerythrin (C-PC), allophycoerythrin (A-PC), and phycoerythrin (PE) in the feed, extract and waste phases of a single-stage C-phycoerythrin case study system. . . . .	83
4.7	A schematic to illustrate the multi-stage extraction set-up. . . . .	84
4.8	Ultraviolet-visible (UV-vis) spectra of the extract, waste and feed of a C-phycoerythrin case study five-stage counter-current ATPS. System was spiked with C-phycoerythrin stock 1 in stage three. As operated using gravity and centrifuge separation. . . . .	86
4.9	Amount of C-phycoerythrin (C-PC), allophycoerythrin (A-PC) and phycoerythrin (PE) in the extract and waste phases of each stage of a C-phycoerythrin case study five-stage counter-current ATPS. The system was spiked with C-phycoerythrin stock 1 in stage three. As operated using gravity separation and centrifuge operation. . . . .	87
4.10	Amount of C-phycoerythrin (C-PC), allophycoerythrin (A-PC), and phycoerythrin (PE) in the extract and waste phases of each stage of a C-phycoerythrin case study system five-stage counter-current ATPE. System was spiked with C-phycoerythrin stock 2 in stage three. As operated using gravity separation and centrifuge operation. . . . .	89
4.11	UV-vis spectra of the extract, waste and feed of a C-phycoerythrin case study five-stage counter-current ATPS. System was spiked with C-phycoerythrin stock 2 in stage three. As operated using gravity separation and centrifuge separation. . . . .	90
4.12	Amount of C-phycoerythrin (C-PC) and phycoerythrin (PE) in the extract and waste phases of each stage of a C-phycoerythrin case study three-stage counter-current ATPS spiked with C-phycoerythrin stock 3. As operated using gravity separation and centrifuge operation. . . . .	92
4.13	UV-vis spectra of the extract, waste and feed of a C-phycoerythrin case study three-stage counter-current ATPS spiked with C-phycoerythrin stock 3. As operated using gravity separation and centrifuge separation. . . . .	93
4.14	A schematic to demonstrate the general trends seen across the six Multi-stage Extraction (MSE)s carried out. . . . .	95
5.1	A diagram to show the different options for distribution of material in ATPE, adapted from Albertsson (1971). . . . .	103

---

5.2	Distribution of 3 mg of haemoglobin in the different 1600 $\mu$ L PEG 1500 - potassium phosphate pH 8.0 systems screened. . . . .	106
5.3	Calibration curves of haemoglobin in different concentrations of phase forming components, respective of concentrations used during experimentation. . . . .	107
5.4	The partitioning of haemoglobin in the haemoglobin case study system.	108
5.5	Volume of the horizontal interface as a percentage of the total volume in the haemoglobin case study system. . . . .	110
5.6	The UV-vis analysis of the extract and waste phases of a three-stage counter-current haemoglobin case study ATPE . . . . .	110
5.7	The amount of protein in the extract and waste phases of a three-stage counter-current haemoglobin case study ATPE with the feed in stage 1 . . . . .	111
5.8	The partitioning of C-phycoerythrin in the top, bottom, and horizontal interface region with respect to the total C-phycoerythrin concentration in the C-phycoerythrin case study . . . . .	113
5.9	The amount of C-phycoerythrin in the extract and waste phases of a four-stage count-current ATPE with a feed at stage one the C-phycoerythrin case study system . . . . .	114
5.10	The partitioning of lysozyme in the top, bottom, and horizontal interface region with respect to the total lysozyme concentration in the C-phycoerythrin case study system . . . . .	116
5.11	Schematic representing a MSE design of C-phycoerythrin from lysozyme in the C-phycoerythrin case study system. . . . .	117
6.1	Dispersion height diagrams for systems A, B, C, and D. . . . .	128
6.2	Turbidity measurements at 555 nm through the bottom, continuous phases of systems A, B, C, and D. The readings shown are from the start to the end of separation, the dotted red line indicates the point at which a distinct horizontal interface had formed. . . . .	130
6.3	Turbidity measurements at 555 nm through the bottom, continuous phases of systems A, B, C, and D. The readings shown are from the start of separation to 20 minutes after separation began, the dotted red line indicates the point at which a distinct horizontal interface had formed. . . . .	131
6.4	Dispersion height diagram for the C-phycoerythrin system. . . . .	132

6.5	Turbidity measurements at 555 nm through the bottom, continuous phases of the C-phyco cyanin system. The dotted red line indicates the point at which a distinct horizontal interface had formed for a system of this height. . . . .	134
6.6	Microscope images taken of the C-phyco cyanin system separating. The top row represents the top PEG-rich phase of the system, the second row represents the horizontal interface images and the bottom row represents the bottom phosphate-rich phase of the system. In a system of this height, the horizontal interface has formed after 5 minutes of separation . . . . .	136
6.7	Microscope images taken of the C-phyco cyanin system separating. The top row represents the top PEG-rich phase of the system, the second row represents the horizontal interface images and the bottom row represents the bottom phosphate-rich phase of the system. . . .	137
6.8	The number of stages required to reach varying yields around that which is achieved in a two-stage process. Shown are the results for $\lambda = 1, 1.63,$ and $7$ . The number of runs refers to the number of different $\beta$ values tested within the model. . . . .	144
6.9	The number of stages required to reach varying yields around that which is achieved in a three-stage process. Shown are the results for $\lambda = 1, 1.63,$ and $7$ . . . . .	145
6.10	The number of stages required to reach varying yields around that which is achieved in a four-stage process. Shown are the results for $\lambda = 1, 1.63,$ and $7$ . . . . .	146
6.11	The number of stages required to reach varying yields around that which is achieved in a >four-stage process. Shown are the results for $\lambda = 1, 1.63,$ and $7$ . . . . .	147
7.1	Calibration curves of C-phyco cyanin stock 1 in the extract and waste phases of a C-phyco cyanin case study system. As operated using gravity separation and centrifuge operation. . . . .	178

# List of Tables

2.1	Applications of Aqueous Two-Phase Extraction (ATPE) shown within the literature. . . . .	8
2.2	A comparison between traditional Liquid-Liquid Extraction (LLE) and ATPE (Albertsson, 1971; Seader et al., 2006). . . . .	22
2.3	Equating mechanisms and variables in Polyethylene Glycol (PEG)-salt Aqueous Two-Phase Systems (ATPS) . . . . .	28
2.4	Equating mechanisms and variables in PEG-salt ATPS . . . . .	29
2.5	Coefficients for kinetics equation of PEG-salt ATPS as determined by Mistry et al. (1996) . . . . .	39
3.1	ATPS used in this thesis . . . . .	49
4.1	Estimates from the literature of the isoelectric point and Molecular Weight (MW) of protein within feed stocks used in the model ATPE . . . . .	77
4.2	The concentration of C-phycoerythrin, allophycocyanin, and phycoerythrin protein in each of the stock solutions used in this study. . . . .	81
4.3	The 620 to 280 nm purity ratio of each of the feed stocks and extract phase of a single-stage C-phycoerythrin case study system as operated under centrifuge-operation. . . . .	84
4.4	The purity ratio of each of the C-phycoerythrin stock 1 feed and extract phases of a five-stage C-phycoerythrin case study system with a feed at stage three as operated with a centrifuge and gravity. . . . .	85
4.5	The purity ratio of each of the C-phycoerythrin stock 2 feed and extract phases of a five-stage C-phycoerythrin case study system with a feed at stage three as operated under centrifuge-operation and gravity. . . . .	90
4.6	The purity ratio of each of the C-phycoerythrin stock 3 feed and extract phases of a three-stage C-phycoerythrin case study system as operated under centrifuge operation and gravity. . . . .	94
4.7	The purity ratio and % of C-phycoerythrin lost in the waste output with respect to the feed for all extractions carried out. . . . .	95

5.1	Position of the horizontal interface in a 1600 $\mu\text{L}$ sample of the PEG 1500 - potassium phosphate pH 8.0 systems screened . . . . .	105
5.2	Comparison of the amount of haemoglobin in each phase between the experimental data, the Liquid-Liquid (LL) distribution model, and the Liquid-Interface-Liquid (LIL) distribution model. The feed in this system was at stage 1. . . . .	112
5.3	Comparison of the amount of C-phycoerythrin in each phase between the experimental data, the LL distribution model, and the LIL distribution model for the four-stage extraction with the feed at stage one. . . . .	114
5.4	Comparison of the amount of C-phycoerythrin in each phase between the experimental data, the LL distribution model, and the LIL distribution model. The feed in this system was at stage 3 . . . . .	115
5.5	Predicted percentage removal of lysozyme from the C-phycoerythrin case study system. . . . .	117
5.6	Predicted percentage recovery of C-phycoerythrin from the C-phycoerythrin case study system. . . . .	117
6.1	The amount of C-phycoerythrin measured in each of the top and bottom phases of the C-phycoerythrin system at various time points after the separation began up until equilibrium had been reached. Also shown is the amount of material not accounted for; this is listed under 'Remaining'. . . . .	139
6.2	The calculated values for $\beta$ and $SE(\beta)$ from Deming regression using $\lambda$ values of 1, 1.62 and 7 and linear regression. . . . .	143
6.3	The calculated yield of haemoglobin for a varying number of stages in a counter-current multi-stage operation using the haemoglobin system, using the same feed and extract and waste sizes as used in the experimentation. Shown is the stage-wise results for $\beta - 2SE(\beta)$ , $\beta - SE(\beta)$ , $\beta$ , $\beta + SE(\beta)$ and $\beta + 2SE(\beta)$ as calculated when $\lambda = 7$ . . . . .	143

# Glossary

<b>Abbreviation</b>	<b>Description</b>	<b>Page</b>
ATPAP	Aqueous Two-Phase Affinity Partitioning	13, 23, 94
ATPE	Aqueous Two-Phase Extraction	v, ix, x, xiii– xv, xvii, 1–6, 9, 11–13, 15– 23, 25, 30, 32, 34, 35, 38–41, 43, 48, 50, 53, 54, 56, 57, 60, 61, 65, 69–75, 79, 80, 82–84, 86, 87, 89, 95– 104, 108–110, 112, 113, 116– 119, 121–124, 138–140, 146– 153, 155

<b>Abbreviation</b>	<b>Description</b>	<b>Page</b>
ATPS	Aqueous Two-Phase Systems	ix, xiii, xiv, xvii, 1, 2, 5, 13–15, 18, 19, 21–23, 25–30, 32–37, 39, 43–48, 50, 52, 54, 57, 60, 61, 69, 70, 72, 73, 75–80, 84, 85, 88, 90, 91, 95, 96, 107, 121–124, 131, 136, 139, 148, 149, 152, 175
CAC	Continuous Annular Chromatography	8
CCC	Counter-Current Chromatography	18
CCTC	Continuous Counter-Current Tangential Chromatography	9
CHO	Chinese Hamster Ovary	11, 13, 17, 39, 40, 70, 99, 100, 116
CPC	Centrifugal Partition Chromatography	18
IgG	Immunoglobulin G	13, 16–18, 23, 24, 39, 40, 70, 99, 100, 116
LI	Liquid-Interface	100, 102, 103, 106
LIL	Liquid-Interface-Liquid	xi, xviii, 60, 62, 63, 66, 68, 100, 103, 107–113, 119, 140, 142–144, 149–152

---

<b>Abbreviation</b>	<b>Description</b>	<b>Page</b>
LL	Liquid-Liquid	xi, xviii, 60, 62, 100, 103, 106–113, 118, 119, 149, 150
LLE	Liquid-Liquid Extraction	x, xvii, 2, 14, 15, 17, 19, 20, 25, 28, 40, 69, 99, 102, 153
MAb	Monoclonal Antibody	3–8
MCSGP	Multi Column Counter Current Solvent Grade Purification	8
MSE	Multi-stage Extraction	v, xi, xiv, xv, 4, 43, 48–52, 54, 55, 60, 66, 69, 70, 74, 76, 80, 82–84, 86, 89, 92–97, 100–102, 105, 107, 108, 110, 111, 114–119, 122, 123, 148–150
MW	Molecular Weight	xvii, 44, 45, 47, 50, 75, 94, 118
PCCC	Periodic Counter-Current Chromatography	7, 8

---

<b>Abbreviation</b>	<b>Description</b>	<b>Page</b>
PEG	Polyethylene Glycol	xiii, xv–xviii, 1, 13, 16–20, 22, 23, 25–27, 29–31, 34, 37, 39, 44–47, 50– 52, 58, 60, 69, 70, 73–76, 79, 80, 94, 99, 102– 105, 122, 124, 125, 127, 130, 134–136, 140, 147, 149, 175
PRDC	Perforated Rotating Disk Contactors	17
RSM	Response Surface Methodology	35
SMB	Simulated Moving Bed	8
TLL	Tie Line Length	16, 27, 31, 75, 95
TMB	True Moving Bed	8
UV-vis	Ultraviolet-visible	x, xiv, xv, 44, 48–53, 55, 57– 59, 70, 78, 84, 88, 91, 107, 108, 117, 122– 125, 127, 130, 131, 133, 137, 139, 146, 151, 153

# Notation

## Phase Descriptions

<i>Bottom</i>	Bottom phase
<i>E</i>	Extract phase
<i>HI</i>	Horizontal interface
<i>Top</i>	Top phase
<i>Total</i>	Total system
<i>W</i>	Waste phase
<i>x</i>	Phase protein is being moved from
<i>y</i>	Phase protein is being moved to

## Roman Letters

$A_{WL}$	Absorbance at wavelength WL
$b$	Estimate of horizontal interface slope for haemoglobin partitioning
$B$	Binary variable
$C$	Concentration, $mg/mL$
$\hat{C}_{HI}$	True estimate of horizontal interface concentration, $mg/mL$
$\hat{C}_{Total}$	True estimate of total concentration, $mg/mL$
$d_d$	Diameter of globule
$e$	Molar absorptivity, $L/gcm$
$H_{extraction}$	Extraction height above the horizontal interface, $cm$
$i$	Data points in experiment
$I$	Total data points in experiment
$j$	Repeats in experiment
$J$	Total repeats in experiment
$k_{b1}$	Protein partitioning coefficient for bottom phase, $mL/mg$
$k_{b2}$	Protein partitioning coefficient for bottom phase
$k_{t1}$	Protein partitioning coefficient for top phase, $mL/mg$
$k_{t2}$	Protein partitioning coefficient for top phase

---

$K_{biosp}$	Partitioning coefficient as a result of biospecific affinity
$K_{conf}$	Partitioning coefficient as a result of conformation
$K_{el}$	Partitioning coefficient as a result of electrochemical potential
$K_{hfob}$	Partitioning coefficient as a result of hydrophobicity
$K_{size}$	Partitioning coefficient as a result of size
$K_0$	Partitioning coefficient as a result of other factors
$l$	Path length, <i>cm</i>
$m$	An experimental measurement
$M$	Mass of protein, mg
$n$	Stage number
$N$	Total number of stages in the process
$N_{max}$	Maximum number of stages considered in the model
$PR$	Purity ratio
$r$	Runs / number of phase changeovers performed
<i>radius</i>	Radius of vessel where extractions were carried out, <i>cm</i>
$Re$	Reynolds number
$s$	A sample
$S$	Stage-wise result
$SD$	Standard deviation
$t$	T-distribution
$t_m$	Mixing time
$T$	Required recovery or removal
$V$	Volume, <i>mL</i>
$Var$	Variance
$v_1$	Separation rate coefficient, <i>m/s</i>
$v_2$	Separation rate coefficient
$v_3$	Separation rate coefficient
$v_4$	Separation rate coefficient
$V_a$	Coefficient describing horizontal interface size
$V_b$	Coefficient describing horizontal interface size, <i>mg/mL</i>
$V_c$	Coefficient describing horizontal interface size, <i>mL/mg</i>
$V_{critical}$	Threshold value for volume of horizontal interface, <i>mL</i>
$V_{HI}$	Size of the horizontal interface as a percentage volume of the total system height
$V_s$	Sedimentation velocity, <i>m/s</i>
$We$	Weber number
$Z$	Calculated value

### Greek Letters

---

$\alpha$	Significance level
$\beta$	Protein partitioning coefficient for the horizontal interface
$\beta_1$	Protein partitioning coefficient for the horizontal interface, $mL/mg$
$\beta_2$	Protein partitioning coefficient for the horizontal interface
$\hat{\beta}$	True estimate of horizontal interface slope for haemoglobin partitioning
$\hat{\beta}_{-i}$	The estimate of $\hat{\beta}$ without the data set $(C_{Total,i}, C_{HI,i})$
$\hat{\beta}_i^*$	The $i^{th}$ pseudo-variate of $\hat{\beta}$
$\hat{SE}(\hat{\beta})$	Standard error of $\hat{\beta}$
$Var_{Jackknife}(\hat{\beta})$	Variance of $\hat{\beta}$ as determined by the Jackknife method
$\epsilon$	Normally distributed error, $mg/mL$
$\theta$	Data set
$\lambda$	Error ratio
$\mu$	Mean of experimental data points
$\mu_C$	Viscosity of the continuous phase, $kg/ms$
$\mu_D$	Viscosity of the dispersed phase, $kg/ms$
$\Delta\rho$	Density difference between the two phases, $kg/m^3$
$\rho_C$	Density of the continuous phase, $kg/m^3$
$\sigma$	Interfacial tension between the two phases, $N/m$
$\sigma_W$	Surface tension of the air-water interface at 20 °C, $7.28 \times 10^{-2} N/m$



# Chapter 1

## Introduction, Aims and Objectives

This chapter is an introductory chapter which outlines the background and context for the research contained in this thesis. The first section outlines how [Aqueous Two-Phase Extraction \(ATPE\)](#) works as an extraction process. The section also outlines the reason there is a need to develop continuous processes like [ATPE](#) for protein purification, followed by the technology gaps in [ATPE](#) which need to be met for [ATPE](#) to be used industrially. The chapter also describes the biopharmaceutical market as well as the latest use and development of [ATPE](#) for the extraction of therapeutic proteins. Lastly, this section outlines the hypothesis, aims, and objectives for this thesis which have been chosen to help [ATPE](#) become more attractive as an industrial process.

### 1.1 [ATPE](#) as a process

[Aqueous Two-Phase Systems \(ATPS\)](#) form semi-miscible phases when sufficient concentrations of phase forming material (polymer(s)) and / or salt(s)) are used in water. These phases separate due to the polarity of the phases, and it has been shown by [Albertsson \(1986\)](#) that up to 18 phases can be seen in a single system. However, two phases are often used for practicality to partition proteins. In this type of two-phase system, one phase is considered the relatively hydrophilic phase and one the relatively hydrophobic phase. For instance, in a [Polyethylene Glycol \(PEG\)](#)-salt system, the salt-rich phase would be considered the hydrophilic phase, and the [PEG](#)-rich phase the hydrophobic phase. When protein, solutes, or cells are added to a system, they will preferentially partition into one of the phases because of the properties of the protein and the system conditions. The system conditions

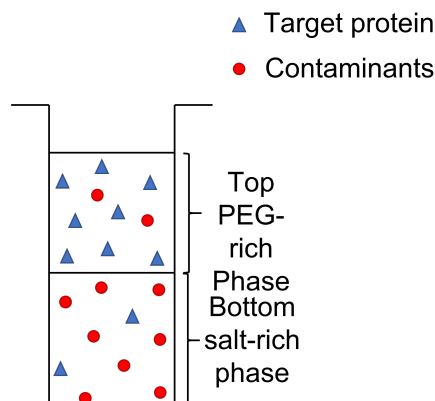


Figure 1.1: A schematic of an [ATPE](#)

can be manipulated to change the protein partitioning. This means that the system can be used as a separation technique. A schematic of an extraction using [ATPS](#) is shown in [Figure 1.1](#)

## 1.2 Background

[ATPE](#) is a non-traditional protein purification technique in which there has been a renewed interest as the biopharmaceutical industry undergoes a paradigm shift. The industry has typically been conservative in that it employs batch manufacturing techniques, values a first to market approach, has little concern for costs, and has very stringent health and safety regulations. However, the industry must adapt to increase its manufacturing capacity and drive down its costs while still meeting the stringent safety standards. This is due to the expiration of patents and the subsequent emergence of biosimilars which have driven down prices. The industry is also facing an increasing demand for products. It has been suggested that this should be achieved through the use of continuous manufacturing; this has been further encouraged by safety boards, such as the FDA, as it is expected to improve the quality and consistency of the products ([Konstantinov and Cooney, 2015](#)). As a result, there has been a need to either convert the current batch purification techniques to a continuous mode of operation or replace them.

Up until recently, significant effort has been focused upon improving and converting the upstream unit operations into continuous processes. These improvements have meant that, theoretically, large antibody titres can be achieved in continuous cell cultures at an industrial scale ([Hodge, 2005](#); [Clincke et al., 2013](#)). The increase in material from the upstream processing has resulted in the downstream processes being unable to cope with required throughputs ([Azevedo et al., 2009a](#)). This issue

is further compounded by the high cost of downstream processing which can account for up to 80% of the manufacturing costs (Roque et al., 2004). As such, it would be desirable to both intensify and integrate downstream unit operations in order to increase the amount of material handled as well as decrease the costs. An alternate unit operation which is considered to be capable of meeting all of these demands is ATPE.

ATPE is a Liquid-Liquid Extraction (LLE) process suitable as a continuous purification technique for biological products. ATPE is a gentle, low shear extraction technique which is unlikely to damage or denature biological products (Asenjo and Andrews, 2011a). The technique has an added advantage of having comparatively cheaper economics when compared with more traditional downstream purification techniques (Azevedo et al., 2009a). This is due to the cheap, recyclable phase forming material, simple equipment requirements, and its ability to be run in a continuous manner. The process works by using high enough concentrations of phase forming polymer(s) and / or salt(s) to form two aqueous, semi-miscible phases. Protein, cells, and solutes can then be partitioned by setting the conditions so that the target product partitions into one phase and the contaminants partition into the other, thereby purifying the target product. ATPE has been demonstrated at lab scale to be capable of purifying a number of biological products including: monoclonal antibodies (Andrews et al., 1996), protease inhibitors (Harris et al., 1997), and cells (Walter et al., 1992).

The first recorded observation of aqueous two-phase partitioning was made by a Dutch microbiologist in 1886 when it was discovered that the water soluble polymers agar and starch would separate into two aqueous phases (Beijerinck, 1886). A use for ATPS was not discovered until the 1950's when Albertsson (1958) used it to partition protein. During the course of his career, Albertsson (1986) was instrumental in developing the process as a protein purification technique, including suitable equipment and scaling up the process so that it is capable of being run at an industrial scale (Blomquist and Albertsson, 1972).

However, the process has two major drawbacks; a lack of understanding of the phase forming mechanisms, and a low resolution being achieved through a single step. These drawbacks have led to the process design and optimisation being heavily reliant on both 'trial and error' and individual expertise. This has made the process development expensive with no guarantee of yielding desirable results. As a result, there is a reluctance to use the process industrially and the process was overshadowed in the 1990's by chromatography, a process which was better understood and well suited to the batch operations being used at the time.

### 1.3 Industry and ATPE

The biopharmaceutical industry is a large and fast-growing industry. It was valued at around \$325 billion in 2020 with an estimated compound annual growth rate of around 7.3 % between 2021 and 2026 (MordorIntelligence, 2021). The key market players include Amgen Inc, Abbvie Inc, Bristol Myers Squib, Eli-Lilly, Roche and Novo Nordisk (MordorIntelligence, 2021; IndustryArc, 2019). These key market players often supply key blockbuster drugs to the market which treat some of the most challenging diseases like cancer or autoimmune diseases. For example, Genentech (owned by Roche) produce Avastin (Bevacizumab) to treat number of difficult to treat cancers including non-squamous non-small cell lung cancer and recurrent glioblastoma (Genentech, 2021). The Monoclonal Antibody (MAb) works by targeting VEGF, thereby limiting the growth of new tumour blood vessels (Genentech, 2021). Avastin recorded sales of \$7.12 billion in 2019; however, this is predicted to drop drastically to \$1.7 billion by 2026 after Amgen and Allergan bought cheaper biosimilars of Avastin to market at the end of 2019 (FiercePharma, 2020).

There is a growing acceptance of ATPE within industry which is being driven by the need to reduce costs of bio-processes as the emergence of biosimilars lowers the market price of therapeutic proteins. McQueen and Lai (2019), who work within the drug development and processing departments of GlaxoSmithKline, published a mini-review on the increasing acceptance of ATPE within the pharmaceutical and biopharmaceutical industries. They comment the barriers to adopting ATPE as an industrial technology were theoretically low. Research into this area is increasingly showing that high yields and purities of therapeutic proteins can be achieved from crude starting materials; for instance, lysed cell supernatant or cultivation broth. Kruse et al. (2019) combined ATPE with a membrane-based separation to purify MAbs directly from a cultivation broth. They achieved high MAb yields, up to 93 %, while removing DNA and host cell protein.

Aside from its use in the purification of therapeutic proteins, ATPE is also breaking into diagnostics. A major author in the field, Boris Zaslavsky, has set up a spin out company (Cleveland Diagnostics) which uses ATPE in cancer diagnostics (ClevelandDx, 2021). The company has recently raised a series D funding round of around \$19 million. The technology evaluates differences in partitioning coefficients in cancer markers. They state partitioning coefficients of common cancer biomarkers change as result in changes in protein structure in cancerous patients (Zaslavsky et al.). The technology allows for more accurate and earlier screening of patients, aiming to improve treatment outcomes by catching cancer cases earlier.

## 1.4 Research aims and objectives

To improve the low resolution of [ATPE](#), [Multi-stage Extraction \(MSE\)](#) can be utilised. Improving low resolution, cheap separation processes through the use of additional stages has been a technique commonly used across the chemical processing industry, with the most well known example being distillation. Using [MSE](#) has the added benefit of reducing the amount of system screening required, as less desirable conditions can be accepted. To use [ATPE](#) as a multi-stage technique, there needs to be a firm understanding of how the process behaves across multiple stages and which parameters need to be controlled.

As such, this thesis aims to evaluate multi-stage [ATPE](#) and develop a method for the design and its implementation. The overarching aim of this report is to reduce both the ‘trial and error’ and individual expertise required in the design of [ATPE](#) for protein purification and therefore increase the success in [ATPE](#) design. As such the project was divided as follows:

1. Literature surrounding [ATPE](#)
2. Materials and methods
3. Experimental investigations of multi-stage [ATPE](#)
4. Multi-stage [ATPE](#) modelling at equilibrium
5. Kinetics of [ATPE](#) and robustness testing
6. Conclusions and future work



## Chapter 2

# Literature Review

### 2.1 Introduction

This section outlines the relevant literature surrounding [Aqueous Two-Phase Extraction \(ATPE\)](#) and is divided into four parts. The first section looks at the background, uses, advantages and challenges of [ATPE](#). The second section covers how [Aqueous Two-Phase Systems \(ATPS\)](#) behave, along with the partitioning behaviour of protein, cells and solutes. The third section contains information on the kinetics of the phase separation and the last section outlines the different modelling approaches used in [ATPE](#).

#### 2.1.1 Applications of [ATPE](#)

[ATPE](#) has been demonstrated to be capable of purifying a wide range of biological products at lab scale which are shown in [Table 2.1](#). It can be seen that the process is capable of handling [Monoclonal Antibody \(MAB\)s](#). [MABs](#) are the most sought after and profitable therapeutic proteins in the biopharmaceutical industry. In 2016, the pharmaceutical industry statistics show that 6 out of the top 10 grossing pharmaceutical products were [MAB](#), with a further two also being biopharmaceutical products ([Hall et al., 2017](#)). As a result, a significant amount of the research surrounding protein purification techniques looks at the purification of [MABs](#). Despite this focus, there is a wide range of biological products which also need purification including: enzymes ( $\alpha$ -amylase, proteases), amino-acids (L-Arginine, L-glutamic acids), antibiotics (tetracyclines, celaphosporins, penicillins) natural pigments (C-phycoyanin,  $\beta$ -carotene), and therapeutic cells (CAR-T cells, synthetic blood) ([Doran, 2013](#)). As the number of products available increases, the diversity in manufacturing requirements also increases; this creates a need to develop more novel manufacturing techniques surrounding purification of biological products.

Use	System Type	Reference(s)
Enzymes	Polymer-Salt	( <a href="#">Kula et al., 1982</a> ; <a href="#">Prinz et al., 2014</a> )
MAbs	Polymer-Salt	( <a href="#">Rosa et al., 2013</a> ; <a href="#">Andrews et al., 1996</a> )
	Polymer-Polymer	( <a href="#">Azevedo et al., 2009b</a> )
Antibiotics	Polymer-Hydrophobic Ionic Liquids	( <a href="#">Jiang et al., 2009</a> )
Protease inhibitors	Polymer-Salt	( <a href="#">Harris et al., 1997</a> )
Cells	Polymer-Polymer	( <a href="#">Walter et al., 1992</a> )
Metal Ions	Polymer-Salt	( <a href="#">Rogers and Bauer, 1996</a> )
Small Organic Species	Polymer-Salt	( <a href="#">Willauer et al., 2002</a> )
Nano and Micro - Solid Particulates	Polymer-Polymer	( <a href="#">Helfrich et al., 2005</a> )

Table 2.1: Applications of [ATPE](#) shown within the literature.

### 2.1.2 Competing Technologies

Currently, the downstream processing of biologics is heavily reliant on resin-based chromatography. In resin-based chromatography, a mobile phase which contains the target protein and contaminants is run through the stationary phase, i.e. the resin bed. The target protein and contaminants interact with the resin differently depending on their properties. Typical properties exploited to separate contaminants from target protein include ([Doran, 2013](#)):

- Charge
- Size
- Hydrophobicity
- Biospecific affinity

Either the contaminants or target protein are bound to the column. If the contaminants are bound to the column, the column can be operated continuously until the solid resin is saturated and either needs to be cleaned or replaced. If the target protein is bound to the column, as is common, then once the mobile phase has been run through the column, the conditions of the column are changed (usually through pH adjustment) and the target protein is eluted off the column. Due to the up stream processes and high regulatory standards, processes are often run as campaigns and purification is carried out in batch with equipment and resins cleaned or replaced after every individual operation. As a result, protein purification is run as an inherently batch process.

Chromatography columns are recognised as the backbone of protein purification due to the high product quality which can be achieved easily and rapidly to meet the minimum driving factors of the biopharmaceutical industry ([Konstantinov and Cooney, 2015](#)). However, as they are run as an inherently batch operation, the process cannot deliver the required throughput at a competitive cost. There are ways to alter the operation of chromatography columns to be run in a more continuous manner to increase throughput and decrease costs; this is described later in this section.

Another disadvantage of chromatography is the high cost of the process; up to 80% of the downstream processing costs of protein can be attributed to the chromatographic unit operations ([Azevedo et al., 2009a](#)). Mostly, this is a result of the long processing times and high cost of the resin. A particular cost to highlight is the protein A resins, commonly used in an affinity capture step of MABs, which typically cost between \$6,000 and \$15,000 per litre ([Lain, 2009](#); [Petrides et al., 2014](#)). [Petrides et al. \(2014\)](#) carried out economic analysis of the batch production of MABs. It was found that the protein A resin accounted for 73% of the consumables cost, with a further 15% attributed to other resins. In comparison, filtration membranes accounted for only 10% of the consumables costs. When considering the total operating costs it was found that protein A resin alone accounted for 11.7%, even if the lower range of protein A (\$6000/L) cost and a use of 60 cycles were assumed.

The last major disadvantage associated with the use of chromatography columns is that they are unable to deal with large or varying amounts of material ([Azevedo et al., 2009a](#)). This is becoming increasingly important because of the improvements being made in the upstream processes. These improvements have resulted in both higher MABs titres, as well as increasing production scales. Consequently, there are larger amounts of material for the downstream processes to deal with.

These disadvantages along with the current trends in bioprocessing mean that in order for the industry to advance, it is imperative that either the process of chromatography be improved or replaced, either partially or fully, by an alternative process ([Konstantinov and Cooney, 2015](#)). In order to meet the demand to improve chromatography processes, advances have been made which allow the process to run continuously, thereby reducing costs, increasing throughput, and decreasing column size requirements. This has been achieved through both a multi-column and a single-column approach. A multi-column approach involves having each column at a different stage of the operation (e.g. loading, washing, elution, cleaning in place, and equilibration), thereby creating a continuous operation.

There are several different ways of approaching multi-column chromatography; the most common and simple of which is called [Periodic Counter-Current Chro-](#)

matography (PCCC). In PCCC, the columns are switched between each mode of operation. This technique has been demonstrated using both MABs and enzymes, where it both improved the process economics (through increasing the resin usage) and decreased the equipment and facility size (Godawat et al., 2012). The use of PCCC was investigated commercially by GE Healthcare (2015) where it was found that PCCC increased production capacity by 56% when compared with a batch chromatography operation.

Another multi-column approach is called Simulated Moving Bed (SMB) chromatography. In this, the solid resin bed is kept stationary, but the point at which the mobile phase(s) is added is moved simulating a counter-current flow. This effectively creates columns at different points of the operation. This technique has been offered at both a small and commercial scale by PALL, Sigma-Aldrich, and other bioprocessing manufacturers (PALL Biopharmaceuticals, 2017; Sigma-Aldrich, 2017). For SMB to work, a resin which binds much more preferentially to the product than the impurities is required (for example a protein A resin for MABs) or acceptance of only achieving a partial separation in a single step (Müller-Späth et al., 2008). As a result, this technique has been modified in order to provide three fractions, as opposed to two. Having three fractions allow for the product to be separated from both weakly and strongly binding impurities. This technique is called Multi Column Counter Current Solvent Grade Purification (MCSGP) (Liu and Morrow, 2017). MCSGP has been shown by Liu and Morrow (2017) to be capable of purifying a target MAB from two other MAB variants using a cation exchange chromatography column to achieve a purity and yield of over 90%. An alternative, theoretical, multi-column approach is True Moving Bed (TMB) chromatography, where the stationary and mobile phases are moved counter-current to each other. However, it is impractical to move the stationary phase in resin based chromatography (Sá Gomes and Rodrigues, 2012).

In terms of a single-column chromatography approach, a technique called Continuous Annular Chromatography (CAC) can be used. In this approach, the column along with the stationary phase is rotated and the mobile phase moves cross-current to the stationary phase. CAC has been demonstrated at lab scale to be suitable for bioseparations but is not yet available commercially (Hilbrig and Freitag, 2003; Zydney, 2016).

These efforts to develop continuous chromatography techniques have increased the resin life span as well as the throughput of the process. However, the repeated use of the resin can result in column fouling which means a decrease in performance over time (Staby et al., 1998; Close et al., 2013; Doran, 2013). While cleaning in place techniques can be used to remove or reduce column fouling, some fouling is

irreversible (Jin et al., 2010). To slow the process of irreversible column fouling, more upstream purification processes can be used to protect more expensive resins; however, eventually they will still need to be replaced.

Other alternative continuous purification techniques which are being considered include (Zydney, 2016):

- Continuous Counter-Current Tangential Chromatography (CCTC) (Dutta et al., 2015)
- Radial chromatography (Lay et al., 2006)
- Protein precipitation\* (Hammerschmidt et al., 2014)
- Crystallisation\* (Zang et al., 2011)

\*Batch operations which can be modified using a tubular reactor to run continuously.

While chromatography is a very useful technique in the processing of biologics, the trends of the industry and disadvantages of the process mean that research into better operational methods of chromatography, cheaper resins, or even alternative processes are required. An alternative process which is considered capable of meeting the current demands of the industry is ATPE.

### 2.1.3 Advantages of ATPE

One of the advantages to using ATPE which has re-captured interest in the process is that it is easily run in a continuous manner. ATPS has two liquid phases, rather than a solid phase and a liquid phase, meaning that during operation:

1. Both phases are mobile
2. Cleaning of the phases is easier to achieve
3. Replacement of the phases is easier to achieve

It is these three advantages which make the system particularly suitable to continuous operation. This is particularly relevant because of the recent push towards continuous manufacturing in the biopharmaceutical industry. This has been encouraged by the FDA as a result of a demand to reduce the cost of biologics. Furthermore, a product of a continuous manufacturing method is likely to be of a more consistent and higher quality (Rathore et al., 2016; Konstantinov and Cooney, 2015). This is because the time to manufacture the product would vary less, resulting in a more consistent glycosylation profile (Robinson et al., 1994; Pacis et al., 2011; Konstantinov and Cooney, 2015).

Decreasing costs is an essential challenge to biopharmaceutical companies who originally developed a product and must now compete with companies bringing out biosimilars. Biosimilars are therapeutic protein products which have been shown to have no meaningful difference clinically (in terms of safety, efficacy and quality) to an original product. The process of developing therapeutic proteins is expensive and lengthy, especially for completely novel products which must undergo the most extensive research and development processes as well as more extensive clinical testing. A lot of therapeutic protein products are beginning to reach the end of their patents. This means that other companies who have not had to bear the brunt of the research and clinical testing costs can develop biosimilars ([Blackstone and Joseph, 2013](#)). In order to compete with companies producing biosimilars of their product, companies are looking for cheaper manufacturing methods to reduce costs, for instance, by switching from a batch manufacturing technique to a continuous one.

The use and benefits of continuous manufacturing have been shown to be effective across a wide array of manufacturing industries. These include; chemical, food, steel casting, and pharmaceutical industries ([Anderson, 2001](#); [Reay et al., 2013](#)). The benefits of using a continuous manufacturing process include ([Konstantinov and Cooney, 2015](#)):

- Reduced equipment size
- Higher productivity
- Reduced capital
- Reduced operating cost
- Steady state operation
- Low cycle times
- Streamlined process flow

The reduction in equipment size and higher productivity is the result of a continuous output of a small amount of product, rather than a large amount of product being produced at the end of a campaign ([Utterback, 1994](#)). The smaller equipment also means that smaller spaces are required for manufacturing plants which reduces the capital required to set up a manufacturing process. This reduced cost and reduced need for upfront capital would allow companies to invest in the development and manufacture of more biological products. This is especially relevant when considering treatments for conditions and diseases which are less prevalent and therefore

less profitable. A greater number of biological products which are cheaper to produce will increase the number of treatable diseases as well as increase treatment availability worldwide. In terms of the biopharmaceutical industry, it will increase both profit margins and the number of products which can be sold. However, there are some concerns with continuous manufacturing; a key concern is that production would effectively be halted should one unit operation fail or become contaminated.

Aside from continuous operation, [ATPE](#) has several other advantages which includes:

- Flexible operation
- Flexible material handling
- Low cost
- Low toxicity and low shear
- Easily scale up
- Process integration

[ATPE](#) is a flexible process which can be operated in a number of different configurations. It has been shown that it can be operated in a batch or a continuous mode as a single or a multi-stage process, with the multi-stage processes being operable as both a counter-current and a cross-current configuration ([Walter et al., 1994](#)). This allows for the process to be easily adapted to the individual needs of a manufacturing processes. The process is also flexible in the way it handles material; it has been shown that [ATPE](#) is capable of dealing with both large and varying feeds. This is particularly relevant as continuous upstream operations, such as high cell density perfusion systems, have been shown to express large titres which can vary ([Hodge, 2005](#); [Clincke et al., 2013](#)).

[ATPE](#) has also been shown to be capable of dealing with very crude material, including [Chinese Hamster Ovary \(CHO\)](#) cell supernatant and [PER.C6](#) cell supernatant, a cell line derived from human embryonic retinal cells ([Rosa et al., 2009b, 2013](#)). [ATPE](#) has also been shown to be capable of handling very viscous material (for instance chicken egg white) which chromatography columns would typically find difficult to handle ([Lu et al., 2013](#); [Dembczyński et al., 2010, 2013](#)). Handling of viscous and crude material is becoming more valuable as novel upstream manufacturing methods are being developed which aim to decrease costs and increase manufacturing capacity. An example of where [ATPE](#) could be beneficial is as a purification technique for novel upstream manufacturing methods is in the purification of chicken egg white containing biological products. The novel technique of

using transgenic chickens to produce biological products has been achieved; however, the manufacturing techniques surrounding the downstream processes need to be capable of handling very viscous material to make this a viable way to produce biological products (Herron et al., 2018). The use of biological products in transgenic chicken eggs would drastically decrease the costs associated with production. As the techniques to produce biologics improve and novel manufacturing methods are developed, this capability to handle varying types and amounts of crude material will make the diversity and robustness of ATPE invaluable.

A further advantage of ATPE is the low cost of the phase forming materials and the process in comparison with chromatography. This is particularly true if a polymer-salt system is used and recycling of the more expensive polymer phase using back extraction and washing steps is carried out (Rosa et al., 2013). The use of two aqueous phases also makes ATPE a very mild, low shear process with low toxicity, which is unlikely to damage or denature the biological product (Asenjo and Andrews, 2011a). Lastly, it has been shown that ATPE can combine two or more unit operations. For instance: clarification, purification, and viral inactivation (Schügerl and Hubbuch, 2005; Benavides and Rito-Palomares, 2008; Asenjo et al., 1994; Hart et al., 1994). It has also been shown that the system is easily scaled up which allows for easy transition from bench scale to an industrial scale operation.

Together, these advantages have led to ATPE being reconsidered as a purification technique for biological products considering the current trends seen in bioprocessing. The unit operation provides an alternative to chromatography which can: reduce costs, be easily operated in a continuous manner, and can intensify and integrate downstream unit operations.

#### 2.1.4 Challenges Establishing ATPE as an Industrial Process

While interest in ATPE has recently been reignited due to the biopharmaceuticals industry's interest in continuous manufacturing, there are a number of challenges which must be overcome in order for the unit operation to be used as an industrial process. Most importantly, the process needs to effectively compete with the industrially used protein purification techniques (in particular, chromatography) in terms of process economics, yield and purity (Azevedo et al., 2009a). While the process is much cheaper to run than chromatography, single-stage ATPE has a low resolution which has an impact on the purity and yield of the process (Ruiz-Ruiz et al., 2012). High levels of purity are needed in order to comply with the high safety standards applied to the biopharmaceutical industry, and the yield of the system would affect the economics of the process.

There are two ways to overcome the low purity and yield achieved using ATPE.

The first is to use a multi-stage purification process. Rosa et al. (2013) reported that they achieved an 80% yield and greater than 99% purity of Immunoglobulin G (IgG) from CHO cell supernatant when a multi-stage, counter-current continuous Polyethylene Glycol (PEG)-phosphate system was used. Another way to improve the resolution is to use Aqueous Two-Phase Affinity Partitioning (ATPAP) (Azevedo et al., 2009a). In this approach, at least one of the phase forming polymers is chemically attached to an affinity ligand specific to the target protein. The technique has been shown to be capable of purifying IgG to 90% purity and yield in a single step. Ligands can also be added in solution to a system to improve the resolution (Andrews et al., 1990).

The other limitation of ATPE is the lack of understanding of the mechanics behind the phase separation and the protein partitioning behaviour. This has led to a lack of reliable modelling of the system, which has in turn contributed to ATPE's reputation as a low resolution, unreliable technique (Asenjo et al., 1994, 2002a; Rito-Palomares, 2004). Modelling is required in the optimisation of the process, system and reactor design to maximise the efficacy of the system. This lack of reliable modelling has resulted in a need for both 'trial and error' as well as individual expertise in system selection which is time consuming and expensive. There have been efforts to combat this through the use of robotic-aided strategies, but these are costly (Bensch et al., 2007).

Another limitation of ATPE is the difficulty in removing the polymer phase material after the extraction. To avoid this, a second back-extraction step can be used where the polymer phase containing the target protein is contacted with a fresh salt phase. The conditions are set so as to partition the target protein into the salt-rich phase Mistry et al. (1996). A salt-rich phase is much easier to clean downstream than a polymer-rich phase. The removal of salt can be achieved easily with filtration, and the more expensive polymer phase can then be recycled and reused with this method.

### 2.1.5 System Representation

ATPS are often graphically represented using a phase diagram. These show information on the system at equilibrium. A typical representation of a binodal curve is shown in Figure 2.1. The phase diagram depicts the binodal curve which shows the critical concentration at which the system will shift from forming a single-phase to forming a two-phase system. Below the curve, a single phase is formed and above the curve two phases are formed. A binodal curve is usually determined experimentally using the cloud point method (Hatti-Kaul, 2000). In two-phase systems, the separation can be represented by a tie line. On the phase diagram below, the line

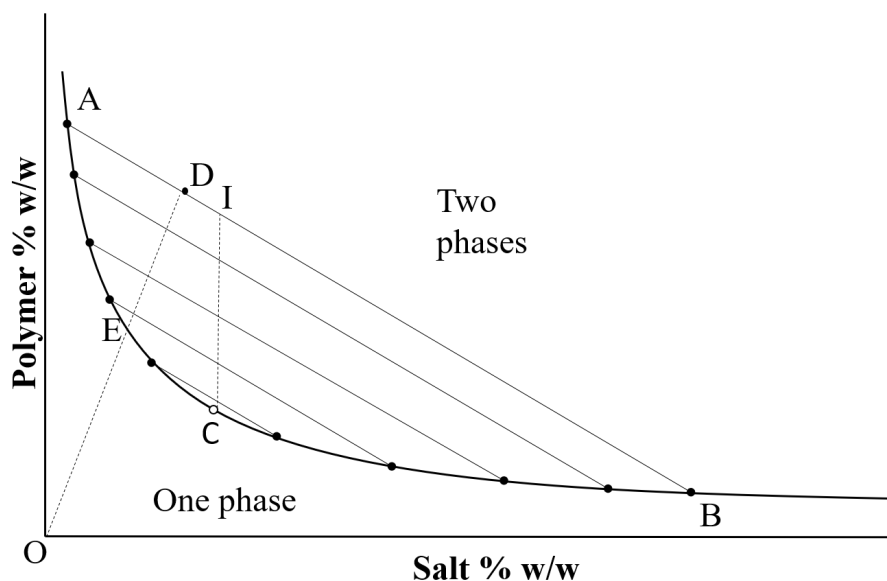


Figure 2.1: A typical representation of a binodal curve which shows the critical point, tie lines and the points at which the system shifts from forming a single to a two-phase system.

AB and the lines parallel represent the systems tie lines. In the example tie line AB, the point D represents the concentration of an entire system. This point D can be anywhere along the tie line. As the system separates, the concentration of each phase moves along the tie line until one phase reaches the concentration at point A and the other phase the concentration at point B. At this point, the system is at equilibrium. It has been shown experimentally that systems with different total compositions resting along a tie line will have the same equilibrium composition in each phase (with different phase volumes) (Albertsson, 1971). It has been shown experimentally that tie lines in the same ATPS are considered to run parallel to each other (Albertsson, 1986; Zaslavsky, 1995; Hatti-Kaul, 2000; Raja et al., 2011); this is not the case in traditional Liquid-Liquid Extraction (LLE) (Seader et al., 2006).

Another important feature on the binodal curve is the critical point, C. This is a theoretical point at which the compositions and volumes of the two phases are equal. The critical point can be determined experimentally by extrapolating through the midpoints of several tie lines (Hatti-Kaul, 2000). Another important feature shown on phase diagram is the phase inversion point, represented by the point I. This point is the concentration at which the phase continuity of the system is reversed. In polymer-salt phases, this is always determined by a critical salt concentration and is known to cut through the critical point (Kaul et al., 1995; Salamanca et al., 1998).

Systems are often described in terms of their volume ratios which can be determined using the phase diagram. There are two types of volume ratio: the stability ratio, and the relative difference. These can be worked out using a phase diagram using the following equations, assuming the point O represents the origin of the phase diagram (Salamanca et al., 1998):

$$\text{Stability Ratio} = \frac{DE}{DO} \quad (2.1)$$

$$\begin{aligned} \text{Relative Difference} &= \frac{DI}{IB} \\ &= \frac{DI}{IA} \end{aligned} \quad (2.2)$$

### 2.1.6 ATPE Process Operation

ATPE can be operated in two ways:

1. A two-phase system is mixed and allowed to separate
2. A single-phase system is altered to form two phases and allowed to separate

Overwhelmingly, ATPE is operated by mixing a two-phase system and allowing it to separate; most of this report assumes that the system is operated as such and this type of operation is discussed throughout. This form of operation is the only option for most traditional LLE systems as they are completely immiscible. As a result, the conditions required for single-phase formation, if there are any, are extreme and unusable. However, for ATPE, semi-miscible phases are formed with conditions to form a single phase readily achievable at room temperature and pressure. This means that the operation through shifting a single-phase system to a two-phase system is easily attainable.

Operation of ATPE has been explored through the use of thermoseparating polymers. In these systems, a temperature increase above a critical point will force a phase shift from a single phase to a bottom polymer-rich phase and a top water-rich phase (Ferreira et al., 2008). This type of system is useful in a multi-stage extraction, where in the first step normal ATPS are used for extraction of the target into the polymer-rich phase. A temperature increase is then used to extract the target protein into the water-rich phase so that the thermoseparating polymer can be recycled (Li et al., 1997; Kepka et al., 2004). This is a cheaper, more sustainable process which is easier on the downstream processes.

The use of temperature to alter the system equilibrium can be of some concern for protein purification as biomolecules are sensitive to temperature changes.

However, shifts in equilibrium can be achieved with very small temperature changes at room temperatures. Furthermore, some molecules are stable at higher temperatures, for instance, [IgG](#) (the biomolecule which accounts for the largest proportion of biopharmaceutical revenue) has been found to be stable up to a temperature of around 55°C ([Vermeer and Norde, 2000](#)). [Indyk et al. \(2008\)](#) showed that once [IgG](#) has been freeze dried, there is no effect from the heat treatment on the molecule.

Phase shift operation has also been used to study systems. [de Belval et al. \(1998\)](#) used a temperature increase to manipulate system equilibrium in [PEG-salt](#) systems. In this study, the effect a system's [Tie Line Length \(TLL\)](#) had on the protein partitioning was evaluated, in particular systems which were close in composition to the critical point. It was found that using a temperature control to alter the [TLL](#) produced less error than altering the system composition. This was because very small changes in composition alter the [TLL](#) when the system is close to the critical point ([de Belval et al., 1998](#)).

### 2.1.7 Equipment Design

Typically, [ATPE](#) is operated using a system that forms two phases which is mixed and then allowed to separate. The system operation is performed in either a gravity settler or a centrifuge. Gravity settlers are simpler to scale up and less expensive as they require less energy to operate ([Kaul et al., 1995](#)). The scale up of systems in a gravity settler is related simply to the height of the system and can be evaluated through the kinetics; the kinetics are discussed later in this thesis. [Kaul et al. \(1995\)](#) carried out studies on scaling up [PEG 4000-phosphate](#) systems from 5 g to 1300 g and determined that the kinetics of the system are independent on the horizontal area of the system. In terms of equipment designs for the continuous operation of [ATPE](#); there are three main types ([Espitia-Saloma et al., 2014](#)):

- Column Contactors
- Mixer-Settler Units
- Other Contactors

Out of the three types, column contactors have had the most success in the chemical processing industry and have therefore been studied most extensively. There are multiple different types of column contactors including:

- Pulsed Cap Columns
- Spray Columns

- [Perforated Rotating Disk Contactors \(PRDC\)](#)
- Packed Columns
- Sieve Plate Columns
- Vane Agitated Columns

The major difference between these columns is how the mass transfer is facilitated and the promotion of the phase mixing. These columns experience the following problems with their operation ([Espitia-Saloma et al., 2014](#)):

- Time to reach steady state
- Back mixing
- Flooding
- Emulsification
- Poor phase separation
- Complexity of the device

These problems are experienced to a greater degree in [ATPE](#) than in traditional [LLE](#) because of both the small density difference between the phases and because the phases are so similar (both phases have water as the solvent). This means that the phase separation / time to reach steady state can be slow, particularly in tall columns. The low density difference also contributes to the systems experiencing back mixing if the feed velocities are too high. An emulsion forms in columns where the phase dispersion mechanism creates globules which are too small.

Together, these disadvantages mean that operating columns for [ATPE](#) can be difficult. Despite this, they have been used successfully; [Rosa et al. \(2011\)](#) used a packed column to continuously purify [IgG](#) from [CHO](#) cell supernatant. A yield of 85% of the target protein was achieved with 85% of protein contaminants and 50% of the total contaminants in the system were removed.

Another widely used type of separation equipment in the chemical industry for [LLE](#) are mixer-settler batteries. These are simple, scalable, and cheap systems with low energy requirements that are easy to clean. They do require systems which separate easily with rapid separation rates. Mixer-settler batteries have been used with success for [ATPE](#); [Rosa et al. \(2013\)](#) used a multi-stage counter-current [PEG-salt ATPE](#) to purify [IgG](#) from [CHO](#) cell supernatant. A yield of 80% of the target protein was achieved with a purity of 99%.

**Counter-Current Chromatography (CCC)** columns offer a further equipment option to consider that use centrifugal force. There are two categories of **CCC** columns: hydrostatic columns and hydrodynamic columns. In both columns, a stationary phase is created by holding the denser liquid phase in geometrical channels by a centrifugal force and the lighter mobile phase is pushed through the stationary phase. Hydrostatic columns use a pump to push the mobile phase, whereas hydrodynamic columns utilise an Archimedean screw effect (Mekaoui et al., 2012).

**CCC** columns allow for a large number of extraction steps (over 250 theoretical steps) and are scalable. However, with **ATPE**, there are some problems with retention of the stationary phase, particularly in hydrodynamic columns. In hydrodynamic columns, often under 20% of the volume of liquid stationary phases is retained in the **CCC** column over the column volume (Mekaoui et al., 2012). Such a low stationary phase retention does not allow for satisfactory protein separation. Low retention of stationary phases arises because of the low density difference between the phases and low interfacial tension. To improve the density difference between the phases, work has been carried out by Ruiz-Angel et al. (2007) to develop **ATPE** which uses room temperature ionic liquids as a second phase instead of a polymer like **PEG**. This still limits the types of systems that can be used with this equipment which can conflict with system selection for a desirable protein purification. For instance, in order to maximise the density difference between the phases, a lighter polymer (400-1000 MW) should be selected; however, successful purification of **IgG** has mostly been achieved with heavier polymers around 4000 MW. Despite these challenges, **Centrifugal Partition Chromatography (CPC)** has been used to successfully purify lysozyme from myoglobin by Sutherland et al. (2011).

## 2.2 **ATPS Behaviour**

### 2.2.1 Overview

**ATPS** form semi-miscible phases when sufficient concentrations of phase forming material (polymer(s)) and / or salt(s) are used in water. These phases separate due to the polarity of the phases, and it has been shown by Albertsson (1986) that up to 18 phases can be seen in a single system. However, two phases are often used for practicality to partition proteins. In this type of two-phase system, one phase is considered the relatively hydrophilic phase and one the relatively hydrophobic phase. For instance, in a **PEG**-salt system, the salt-rich phase would be considered the hydrophilic phase, and the **PEG**-rich phase the hydrophobic phase. When protein, solutes, or cells are added to a system, they will preferentially partition into one of the phases because of the properties of the protein and the system conditions.

The system conditions can be manipulated to change the protein partitioning. This means that the system can be used as a separation technique. This section describes the variables and theory behind both the system and protein behaviour.

### 2.2.2 Comparison to Traditional [LLE](#)

[ATPE](#) can be compared with and operates similarly to more traditional [LLE](#) techniques, i.e. aqueous-organic systems, which is an established process in the chemical industry. Some parallels can be drawn between the two processes which mean the field of [ATPE](#) can benefit from the more mature field of traditional [LLE](#). It is also helpful to recognise the differences between the two processes when drawing comparisons. A comparison between the two different systems is detailed in [Table 2.2](#).

The first major variance is that two different immiscible solvents are used in traditional [LLE](#), one phase is aqueous and the other is organic. In these systems, charged solutes will partition to the aqueous phase and non-charged solutes will partition to the organic phase. In [ATPE](#), only a single solvent (water) is used, and the phases separate as a result of the phase forming constituents.

This has a knock on effect in its behaviour; for instance, in a [PEG-salt](#) system, the phases partition partially because of the relative hydrophobicity of the [PEG](#)-rich phase relative to the salt-rich phase. Solutes and particulates added to this system will then partition only partially because of their polarity. Whereas in traditional [LLE](#), non-polar solutes partition to the more hydrophobic phase, and polar solutes partition to the more hydrophilic phase. More detailed theories behind the partitioning of phases and solutes in [ATPE](#) are discussed in more detail in a later section.

In [ATPE](#), the phases are partially soluble in one another as the solvent is the same for both phases. Therefore, a critical concentration of phase forming constituents are required for multi-phase formation. This is not true for aqueous-organic systems as immiscible phases are used and single-phase systems would be difficult to achieve.

In [ATPE](#), there is very little difference in the density of the phase as a result of most of the phases consisting mostly of water. The similarity between the phases and aqueous environment is what makes [ATPE](#) so suitable for protein purification ([Merchuk et al., 1998](#)). This is also what makes the separation of the phases so difficult and slow. Proteins have a low solubility in organic media and the harsh conditions of traditional [LLE](#) mean that protein would be damaged and make aqueous-organic systems unsuitable for protein separation ([Huenupi et al., 1999](#)).

<b>Traditional LLE</b>	<b>ATPE</b>
Two solvents: An aqueous and an organic phase (for example toluene and water).	One solvent: Water is the only solvent, phase forming constituents are used to form the phases (for example PEG and phosphate).
Phases are generally immiscible or sparingly soluble in each other.	Phases are semi miscible: Phases are partially soluble in each other, and a high enough concentration of phase forming constituents is required to form more than one phase.
Solute partitioning a result of polarity or ligand affinity: Charged / polar solutes to the aqueous phase, non-charged / non-polar solutes to the organic phase.	Solute partitioning is partially a result of the relative hydrophobicity: Solutes partition due to many reasons which are discussed in the next sections, but generally polar solutes move to the more hydrophilic phase and the non polar solutes more to the more hydrophobic phase.
Solute partitioning manipulated through manipulating the solutes charge(for example complexing agents, reducing agents, etc) or ligand affinity.	Solute partitioning manipulated through system conditions: for example PEG molecular weight, pH, temperature. Partitioning can be influenced through affinity interactions. This is discussed in more detail in later sections.
Unsuitable for protein separation: Organic phase contains no / very little water, which would damage the protein.	Suitable for protein separation: As the solvent for both phases is water, this provides a suitable, gentle extraction environment for protein.

Table 2.2: A comparison between traditional LLE and ATPE (Albertsson, 1971; Seader et al., 2006).

### 2.2.3 Phase Separation

In [ATPE](#), there is an incomplete understanding of the mechanisms behind the phase separation and the mechanisms are different in polymer-polymer and polymer-salt systems. However, there are some commonalities between these two systems and it is known that phase separation is a result of how the phase forming components interact both with each other and with water ([Huddleston et al., 1991](#); [Cabezas, 1996](#)). It is theorised that there are three stages of separation:

1. For dilute solutions of polymers, there are many layers of solvent separating the individual polymer molecules. As the polymer concentration approaches zero, there is no interaction between the phase forming components. At this point, the system is a truly homogeneous phase and there is no phase separation at any level ([Dobry and Boyer-Kawenoki, 1947](#)). The concentration range for which this holds true is dependent on the properties of the phase forming components, and is likely only true for low concentrations.
2. It has been theorised by [Dobry and Boyer-Kawenoki \(1947\)](#) that there is an intermediate stage between a truly homogeneous system and systems which have multiple phases at a macroscopic level. [Dobry and Boyer-Kawenoki \(1947\)](#) suggested that in this intermediate stage, the different molecules begin to weakly interact with each other and this interaction leads to phase separation at the microscopic level. This phase separation cannot be observed by eye and the system will still appear as a single phase at the macroscopic level. This is supported by the need for dilutions of phases by 1-4 times their weight with water when separated phases are analysed in a UV-visible spectrophotometer as the microscopic phase separation interferes with readings ([Albertsson, 1971](#)).
3. At higher polymer concentrations, the polymers form a mesh or lattice-like structure ([Cabezas, 1996](#)). These structures grow as the polymer concentration increases. In systems with more than one polymer phase, there is an incompatibility between some types of polymers. This results in separate mesh structures and therefore multiple polymer phases as they separate due to steric exclusion ([Asenjo and Andrews, 2011b](#)). There is also an incompatibility between polymers and inorganic salts. The mechanism is unclear, however, it is related to the hydration of the salts and the Hofmeister series ([Ananthapadmanabhan and Goddard, 1987](#)). As the salt concentration increases, more water is required to dissolve the salt as the salt captures the water. This happens in conjunction with the polymer lattice formation in the polymer-rich phase ([Asenjo and Andrews, 2011b](#)). Eventually, it becomes more energetically

favourable to form two phases.

#### 2.2.4 Protein Behaviour

In [ATPE](#), a feed is often complex but can contain a mixture of cells, cell debris, organelles, protein, particulates, and solutes. When a feed is added to a system, it will partition between the phases. Generally, more hydrophilic or charged components partition to the salt-rich bottom phase and more hydrophobic or neutral components partition to the [PEG](#)-rich top phase ([Harris, 1989](#)). The partitioning behaviour of a component (cells, cell debris, organelles, protein, particulates, and solutes) within a system is dependent on the properties of the component and the system itself; component properties which should be considered are ([Harris, 1989](#); [Albertsson, 1986](#); [Asenjo and Andrews, 2011b](#); [Grilo et al., 2016](#)):

- Size ([Luechau et al., 2009](#))
- Hydrophobic character ([Andrews and Asenjo, 2010](#))
- Electrochemical potential ([Asenjo and Andrews, 2011b](#))
- Bio-specific affinity ([Ruiz-Ruiz et al., 2012](#))

Separation based upon size is usually for larger components such as proteins, organelles, and cells. The separation is based upon the surface area and size of the component. The partitioning is a result of the ‘free volume effect’; the volume available for the components in each phase is strongly affected by the steric effects of the phases forming constituents. When this effect is too great, larger particles like protein, organelles, or cells will partition to the horizontal interface, rather than one of the phases as there is not enough free volume available in either one of the phases. For smaller compounds, this effect has a much lower influence on the partitioning.

Separation based upon the hydrophobic character of a component refers to protein partitioning; this is based upon a protein’s 3D structure and the hydrophobicity of surface amino acids ([Asenjo and Andrews, 2011b](#)). The relative hydrophobicity of the phases is dependent on the nature of the phases used in the system. While all phase forming constituents in an [ATPS](#) are hydrophilic, one is considered to be hydrophobic relative to the other phase forming constituent. For instance, in a polymer-salt system, the polymer-rich phase would be hydrophobic relative to the salt phase because the polymer’s hydrophilic functional groups are confined to the extremes of the molecule, whereas the rest of the molecule would be hydrophobic (as long as a hydrophilic side chain is not present). In comparison, the salt-rich phase will readily capture the water in the system. A protein which has lots of hydrophobic

surface amino acids will favour the relatively hydrophobic phase and a protein with lots of hydrophilic surface amino acids will favour the relatively hydrophilic phase.

Separation based on electrochemical potential is a result of the charge of a component determining the partitioning. The use of charged phase forming consistent (NaCl which dissociates within the system) has been shown to significantly increase the separation of protein which was positively charged; it was suggested this was a result of NaCl increasing the negativity of the PEG-rich phase ([Andrews et al., 2005](#); [Asenjo and Andrews, 2011b](#)). A proteins charge can be manipulated through the use of its isoelectric point and other components expected within a system are also charged, for instance, DNA which is negatively charged.

Lastly, affinity ligands with biospecific affinity to a protein will affect the partitioning of that protein. Ligands have been used in systems as free ligands and coupled to a phase forming component (usually to PEG) to increase system selectivity ([Benavides et al., 2011](#)). Affinity interactions have also been suggested as a mechanism of partitioning between a biomolecule and the PEG ([Luechau et al., 2009](#)).

There is disagreement between the most respected authors in the field of ATPS over which mechanism is driving the partitioning of molecules in systems ([Grilo et al., 2016](#)). [Luechau et al. \(2009\)](#) concluded that the partitioning of nucleic acids in PEG-phosphate systems could be described using the excluded volume theory. However, the work of [Andrews and Asenjo \(2010\)](#) uses hydrophobic interactions to explain partitioning. Other works conclude that hydrophobic interactions should be used to explain the partitioning in systems using higher molecular weight PEG, but not lower molecular weight PEG. [Rocha and Nerli \(2013\)](#) found that partitioning of bromelain in PEG 600-citrate and PEG 1000-citrate systems could not be explained by either the molecular weight or the isoelectric point of the enzyme. They proposed that there was some affinity interaction between the low molecular weight PEG and bromelain. Other prominent authors such as Aires-Barros and Azevedo conclude that systems generally will be dependent on all of the above interactions, and in some cases there can be a synergistic effect ([Grilo et al., 2016](#)).

One way to explain behaviour is that the partitioning behaviour is more dependent on different interactions for different types of system. For instance, a standard PEG-salt system with small solutes in would be primarily partitioned based on the electrochemical potential or hydrophobic interactions (for a small protein). If larger proteins were added, the partitioning would be still dependant on the hydrophobic character of the system but would also be largely dependent on the excluded volume theories. A more specialist system such as ATPAP with protein A ligands used to partition IgG from contaminants would be mostly dependant on affinity interactions

of the [IgG](#) and the protein A ligands.

### 2.2.5 System Variables

System variables are system properties or environmental conditions that can be manipulated to change partitioning. These include ([Harris, 1989](#); [Albertsson, 1986](#)):

- Type of polymer
- Polymer molecular weight
- Type of salt
- Concentration of phase forming constituents
- System pH
- Use of additional salt
- Use of additional ligands
- Temperature

The different properties of the protein / components within the system can be manipulated with the above variables in order to facilitate separation.

If the governing mechanism to facilitate separation is size dependency, then the steric effects of the phase forming components should be considered ([Asenjo and Andrews, 2011b](#); [Ananthapadmanabhan and Goddard, 1987](#)). Variables which can be manipulated include: molecular weight of polymer, concentration of polymer, inclusion of a branched polymer, and ionic strength of salt. Increasing polymer molecular weight, polymer concentration, or ionic strength of salt will result in the reduction of free volume available. Inclusion of a branched polymer generally increases the free volume available.

In terms of the hydrophobic effects of the system, there are two known mechanisms: the hydrophobicity, and the salting out effect. With regards to the former, the polymer phase becomes more hydrophobic as the polymer molecular weight or concentration increases. It should also be noted that as phase forming constituent concentration increases, water concentration decreases. This leads to a decrease in free water. High concentrations of additional salts, such as NaCl, would affect free water through the salting out effect. The salting out effect can also be considered through the Hoffmeister series ([Ananthapadmanabhan and Goddard, 1987](#)). Both of the above mechanisms result in hydrophobic molecules favouring the more hydrophobic phase. For phases relative hydrophobicity, it is dependent on both the concentration and chemical properties of the phase forming constituents.

The electrochemical dependency of a protein can be manipulated through its isoelectric point by altering the pH of the salt phase. If the isoelectric point of a protein is below the pH of the system, it will push the protein towards the PEG-rich phase. The isoelectric point of the protein is the point at which the protein's net charge is equal to zero and is therefore the point at which a protein is least soluble in a hydrophilic phase. A protein's charge is negative when a systems pH is above the protein's isoelectric point and is positive when a systems pH is below it. Less free water is available in systems with a higher pH salt-rich phase, which pushes the target protein out of the salt-rich phase. The use of charged phase forming constituents can also then be used to manipulate partitioning (Andrews et al., 2005).

From this information, these variables can be tied to the mechanisms described in the previous section; examples for a PEG-salt system are shown in Tables 2.3 and 2.4.

## 2.3 Kinetics of Phase Separation

### 2.3.1 Overview

The operation of ATPS can be achieved using two different approaches; either by changing the system from a single-phase system to a two-phase system, therefore by initiating phase separation, or by mechanically mixing a two-phase system and then allowing it to separate (Sawant et al., 1990). A change from a single-phase system to a two-phase system can be achieved through either the addition of phase forming components or change in system conditions, for example, an increase in temperature or pH. However, a phase-shift method of operation is not commonly used. Mostly, a system which forms two-phases is selected and the conditions of the system selected are kept constant. This system is then mechanically agitated so that the solutes can transfer between the phases and the phases are left to separate. This is the preferred operational method and also the method used in the operation of traditional LLE. A system which is defined as being in equilibrium has two separated phases. For a separated system, the two phases will be separated by a distinct horizontal interface and there will be no net change in the composition of the phases (Tidhar et al., 1986).

In ATPE, the separation of the phases is a time dependant process in which the mechanism for phase separation is the same for all types of systems (Kaul et al., 1995). For a separating system, there will be a continuous phase and a dispersed phase. In the continuous phase, globules of the dispersed phase form at the coalescence front and rise or sink (depending on the continuity of the phases) towards

<b>System Variable</b>	<b>Effect on system</b>	<b>Effect on partitioning</b>	<b>Mechanism(s) responsible</b>
Use of hydrophobic branched polymer	Increase in hydrophobicity of polymer phase  Change in steric effects of polymer in polymer phase	Increase attractiveness of polymer phase to hydrophobic protein and decrease for hydrophilic protein Change in available free water in polymer phase	Hydrophobicity effects  Size exclusion theory
Increase polymer molecular weight	Increase in hydrophobicity of polymer phase  Increase in steric effects of polymer in polymer phase	Increase attractiveness of polymer phase to hydrophobic protein and decrease for hydrophilic protein Decrease in available free water in polymer phase	Hydrophobicity effects  Size exclusion theory
Increase in polymer concentration	Increase in hydrophobicity polymer of phase  Increase in steric effects of polymer in polymer phase	Increase attractiveness of polymer phase to hydrophobic protein and decrease for hydrophilic protein Decrease in available free water in polymer phase	Hydrophobicity effects  Size exclusion theory
Increase in salt concentration	Salt phase captures more water  Increase salting out effect in salt phase	Decreases systems ability to partially hydrate protein Salts protein out of phase	Hydrophobicity effects

Table 2.3: Equating mechanisms and variables in [PEG-salt ATPS](#)

<b>System Variable</b>	<b>Effect on system</b>	<b>Effect on partitioning</b>	<b>Mechanism(s) responsible</b>
Increased salting out ability of salt	Salt phase captures more water  Increase salting out effect in salt phase	Decreases systems ability to partially hydrate protein Salts protein out of salt phase	Hydrophobicity effects
Use of additional NaCl	Increase salting out effect in salt phase  NaCl dissociates and splits between the phases ( $Na^+$ into the salt phase, $Cl^-$ into the polymer phase)	Salts protein out of salt phase;  Increases separation of charged particles	Hydrophobicity effects  Electrochemical effects
Increase in pH	Decrease in available free water in salt phase	Shift in pH changes charge on protein and alters solubility in phases	Hydrophobicity effects
Increase in temperature	Increase in <a href="#">TLL</a>  Increase in relative hydrophobicity of phases	Decrease in available free water Increase attractiveness of polymer phase to hydrophobic protein and decrease for hydrophilic protein	Size exclusion theory Hydrophobic effects
Use of ligands	N/A	Attract protein to polymer phase if ligand is attached to polymer backbone Create new compound which has a different solubility altering partitioning	Affinity interactions  Hydrophobicity and Electrochemical effects

Table 2.4: Equating mechanisms and variables in [PEG-salt ATPS](#)

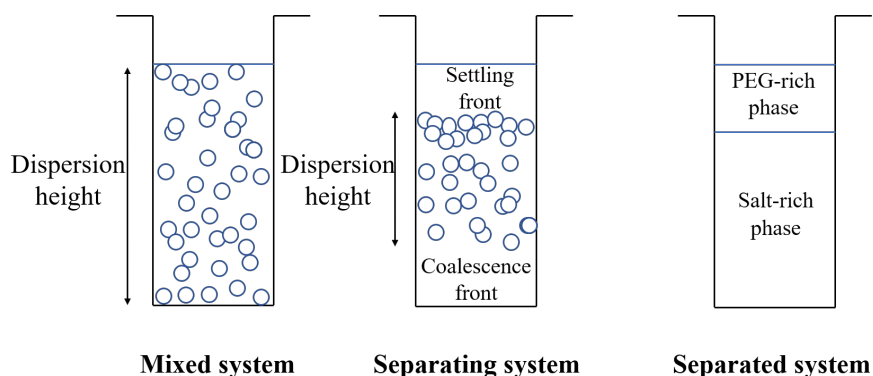


Figure 2.2: A schematic of an [ATPS](#) with a continuous bottom phase undergoing separation.

their native phase. At the settling front, the globules will queue until they coalesce and join their native phase. The settling front is where the horizontal interface will eventually form. The turbid region between the coalescence front and the settling front is described as the dispersion front and the height of the dispersion front is used to measure the separation ([Kaul et al., 1995](#)). This is represented in [Figure 2.2](#). The rate of separation of the phases of [ATPS](#) is measured by the rate of change of the dispersion height. This is measured by eye in a graduated tube. A phase diagram can be used to determine the continuity of the phases, this is shown below in [Figure 2.3](#).

### 2.3.2 Mechanism

During phase separation, there are two processes happening: globule coalescence, and globule rise or fall ([Kaul et al., 1995](#)). A separating system is dominated by one of these processes. This can be observed at eye level; a system which is seen to have queuing at the horizontal interface has the rate of separation controlled by the coalescence of the globules. For most [ATPS](#), this is the rate-controlling process and the queuing at the horizontal interface is characteristic ([Asenjo et al., 2002a](#); [Salamanca et al., 1998](#)). The horizontal interface acts as a barrier between the two phases and globules must have enough energy to pass through this barrier. [ATPS](#) have more similar phases to each other compared with more traditional [LLE](#) systems. This means that the repulsion between the phases is not as great as what is observed in aqueous-organic systems. This effect is so great that [ATPS](#) form semi miscible phases rather than immiscible phases. The rate of coalescence is not well understood, however, it is known to be controlled by both the settler and the system properties ([Jeffreys and Hawksley, 1965](#)).

For a separating globule, there are three forces acting on it: gravity, friction,

and buoyancy. The more dominant force is dependent on the properties of the system. The gravitational force is dependent on the density and size of the globule. The friction and buoyancy forces are dependent on the rheological properties of the system as well as the size of the globule. In [ATPS](#), there is very little density difference between the two phases, however, in [PEG-salt](#) systems there are large viscosity differences between the phases. The viscosity of the [PEG-rich](#) phase is often much greater than the salt-rich phase. This has a large effect on the separation rates of the system which is discussed in more detail in Section [2.3.3](#).

In terms of the coalescence behaviour of globules, these three forces all have an effect on the system, as well as the interfacial tension between the phases both at the horizontal interface and at a globule interface ([Salamanca et al., 1998](#)).

### 2.3.3 Phase Continuity

In a separating [ATPS](#), one of the phases can be observed as being the continuous phase, and the other as the dispersed phase ([Kaul et al., 1995](#)). This can be done by eye by observing the direction the globules travel. For example, a system with a continuous top phase would have globules descending towards the bottom phase and a system with a continuous bottom phase would have globules ascending towards the top phase. The dispersed phase is static and grows in size as globules join it. For a continuous polymer phase, the globule sizes are much smaller than for that seen in a continuous salt phase and are not easily observed without magnification ([Salamanca et al., 1998](#)). The increased viscosity of the polymer phase makes it more difficult for globules of the opposing phase to coalesce and form larger globules, resulting in a smaller average size of globule.

The continuity of the phases is determined by the concentration of phase forming constituents. The fixed concentration at which the phase continuity inverts is called the phase inversion point ([Kaul et al., 1995](#)). This point has been shown to coincide with the critical point and is represented in Figure [2.3](#) ([Merchuk et al., 1998](#)). However, there is an ambiguity where the continuity of the phases is determined by both the system composition and the fluid dynamics of the system ([Merchuk et al., 1998](#)). In this range, it was shown that gentle agitation of a [PEG-salt](#) system led to a continuous bottom phase and strong agitation led to a continuous top phase. As a result, this is sometimes demonstrated on a phase diagrams as a pair of phase inversion lines.

Phase continuity is one of the most important factors in the system kinetics in polymer-salt systems. [Albertsson \(1986\)](#) noticed that above a certain volume ratio, the rate of separation rapidly increases. However, it was [Walter \(1985\)](#) who linked the change in volume ratio to an inversion of the phase continuity. In polymer-salt

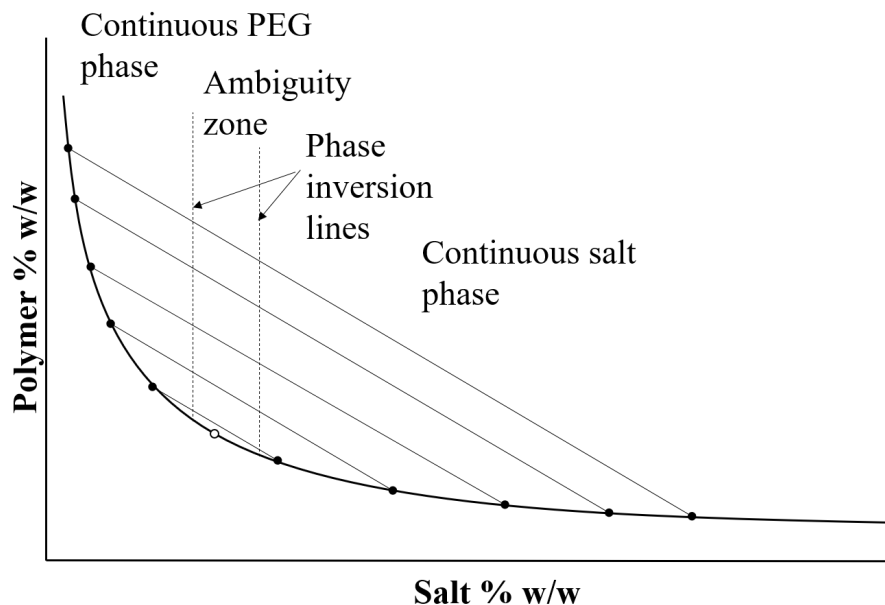


Figure 2.3: A typical representation of a binodal curve which shows the phase inversion point.

phases, the bottom, salt-rich phase is much less viscous than the top, polymer-rich phase. As a result, when the bottom phase is continuous, the phase separation happens at a much faster rate (Kaul et al., 1995; Salamanca et al., 1998; Asenjo et al., 2002a). This is a result of globules moving through a phase with low viscosity will experience less friction than those moving through a more viscous phase. Globules in a less viscous phase will also be able to coalesce more easily as the interface surface tension would be lower. This results in larger globules which move more rapidly through the phase and coalesce more quickly at the horizontal interface.

In ATPS, the coalescence of globules at the horizontal interface has been observed as the rate determining process for the phase separation in many systems (Asenjo et al., 2002a; Salamanca et al., 1998). Kaul et al. (1995) suggest that globule coalescence in ATPE is thought to be largely dependent on the interfacial tension of the system. It is known that larger globules have a lower surface charge and therefore experience less electrical repulsion which speeds up the rate of coalescence at the horizontal interface (Salamanca et al., 1998). Salamanca et al. (1998) observed that smaller globules form in systems with continuous PEG-rich phases which correlates with slower separation rates for systems with continuous PEG-rich phases. It is also known that coalescence rates are dependent on liquid composition; deionised water is known to coalesce at much faster rates than water containing salts (Doran, 2013). Polymer-salt systems contain very high concentrations of salts (as well as polymers)

and can be very slow to separate and coalesce. [Salamanca et al. \(1998\)](#) showed that systems which sit on intermediate sections of the binodal with a high enough salt concentration to have a continuous salt-rich phase have the fastest separation rates. This correlates with the lowest concentrations of salt (and polymer) possible to have a continuous bottom phase, therefore resulting in the fastest separation rates.

#### 2.3.4 System Properties and Phase Separation

The type of system has a large effect on the rate of separation of a system. Polymer-salt systems have much more desirable kinetics than polymer-polymer systems. This is a result of the lower viscosity of the salt phase in the polymer-salt systems resulting in faster separation times ([Hart et al., 1994](#)).

Rate of separation can also be linked to a systems binodal curve in terms of both types of volume ratios: stability ratio, and relative distance ([Salamanca et al., 1998](#)). PEG-sulphate systems were used to show that the rate of separation is faster for systems with smaller relative distances. Systems with small relative distances sit in intermediate positions on the binodal curve. For systems with small relative distances, an increase in TLL will increase the separation rate ([Asenjo et al., 2002a](#)). It is theorised that this is a result of an increase in difference between the phases, making the separation easier.

[Salamanca et al. \(1998\)](#) showed that systems with large volume ratios have a ‘lag’ phase in the separation during which time there is little change in the dispersion height. Systems with larger volume ratios sit in the extremes of the binodal curve and have higher concentrations of phase forming constituents. This results in a higher interfacial tension at the horizontal interface and an increase in viscosity for those systems with higher concentrations of a polymer ([Kaul et al., 1995](#)).

The use of additional salt, NaCl, was shown by [Asenjo et al. \(2002a\)](#) to have a negligible effect on the viscosity of the system. However, it has been observed to decrease the separation rate [Kaul et al. \(1995\)](#). It is theorised this would be the same for all additional salts.

#### 2.3.5 Effect of Protein

The introduction of protein into a system can affect the system’s behaviour both in terms of the separation and kinetics. This is particularly the case if the target is large, for instance, large proteins or cells ([Asenjo et al., 2002a](#)). It is thought this is because the protein interacts with the phase forming constituents and alters the system behaviour. The addition of protein also alters the density difference between the phases and hence the rate of separation ([Kaul et al., 1995](#)).

## 2.4 Modelling Approaches

### 2.4.1 Overview

The optimisation of [ATPE](#) processes is often achieved through experimental ‘trial and error’ based on individual expertise. This is due to the lack of understanding of the behaviour of systems and a large number of parameters which control the behaviour. The optimisation of [ATPS](#) is vital in order to meet the desired purity and yield requirement; however, this can be both time consuming and expensive with no guarantee that the experimentation will yield the required results. In an effort to overcome the learning curve of researchers and engineers who are new to the process, there have been papers published by experts in the field detailing ‘practical guidelines’ in system selection and design ([Benavides and Rito-Palomares, 2008](#)). While these rules generate a starting point in system selection, there are still many parameters to be tested. It has been suggested that high throughput robotic-aided strategies could be employed to enable this number of parameters to be tested quickly ([Bensch et al., 2007](#)). However, this approach would drastically raise capital and operating costs. There have been attempts to offset the material costs of high volume testing by using miniaturized microfluidic platforms ([Bras et al., 2017](#)). The alternative approach is to use modelling strategies to understand the system behaviour and therefore reduce the experimental workload.

Mathematical models are used in several ways to describe [ATPS](#) and their use as an extraction process:

- Equilibrium modelling
- Kinetics modelling
- Mixing modelling

The equilibrium modelling is used to describe the phase separation and protein partitioning of the system. In this type of modelling, some models are there to describe the separation and others are used to predict the partitioning of the system. These are used to design system extraction protocols which have satisfactory yields and purities. The kinetics modelling is used to describe the rate of the phase separation and is used in both system selection and in the design of appropriate equipment. Modelling of the mixing of the phases is less extensively studied as it is considered easier to achieve appropriate mixing conditions; however, it is considered in the equipment design.

This following section goes through each of these types of modelling in more detail.

### 2.4.2 Modelling Partitioning

The partitioning of a protein in an [ATPS](#) can be described by the protein partitioning coefficient,  $K$  ([Albertsson, 1971](#)):

$$K = \frac{C_{Top}}{C_{Bottom}} \quad (2.3)$$

Where  $C_{Top}$  is the concentration (mg/mL) of the protein partitioned to the top phase when the system is at equilibrium and  $C_{Bottom}$  is the concentration (mg/ mL) of the protein partitioned to the bottom phase when the system is at equilibrium.

$K$  can also be described in terms of the partitioning factors ([Albertsson, 1971](#)):

$$K = K_0 \cdot K_{hfov} \cdot K_{el} \cdot K_{biosp} \cdot K_{size} \cdot K_{conf} \quad (2.4)$$

Where the partitioning is a result of the hydrophobicity ( $K_{hfov}$ ), the electrochemical potential ( $K_{el}$ ), the molecular size of the protein ( $K_{size}$ ), the biospecific affinity ( $K_{biosp}$ ), the conformation of th protein ( $K_{conf}$ ) and any other factors ( $K_0$ ).

While the partitioning of protein is described as a function of the top and bottom phase concentration, [Andrews and Asenjo \(1996\)](#) found that it was common for protein to partition into the horizontal interface of a system. They found that true partitioning between the top and bottom phase of a system was only ever true at very dilute protein concentrations, although some systems experience partitioning into the horizontal interface even at very dilute protein concentrations. Furthermore, [Asenjo and Andrews \(2011b\)](#) state that protein partitioning is known to change as protein concentration increases.

### 2.4.3 Phase Equilibrium Modelling

While the previous two sections are also concerned with representing system equilibrium, this section looks at the modelling surrounding the partitioning theories. However, there is no single underpinning theory to describe the partitioning of [ATPS](#). As a result, there are a number of modelling approaches. Typically, each of these models is most applicable to a different range of conditions, and the models deviate from experimental data outside of these conditions. [Cabezas \(1996\)](#) described four general modelling approaches:

- Osmotic Virial Expansions
- Extensions of the Lattice theories, i.e. the Flory Huggins Theory
- Integral Equation Theory

- Other Approaches, i.e. Group Contribution Schemes, Excluded Volume Approximations

The main way these theories differ is in their assumptions surrounding the mechanisms for phase separation. Osmotic virial expansions assume phase separation is primarily a result of the properties of water, whereas lattice theories assume separation is primarily a result of the lattice formation of polymers. Integral equation theory combines these two assumptions (Zaslavsky, 1995). As a result of the differences in the underlying assumptions, these models are only suitable for particular phase forming constituent types and concentration ranges; these generally differ for the different models. As osmotic virial expansions assume phase formation is a result of the properties of water, they are most applicable to ATPS with a dilute polymer concentration. As more concentrated regimes of polymers are used, higher order terms are required to account for the increased solute interaction within the system. This is particularly true of polymer-salt systems which require higher concentrations of phase forming polymers to form two-phase systems. Lattice theories are most appropriate for concentrated polymer regimes. Johansson et al. (1998) successfully predicted the partitioning of several proteins in PEG-dextran systems using lattice theories, including serum albumin and phycoerythrin. However, Zaslavsky (1995) states that this model is inappropriate for polymer-salt ATPS because the strong salt-water and some of the salt-polymer interactions mean that it cannot be assumed that the salt has no effect on the polymer-water interactions.

A more sophisticated method to modelling partitioning behaviour of ATPS is the integral equation theory which combines different models using a statistical approach. This procedure was used by Kenkare and Hall (1996) to describe the partitioning of PEG-salt systems. The model aimed to describe the effect temperature has on the equilibrium conditions of PEG-salt ATPE. The model was partially successful. Firstly, it was able to predict that increasing salt concentration lowered the temperature at which the phases separate. Secondly, it was able to predict that increasing temperature and increasing PEG molecular weight increases the size of the biphasic region. Lastly, it was able to determine that increasing the anion charge of the salt decreases the salt concentration at which separation occurs. However, there were some deviations when the model was compared with the experimental data, for instance, the salt concentrations in each phase at equilibrium. This was attributed to the assumption the model makes that the ion-solvent interactions were unimportant.

Another way to use equilibrium modelling is in process optimisation. In terms of process optimisation of conditions, it has been estimated that there are over one billion possible systems to explore for any given separation problem (Selber et al., 2000;

Torres-Acosta et al., 2019). There are also difficulties in mathematical handling of the experimental data of ATPS as it is prone to having large errors associated with it (Selber et al., 2000). As a consequence, models need to be sufficiently robust to handle large data errors, as well as being capable of exploring a large area for solutions. This means there is still an opportunity for improvement in the area of predictive modelling. Currently, common strategies for optimisation are univariate optimisation and Response Surface Methodology (RSM). Univariate optimisation is a commonly explored strategy which involves a simple and methodical approach to optimise a single parameter at a time. It has been used with success for multiple proteins including: invertase, B-phycoerthrin, C-phycoerythrin, and lutein (Akardere et al., 2010; Karkas, et al., 2012; Benavides and Rito-Palomares, 2008). While this method can be highly valuable, the optimum conditions may be missed as only a single parameter can be evaluated at a time. RSM provides the opportunity to explore multiple parameters to obtain optimum conditions. It uses a statistical approach which evaluates an experimental study where several parameters are varied. The results are then reduced to a 2<sup>nd</sup> order model so that an optimum can be calculated. This has been used in a wide range of applications within the scope of ATPE including for the recovery of monoclonal antibodies and enzymes (Azevedo et al., 2007; Alhelli et al., 2016).

#### 2.4.4 Mixing Modelling

ATPS are typically operated through mixing the system and then allowing it to separate. This is the point at which the majority of the mass transfer of solutes and particulates between the phases happens. The mixing is also partially responsible for determining the globules mean diameter; this is also determined by the interfacial tension and hydrodynamic conditions within the mixer. For a stirred mixer, the mixing can be described as a function of the following (Asenjo et al., 2002a):

$$d_d = f(Re, We, t_m) \quad (2.5)$$

Where  $d_d$  is the diameter of the globule,  $Re$  is the Reynolds number,  $We$  is the Weber number, and  $t_m$  is the mixing time.

Due to the low interfacial tension of ATPS, an equilibrium is reached between the globule coalescence and globule break after a relatively short agitation (Kaul et al., 1995; Asenjo et al., 2002a). After this time point, any extra time spent on mixing is not thought to affect the system's behaviour. As a result, the research focus has been on other aspects of the system, such as phase separation and partitioning behaviour.

### 2.4.5 Kinetics Modelling

The simplest way to model the process of sedimentation is to use Stokes' Law. This has been considered by some researchers because the law is applicable if the globules are allowed to travel uninterrupted (Kaul et al., 1995). This assumes that the globules rise or sink towards their native phase undisturbed and if the model is used to describe the separation time, that the time taken for globules to coalesce is negligible. These conditions have only been shown to be met in very viscous systems, where the rise or fall of globules in a system can take hours (Kaul et al., 1995). Generally speaking, the law is not applicable to ATPS for a number of reasons. Firstly, in fast separating systems there are swarms of globules in ATPS which can interact with each other (Kaul et al., 1995). These interacting globules sometimes coalesce meaning that there is a change in globule diameter which affects Stokes' Law. Secondly, globule diameter can also change due to diffusion over time. In order to account for these factors, a globule population balance can be used. However, it would still be expected that there would be differences between the calculated and experimental values. Aside from globule interaction, the rate controlling process for the separation of most ATPS is globule coalescence. This makes Stokes' Law a bad model to use for the process of separation.

The most accepted way to measure the rate of separation of ATPS is to measure the rate of change of the dispersion height; this is represented in Figure 2.4 (Asenjo et al., 2002a). This measurement has been used for both ATPS and aqueous-organic systems and has been used in the modelling of the kinetics of the phase separation of both ATPS and aqueous-organic systems. The model was first established by Golob and Modic (1977) for aqueous-organic systems and is shown below:

$$V_S = v_1 \left( \frac{\mu_C}{\mu_D} \right)^{v_2} \left( \frac{\Delta\rho}{\rho_C} \right)^{v_3} \left( \frac{\sigma}{\sigma_W} \right)^{v_4} \quad (2.6)$$

Where  $V_S$  is the sedimentation velocity ( $m/s$ ),  $\mu_C$  is the viscosity of the continuous phase ( $kg/ms$ ),  $\mu_D$  is the viscosity of the dispersed phase ( $kg/ms$ ),  $\Delta\rho$  is the density difference between the two phases ( $kg/m^3$ ),  $\rho_C$  is the density of the continuous phase ( $kg/m^3$ ),  $\sigma$  is the interfacial tension between the two phases ( $N/m$ ),  $\sigma_W$  is the surface tension of the air-water interface at 20 °C ( $7.28 \times 10^{-2} N/m$ ), and the constants  $v_1$ ,  $v_2$ ,  $v_3$  and  $v_4$  are determined by regression analysis of the experimental data.

In terms of a polymer-salt ATPS, there are two different types of system to be characterised due to the large difference in the viscosity of the phases: a system with a continuous top polymer-rich phase, and a system with a continuous bottom salt-rich phase (Asenjo et al., 2002a).

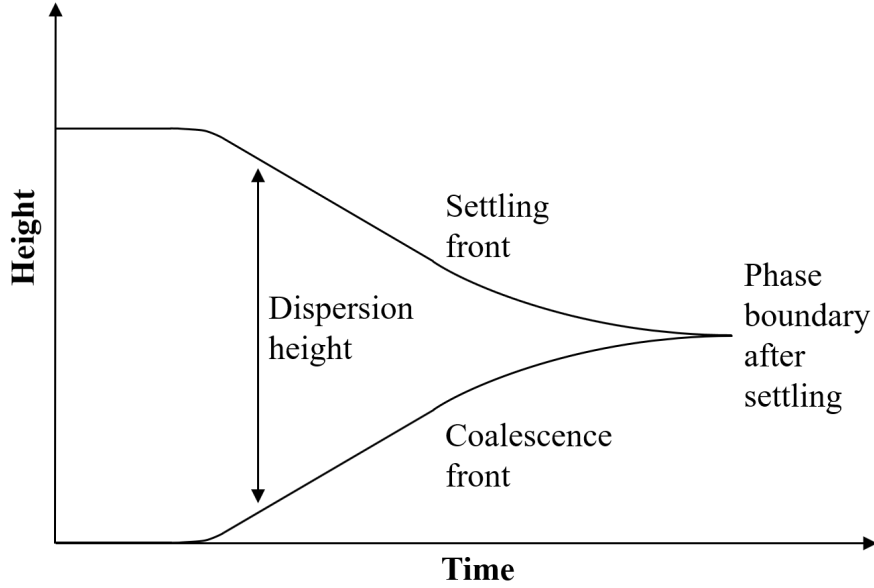


Figure 2.4: A typical representation of a dispersion height graph of a [ATPS](#).

Coefficient	Continuous Top Phase	Continuous Bottom phase
$v_1$	$1.435 \times 10^{-5}$	$2.04 \times 10^{-5}$
$v_2$	2.148	0.144
$v_3$	-1.062	-0.555
$v_4$	-0.971	-0.079

Table 2.5: Coefficients for kinetics equation of [PEG-salt ATPS](#) as determined by [Mistry et al. \(1996\)](#)

Equation 2.6 was then modified by ([Mistry et al., 1996](#)) to measure the rate of separation of [ATPS](#) in terms of the rate of change of the dispersion height of the system to the following:

$$\left(\frac{\delta h}{\delta t}\right)\left(\frac{u_C}{\sigma}\right) = v_1\left(\frac{\mu_C}{\mu_D}\right)^{v_2}\left(\frac{\Delta\rho}{\rho_C}\right)^{v_3}\left(\frac{\sigma}{\sigma_W}\right)^{v_4} \quad (2.7)$$

The coefficients are different depending on which of the phases are continuous, this is shown in Table 2.5. It can be seen from the coefficients that the viscosity of the system plays a much more important role in the phase separation in a system with a continuous top polymer-rich phase. In a system with a continuous bottom salt-rich phase, density is the most important factor in the phase separation. The equation was also modified by [Salamanca et al. \(1998\)](#) to be written to add the terms for the volume ratios (either the relative distance or the stability ratio).

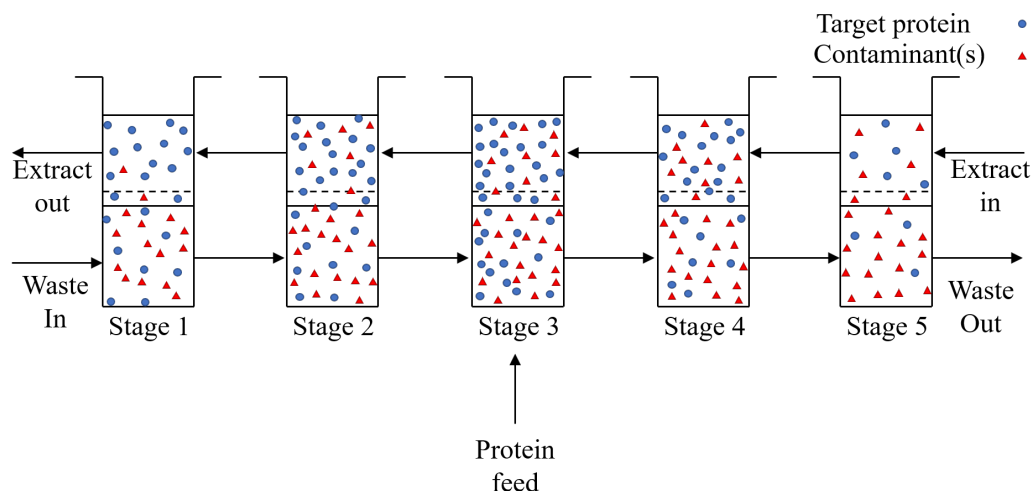


Figure 2.5: A schematic to illustrate a five stage counter-current ATPE with a feed at stage three

#### 2.4.6 Multi-stage Modelling

Multi-stage involves using multiple ATPE in series to improve the resolution of an extraction. A schematic to illustrate a multi-stage extraction is shown in Figure 3.4. For multi-stage modelling for ATPE, there are two approaches. The first is a multi-step approach, and the second is a multi-stage approach. In a multi-step approach, different system conditions are chosen to partition different proteins or move the target protein into a different phase. In the multi-stage approach, the same extraction conditions are used to improve the resolution of the process.

Multi-step extractions have been carried out with success with ATPE. Kroner et al. (1982) successfully used multi-stage ATPE with four sequential systems being used to extract formate dehydrogenase from *Candida boidinii* homogenate. The extractions were carried out in mixer-settlers, and at each step, the following were removed: cell waste, nucleic acids, bulk proteins, and finally salts and remaining proteins. Despite the number of stages, a 70% yield was achieved along with technical grade purity (>70%). The study also compared this purification process with two other processes. The first process was composed of precipitation, centrifugation and three chromatographic steps, and the second process was composed of two ATPE steps, ultra-filtration, and a chromatographic step. The study showed that the multi-stage ATPE was less time consuming and had higher productivities than other possible isolation routes.

Multi-step ATPE has also been used to back extract the target for ease of down-

stream processing. Hummel et al. (1983) carried out a larger scale two-stage ATPE of D-lactate dehydrogenase from *Lactobacillus confuses* homogenate. The first step was carried out at a 120 kg scale using a PEG-salt ATPS in an open stack separator at a flow rate of 60 L h<sup>-1</sup> and was designed to remove cell debris. The top PEG-rich phase containing D-lactate dehydrogenase was then contacted with a second salt phase to back extract the target into the salt-rich phase both for ease of downstream processing and to further purify the product. This step was carried out at a volume of 200 L in a gravity settler which was left overnight.

A lack of predictive design has been recognised as a major weakness in ATPE (Soares et al., 2015). The use and amount of NaCl as an additional salt has been identified as a key performance parameter in protein partitioning, and is often used in multi-step extractions to control extraction and back extraction steps (Rosa et al., 2007; Ahmad et al., 2008; Mao et al., 2010; Patel et al., 2018). As a result of this, a significant proportion of the predictive process modelling in ATPE has been centred around manipulating the system using NaCl concentration of PEG-salt systems (Mistry et al., 1996; Huenupi et al., 1999; Mündges et al., 2015). The initial research conducted by Mistry et al. (1996) used a sigmoidal Boltzmann curve to describe the partition coefficient (log K) of the target protein ( $\alpha$ -amylase) as a function of the NaCl concentration for a system with a large PEG phase. The contaminant partition coefficient remained constant over the varying NaCl concentration. In the first step, a high NaCl concentration was used to extract the target protein into the PEG-rich phase. In the second step, a fresh bottom phase with a low NaCl concentration was contacted with the PEG-rich phase containing the target protein to back extract it into the salt-rich phase. This is done to recycle the more expensive PEG-rich phase and because a salt-rich phase is easier to process downstream. Extensions on this work show that recycling of up to 40% w/w of the PEG-rich phase had little effect on the system performance over ten cycles (Mündges et al., 2015). Lastly, modelling has been used to design control systems for ATPE processes which are run continuously, specifically looking at different volumetric hold ups (Simon and Gautam, 2004).

Other multi-stage techniques involve using multiple stages of the same system in order to improve the low purity and yield typically seen in ATPE. Multi-stage extraction has been used with great success in ATPS; Rosa et al. (2013) used a multi-stage counter-current PEG-salt ATPE to purify IgG from CHO cell supernatant to a purity of 99% and a yield of 80%. A common method for stage-wise optimisation of equilibrium binary separations is McCabe Thiele (Richardson et al., 2002). This was originally used in the chemical industry to determine the required number of stages for binary distillation; an application for which it is still used.

The McCabe Thiele method was modified by [Warade et al. \(2011\)](#) to be suitable for traditional [LLE](#) and has been demonstrated by [Rosa et al. \(2009a,b\)](#) to be suitable for ATPS specifically. In the [Warade et al. \(2011\)](#) study, a single operating line was used to optimise the number of stages for a specified purity in multi-stage counter-current [LLE](#) systems. In the [Rosa et al. \(2009a,b\)](#) studies, a single operating line was also used to determine a required yield rather than a required purity. In all three of these studies, only the target component concentration was used in the models and the contaminants are not considered in the stage-wise determination. In [Rosa et al. \(2009b\)](#), equilibrium curves of different fractions of [CHO](#) cell supernatant were used to predict the success of each fractions extraction from [IgG](#); however, the number of stages was not determined.

## 2.5 Conclusion

This literature review outlines the relevant literature surrounding [ATPE](#) for this thesis. The review begins by looking at the background of [ATPE](#) and its place within the bioprocessing industry. It was found that [ATPE](#) represents an opportunity for a protein purification process which is cheap and geared towards running continuously at a time that the bioprocessing industry is looking to move to a continuous manufacturing process as well as reducing costs. However, the process is not widely accepted within industry due to two major problems with the process: the lack of understanding of the phase forming mechanisms, and the low process resolution. These two problems have meant that the process design is overly reliant on individual expertise and trial and error.

In system design, there are two major criteria which need to be considered: the phase separation rates, and the resolution of the system. Section [2.2](#) focussed on the phase separation behaviour of systems. Currently, there is no one underpinning theory outlining the mechanisms behind phase separation and partitioning. Mechanisms can be divided into four categories: size, electrochemical dependency, hydrophobicity, and bio-affinity, with the dominant mechanism varying between systems and components within the system.

Section [2.3](#) evaluates the literature surrounding the phase separation of the system. In [LLE](#), settler design and the amount of material processed within a system is highly dependent on the phase separation kinetics of a system. In [ATPE](#), the separation rates are measured by eye and the formation of a distinct horizontal interface. Separation rates were shown in the literature to be highly dependent on the system viscosity of the phases and which phase was the ‘continuous phase’.

Section [2.4](#) outlines the modelling approaches within [ATPE](#), for prediction /

evaluation of key performance parameters in phase equilibrium, protein partitioning, phase separation rates and system design. It was found that one practical way of both reducing experimental workload and improving system performance was to use multi-stage extraction.

As a result of the literature review, this thesis focusses on ways to improve system performance while reducing experimental workload. Chapter 4 experimentally evaluates multi-stage extraction in [ATPE](#), looking at if the technique can be used to improve system resolution and if operational techniques (centrifuge and gravity operation) effect the multi-stage resolution. Chapter 5 looks at multi-stage modelling for [ATPE](#) and compares the modelling to several experimental case study extractions. Chapter 6 looks at in more detail factors which can effect multi-stage [ATPE](#), in particular the kinetics of the phase separation and variations in the equilibrium data used for the modelling in Chapter 5.



# Chapter 3

## Materials and Methods

### 3.1 Introduction

This chapter outlines the materials and methods used in this thesis. There are two main sections to this chapter: the experimental materials and methods, and the computational methods. Experimental methods are used in all three data chapters (Chapters 4, 5 and 6) and computational methods are used in Chapters 5 and 6.

In this thesis, several [Aqueous Two-Phase Systems \(ATPS\)](#) are studied with two target model proteins: C-phycoyanin and haemoglobin. These proteins were chosen because of their pigments which made them easy to analyse. The model contaminants considered in this thesis were: allophycoyanin, phycoerythrin and lysozyme.

In Chapter 4, experimental investigations were carried out surrounding the extraction of C-phycoyanin from contaminants using multi-stage [Aqueous Two-Phase Extraction \(ATPE\)](#). In Chapter 5, multi-stage [ATPE](#) (where the separation at each stage has reached equilibrium) is modelled and experimentally validated against both multi-stage extractions of a single, pure protein (haemoglobin) and a protein (C-phycoyanin) in contaminants. In the final data chapter, Chapter 6, two variables which were shown to impact multi-stage [ATPE](#) were investigated; these variables were the kinetics of the phase separation after the horizontal interface formation, and the impact variation in horizontal interface partitioning had on [Multi-stage Extraction \(MSE\)](#). The kinetics of the phase separation were investigated experimentally, whereas the impact of variable horizontal interface partitioning was investigated computationally. This chapter outlines the materials and methods carried out for this thesis.

## 3.2 Experimental Materials and Methods

### 3.2.1 Materials

The phase forming materials used in the ATPSs in this thesis were deionised water, phosphate buffers, and Polyethylene Glycol (PEG) of varying weights. PEG with a Molecular Weight (MW) of 6000 Da was obtained from Alfa Aesar (Heysham, England). PEG with MWs of 4000 Da and 1500 Da were obtained from Sigma-Aldrich (Dorset, England). Potassium phosphate dibasic (>98%),  $K_2HPO_4$ , was obtained from Acros Organics and potassium dihydrogen phosphate (>98%),  $H_2KPO_4$ , was obtained from Alfa Aesar. Ammonium phosphate monobasic and dibasic (>98%),  $NH_4H_2PO_4$  and  $(NH_4)_2HPO_4$  respectively, were obtained from Sigma Aldrich.

Food grade C-phycoerythrin was obtained from three sources; as a result, the different stocks contained different mixtures of contaminants. The first two sources were commercially available blue food colourings obtained from Sainsbury's Supermarkets Ltd. in a liquid form, and SooperGood Foods in a powder form; both of these contained C-phycoerythrin from *Spirulina sp.*. As food colourings, both of these forms will have been partially purified although they still contained other contaminants, including allophycoerythrin and phycoerythrin. The last form of C-phycoerythrin was supplied by Professor Gilmour's microalgae research lab in the Molecular Biology and Biotechnology department at Sheffield University in a liquid form that had undergone centrifugation to remove cell debris. The C-phycoerythrin was produced by *Galdieria Sulphuraria* using a novel method which does not result in the expression of the contaminant allophycoerythrin. This means that the 615 nm and 652 nm peaks were only generated by C-phycoerythrin; however, this stock still contained the contaminant phycoerythrin which absorbs strongly at 562 nm. All three C-phycoerythrin sources were analysed to obtain information on composition using a Ultraviolet-visible (UV-vis) absorption method discussed in section 3.2.7. The other model target protein, human haemoglobin, was obtained from Sigma Aldrich. The model contaminant, lysozyme from chicken egg white, was also obtained from Sigma Aldrich.

### 3.2.2 Model protein

For the model separations, two pigmented proteins were chosen for investigation: C-phycoerythrin and Haemoglobin. Primarily, these proteins were chosen for ease of analysis using a UV-vis.

C-Phycoerythrin is a light-harvesting blue-pigmented protein which is an accessory pigment to chlorophyll. The blue pigmentation is a result of the phycoerythrin chromophores, 3 of which are covalently bound to each of the 6 monomers which

make up the hexamer C-phycoyanin (Schirmer et al., 1985). The protein when produced in *Spirulina platensis*, is acid sensitive (<pH 5), light-sensitive and temperature sensitive (>45 °C) (Wu et al., 2016a). C-Phycocyanin produced in *Galdieria Sulphuraria* is slightly more stable and is able to withstand temperatures up to 60 °C and below pH 5 for extended periods of time (Wan et al., 2021).

Haemoglobin is a transport protein which is found in many organisms. It responsible for transporting oxygen from lungs to tissues throughout an organism, as well as facilitating the return of carbon dioxide. Haemoglobin is comprised of four subunits, each of which has a polypeptide chain and a heme group where oxygen binds reversibly to the ferrous iron atom within the heme group (Marengo-Rowe, 2006).

The C-Phycocyanin stocks were partially purified; however, they still contained other impurities, most notably allo-phycoyanin and phycoerythrin (also pigmented). The haemoglobin stocks only contained haemoglobin. Using simplified experimental systems which have minimal impurities comes with both advantages and disadvantages. *ATPS* are generally considered complex extractions which are difficult to predict. Using simplified systems allowed a thorough evaluation the behaviour of a single protein in an *ATPS*. However, by simplifying the systems the extraction and behaviour may not accurately represent an industrial extraction. As a result, it would be expected that future work would look at building up system complexity with more crude and complex protein stocks.

### 3.2.3 Stock and System Preparation

For this thesis, *ATPS* and stock solutions were prepared by weight unless otherwise stated. This is standard for *ATPS* as the polymers used create very viscous solutions and as a result conducting experimentation by volume generates very large errors (Albertsson, 1986).

*ATPS* were prepared using stock solutions of 50% w/w PEG (MWs: 1500, 4000, 6000) and 20% w/w buffer stocks were prepared using 20% w/w salt stock solutions ( $K_2HPO_4$ ,  $H_2KPO_4$  and  $NH_4H_2PO_4$  and  $(NH_4)_2HPO_4$ ). Three salt buffers were used in this thesis: two ammonium phosphate buffers (20% w/w) at pH 7.4 and 7.0, and a potassium phosphate buffer (20% w/w) at a pH of 8.0. Different system conditions were used for different proteins. Systems studied in the kinetics studies were based upon past work by Asenjo et al. (2002a). The ammonium phosphate buffer stock solution was prepared using 20% w/w stock solutions of ammonium phosphate monobasic and ammonium phosphate dibasic, and the pH was determined using a Mettler Toledo FiveEasy Benchtop pH meter. The potassium phosphate buffer stock solution was made up in the same way using 20% w/w potassium phosphate dibasic

and potassium dihydrogen phosphate stock solutions.

Several [ATPS](#) are routinely used throughout this thesis; their composition is shown in [Table 3.1](#) along with how they are referred to throughout this thesis.

To make up protein stocks, the powder form of C-phycoerythrin was made up to 30 mg/mL in deionised water and the two liquid C-phycoerythrin forms were used as received. These stocks were stored in a dark fridge at 4 °C as C-phycoerythrin degrades in light. For clarity, the C-phycoerythrin stocks were given labels: the liquid *Arthrospira platensis* stock was termed ‘C-phycoerythrin stock 1’, the powder *Arthrospira platensis* stock was termed ‘C-phycoerythrin stock 2’, and the *Galdieria* stock was termed ‘C-phycoerythrin stock 3’. Haemoglobin stock was made up to 10 and 30 mg/mL in deionised water and stored at 4 °C. Lysozyme stock was made up to 14 mg/mL in deionised water and stored at 4 °C.

### 3.2.4 Binodal Curve Determination

Binodal curves are used to determine the single and two-phase regions of [ATPS](#). The position of a system within this curve can be used to determine some system characteristics. The cloud point method was used to determine the position of the binodal curve for a [PEG 6000](#) - ammonium phosphate pH 7.4 [ATPS](#) (conditions used in C-phycoerythrin case study [ATPS](#)) as described in [Hatti-Kaul \(2000\)](#). This method uses the basis that a single-phase system will be clear; however, once the system shifts to a two-phase system, it will become turbid as the phases begin to form and separate. As a result, the shift from a single to a two-phase system can easily be detected by eye.

To determine the binodal curve of an [ATPS](#), stock solutions of each of the phase forming components were required. In this case, the phase forming components were [PEG 6000](#) and ammonium phosphate buffer at pH 7.4. First, one of these stock solutions was weighed into a beaker and the other stock solution was then added drop-wise while continuously stirring. When the solution turned turbid, the additional weight was recorded. Deionised water was then used to shift the composition of the [ATPS](#) back to a single-phase system and the weight was recorded. This was repeated until the stock solution originally weighed into the beaker had been diluted by just over half its weight, giving half of the binodal curve. The stock solutions were then switched to give the opposing half of the binodal curve. This was carried out in triplicate.

Table 3.1: **ATPS** used in this thesis

<b>Label</b>	<b>Buffer pH</b>	<b>Phosphate Buffer Type</b>	<b>Phosphate Buffer % w/w</b>	<b>PEG MW</b>	<b>PEG % w/w</b>
C-phycoerythrin case study system	7.4	Ammonium Phosphate	12.5	6000	9.0
Haemoglobin case study system	8.0	Potassium Phosphate	11.2	1500	13.0
Kinetics A	7.0	Ammonium Phosphate	10.0	4000	14.0
Kinetics B	7.0	Ammonium Phosphate	10.0	4000	16.0
Kinetics C	7.0	Ammonium Phosphate	10.0	4000	18.0
Kinetics D	7.0	Ammonium Phosphate	10.0	4000	20.0
Haemoglobin Screening A	8.0	Potassium Phosphate	12.6	1500	9.7
Haemoglobin Screening B	8.0	Potassium Phosphate	14.4	1500	9.5
Haemoglobin Screening C	8.0	Potassium Phosphate	16.2	1500	9.4
Haemoglobin Screening D	8.0	Potassium Phosphate	9.3	1500	13.2
Haemoglobin Screening E	8.0	Potassium Phosphate	11.2	1500	13.0
Haemoglobin Screening F	8.0	Potassium Phosphate	13.1	1500	12.8
Haemoglobin Screening G	8.0	Potassium Phosphate	15.0	1500	12.6
Haemoglobin Screening H	8.0	Potassium Phosphate	5.8	1500	16.9
Haemoglobin Screening I	8.0	Potassium Phosphate	7.9	1500	16.6
Haemoglobin Screening J	8.0	Potassium Phosphate	9.9	1500	16.3
Haemoglobin Screening K	8.0	Potassium Phosphate	11.8	1500	16.0
Haemoglobin Screening L	8.0	Potassium Phosphate	13.7	1500	15.8

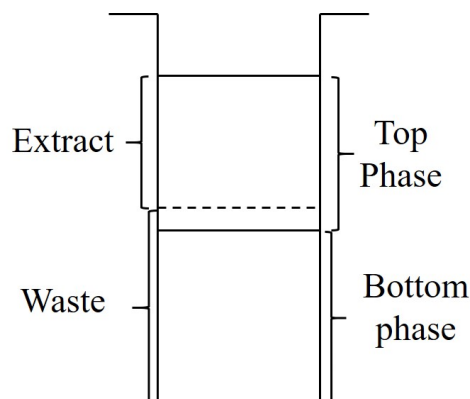


Figure 3.1: A schematic to illustrate the top, bottom, extract and waste phases in an [ATPE](#)

### 3.2.5 Treatment of Phases

Practically speaking, it is very difficult to completely separate out the top and bottom phases of an [ATPS](#), particularly when extractions are carried out at speed (as is the case in [MSEs](#) operated to a separation time). As such, systems were operated using a ‘waste’ and an ‘extract’ phase. This allows the operational phases to consist of an amount of each phase and is demonstrated in [Figure 3.1](#).

### 3.2.6 Single Protein Analysis

For systems with a single protein in them, analysis could be carried out using a [UV-vis](#) spectrophotometer because of the proteins pigment (haemoglobin) or the quantities at which it was used (lysozyme). To determine protein concentration, calibration curves at the appropriate wavelengths were constructed. Lysozyme curves were constructed at 280 nm and haemoglobin at 405 nm.

As for these systems, only a single protein was being considered which absorbs strongly at 405 nm due to its pigment or at 280 nm, Beers’ Law dictates that a correlation between its absorbance and known concentration could be used. Beers’ Law is defined as ([Swinehart, 1962](#)):

$$A = elC \quad (3.1)$$

where  $A$  is absorbance,  $e$  is molar absorptivity ( $L/gcm$ ),  $l$  is the path length ( $cm$ ), and  $C$  is the concentration ( $g/L$ ) of the solution.

To construct a calibration curve samples were measured against suitable blanks; these were made up of the same concentration of phase forming components or deionised water. Samples with the phase forming components were spiked with

varying volumes of protein stocks of known concentrations. The sample's [UV-vis](#) absorption spectra were recorded using a VWR 6300PC Double Beam Spectrophotometer calibrated between 190-900 nm.

Calibrations of haemoglobin in the haemoglobin case study system were required in both equilibrium curves and [MSE](#) phases. This was because different dilution rates were used between top and bottom phase analysis of the equilibrium curves and extract and waste phase analysis of the [MSE](#). In the top and bottom phases, 500  $\mu\text{L}$  samples were diluted by 750  $\mu\text{L}$  of deionised water. In the extract and waste phases, 650  $\mu\text{L}$  samples were diluted with 650  $\mu\text{L}$  of deionised water. These lower dilutions were used in the extract and waste phase analysis because very low concentrations of protein were seen in some samples.

The calibration curve for the haemoglobin screening systems (shown in [Table 3.1](#)) was conducted in water. To be completely accurate, calibration curves should be carried out against each system; however, as this would be very time consuming and only a rough estimate of system behaviour was needed at this stage, it was deemed unnecessary.

The calibration curve for lysozyme was also carried out in deionised water at 280 nm as a lower degree of accuracy was acceptable.

All experimentation was carried out in triplicate and errors were calculated using error propagation with 95% confidence intervals.

### 3.2.7 Phycocyanin Data Analysis

For systems with multiple proteins in it, different analysis was carried out. In this study, multi-protein mixtures were made up of the phycocyanins: C-phycocyanin, allophycocyanin and phycoerythrin. These proteins have been widely studied and have been shown to have distinctive fingerprints under [UV-vis](#) analysis. These have lead to a standardised analytical technique for phycocyanin quantification determined by [Bennett and Bogorad \(1973\)](#).

Analysis of protein concentration was carried out using a VWR 6300PC Double Beam Spectrophotometer calibrated between 190-900 nm. Blanks were made up of the same concentrations of the phase forming components for each sample. The widely used method to analyse C-phycocyanin devised by [Bennett and Bogorad \(1973\)](#) is carried out as follows.

To obtain C-phycocyanin concentration:

$$C_{C-PC} = \frac{A_{615} - 0.474A_{652}}{5.34} \quad (3.2)$$

To obtain A-PC concentration:

$$C_{A-PC} = \frac{A_{652} - 0.208A_{615}}{5.09} \quad (3.3)$$

To obtain PE concentration:

$$C_{PE} = \frac{A_{562} - 0.241C_{C-PC} - 0.849C_{A-PC}}{9.62} \quad (3.4)$$

where  $A_{WL}$  is absorbance at wavelength  $WL$  nm.

A common method to determine the purity of C-phycoerythrin is to use the 620 nm to 280 nm absorbance peak ratio shown in equation 3.5. Generally, a ratio  $>0.7$  is considered food grade,  $>3.9$  is considered reagent grade and  $>4.0$  is considered analytical grade (Kuddus et al., 2015).

$$PR = \frac{A_{620Peak}}{A_{280Peak}} \quad (3.5)$$

This method was adjusted slightly to account for the high phase viscosity leading to inaccuracies of pipetting in ATPE. The top PEG-rich phase of ATPS is highly viscous, particularly with higher MW PEG like that being used in these studies. As a result, studies of ATPS are often carried out by percentage weight (% w/w) as the use of volume can be inaccurate. As such, calibrations of each of the protein stocks of C-phycoerythrin in each of the phases of the case study ATPS were determined, these are shown in appendices in Chapter 7.2. It was unknown if there would be a significant difference in the calibration curves of systems operated under gravity or through the use of a centrifuge, so calibration curves were carried out for each. All protein absorbs strongly around 280 nm, and the blue pigment phycobiliproteins absorb strongly at 562 nm, 615 nm and 652 nm under UV-vis light (Bennett and Bogorad, 1973). As a result, calibration curves were all constructed around these points.

For the calibration curves for C-phycoerythrin, the blanks were made up in the same way as the stock solutions of the extract and waste phases for the C-phycoerythrin case study MSEs. For this, 2 g ATPS were made up as described in section 3.2.3. The system representing gravity operation was allowed to separate for 6 minutes because the system took 5 minutes for a clear horizontal interface to form. Systems representing the centrifuge operation were centrifuged at 2000 g for 10 minutes at 20 °C in a Sigma 4K15 Laboratory centrifuge. A 370  $\mu$ L volume of the top (extract) phase was extracted using a micro-pipette. The rest of the system was vigorously shaken for 30 seconds and a 500  $\mu$ L sample of the ‘waste’ phase was taken. These samples were then stored in 1.5 mL tubes of a known weight. The sample weight was

recorded before a dilution of 500  $\mu\text{L}$  and 300  $\mu\text{L}$  with deionised water for the extract and waste phases, respectively. The dilution weight was recorded. The samples were then centrifuged at 9000 g for 10 minutes at 20 °C. This was done to ensure a sample with no phase separation occurring was achieved before analysis (Albertsson, 1986). These samples were then spiked with a known volume of the C-phycoyanin stocks and mixed using a vortex as well as inversion for at least 30 seconds. Sample UV-vis absorption spectra were then recorded between 190 nm and 900 nm using a VWR 6300PC Double Beam Spectrophotometer.

For the PEG-rich phase extract phases in the MSE, the calibration curves of C-phycoyanin (at 280 nm, 562 nm, 625 nm, found that there was a factor of 1.14 difference between that and the salt-rich phase which was accounted for in calculations using equations 3.2, 3.3 and 3.4.

All experimentation was carried out in triplicate and errors were calculated using error propagation and error bars are shown to 95% confidence intervals.

### 3.2.8 Screening

Several systems were screened in order to select a suitable extraction process for haemoglobin. Kan and Lee (1994) showed that potassium phosphate (pH 8.0)- PEG 1500 systems were suitable for the extraction of haemoglobin. As a result, a range of systems with different concentrations of PEG 1500 and potassium phosphate pH 8.0 were screened; concentrations of systems screened are shown in Table 3.1 under Haemoglobin Screening A-L. 1.5 g systems were made up to the required concentrations of phase forming components in 2 mL centrifuge tubes. Each system was spiked with 100  $\mu\text{L}$  of 30 mg/mL haemoglobin stock. The systems were then thoroughly mixed for 30 seconds through vigorous shaking and inversion. To separate the phases, the systems were then centrifuged at 800 g for 30 minutes to ensure that phases had reached equilibrium. Approximate partitioning volumes were then measured and recorded using the graduations on the centrifuge tube. 500  $\mu\text{L}$  samples of the top and bottom phase were taken carefully using a micro-pipette, ensuring that phases and material at the horizontal interface were not disturbed. The sample weight was recorded. Samples were then diluted by 750  $\mu\text{L}$  of deionised water, the dilution weight was recorded. Samples were then vortexed for 30 seconds to ensure that the samples were forming a single phase. Using the absorbance of the samples at 405 nm, the haemoglobin concentration of samples were then estimated through the use of standard curves constructed in water, as described earlier in Section 3.2.6.

### 3.2.9 Selection of Single Model Contaminant

A different model contaminant, lysozyme, was evaluated in Chapter 5 for the case study C-phycoerythrin system. Lysozyme was expected to partition rapidly into the bottom phase of this system as it has a very high isoelectric point of pH 11.35 (Sigma-Aldrich), and had an advantage over allophycoerythrin as a contaminant as it could be evaluated separately from C-phycoerythrin and, therefore, at higher concentrations than with allophycoerythrin.

### 3.2.10 Equilibrium Curves

Equilibrium curves were used to determine the behaviour of protein in a given case study ATPSs across a range of protein concentrations. This curve was used in the modelling to determine partitioning.

For C-phycoerythrin in the C-phycoerythrin case study system (defined in Table 3.1), 2 g systems were made up as described in section 3.2.3. The ATPS were then spiked with a known volume of the C-phycoerythrin stock 1. Systems were shaken vigorously through inversion for 30 seconds before centrifugation at 2000 g for 10 minutes at 20 °C. A 350 µL sample of the top phase and a 900 µL sample of the bottom phase was carefully extracted and stored in a tube of a known weight. The weight of the sample was then recorded before dilution with deionised water; the top phase was diluted by 1 mL and the bottom phase by 400 µL. At very high C-phycoerythrin concentrations, the samples were diluted by a larger (known) amount to keep the C-phycoerythrin concentration within the appropriate range for UV-vis analysis. These samples did not need adjustment for a PEG phase due to the large dilution. The samples were then centrifuged again at 9000 g for 10 minutes at 20 °C; dilutions and centrifugation was carried out to ensure that the sample was a single phase that was suitable for analysis. Analysis was carried out as discussed in section 3.2.7. This was repeated in triplicate. C-phycoerythrin stock 1 was used in the C-phycoerythrin equilibrium curve as this stock was used in the MSE modelling. The allophycoerythrin concentration was accounted for using the equations described in 3.2.7. A curve for lysozyme was constructed in the C-phycoerythrin case study system using the same methods as used with C-phycoerythrin described above only using UV-vis analysis at 280 nm.

An equilibrium curve for haemoglobin was constructed in the haemoglobin case study system. For this equilibrium curve, the system was made up as described in Section 3.2.3 which was then spiked with a known volume of 10 mg/mL haemoglobin stock up to 10% of the total system volume. Systems were then thoroughly mixed for 30 seconds by inversion. To separate the phases, systems were then centrifuged

at 800 g for 30 minutes. A 300  $\mu\text{L}$  sample of the top phase and a 500  $\mu\text{L}$  sample of the bottom phase was taken from each system, being careful to not disturb material at the horizontal interface of the system. The top phase was then diluted by 900  $\mu\text{L}$  of deionised water and the bottom phase sample was diluted by 700  $\mu\text{L}$  of deionised water. Samples were then thoroughly mixed through inversion and shaking for 30 seconds before [UV-vis](#) analysis. Phase concentrations were calculated using the Beer-Lambert Law, calibration curves and dilution factors. The amount of haemoglobin in the horizontal interface of the sample was determined by mass balance of protein in the top, bottom phase, and total amount.

All experimentation was carried out in triplicate and errors were calculated using error propagation with 95% confidence intervals.

### 3.2.11 Volume Curves

For the haemoglobin extraction, a significant amount of material partitioned into the horizontal interface in such a way that a measurable third phase formed at the horizontal interface. As a consequence, a curve for the volume of the material at the horizontal interface vs. the total protein concentration in the system was constructed. For this, 6 mL of the haemoglobin case study system was made up and spiked with the 10 mg/mL haemoglobin up to 10% of the total system volume. Systems were then allowed to separate overnight to equilibrium. Phase heights of the top, bottom, and horizontal interface of the system were determined using a digital micrometer. The internal diameter of the falcon tube was then used to determine phase volumes.

Volume curves were not necessary for C-phycoerythrin or lysozyme as the visual build up was not large enough (<1 mm height).

All experimentation was carried out in triplicate and errors were calculated using error propagation with 95% confidence intervals.

### 3.2.12 Single-stage [ATPE](#)

Single-stage extractions of C-phycoerythrin in the C-phycoerythrin case study system were carried out in the same way as described in section [3.2.7](#) for each of the C-phycoerythrin feed stocks as operated through separation with a centrifuge. Samples were taken of the top and bottom phase. The extract and waste phase concentrations were calculated via mass balance. Each was carried out in triplicate.

### 3.2.13 Multi-stage ATPE

For the MSEs of C-phycoerythrin in the C-phycoerythrin case study system, each stage was carried out at 1.464 mL scale in 2 mL epindorff centrifuge tubes; the horizontal interface was determined to be at 69.2% of the total system height. The extract phase consisted of 370  $\mu\text{L}$  of the top phase, while the remaining 80  $\mu\text{L}$  and all of the bottom phase made up the waste phase (1014  $\mu\text{L}$ ). While the stock solutions were made up using weight, the extract and waste phases were calculated by volume as speed made this a necessity for the gravity operated extractions and consistency was required across the extractions. For the extractions, stock solutions of the extract and waste phase of the C-phycoerythrin case study systems were made up. This was done for both types of operation.

For a system operated through the use of a centrifuge, larger volumes (*ca.* 50 g) of the case study ATPS were made up and allowed to separate overnight. The required volume of the extract phase calculated using the system density was then extracted from the system and stored as the ‘centrifuge extract phase stock’; the remaining system was stored as the ‘centrifuge waste phase stock’. For the gravity-operated stocks, systems were made up to the same height as the MSEs.

The extract volume (calculated from the system phase densities and total system weight) was taken from the system after being allowed to separate for 6 minutes and stored as the ‘gravity extract phase stock’. The remaining was kept as the ‘gravity waste phase stock’. It was found that if the centrifuge-operated stocks were used for the gravity-operated MSEs, the phase volumes shifted across the multi-stage systems; this is likely because gravity-operated systems are still separating whereas centrifuge-operated systems were not. Both of the waste phase stocks and the gravity-operated extract stocks formed two-phase systems. As a result, when using these stocks, systems were continuously mixed using a magnetic stirrer. This is only suitable for systems which separate extremely slowly, as is the case here.

Multi-stage ATPE were carried out in a counter-current formation; schematics of those used in this thesis are depicted in Figures 3.2, 3.3 and 3.4. Stages between the extract and feed remove contaminants and stages between the waste and feed improve target recovery. As there was allophycocyanin in both C-phycoerythrin stock 1 and 2 feeds, a five-stage extraction with the protein feed in stage three was carried out. As the C-phycoerythrin case study system was designed to remove allophycocyanin and there was no allophycocyanin in C-phycoerythrin stock 3, only a three-stage extraction was carried out with the protein feed in stage one with the waste phase feed was carried out. Each extraction was tested both under centrifuge and gravity separation. Systems were made up using the waste and extract stocks for each respective type of operation by volume. Each system was inverted and

thoroughly mixed for 30 seconds. For the centrifuge operation, the separation was carried out at 2000 g for 10 minutes at 20 °C. For the gravity separation, the individual systems were measured to take 5 minutes to form a horizontal interface at the height operated; as a result, the systems were allowed to separate for 6 minutes to allow for any variation after addition of protein and to ensure that systems had reached ‘equilibrium’. The systems were run for 13 + runs until the extract and waste [UV-vis](#) spectra stopped changing and steady-state was reached. Runs are the number of phase changeovers performed between the stages. At this point, 500  $\mu\text{L}$  of the waste phase and 370  $\mu\text{L}$  of the extract phases of each stage were collected and stored in 2 mL centrifuge tubes of a known weight. The weight of the sample was recorded before the sample was diluted by a 500  $\mu\text{L}$  and 300  $\mu\text{L}$  of deionised water for the extract and waste phases, respectively. The sample was then centrifuged again at 9000 g for 10 minutes at 20 °C to ensure that the sample was a single phase system suitable for [UV-vis](#) analysis.

For validation of the model using C-phycoyanin, the five stage extraction with the feed at stage three using the liquid dye containing C-phycoyanin from the previous chapter was used. The extractions were carried out using a centrifuge-operated separation. A second four-stage extraction, with the feed at stage one using the same C-phycoyanin source was carried out using the same methods for model validation.

For the haemoglobin [MSEs](#) in the haemoglobin case study system, large volumes (*ca.* 15 mL) of the haemoglobin case study system were made up, thoroughly mixed, and allowed to separate over night until equilibrium was reached. The top and bottom phases were then collected using a hypodermic needle, avoiding the horizontal interface, and stored as top and bottom phase stocks. The horizontal interface had been determined to be at 52% of the of the total system volume in section [3.2.11](#). Systems in the [MSE](#) were made up to be 1.5 mL; the extract consisted of 650  $\mu\text{L}$  of the top phase and the waste phase consisted of 780  $\mu\text{L}$  of the bottom phase and 70  $\mu\text{L}$  of the top phase. 54.6  $\mu\text{L}$  of 10 mg/mL haemoglobin was added to the [MSE](#) at stage one with the waste phase. The extraction was carried out in a counter-current formation. Systems were shaken vigorously and allowed to separate until equilibrium. After 15 runs, the waste and extract phases were collected for each stage and analysed using a [UV-vis](#) spectrophotometer at 405 nm.

All experimentation was carried out in triplicate and errors were calculated using error propagation with 95% confidence intervals.

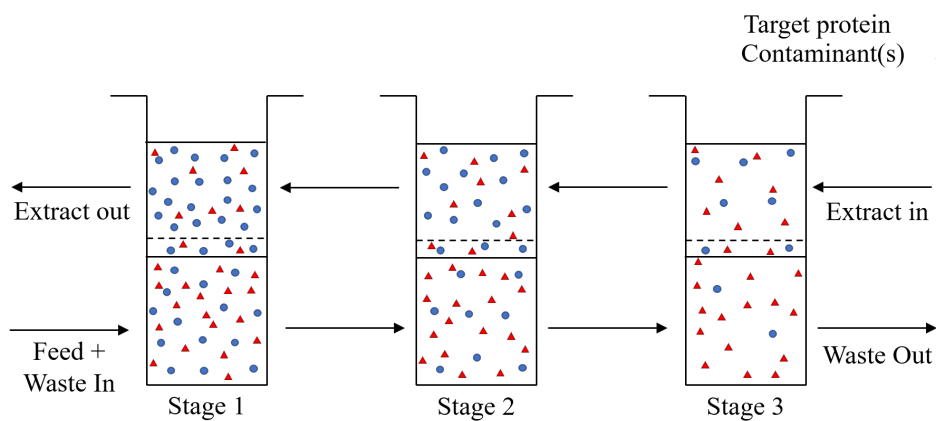


Figure 3.2: A schematic to illustrate a three stage counter-current ATPE with a feed at stage one

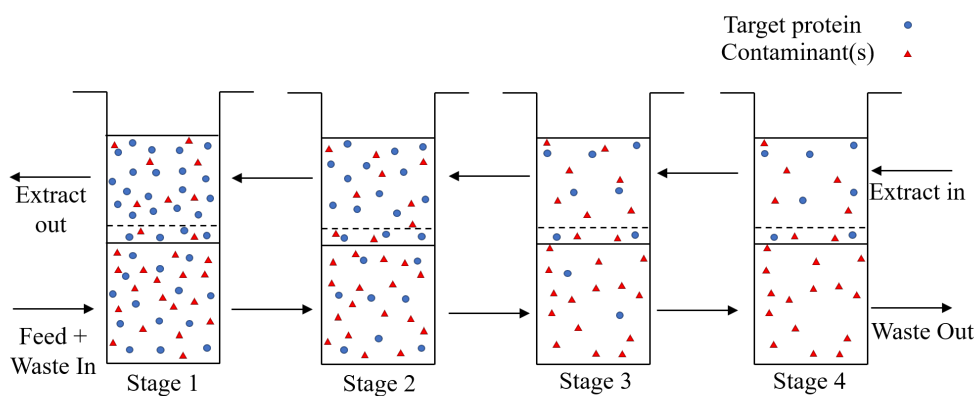


Figure 3.3: A schematic to illustrate a four stage counter-current ATPE with a feed at stage one

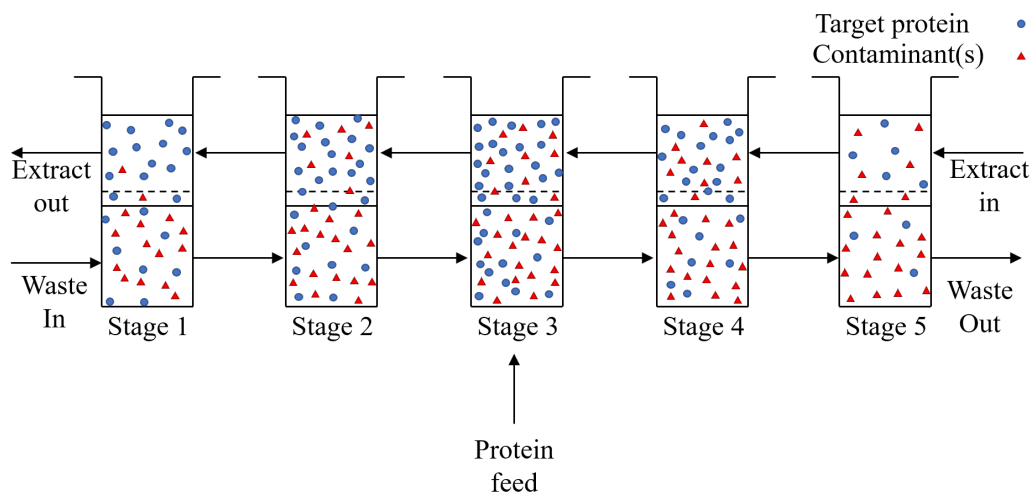


Figure 3.4: A schematic to illustrate a five stage counter-current ATPE with a feed at stage three

### 3.2.14 Conventional Dispersion Height Diagrams

For the dispersion height measurements for the kinetics studies, the C-phycoerythrin case study system and the kinetics systems A-D shown in Table 3.1 were made up in a graduated cylinder with a flat bottom which could be sealed. To mix the system, systems were thoroughly shaken and inverted for 30 seconds before observation of the phase separation. A measurement of the total system height was then taken for time point 0 using the cylinder graduations. Systems were allowed to separate and measurements of the dispersion height and settling fronts were taken by eye using cylinder graduations at various time points until the separation was considered complete. The separation was considered complete when a distinct and flat horizontal interface formed between the top and bottom phase.

All experimentation was carried out in triplicate and errors were calculated using error propagation with 95% confidence intervals.

### 3.2.15 UV-vis Analysis at 555 nm

For the turbidity measurements for the kinetics studies, 3.5 mL of an ATPS was made up in a quartz cuvette with a 1 cm path length. Systems were then mixed through shaking and inversion for 30 seconds. Systems were then allowed to separate under gravity and measurements were taken periodically using a Jenway 6305 UV-vis Spectrophotometer. A blank of deionised water was used for these measurements. The measurements were taken at 555 nm through the bottom, continuous phases of each of the systems. The dispersion height experimentation determined that all the

systems had continuous bottom phases. Each reading was carried out in triplicate. In this experiment, the C-phycoerythrin case study system and the kinetics systems A-D shown in Table 3.1 were tested.

All experimentation was carried out in triplicate and errors were calculated using error propagation and error bars are shown to 95% confidence intervals.

### 3.2.16 Microscopic Observation

The kinetics of the phase separation of the C-phycoerythrin case study system were tested in more detail than the kinetics systems A-D shown in Table 3.1. For this experimentation, the separation of the C-phycoerythrin case study system was observed using a Nikon microscope with a Nikon plan fluor 20x magnification lens. The C-phycoerythrin case study system was pipetted into a quartz cuvette with a 1 mm path length. This cuvette had been modified with a hydrophobic coating to reduce the amount of PEG interacting with the sides of the cuvette. The systems were mixed by vigorously shaking and inverting the cuvette for 30 seconds. Images and videos were taken periodically throughout the experimentation. For scaling of the images, a transmission electron microscopy grid was used; in this, one square was the equivalent of 63.5  $\mu\text{m}$ . Scales were then implemented by hand using the software Image J (Schneider et al., 2012).

For the experimentation, images were taken of the top phase, bottom phase, and horizontal interface of the system. Different volumes of the system were required to get images of the different phases. For the experiments observing the bottom phase, 350  $\mu\text{L}$  of the system was pipetted into the cuvette before thorough mixing; this was the same height as in the C-phycoerythrin kinetics study and UV-vis analysis at 555 nm. The case study system was then observed at approximately 30% of the total system height. For the top phase, 350  $\mu\text{L}$  of the system was used and the system was observed at approximately 88% of the total system height. For the experimentation observing the horizontal interface, 275  $\mu\text{L}$  of the system was used and the system was observed at approximately 69% of the total system height. A smaller system was used to make the horizontal interface easier to follow with the camera.

Systems were not made up in the cuvette as it would be very difficult to make them up accurately by weight within a cuvette with a 1 mm path length at a volume of <350  $\mu\text{L}$ . Instead, for this experiment, larger stock systems were made up to the required C-phycoerythrin case study system concentrations and stored. Samples of this stock solution were then taken for microscopic observation after vigorous shaking and inversion for at least 30 seconds.

All experimentation was carried out in triplicate.

### 3.2.17 Protein Kinetics

The phase separation of C-phycoerythrin case study system was evaluated by spiking the system with C-phycoerythrin and evaluating the amount of C-phycoerythrin in each of the phases at periodic time points. Systems were made up to 1.5 g (1.464 mL) in 2 mL centrifuge tubes and spiked with 50  $\mu\text{L}$  of C-phycoerythrin. Systems were then vigorously shaken and inverted for 30 seconds to mix the system and then allowed to separate under gravity. Each system was allowed to separate for a different length of time, ranging from immediately after the horizontal interface formation to 24 hours after the separation began. For each sample, 200  $\mu\text{L}$  of the top phase and 500  $\mu\text{L}$  of the bottom phase was extracted using a pipette being careful not to disturb material at the horizontal interface. Samples were stored in 1.5 mL centrifuge tubes of a known weight and the sample weight was recorded. Top phase samples were then diluted by 800  $\mu\text{L}$  and bottom phase samples by 450  $\mu\text{L}$  samples with deionised water; the diluted sample weights were then recorded. The samples were then centrifuged at 9000 g for 10 minutes at 20°C to ensure that the sample was a single phase sample which could undergo [UV-vis](#) analysis. Analysis of C-phycoerythrin concentration was then carried out as before in Section [3.2.7](#).

### 3.2.18 Error Calculations

The standard deviation,  $SD$ , of a measurement,  $m$ , was calculated from repeats of that data point,  $i$ , and the total number of repeats in the experiment,  $j$ :

$$SD = \sqrt{\left(\frac{\sum(m_i - \mu)}{j}\right)^2} \quad (3.6)$$

Experimental errors in values calculated from multiple samples, 1 to  $s$ , were calculated via error propagation ([Harvard, 2007](#)). The standard deviation of a calculated value,  $Z$ ,  $SD_Z$  of added or subtracted sample measurements,  $m$ , can be defined as:

$$SD_Z = \sqrt{(SD_1)^2 + (SD_2)^2 + \dots + (SD_s)^2} \quad (3.7)$$

For multiplication or division:

$$SD_Z = Z \sqrt{\left(\frac{SD_1}{m_1}\right)^2 + \left(\frac{SD_2}{m_2}\right)^2 + \dots + \left(\frac{SD_s}{m_s}\right)^2} \quad (3.8)$$

### 3.3 Computational Methods

This thesis uses single-stage data (equilibrium volume curves) to describe multi-stage [ATPE](#). Two different models are compared in this thesis: a [Liquid-Liquid \(LL\)](#) distribution model, and a [Liquid-Interface-Liquid \(LIL\)](#) distribution model. The [LL](#) distribution model assumes that partitioning only occurs between the top and bottom phases of a system and, the [LIL](#) distribution model assumes that distribution occurs between three regions of the system (the top, bottom, and the horizontal interface). Both models use single-stage equilibrium data to determine the behaviour of a protein over multi-stage [ATPE](#).

The model(s) assume the following:

1. The phases are immiscible
2. The process is isothermal
3. Perfect phase mixing was achieved
4. Phases were operated to equilibrium
5. Partitioning assumed to be only a result of phase forming materials and that other proteins added to the mixture did not impact phase partitioning
6. The interface was flat

The first assumption states that the phases were immiscible. Phases are semi-miscible with some salt partitioning into the [PEG-rich](#) phase and some [PEG](#) partitioning into the salt-rich phase. This is a common assumption in [ATPE](#), and is valid as the protein curves are constructed in [ATPS](#) used for the [MSE](#). It should be noted that robust systems should be chosen so that small shifts in composition do not result in large systems changes and therefore partitioning. Systems which are very close to the critical point of the binodal curve could generate more model error as they are prone to large partitioning changes as a result of very small temperature or concentration changes ([de Belval et al., 1998](#)).

The process is also considered to be isothermal so an energy balance is not used ([Mistry et al., 1996](#); [Rosa et al., 2009b,a](#)). System components do not react with each other so a constant temperature should be maintained. Temperature changes within the system (either from a reaction or heating or cooling the system) would alter phase partitioning and contribute to model error.

It was assumed that perfect mixing was achieved at each stage. This is valid as the interfacial tension in [ATPS](#) is very low meaning that an equilibrium point between globule break and coalescence is easily reached ([Kaul et al., 1995](#)).

The phases are also considered to have reached equilibrium. The point at which phase equilibrium is reached in [ATPS](#) is a major topic within this thesis. It is shown that this is valid for systems which have been operated to the point of clear, non-turbid phases. This can be achieved by allowing a system to separate overnight in a temperature-controlled environment, or more quickly in a temperature controlled centrifuge. This thesis shows that should a system simply be operated to a clear horizontal interface the model will not be valid as protein is still moving between the phases in the system.

In [ATPE](#), several components must be considered and can be divided into the phase forming materials (polymer(s), salt(s) and water), and materials which are to be partitioned (proteins, particulates, and cells). The materials to be partitioned are split into the contaminants and target. The partitioning of the protein is assumed to be a result of the phase forming materials. The concentration of the phase forming components and the phase volumes are assumed to be constant across the system ([Rosa et al., 2009b,a](#)). It is likely that in systems with multiple proteins at high concentrations, partitioning is being altered away from the constructed partitioning curves. This is likely mostly true at, or close to protein concentrations where a phase is becoming saturated. At this point, a protein may not be able to partition into its favoured phase and will partition into another phase or precipitate into the interface or to the bottom of the flask.

It was lastly assumed that the horizontal interface was flat. An interface will be curved; however, this would be difficult to accurately account for and the very small changes in the phase volume will not generate huge errors. Upon scale-up the error may be large enough to consider accounting for.

For the multi-stage distribution, if  $V$  is the phase volume (mL),  $x$  is the phase which protein is being moved from,  $y$  is the phase protein is being moved to and  $N$  is the total number of stages, the mass balance is described by:

$$V_x C_{x,0} + V_y C_{y,N+1} = V_x C_{x,N} + V_y C_{y,1} \quad (3.9)$$

Likewise, material balances for stage  $n$  can be written as:

$$V_x C_{x,n-1} + V_y C_{y,n+1} = V_x C_{x,n} + V_y C_{y,n} \quad (3.10)$$

Each stage at each run can then be evaluated using the equilibrium curve describing the phase separation and the stage-wise material balance:

$$\left. \begin{aligned} C_{top/HI/Bottom} &= f(\text{equilibrium lines}) \\ C_{Total,n,r} &= \frac{V_x C_{x,n-1,r-1} + V_y C_{y,n+1,r-1}}{V_{Total}} \end{aligned} \right\} n = 1, \dots, N \quad (3.11)$$

where  $f$  is the function determined for the equilibrium line and  $r$  is the number of runs performed. The equilibrium lines are determined either by a piecewise linear function or a curve of the equilibrium points determined experimentally. In this thesis, they are determined through curves from experimentally determined data points. How the concentration of the extract and waste phases is determined from the top, bottom, and horizontal interface phase concentrations depends on if the model uses a **LL** or **LIL** distribution; this is described in the following two sections.

The number of runs,  $r$ , is determined by the following conditions being met:

$$r > N \quad (3.12)$$

$$-0.00001 < C_{x,N,r} - C_{x,N,r-2} > 0.00001 \quad (3.13)$$

In this chapter, the number of stages was set to the experimental stages carried out in model validation. In the predicted stage design, up to 10 stages were considered for each separation step.

### 3.3.1 **LL** Distribution

In the **LL** distribution model, the partitioning in each stage is determined by:

$$C_{Bottom} = k_{b1}C_{Total}^2 + k_{b2}C_{Total} \quad (3.14)$$

$$C_{Top} = k_{t1}C_{Total}^2 + k_{t2}C_{Total} \quad (3.15)$$

The coefficients  $k_{b1}$  (mL/mg),  $k_{b2}$ ,  $k_{t1}$  (mL/mg) and  $k_{t2}$  were determined experimentally from the equilibrium curve. The phase volumes,  $V_{Bottom}$  (mL) and  $V_{Top}$  (mL), were determined experimentally and remained constant regardless of protein concentration. The extract,  $E$ , and waste,  $W$ , phases can be determined by the following equations:

$$C_{W,n} = V_{Bottom}C_{Bottom,n} + (V_{Top} - V_E)C_{Top,n} \quad (3.16)$$

$$C_{E,n} = V_{E,n}C_{Top,n} \quad (3.17)$$

There are configurations where the extract phase can consist of all of the top phase and part of the bottom phase, and the waste phase consists of the remaining bottom phase. These would follow the same equations as above, just with phases reversed. The material in the horizontal interface is not considered in this model.

### 3.3.2 LIL Distribution

In the LIL distribution model, the material in the horizontal interface was also considered. The concentration,  $C_{HI}$  (mg/mL), of mass in the horizontal interface,  $M_{HI}$  (mg), was calculated with respect to the total system volume rather than with respect to the volume measured at the horizontal interface. This is to avoid potentially large errors with volume measurement being propagated through the model. If a more accurate volume measurement of the horizontal interface could be used, it could be calculated as a true concentration.

$$M_{HI} = C_{Total}V_{Total} - C_{Bottom}V_{Bottom} - C_{Top}V_{Top} \quad (3.18)$$

For the haemoglobin partitioning, the horizontal interface concentration was found to follow the following equation:

$$\frac{M_{HI}}{V_{Total}} = \beta C_{Total} \quad (3.19)$$

For the C-phycoerythrin and lysozyme partitioning, the horizontal interface concentration was found to follow the following equation:

$$\frac{M_{HI}}{V_{Total}} = \beta_1 C_{Total}^2 + \beta_2 C_{Total} \quad (3.20)$$

While the volume of the phase at the horizontal interface was not used in concentration calculations to avoid error propagation, it was used to determine whether the horizontal interface material was part of the ‘extract’ or ‘waste’. It was suitable to use for this as there was a much lower accuracy requirement. In the haemoglobin extraction, larger horizontal interface regions partitioned into the extract and smaller horizontal interface regions partitioned into the waste. Ideally, material in the horizontal interface should remain in the waste phase; however, partitioning of horizontal interface phase material into the extract occurs at higher protein concentrations, i.e. larger horizontal interface volumes. The volume of the horizontal interface,  $V_{HI}$ , was considered as an insoluble phase at the interface boundary between the top and bottom phase:

$$\%V_{HI} = V_a \log_{10} \left( \frac{C_{Total} + V_b}{V_c} \right) \quad (3.21)$$

$$V_{HI} = \%V_{HI} V_{Total} \quad (3.22)$$

where  $a$ ,  $b$  (mg/ml) and  $c$  (mL/mg) were determined experimentally from the horizontal interface volume data.

It was assumed that the mass in the horizontal interface was all in the extract or the waste phase. If the volume of the horizontal interface phase was below a threshold value,  $V_{Critical}$ , then the horizontal interface material partitioned into the waste phase. If the volume of the horizontal interface material was above  $V_{Critical}$  then the horizontal interface material partitioned into the extract.  $V_{Critical}$  is dependant on the extraction method and separation equipment used in the experimental protocol.

$V_{Critical}$  is defined as:

$$V_{Critical} = H_{Extraction} \pi radius^2 \quad (3.23)$$

where  $H_{Extraction}$  (cm) is the extraction height above the horizontal interface and  $radius$  (cm) is the radius of the vessel used for the extraction. The waste and extract phases for each stage,  $n$ , are defined as follows:

If  $V_{HI,n} < V_{Critical}$ :

$$C_{W,n} = V_{Bottom} C_{Bottom,n} + (V_{Top} - V_E) C_{Top,n} + C_{HI,n} V_{Total} \quad (3.24)$$

$$C_{E,n} = V_E C_{Top,n} \quad (3.25)$$

If  $V_{HI,n} \geq V_{Critical}$ :

$$C_{W,n} = V_{Bottom} C_{Bottom,n} + (V_{Top} - V_E) C_{Top,n} \quad (3.26)$$

$$C_{E,n} = V_E C_{Top,n} + C_{HI,n} V_{Total} \quad (3.27)$$

Then, for the stage wise balance (in both distributions),  $C_E$  (mg/mL) and  $C_W$  (mg/mL) are substituted into equation 3.11 to determine the total concentration at each stage. If the contaminants being evaluated, then protein is being removed from the extract phase and  $x = E$  and  $y = W$ . If the target protein is being evaluated, then protein is being removed from the waste phase and  $x = W$  and  $y = E$ .

### 3.3.3 Optimisation

The stage wise optimisation was either carried out with respect to the yield or purity (for a single contaminant) of the system. For a set target recovery or removal, the objective function is:

$$\min \sum_{N=1}^{N_{max}} S_N B_N \quad (3.28)$$

where  $S$  is the stage-wise result,  $B$  is a binary variable,  $N$  is the number of stages in the multi-stage process being considered, and  $N_{max}$  is the maximum number of stages considered. This objective statement is subject to:

$$\sum_{N=1}^{N_{max}} B_N = 1 \quad (3.29)$$

$$B_N \in 0, 1 \quad \forall N \quad (3.30)$$

$$\sum_{N=1}^N S_N B_N \geq T \quad (3.31)$$

$$S_N = Recovery \quad or \quad S_N = Removal \quad (3.32)$$

where  $T$  is the required recovery or removal (for a single contaminant) and the stage-wise result,  $S$ , is the achieved value for the recovery (*Recovery*) or removal (*Removal*) for  $1 \dots N_{Max}$  stages within a process,  $N$ .

To evaluate the loss of target protein, the following equation was used:

$$Recovery = \frac{C_{W,0}V_W - C_{W,N}V_W}{C_{W,0}V_W} \times 100 \quad (3.33)$$

where *Recovery* is the percentage recovery of the target protein and  $C_{W,0}V_W$  is the amount of the target protein in the feed added to the system. In this scenario,  $x$  would represent the waste phase and  $y$  would represent the extract phase.

To evaluate the removal of contaminants:

$$Removal = \frac{C_{E,N}V_E}{C_{E,0}V_E} \times 100 \quad (3.34)$$

where *Removal* is the percentage removal of a contaminant protein and  $C_{E,0}V_E$  is the amount of the contaminant protein in the feed added to the system. In this scenario,  $x$  would represent the extract phase and  $y$  would represent the waste phase.

### 3.3.4 Deming Regression

In this work, the variability and robustness of a model describing multi-stage [ATPE](#) is tested. The model uses single-stage partitioning behaviour as a basis for modelling multi-stage [ATPE](#). The system is then optimised to predict the optimal number of stages for a required yield or required amount of removal of contaminants. The reliability of this result is then tested via randomising the partitioning of material at the horizontal interface, which is the most variable part of the experimental data, and

re-running the model and stage-wise optimisation. The variance of the coefficient  $\beta$  was determined using Deming regression. Deming regression was used because it was necessary to have both a variable  $x$  and  $y$  axis. This was because it was not possible to determine either the total or horizontal interface protein concentration accurately through experimentation. The Deming regression was carried out as follows (Linnet, 1990). This analysis was carried out on the LIL distribution model describing the haemoglobin MSE; this case study system was chosen because it had the largest amount of material partitioning into horizontal interfacehorizontal interface.

The first step was to set a value for the error ratio,  $\lambda$ ; this can be calculated (Equation 3.38) or set. Three values for  $\lambda$  were used as one method to test model robustness: a calculated value from experimental data,  $\lambda = 1$  and  $\lambda = 7$ . These values gave a wide range of  $\lambda$  s to be tested;  $\lambda = 1$  assumed that the  $y$  error was equal to the  $x$  error and  $\lambda = 7$  and  $7\times$  larger than the  $x$  error. The calculated value for  $\lambda$  was determined as follows; firstly, the mean of each set of data,  $\theta$ , at every data point,  $i$ , is calculated from repeats carried out at each data point,  $j$ :

$$C_{\theta,i} = \frac{\sum_{j=1}^{J_i} C_{\theta,i,j}}{J_i} \quad (3.35)$$

Where the total number of repeats at each data point is represented by  $J_i$  and  $\theta$  is a place holder for *Total* ( $x$  axis) and *HI* ( $y$  axis). The true concentration,  $\hat{C}_\theta$  (mg/mL) can be related to the measured concentration  $C_\theta$  (mg/mL) by the normally distributed error  $\epsilon_\theta$  (mg/mL) through the following equation:

$$C_\theta = \hat{C}_\theta + \epsilon_\theta \quad (3.36)$$

Then variance of each data set was calculated by:

$$Var(\epsilon_\theta) = \frac{\sum_{i=1}^I \sum_{j=1}^{J_i} (C_{\theta,i,j} - C_{\theta,i})^2}{\sum_{i=1}^I J_i - 1} \quad (3.37)$$

The constant error ratio,  $\lambda$  between the two variances,  $Var(\epsilon_y)$  and  $Var(\epsilon_x)$ , of the  $x$  and  $y$  data set respectively may then be calculated by:

$$\lambda = \frac{Var(\epsilon_y)}{Var(\epsilon_x)} \quad (3.38)$$

For this process, the  $x$  data set is set as  $C_{Total}$  and the  $y$  data set is represented by  $C_{HI}$ .

As it is known that the equation goes through the origin, the ‘true estimates’ of  $\hat{C}_{Total}$  and  $\hat{C}_{HI}$ , for each pair of  $(C_{Total,i}, C_{HI,i})$  measurements for haemoglobin in the haemoglobin case study system, can be defined as:

$$\hat{C}_{HI} = \hat{\beta}\hat{C}_{Total} \quad (3.39)$$

And the estimate of the slope,  $\beta$ , can be calculated as:

$$\hat{\beta} = -\frac{b}{2} + \frac{1}{2}\sqrt{b^2 + 4\lambda} \quad (3.40)$$

where:

$$b = \frac{(\lambda u - q)}{p} \quad (3.41)$$

$$u = \sum_{i=1}^I C_{Total,i}^2 \quad (3.42)$$

$$q = \sum_{i=1}^I C_{HI,i}^2 \quad (3.43)$$

$$p = \sum_{i=1}^I C_{Total,i}C_{HI,i} \quad (3.44)$$

The jackknife method was then used to calculate the standard error of  $\hat{\beta}$ ,  $\hat{SE}(\hat{\beta})$ . The jackknife method has been shown to be suitable for use in Deming regression (Linnet, 1990). Firstly, to compute  $\hat{\beta}$ , the estimate of  $\hat{\beta}$  using all available data, was calculated. Then for  $i = 1 \dots I$ ,  $\hat{\beta}_{-i}$ , the estimate of  $\hat{\beta}$  without the data set  $(C_{Total,i}, C_{HI,i})$  was calculated. From this data set, for  $i = 1 \dots I$ , the  $i^{th}$  pseudo-variate  $\hat{\beta}_i^*$  was calculated as:

$$\hat{\beta}_i^* = I\hat{\beta} - (I-1)\hat{\beta}_{-i} \quad (3.45)$$

The jackknife estimator,  $\hat{\beta}_{Jackknife}$ , is then computed as:

$$\hat{\beta}_{Jackknife} = \sum_{i=1}^I \frac{\hat{\beta}_i^*}{I} \quad (3.46)$$

The variance of  $\beta$ ,  $Var_{Jackknife}(\hat{\beta})$ , can then be calculated as:

$$V_{Jackknife}(\hat{\beta}) = \sum_{i=1}^I \frac{(\hat{\beta}_i^* - \hat{\beta}_{Jackknife})^2}{(I-1)} \quad (3.47)$$

Finally  $\hat{SE}(\hat{\beta})$  can be calculated as:

$$\hat{SE}(\hat{\beta}) = \sqrt{\frac{Var_{Jackknife}(\hat{\beta})}{I}} \quad (3.48)$$

The confidence intervals of  $\beta$ , with a  $100(1 - \alpha)\%$  confidence interval, can be calculated as:

$$\hat{\beta} \pm t_{1-\alpha, I-2} \hat{SE}(\hat{\beta}) \quad (3.49)$$

For each of the distributions of  $\beta$  as calculated by the three  $\lambda$  values, 1000 random values for  $\hat{\beta}$  were generated which were then used in the model developed for the [LIL](#) distribution to determine an optimal number of stages for a required yield.

## Chapter 4

# Experimental Investigations of Multi-stage Aqueous Two-Phase Extraction

### 4.1 Introduction

[Aqueous Two-Phase Systems \(ATPS\)](#) are a promising alternative processing option for protein purification due to a reduced comparative cost compared with traditional techniques (such as chromatography) and ease at which they can be operated continuously. For [ATPS](#) to be used industrially, there are two major issues to be resolved: the lack of understanding of the phase forming mechanisms, and the low resolution achieved in a single extraction step. This chapter experimentally explores the use of multi-stage [Aqueous Two-Phase Extraction \(ATPE\)](#) to improve the resolution of the process. While multi-stage [ATPEs](#) are simple to operate, there are two operational methods which have both been explored in this chapter: operation through the use of a centrifuge, or under gravity. During this chapter, the extraction of a model protein, C-phycoyanin, was explored using a case study system of 9% w/w [Polyethylene Glycol \(PEG\)](#) 6000 and 12.5% w/w ammonium phosphate buffer at pH 7.4. To evaluate the robustness and repeatability of the results, different contaminant mixes were used.

The use of [Multi-stage Extraction \(MSE\)](#) has been used successfully across the chemical processing industry with cheap and low yield processes in order to improve the process performance; a key example is column distillation ([Seader et al., 2006](#); [Richardson et al., 2002](#)). Multi-stage operation has also been applied to both traditional [Liquid-Liquid Extraction \(LLE\)](#) and [ATPE](#) with success ([Seader et al., 2006](#); [Rosa et al., 2013](#)). In [ATPE](#), [MSE](#) can be utilised in two ways to improve

process performance: either the extraction conditions remain the same with each additional step removing more of the same contaminants, or the extraction conditions are modified with each step.

Altering the system conditions with each step has multiple uses. Firstly, it has been used to remove different contaminants at each stage. For example, [Kroner et al. \(1982\)](#) used four sequential systems to extract formate dehydrogenase from *Candida boidinii* homogenate. The extractions were carried out in mixer settlers and at each step the following were removed: cell waste, nucleic acids, bulk proteins, and finally salts and remaining proteins. Despite the number of stages, a 70% yield was achieved along with technical grade purity (>70%). Secondly, [MSE](#) with different system conditions at each step has been applied to move the target from the [PEG-rich](#) to the salt-rich phase for ease of downstream processing in a backwashing step. [Hummel et al. \(1983\)](#) carried out a larger scale two-stage [ATPE](#) of D-lactate dehydrogenase from *Lactobacillus confuses* homogenate. The first step was carried out using a [PEG-salt ATPS](#) and was designed to remove cell debris. The top [PEG-rich](#) phase containing D-lactate dehydrogenase was then contacted with a second salt-rich phase to back-extract the target into the salt-rich phase both for ease of downstream processing and to further purify the product. Lastly, multi-step extraction has been used in ‘washing’ steps, where protein remaining in the [PEG-rich](#) phase is removed after product back-extraction, in order to recycle the more expensive polymer phases in a [PEG-salt ATPS](#). [Rosa et al. \(2013\)](#) implemented a 6+ stage process where all of these techniques were used. A multi-stage counter-current process with the same conditions was used to remove contaminants by extracting the target protein, [Immunoglobulin G \(IgG\)](#) into the [PEG-rich](#) phase. The system conditions were then changed to back-extract the target into the salt-rich phase for easier downstream processing. Finally, the [PEG-rich](#) phase waste from the back-extraction was washed in order to recycle it. An 80% yield and a 99% purity of [IgG](#) from [Chinese Hamster Ovary \(CHO\)](#) cell supernatant was achieved using this approach.

For this chapter, C-phycoyanin was chosen as the target in the [MSE](#) experimentation because it is a blue-pigmented protein which absorbs strongly at around 620 nm. This makes it easy to analyse with a [Ultraviolet-visible \(UV-vis\)](#) spectrophotometer. While C-phycoyanin has undergone some investigation as an ‘anti-cancer’ protein, it has most commonly been produced as a natural food colouring ([Jiang et al., 2018](#); [Carle and Schweiggert, 2016](#)). C-phycoyanin can still require purification to be sold even though the purity standards of the food industry are much lower than that of the bio-pharmaceutical industry. The purity of C-phycoyanin is assessed by [UV-vis](#) spectroscopy where its characteristic peak absorption wave-



Figure 4.1: Structures of phycoerythrin, C-phycoerythrin and allophycoerythrin as depicted by [Sonani \(2016\)](#).

length of 620 nm is compared with a general protein absorption peak at 280 nm. The comparison of absorption between these two wavelengths then gives the purity ratio which must be above 0.7 to be sold as a food product ([Kuddus et al., 2015](#)). The 620 nm peak can be used to evaluate the C-phycoerythrin concentration as this blue protein absorbs strongly at this wavelength. The 280 nm peak evaluates total protein concentration. Protein usually absorbs strongly at this wavelength because of the presence of two aromatic amino acids, tryptophan and tyrosine, and to a smaller extent the presence of cystine which is responsible for the disulphide bond ([Schmid, 2001](#)).

While the purity standards are lower in the food industry, the cost of production must also be much lower and the throughput much higher. The many advantages of [ATPE](#) make it a viable option for processing of C-phycoerythrin. These advantages include low cost, low energy requirements (if operated using gravity), scalability, continuous operation, and the option of recycling raw material. Seeking to use [ATPE](#) in the food and beverage industry may also provide an opportunity to explore the process on an industrial scale without having to compete with chromatography, as chromatography is generally used for quality control rather than processing in the food and beverage industry ([Bio-Rad, 2020](#)).

C-phycoerythrin can be produced in cyanobacteria and is of the phycophiliprotein family; blue-pigmented proteins in this family are made up of monomers composed of similar  $\alpha$  and  $\beta$  subunits. C-phycoerythrin has an overall structure of  $(\alpha\beta)_6$ . A common contaminant found with C-phycoerythrin is allophycoerythrin, which has the structure  $(\alpha\beta)_3$ . The removal of allophycoerythrin from C-phycoerythrin is desired as allophycoerythrin pollutes the blue colouring with a blue/green. Another common contaminant considered in this chapter is phycoerythrin, which is also a hexamer composed of similar  $\alpha$  and  $\beta$  subunits. The purification techniques currently used within the food and beverage industry struggle to separate these compounds from each other.

Alongside choosing suitable extraction conditions, the operational method of [ATPE](#) is another parameter which must be considered. The extraction is based upon the separation of the two phases, one of which contains the target protein and the other contains contaminants. The separation of the phases is commonly achieved using two different methods: phase separation through gravity, or through the use of a centrifuge. Industrial equipment designs are based on one of the two above separation methods. For instance, centrifugal partition columns and counter-current chromatography columns are based on separation through centrifugal force, whereas traditional mixer-settlers and column contactors are based on gravity settling. While operation through centrifugal force can be achieved rapidly, it is more expensive and has higher energy requirements than equipment based on gravity settling. In current [ATPE](#) literature, equilibrium using gravity separation is defined as the point at which a clear horizontal interface is formed between the two phases ([Tidhar et al., 1986](#)). This can be achieved in under 80 seconds in fast separating systems at bench scale, but may take as long as 12 hours in a slow separation system ([Fauquex et al., 1985](#); [Albertsson, 1986](#)). When operating a system using gravity, it is important to choose systems with rapid separations at bench scale as separation time is based upon system height and will therefore increase as systems are scaled up ([Kaul et al., 1995](#)). System separation rate is determined by the system conditions, the most important factor has been determined to be the phase viscosity ([Kaul et al., 1995](#)).

Systems which are separated under centrifugal force will always be operated at or very close to equilibrium as large forces are applied. There may be some heating of the sample upon centrifugation which may shift the equilibrium and therefore the partitioning of the sample. Temperature-controlled centrifuges can be used in order to mitigate this effect; however, this would increase operational costs, particularly at scale. Large-scale systems operated under gravity are not always operated to equilibrium. Generally, the formation of a horizontal interface is considered close enough to equilibrium ([Kaul et al., 1995](#)). Operating close to equilibrium will mean there are very slight changes in the system, however, it has been shown in [ATPS](#) that slight shifts in the concentration can drastically change partitioning behaviour ([de Belval et al., 1998](#)). Fortunately, systems where small changes can have a drastic effect on partitioning behaviour can be predicted by the position on the binodal and can therefore be avoided in process design ([de Belval et al., 1998](#)). These regions are shown in [Figure 4.2](#). Systems which can have drastic behaviour changes are characterised by having an intermediate position on the binodal / or a position very close to the binodal curve. Systems with an intermediate position on the binodal can experience drastic shifts in partitioning behaviour from very small environmental changes, and positions close to the binodal may change to a single-phase system

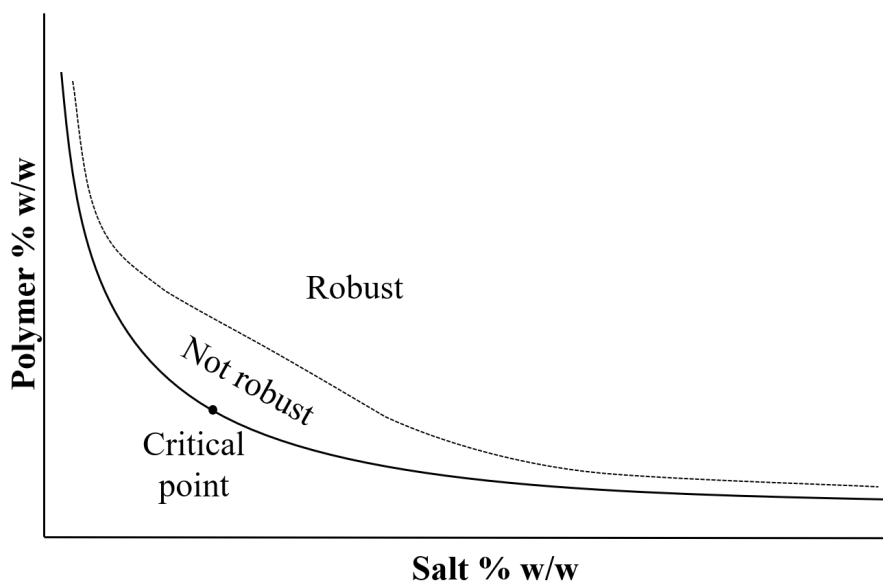


Figure 4.2: A schematic of a binodal curve (represented by the solid black line) illustrating regions which have robust [ATPS](#).

with small environmental changes. Robust system selection in single-stage [ATPS](#) can overcome this problem. However, small changes in a single-stage system may accumulate across a multi-stage system. At best, this may alter separation behaviour or shift the horizontal interface position and reduces performance; at worst, this could result in a system which does not form two phases at extremities of a multi-stage system.

A system which is operated under gravity is considered to be very close to equilibrium once a distinct horizontal interface is formed. This means interchangeability is assumed between the operational methods. Often in experimental studies, systems are separated through 10 or more minutes in a centrifuge at low spin speeds and then left in a controlled temperature environment overnight to ensure equilibrium has been reached ([Albertsson, 1986](#); [Rosa et al., 2009a, 2007](#); [de Barros et al., 2016](#)). In comparison, when kinetics studies are performed, the phase separation is evaluated by eye and without protein in the system ([Asenjo et al., 2002a](#); [Kaul et al., 1995](#)). As a result, evaluating the differences of the operational methods on protein partitioning will provide insight into experimentation and ultimately choosing equipment and system operational methodology upon scale up.

In this chapter, three multi-stage [ATPE](#) systems for C-phycoyanin purification are experimentally evaluated. The guidelines established in [Benavides and Rito-Palomares \(2008\)](#) were used to select a [PEG](#) and salt type for the [ATPS](#). For this [PEG-phosphate ATPS](#), a binodal curve was constructed. A system was selected

from this which is expected to be robust because of its position on the binodal. The partitioning of C-phycoerythrin in this system was then tested through the construction of an equilibrium curve. Three different C-phycoerythrin stocks are then used for the single and MSEs. The first two feeds are commercially available food products of C-phycoerythrin from *Arthrospira platensis*, and the third is C-phycoerythrin produced from *Galdieria Sulphuraria*. The MSE were carried out using gravity operation and centrifuge operation.

## 4.2 Results and Discussion

### 4.2.1 System Selection

Within this study, a model extraction of C-phycoerythrin from other protein contaminants present within cyanobacteria was carried out. Two contaminants which are commonly present and easily identifiable by spectral analysis are the phycobiliproteins allophycoerythrin and phycoerythrin. C-phycoerythrin absorbs strongly at around 620 nm, allophycoerythrin at 652 nm, and phycoerythrin at 562 nm (Bennett and Bogorad, 1973). The exact point of the 620 nm C-phycoerythrin peak varies between around 610 nm and 620 nm depending on the exact structure of the protein. C-phycoerythrin in the three stocks used was found to have a peak at 615 nm. To carry out an extraction, the first step is to decide on the system type. For a protein extraction, both polymer-polymer and polymer-salt ATPE are suitable. However, as polymer-salt systems are more economically favourable than polymer-polymer, the former were used (Benavides and Rito-Palomares, 2008). The characteristics of the target and contaminants are key considerations when choosing PEG and salt types in system selection. Benavides and Rito-Palomares (2008) state that two characteristics which are important in system selection are protein size and the isoelectric point. Table 4.1 shows the expected characteristics of the proteins.

The isoelectric point of the target protein alongside the pH of the phase forming salt buffer has been used in the literature to manipulate target protein partitioning (Benavides and Rito-Palomares, 2008). When extracting a target protein, it is generally pushed into the PEG-rich phase in a polymer-salt system. As the pH of the system increases above a protein's isoelectric point, the free water in the salt-rich phase decreases. This can result in the protein favouring the PEG-rich phase. A pH up to 4 points above the isoelectric point (so as not to push all the contaminants into the polymer-rich phase) is considered suitable (Benavides and Rito-Palomares, 2008). Another consideration involving pH is that C-phycoerythrin has been shown to be unstable when stored in solutions below pH 5, and is generally stored in solutions around pH 7 (Wu et al., 2016b). In terms of protein size, as the size of protein

Table 4.1: Estimates from the literature of the isoelectric point and MW of protein within feed stocks used in the model ATPE

Protein	MW (kDa)	Isoelectric point (pH)	Reference
C-phycoerythrin	242	4.65	(Anaspec, 2020b) (Prozyme, 2019)
Allophycoerythrin	90 - 121	5.1	(Fernández-Rojas et al., 2014) (Bateman, 2019; Kozłowski, 2016)
Phycoerythrin	240 - 292	4.2	(Anaspec, 2020a) (Orta-Ramirez et al., 2000)

increases a lower Molecular Weight (MW) of PEG is required for the target protein to readily partition into the PEG rich phase (Benavides and Rito-Palomares, 2008). This is a result of the excluded volume theory (Grilo et al., 2016). Benavides and Rito-Palomares (2008) state that a PEG MW of less than 4000 is generally preferred for a protein with a MW of more than 10 kDa, whereas a PEG MW of more than 6000 is preferred for a target protein of less than 10 kDa.

From Table 4.1, it can be seen that there are differences between C-phycoerythrin and allophycoerythrin which can be readily exploited in ATPE using the method established by Benavides and Rito-Palomares (2008); both the size and isoelectric point of the proteins are different. There is less difference between phycoerythrin and C-phycoerythrin; both proteins are of a similar size and unfortunately the isoelectric point of C-phycoerythrin lies between that of allophycoerythrin and phycoerythrin. As this is the case, it may be difficult to isolate C-phycoerythrin from both allophycoerythrin and phycoerythrin using the same ATPS on the salt pH of the system alone.

A salt-phase with a pH of 7.4 was selected to push C-phycoerythrin into the PEG-rich phase as well as to stay in the pH stability range of C-phycoerythrin. The three salts used as phase forming components used in ATPE are citrate, sulphate, and phosphate salts. Citrate and sulphate salts are generally used in systems with a lower pH requirement, below pH 6.5, and phosphate salts are used for pH 7 or above (Benavides and Rito-Palomares, 2008). As a result, an ammonium phosphate buffer at pH 7.4 was chosen. A PEG MW of 6000 was chosen because it has been previously used successfully in the literature to extract C-phycoerythrin and it was therefore known that C-phycoerythrin would partition into a PEG 6000 phase (Antelo et al., 2015). Other methods could have been used to manipulate protein partitioning within the system; for instance, using the Tie Line Length (TLL) of the ATPS to change either the size exclusion or hydrophobic effects of the system.

Figure 4.3 shows the binodal curve of a PEG 6000 and ammonium phosphate at

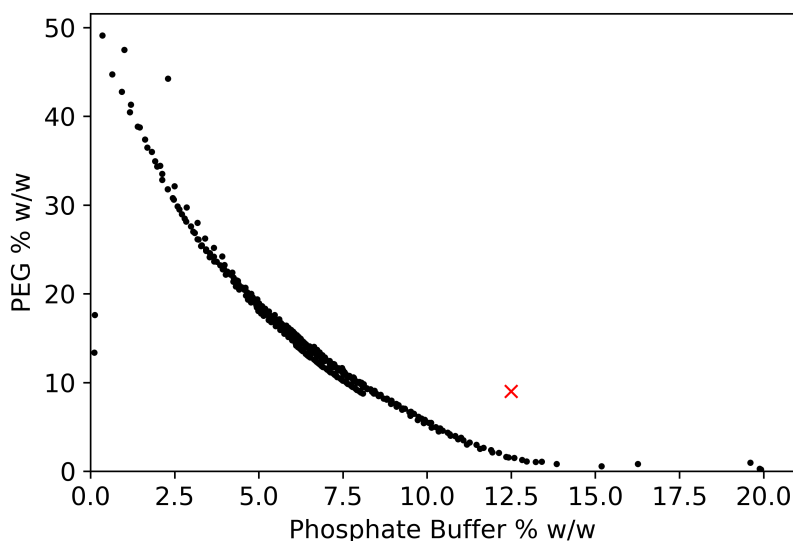


Figure 4.3: Binodal curve of a [PEG 6000](#) - ammonium phosphate at a pH of 7.4 [ATPS](#). The black dots represent the point at which the system shifts from a single phase to a two-phase system. The red cross represents the system chosen for further case study.

pH 7.4 [ATPS](#). The region below the black dots represent the concentrations at which this system forms a single-phase system, and the region above represents the concentrations at which a two-phase system occurs. The red cross represents the system chosen for further study. This system was chosen as it rests at a salt concentration high enough to form a system with a continuous bottom phase, therefore having faster separation kinetics ([Kaul et al., 1995](#)). The system is also still on the edge of the intermediate region of the binodal curve, which are also known to have faster phase separation kinetics as well as volume ratios which are not extremely high or low ([Salamanca et al., 1998](#)). The system is not too close to the binodal curve, and far enough away from a central position to represent a system which is robust. Small concentration or condition changes should not alter the system partitioning or shift the system to a single phase. Together, these traits make the C-phycoyanin case study system suitable for a [MSE](#) process.

[Albertsson \(1971\)](#) and [Andrews and Asenjo \(1996\)](#) state that [ATPS](#) can experience partitioning into the horizontal interface of a system. As a result protein partitioning into the horizontal interface is considered in this thesis. Figure 4.4 shows the partitioning of C-phycoyanin between the top, bottom, and horizontal interface in the case study [ATPS](#). In the majority [PEG-salt](#) systems, the top phase is the [PEG-rich](#) phase and the bottom phase is salt-rich phase. It can be seen

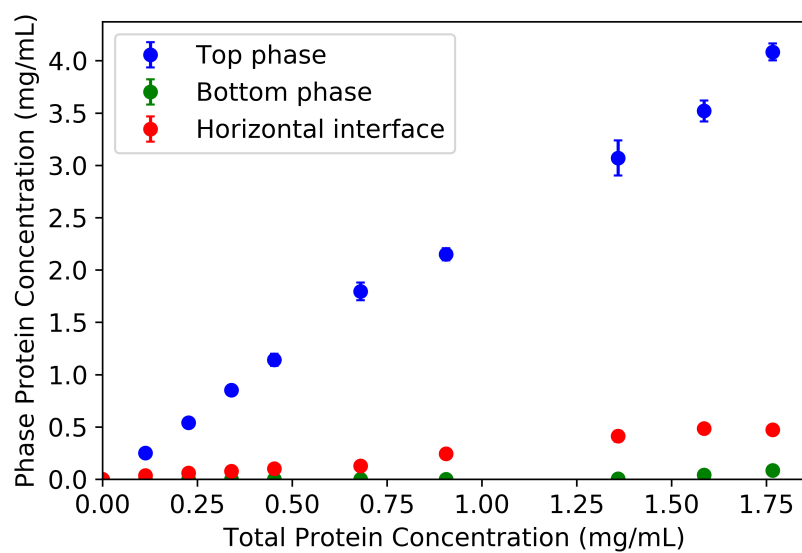


Figure 4.4: The partitioning of C-phycoerythrin into the top, bottom, and horizontal interface in the C-phycoerythrin case study system.

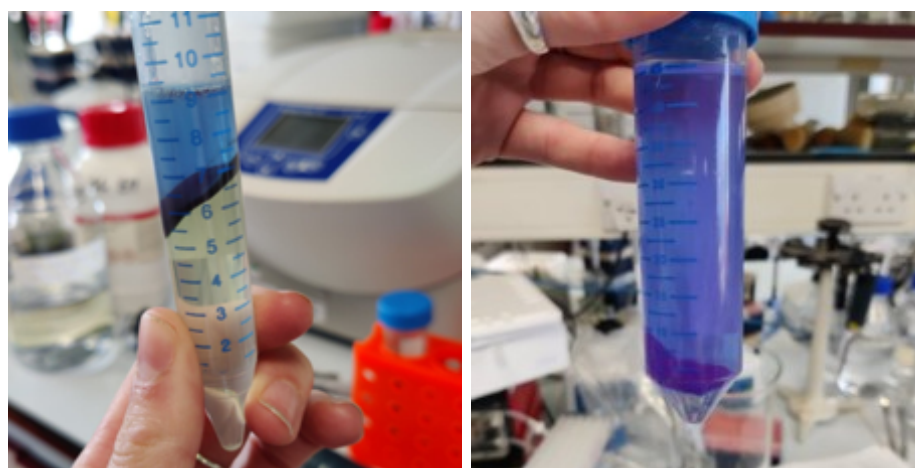


Figure 4.5: ATPS in which material, including protein, has partitioned heavily into the horizontal interface of the system.

from Figure 4.4 that C-phycoerythrin favours the top phase in this system which is where the target protein should be extracted to. The relationship between the total C-phycoerythrin concentration and top phase C-phycoerythrin concentration appears linear at all concentration ranges tested. Almost no C-phycoerythrin partitions into the bottom phase within the range tested. Some protein begins to partition into the bottom phase after a total concentration of 1.5 mg/mL of C-phycoerythrin is reached. It can also be seen that material is partitioning into the system horizontal interface, even at low total system concentrations. ATPS with protein and other materials partitioning into the interface are shown in Figure 4.5. Partitioning into the horizontal interface is discussed in more detail in the next chapter. It should be noted that the concentration in the horizontal interface is taken with respect to the total volume of the system as the volume of the horizontal interface is not easily measured accurately. The top and bottom phases are shown as a concentration of their phase size; in this system, the top phase was shown to be 30.8% of the total system volume, and the bottom phase was shown to be 69.2% of the total system volume. The treatment of the horizontal interface material is discussed in the next chapter.

#### 4.2.2 Feed and System Characterisation

Only protein contaminants are considered in this study rather than small solutes and particulates. Bulk protein was considered using the 280 nm peak, and the target protein and major contaminants using 562, 615 and 652 nm peaks. To evaluate the success of the extractions, the starting feed stocks needed to be evaluated as they had different concentrations of C-phycoerythrin, allophycoerythrin, and phycoerythrin. Table 4.2 shows the calculated concentrations of C-phycoerythrin, allophycoerythrin, and phycoerythrin in each of the feed stocks, as calculated from the equations described in Chapter 3.

The first feed evaluated in this study was a commercially available liquid food colouring which contained C-phycoerythrin from *Arthrospira platensis*; this stock was termed ‘C-phycoerythrin stock 1’. From Table 4.2, it can be seen that UV-vis analysis showed that the product contained 7.29 mg/mL of C-phycoerythrin along with the highest concentrations of allophycoerythrin at 2.42 mg/mL and phycoerythrin at 1.72 mg/mL.

The second feed evaluated in this study was a commercially available powdered food colouring and nutritional product which contained C-phycoerythrin from *Arthrospira platensis*; this stock was termed ‘C-phycoerythrin stock 2’. When 30 mg/mL of the powder was made up in deionised water, it can be seen from Table 4.2 that this stock contained 7.30 mg/mL of C-phycoerythrin, 1.15 mg/mL of allophy-

Table 4.2: The concentration of C-phycoerythrin, allophycoerythrin, and phycoerythrin protein in each of the stock solutions used in this study.

Stock type	C-phycoerythrin mg/mL	Allophycoerythrin mg/mL	Phycoerythrin mg/mL
C-phycoerythrin stock 1	7.29	2.42	1.72
C-phycoerythrin stock 2	7.30	1.15	1.16
C-phycoerythrin stock 3	1.61	0	0.33

erythrin, and 1.16 mg/mL of phycoerythrin. Similar amounts of C-phycoerythrin are seen in C-phycoerythrin stocks 1 and 2; however, a lower amount of phycobiliprotein is seen in the powder stock. As only 9.16 mg/mL of phycobiliprotein is accounted for, there are therefore other contaminants in this feed. Other protein contaminants will be accounted for in bulk at the 280 nm peak, but non-protein contaminants are not. The non-protein contaminants are not considered in this chapter as it is unlikely that a concentration of <21 mg/mL in the stock and a total concentration of <0.45 mg/mL in the [ATPS](#) will interfere with the [ATPE](#). Phase forming components, which control the system behaviour are present in the case study system at concentrations of around 115 mg/mL and 159 mg/mL of [PEG](#) and phosphate salt buffer respectively. These components are in large excess compared with the other contaminants in the system and both strongly influence the behaviour of water. Therefore, these components control the system behaviour. In [ATPE](#), particularly in multi-stage systems, it is important that systems are chosen which are robust enough that feed variation does not strongly influence behaviour.

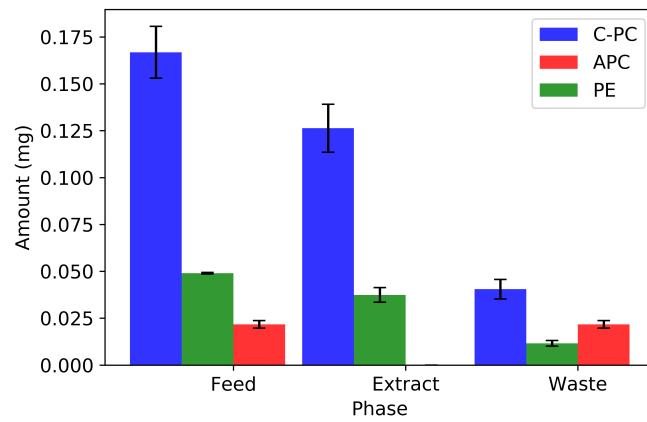
The last feed stock evaluated was a C-phycoerythrin containing sample obtained from a research laboratory at the University of Sheffield. This sample was made using *Galdieria* which was cultured such that undetectable amounts of allophycoerythrin are expressed. This stock was termed ‘C-phycoerythrin stock 3’. It should be noted that the stock still contained the pigmented-protein phycoerythrin, but this protein does not absorb around the 620 nm mark. As the method to manufacture the stock was carried out in a lab, conditions varied more than that in a commercial process and stock solutions obtained could vary in concentration. All feeds were analysed to obtain the exact concentrations used in each experiment; however, while some comparisons could be made between the experiments, only qualitative conclusions could be drawn as a result of this. Generally speaking though, Table 4.2 shows that this stock contained a much lower concentration of C-phycoerythrin and phycoerythrin than the other two stocks.

### 4.2.3 Single-stage Extraction

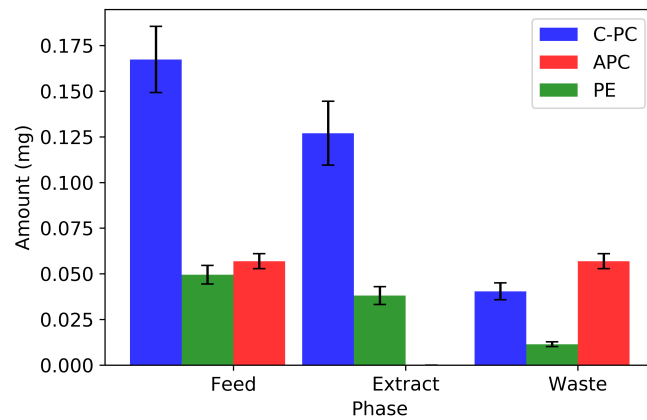
As a comparison to the [MSEs](#), a single-stage extraction using the same case study system was carried out for each of the feed stocks. [Table 4.3](#) shows the 620 / 280 nm purity ratios of the extract phase of a single-stage [ATPE](#) compared with the feed stocks and [Figure 4.6](#) shows the amounts of C-phycoerythrin, allophycoerythrin, and phycoerythrin in the feed stocks compared with the extract and waste phases in a single-stage [ATPE](#). All three extractions were carried out using a centrifuge for the separation.

[Figure 4.6](#) and [Table 4.3](#) show the results for the single-stage [ATPE](#) for all three feeds. It can be seen across all three experiments in [Figure 4.6](#) that C-phycoerythrin consistently behaves as seen in the equilibrium curve in [Figure 4.4](#) and favours the top [PEG](#)-rich phase of this [ATPS](#). It can also be seen that phycoerythrin favours the top [PEG](#)-rich phase. This is in line with the guidelines established by [Benavides and Rito-Palomares \(2008\)](#) as a result of the isoelectric point of the system being far below that of C-phycoerythrin. Allophycoerythrin, as desired, is favouring the salt-rich bottom phase, with all the allophycoerythrin being detected in salt-rich phase for both systems containing the contaminant. The successful removal of allophycoerythrin from the feeds is reflected in the 620/280 nm purity ratios shown in [Table 4.3](#), with both C-phycoerythrin stock 1 and 2 purity ratios being improved. The C-phycoerythrin stock 1, which contains more allophycoerythrin, had the greatest purity ratio increase from 1.84 to 2.86 in a single step compared with C-phycoerythrin stock 2, which had a purity ratio increase of 2.16 to 2.7. The C-phycoerythrin stock 3 also had an increase of purity ratio from 0.81 to 1.09 despite not containing allophycoerythrin, indicating that some other bulk protein contaminant within the feed is being extracted into the bottom phase.

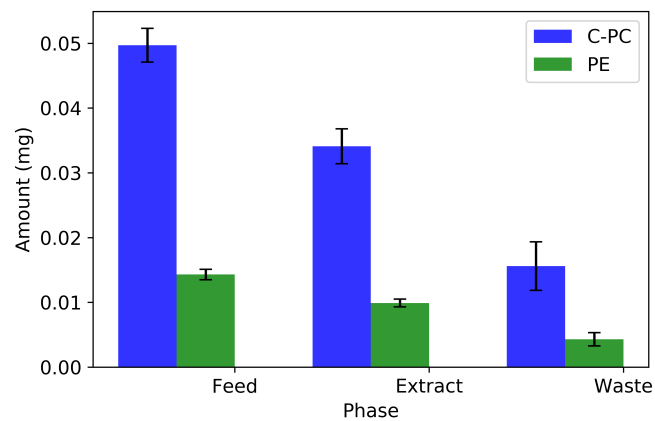
While the purity ratio was increased in all three single-stage extractions, it can be seen from [Table 4.3](#) that a major drawback is that a large proportion of C-phycoerythrin is being lost. While [Figure 4.4](#) shows that the partitioning of the system is such that C-phycoerythrin overwhelmingly favours the top phase, it is difficult in practice to operate a system with complete separation of the phases. As a result, either some of the bottom phase is retained in the extract or some of the top phase is in the waste. Generally speaking, bottom phase in the extract results in a lower purity and top phase in the waste results in a lower yield. In this system, the latter is true, with 80 out of 450  $\mu\text{L}$  of the top phase remaining in the waste phase. This has resulted in a 24.3%, 24.1% and 31.4% loss of C-phycoerythrin in the waste phase in the systems containing the C-phycoerythrin stocks 1, 2 and 3, respectively.



(a) C-phycoerythrin stock 1



(b) C-phycoerythrin stock 2



(c) C-phycoerythrin stock 3

Figure 4.6: Amount of C-phycoerythrin (C-PC), allophycoerythrin (A-PC), and phycoerythrin (PE) in the feed, extract and waste phases of a single-stage C-phycoerythrin case study system.

Table 4.3: The 620 to 280 nm purity ratio of each of the feed stocks and extract phase of a single-stage C-phycoerythrin case study system as operated under centrifuge-operation.

Stock type	Purity ratio		C-phycoerythrin loss
	Feed	Single-stage extract	
C-phycoerythrin stock 1	1.84	2.86	24.3%
C-phycoerythrin stock 2	2.16	2.70	24.1%
C-phycoerythrin stock 3	0.81	1.09	31.4%

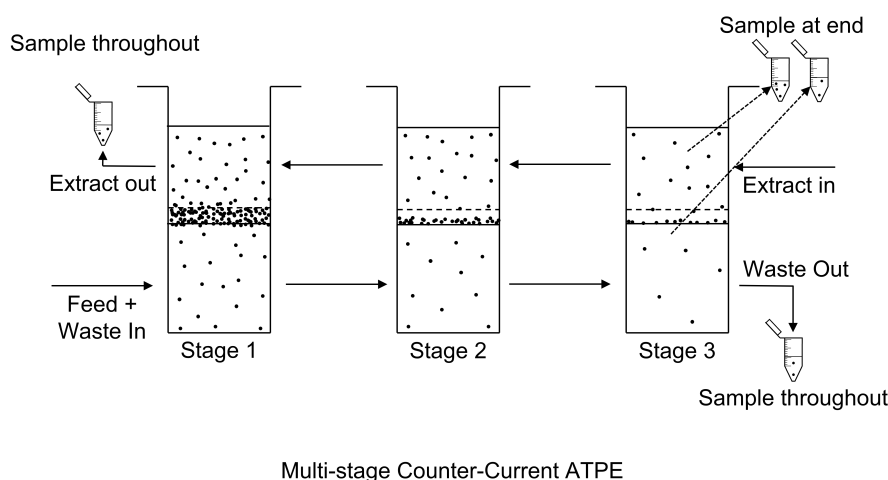


Figure 4.7: A schematic to illustrate the multi-stage extraction set-up.

#### 4.2.4 C-phycoerythrin Stock 1 MSE

The first MSE carried out was a five-stage counter-current ATPE with the case study system with C-phycoerythrin stock 1 feedstock added at stage three. An example set-up is illustrated in Figure 4.7. In this extraction, the aim was to partition C-phycoerythrin into the top phase and the contaminants into the waste phase. Stages to the left of the feed were used to improve the purity, and to the right were used to improve the yield. The extraction was carried out both with the use of a centrifuge and with a gravity separation using the same feed stocks. The results for this MSE are shown in Table 4.4 and in Figures 4.8 and 4.9.

Firstly, it can be seen that the overall purity ratio was improved from 1.84 in the feedstock to 2.98 in a MSE operated with a centrifuge and 2.35 with a MSE operated through the use of gravity. This is shown in Figure 4.8 in which the purity ratios for the extracts out of the MSE are different, with the 620 nm peaks shown to be very similar. However, the 280 nm peak for the centrifuge operation is much lower than that of the gravity operation peak. When comparing both extracts with the feed, the purity ratio has been improved for both, with the 280 nm peak of the

Table 4.4: The purity ratio of each of the C-phycoerythrin stock 1 feed and extract phases of a five-stage C-phycoerythrin case study system with a feed at stage three as operated with a centrifuge and gravity.

Stage	Purity ratio	
	Centrifuge-operation	Gravity-operation
C-phycoerythrin stock 1	1.84 $\pm$ 0.09	
Stage 1	2.98 $\pm$ 0.15	2.35 $\pm$ 0.15
Stage 2	2.71 $\pm$ 0.14	2.37 $\pm$ 0.14
Stage 3	2.47 $\pm$ 0.09	2.24 $\pm$ 0.09
Stage 4	2.09 $\pm$ 0.08	2.10 $\pm$ 0.08
Stage 5	1.71 $\pm$ 0.27	1.87 $\pm$ 0.27

feed above that of both the extracts and the 620 nm peak below that of the extracts, showing that the purification was successful. The shoulder at 652 nm seen in the feed has been removed in the extract spectra and the waste stream spectra shows a very pronounced hump at 652 nm, indicating that allophycoerythrin is leaving in the waste stream. When comparing both the [MSEs](#) with the single-stage extraction, the centrifuge-operated [MSE](#) just outperformed the single-stage extraction in terms of purity, which had an extract purity of 2.86, but the gravity operated [MSE](#) did not. This is likely because the gravity operated separation was still undergoing separation.

Between the feed and waste exit, the amount of C-phycoerythrin is reduced in both stages at each step, therefore increasing the yield of the system. Between the extract exit point and the feed, there is a dilution of the C-phycoerythrin. This trend is also observed in the behaviour of phycoerythrin which also partitions into the top phase. However, there was no dilution effect observed with allophycoerythrin in the waste phases between the feed and the waste exit. This was because the waste phase contains the entirety of the bottom phase and allophycoerythrin overwhelmingly favours the bottom phase.

From Figures [4.9a](#) and [b](#), it can be seen that the [MSEs](#) lost 19.4% and 21.1% of the target protein to the waste in the centrifuge operated and gravity operated [ATPE](#), respectively. The centrifuge-operated system marginally outperformed the gravity operated system, and both were only a marginal improvement over the single-stage extraction which was unexpected.

When looking at the final stage in Figures [4.9a](#) and [b](#), it can be seen that the partitioning of C-phycoerythrin between the two phases seems to have altered. In this final step, there is around the same amount of C-phycoerythrin in the waste phase as in the extract phase for both types of operation. This could be for three reasons; firstly, the system conditions could have been altered in the [MSE](#) enough

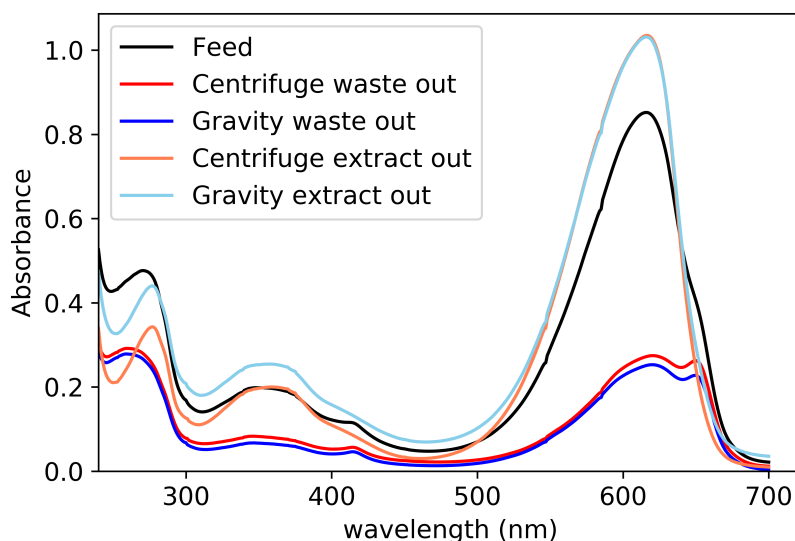
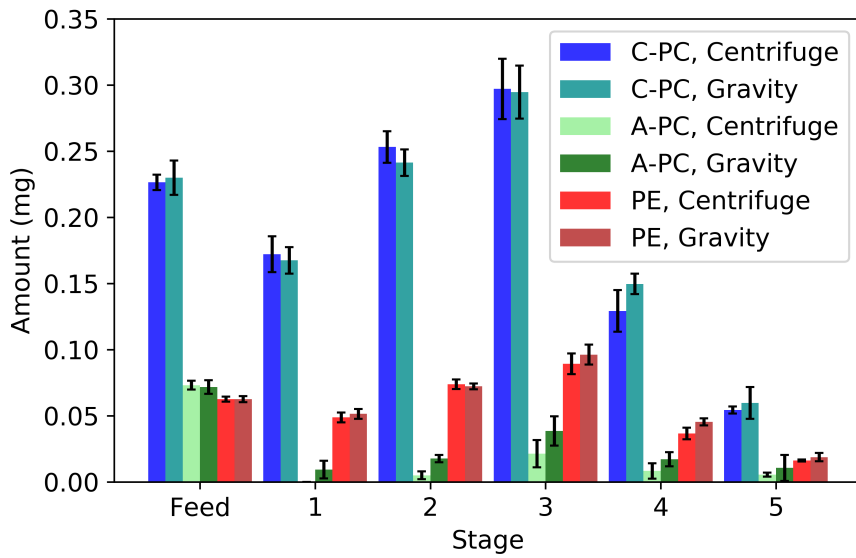


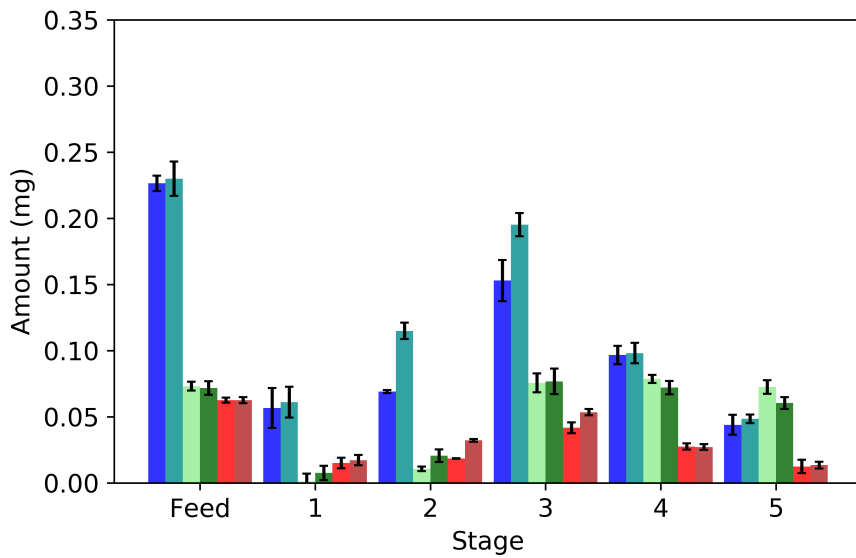
Figure 4.8: UV-vis spectra of the extract, waste and feed of a C-phycoerythrin case study five-stage counter-current ATPS. System was spiked with C-phycoerythrin stock 1 in stage three. As operated using gravity and centrifuge separation.

to shift the partitioning conditions. This is unlikely as no shift in the position of the horizontal interface was observed in these systems. Secondly, a contaminant could be collecting in the bottom phase of the ATPE and is at its highest concentration at stage five, at which point it is at a high enough concentration to shift the partitioning conditions for other proteins in the system. Lastly, a small amount of protein could have become precipitated in the horizontal interface at each step which could not redissolve under the conditions used in the MSE (Albertsson, 1971). This would be more likely to happen in a system operated with a centrifuge and at high protein concentrations as both of these would force protein into the horizontal interface. If protein precipitates in the horizontal interface, it would build up over each step and be seen most prevalently at stage five where the waste phase containing the horizontal interface exits the MSE. Once the phases were extracted for analysis at the end of the experiment, the protein in the horizontal interface would be more likely to redissolve once phases were diluted for analysis and re-shaken. The protein that was able to redissolve under these new conditions would then be able to be detected with UV-vis analysis.

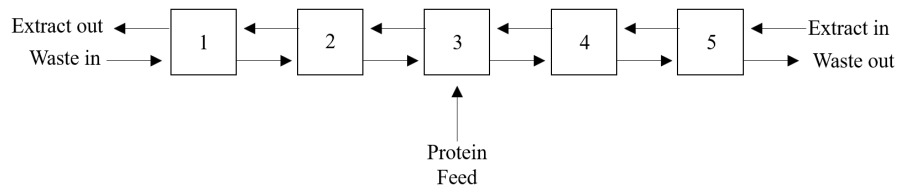
Figure 4.9 shows there is more C-phycoerythrin and phycoerythrin measured in the waste of the system operated through gravity settling than the system operated through the use of a centrifuge in stages two and three. Despite this, the centrifuge operation only had a marginal overall improvement of yield which was within error.



(a) Extract Phase



(b) Waste Phase



(c) Block diagram

Figure 4.9: Amount of C-phycoerythrin (C-PC), allophycoerythrin (A-PC) and phycoerythrin (PE) in the extract and waste phases of each stage of a C-phycoerythrin case study five-stage counter-current ATPS. The system was spiked with C-phycoerythrin stock 1 in stage three. As operated using gravity separation and centrifuge operation.

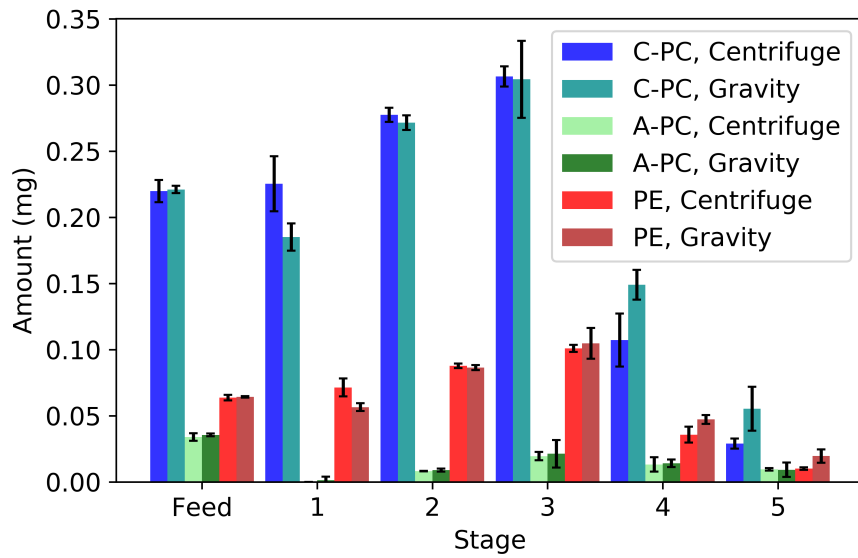
Figure 4.9 shows that there is some allophycocyanin observed in the extract phase when the system is operated with a gravity separation, whereas with a system operated with a centrifuge does not have any allophycocyanin in the extract phases of stage one and two. It was not expected that allophycocyanin would be found in the extract phases of the experimental MSE, as there are very low concentrations of allophycocyanin in the system, and other data shown in the equilibrium curves and single-stage extractions all show allophycocyanin partitioning into the bottom phase. It is possible the partitioning of the system changed for the reasons discussed above. Another option is that it was observed that the systems operated under gravity were still cloudy, despite the formation of the horizontal interface, whereas the centrifuged systems were clear. It is possible that small globules of the bottom phase were still moving out of the top phase, taking allophycocyanin with them. This is discussed more in Chapter 6. This behaviour was reflected in the purity ratio and the purity ratio was shown to be better in the centrifuge-operated system than the gravity-operated system.

#### 4.2.5 C-phycoyanin Stock 2 MSE

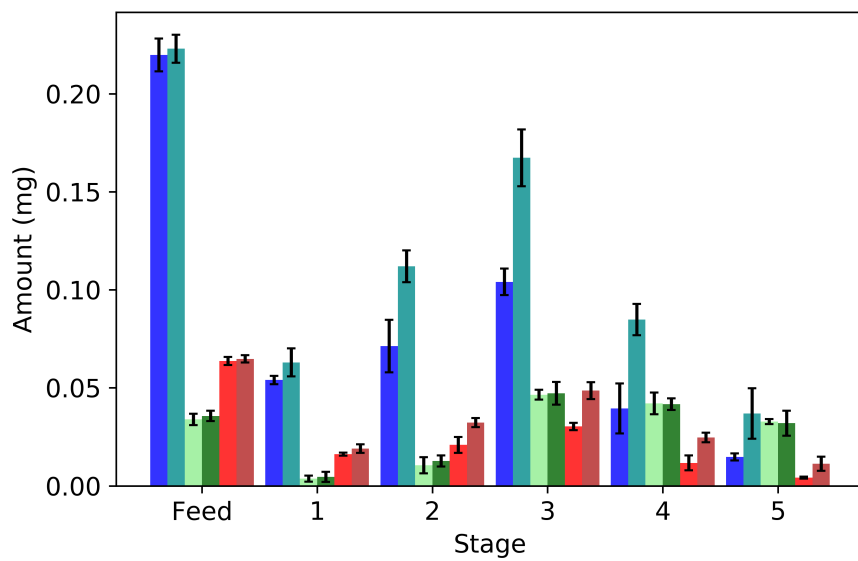
The next MSE which was carried out was a five-stage counter-current ATPE with the case study system with C-phycoyanin stock 2 feedstock added at stage three. In this extraction, the aim was to partition C-phycoyanin into the top phase and allophycocyanin into the waste phase. Stages to the left of the feed were used to improve the purity, and stages to the right of the feed were used to improve the yield. The extraction was carried out both with the use of a centrifuge and with gravity separation. The results for this MSE are shown in Table 4.5 and Figures 4.10 and 4.11.

It can be seen that the purity ratio was improved from 2.16 in the feedstock to 2.7 in a single-stage extraction, 2.65 in a MSE operated with a centrifuge, and 2.5 with a MSE operated through the use of gravity. The loss of C-phycoyanin was 24.1% in a single-stage system, 6.7% in a multi-stage system operated with a centrifuge, and 16.5% in a multi-stage system when operated through gravity.

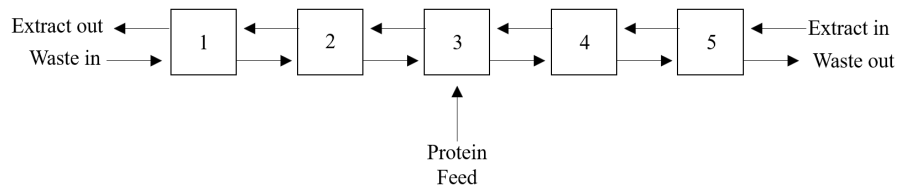
The behaviour of C-phycoyanin follows the same general trend across the stages for both system operations. Between the feed and the waste exit, the amount of C-phycoyanin is reduced in both stages at each step, therefore increasing the yield of the system. However, between the feed and the extract exit, there is still a dilution of the C-phycoyanin. The amount of allophycocyanin is reduced in the extract phase between the feed and the extract exit, thereby increasing the system purity, and is not diluted between the feed point and waste exit point; this can also be seen in the C-phycoyanin stock 1 MSE.



(a) Extract Phase



(b) Waste Phase



(c) Block diagram

Figure 4.10: Amount of C-phycoerythrin (C-PC), allophycoerythrin (A-PC), and phycoerythrin (PE) in the extract and waste phases of each stage of a C-phycoerythrin case study system five-stage counter-current ATPE. System was spiked with C-phycoerythrin stock 2 in stage three. As operated using gravity separation and centrifuge operation.

Table 4.5: The purity ratio of each of the C-phycoyanin stock 2 feed and extract phases of a five-stage C-phycoyanin case study system with a feed at stage three as operated under centrifuge-operation and gravity.

Stage	Purity ratio	
	Centrifuge-operation	Gravity-Operation
C-phycoyanin stock 2	2.16 $\pm$ 0.15	
Stage 1	2.65 $\pm$ 0.10	2.50 $\pm$ 0.04
Stage 2	2.40 $\pm$ 0.03	2.37 $\pm$ 0.04
Stage 3	2.23 $\pm$ 0.04	2.21 $\pm$ 0.11
Stage 4	1.86 $\pm$ 0.11	2.14 $\pm$ 0.07
Stage 5	1.23 $\pm$ 0.15	1.80 $\pm$ 0.34

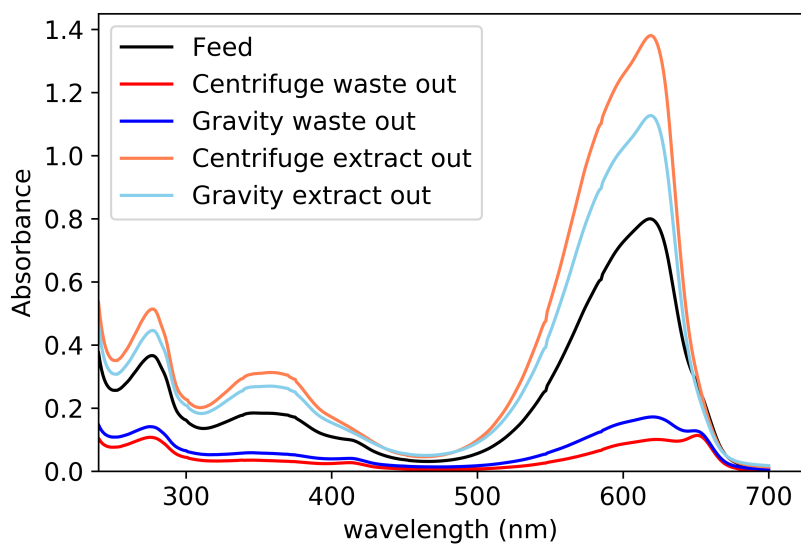


Figure 4.11: UV-vis spectra of the extract, waste and feed of a C-phycoyanin case study five-stage counter-current ATPS. System was spiked with C-phycoyanin stock 2 in stage three. As operated using gravity separation and centrifuge separation.

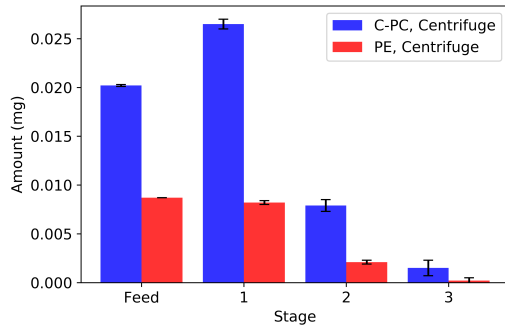
The spectra analysis shown in Figure 4.11 shows the same patterns as seen in the C-phycoerythrin stock 1 MSE. Not only is the purity ratio better for the centrifuge operation, but the 652 nm peak in the feed is removed in the extract and is pronounced in the waste feed. The purity ratio of the system was improved over that of the feed but was not improved compared with the single-stage system. It is possible this is because phycoerythrin, or another protein contaminant, is being concentrated into the extract phase at a greater rate than C-phycoerythrin over the multiple stages. It could be expected that phycoerythrin would partition more readily into the top phase than C-phycoerythrin because phycoerythrin has a lower isoelectric point.

#### 4.2.6 C-phycoerythrin Stock 3 MSE

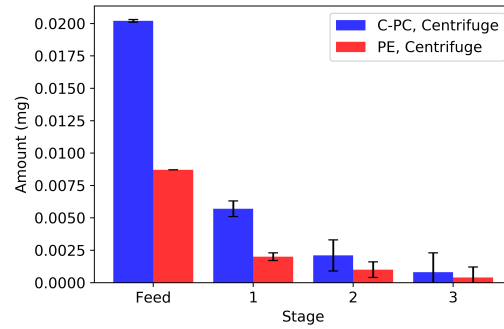
The last MSE carried out was a three-stage counter-current ATPE with the C-phycoerythrin stock 3 stock added in stage one. As there was no allophycoerythrin in this system, no stages were placed to the left of the feed. The aim of the experiment was to see if a MSE could be used to improve the yield of the process and if there is a difference in system behaviour when the ATPE was operated using a gravity separation versus using a centrifuge. While it should be noted that the feeds varied because of the way the C-phycoerythrin was produced, some qualitative comparisons and observations can be made in conjunction with the other extractions. The results for this MSE are shown in Table 4.6 and Figures 4.12 and 4.13.

From Table 4.3 and Figure 4.12 it can be seen that the loss of C-phycoerythrin in the single-stage system was 31.4% of the feed, whereas in the MSEs the loss of C-phycoerythrin was 4.0% and 14.3% in the centrifuge-operated and gravity-operated system, respectively. The centrifuge-operated system had a higher yield than the gravity-operated system; this could be a result of having a lower protein concentration in the feed as well as the mode of the operation.

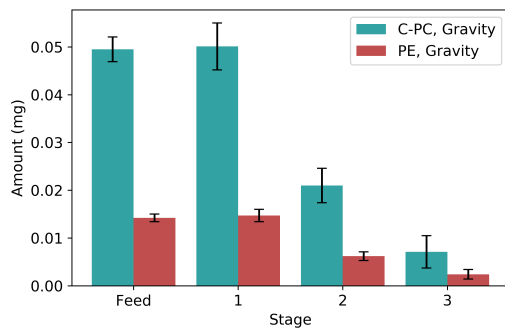
Interestingly, Figure 4.13 shows that even though the feed used in the centrifuge operation had a much lower purity ratio than that used in the gravity operated multi-stage operation, a higher ratio was achieved in the extract. For the centrifuge operation, a feed with a purity ratio of 0.58 was introduced into the system, and the purity was improved to 1.22 in the extraction. For the gravity operation a feed with a purity ratio of 0.82 was introduced into the system and only a 1.03 purity ratio was achieved in the extract. This could be due to several reasons. Firstly, a higher protein loading in the system; however, this is unlikely as the total concentration of both of these extractions is significantly lower than that used in both C-phycoerythrin stock 1 and 2 extractions. Secondly, in the feed introduced with the centrifuge operation there is a protein contaminant which is present in significantly



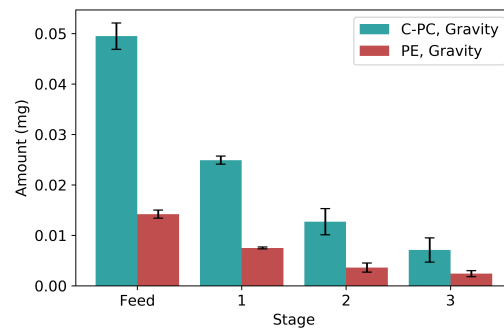
(a) Extract Phase, Centrifuge



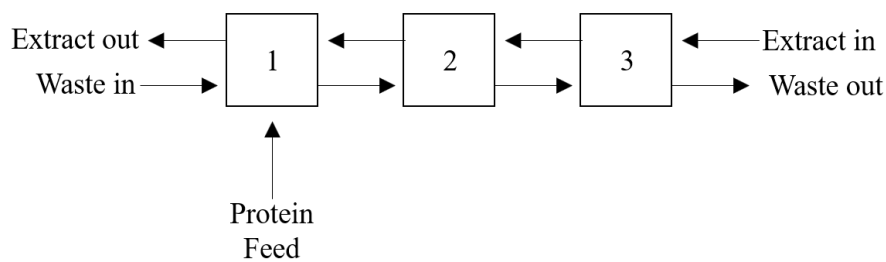
(b) Waste Phase, Centrifuge



(c) Extract Phase, Gravity

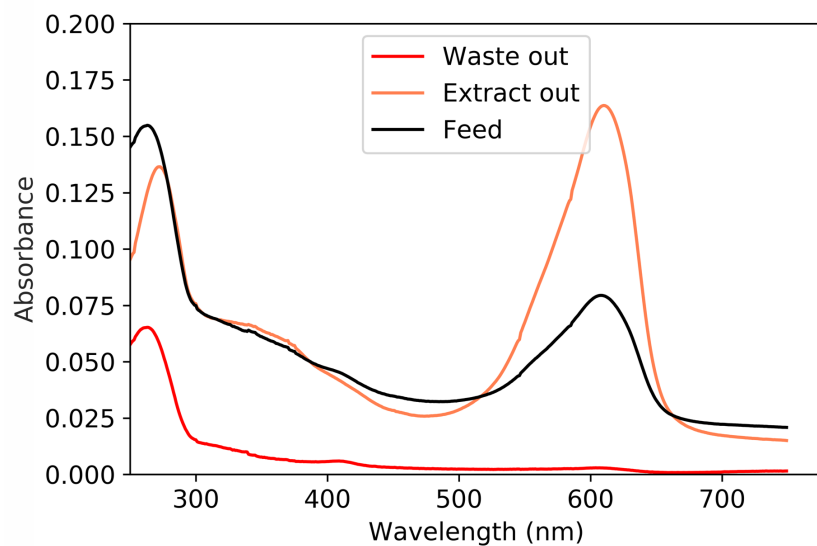


(d) Waste Phase, Gravity

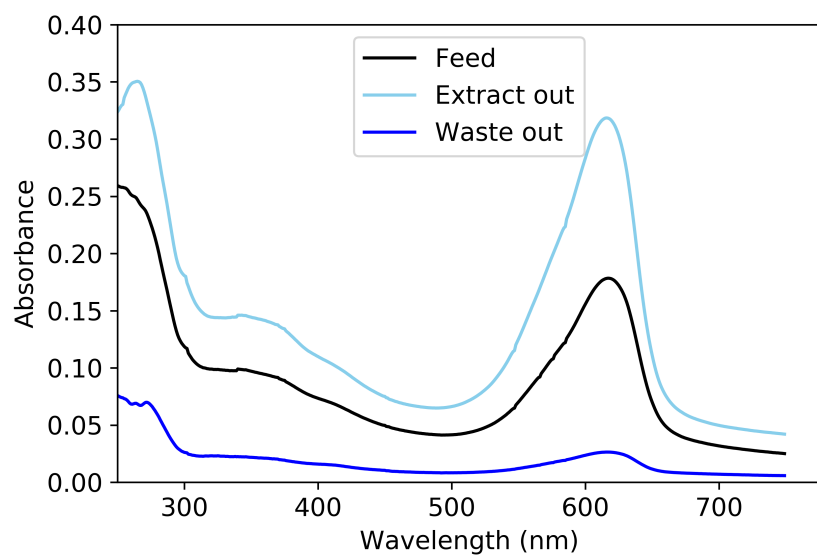


(e) Block diagram

Figure 4.12: Amount of C-phycoerythrin (C-PC) and phycoerythrin (PE) in the extract and waste phases of each stage of a C-phycoerythrin case study three-stage counter-current ATPS spiked with C-phycoerythrin stock 3. As operated using gravity separation and centrifuge operation.



(a) Centrifuge Operation



(b) Gravity Operation

Figure 4.13: UV-vis spectra of the extract, waste and feed of a C-phycoerythrin case study three-stage counter-current ATPS spiked with C-phycoerythrin stock 3. As operated using gravity separation and centrifuge separation.

Table 4.6: The purity ratio of each of the C-phycoerythrin stock 3 feed and extract phases of a three-stage C-phycoerythrin case study system as operated under centrifuge operation and gravity.

Stage	Purity ratio	
	Centrifuge-operation	Gravity-operation
C-phycoerythrin stock 3 Feed	0.58 $\pm$ 0.14	0.82 $\pm$ 0.04
Stage 1	1.22 $\pm$ 0.05	1.03 $\pm$ 0.09
Stage 2	0.80 $\pm$ 0.16	0.79 $\pm$ 0.16
Stage 3	0.35 $\pm$ 0.52	0.52 $\pm$ 0.49

higher concentrations than in the gravity-operated system and this protein either favours the bottom phase or alters the partitioning of the system. Lastly, the mode of operation could have resulted in these changes, as protein may still be separating in the gravity operation.

From Table 4.6, it can be seen that MSE did not improve the purity of the system, but instead made the extraction worse. It is likely that the phycoerythrin contaminant (or another contaminant) is accumulating in the extract phase faster than C-phycoerythrin.

#### 4.2.7 Overview of MSEs

From the three extractions carried out, it can be seen that the use of MSE can be used to improve both the yield and the purity of the process. All of the multi-stage processes decreased the loss of the target protein in the waste output. It can be seen from Table 4.7 that the most successful of the MSEs was the centrifuge operated C-phycoerythrin stock 3 MSE which reduced the waste output from 31.4% in a single extraction to 4%. The purity of the process was also improved in all of the MSEs, with the most successful extraction improving the purity ratio from 1.86 to 2.98 for the centrifuge operated C-phycoerythrin stock 1 MSE. However, there were varying amounts of success achieved across the different extractions which could be a result of a variety of factors including: the modes of operation, differences in feeds (contaminant and target protein concentration), partitioning of protein changing across stages, and contaminants concentrating into the extract phase.

In terms of whole system behaviour, stages towards the extract output improves the purity of the system, and stages towards the waste phase output considers the yield of the system; this is illustrated in Figure 4.14. For each stage added onto the system, there is a stepwise reduction of protein in the phase it does not partition to. The yield of the system is easier to consider. It is a result of the behaviour of the target protein, and while other proteins may influence the target behaviour, how

Table 4.7: The purity ratio and % of C-phycoyanin lost in the waste output with respect to the feed for all extractions carried out.

Feed	Extraction					
	Single-stage		Multi-stage, Centrifuge		Multi-stage, Gravity	
	purity ratio	% C-phycoyanin loss	purity ratio	% C-phycoyanin loss	purity ratio	% C-phycoyanin loss
Stock 1	2.86	24.3%	2.97	19.4%	2.35	21.1%
Stock 2	2.70	24.1%	2.65	6.7%	2.50	16.5%
Stock 3	1.09	31.4%	1.22	4.0%	1.03	14.3%

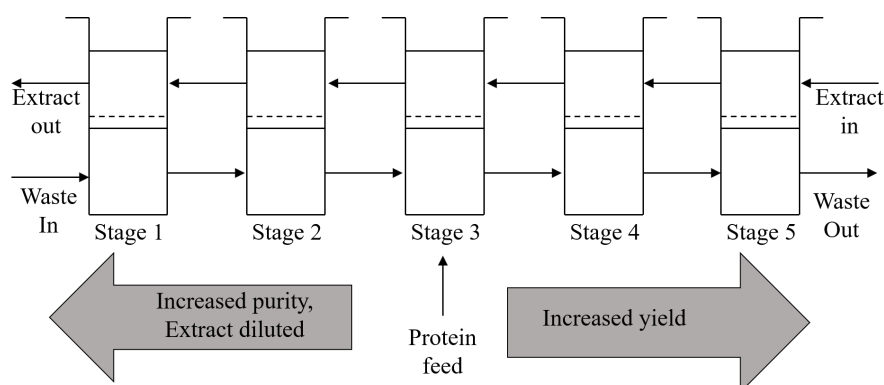


Figure 4.14: A schematic to demonstrate the general trends seen across the six MSEs carried out.

those proteins themselves behave does not affect the yield.

To improve the yield, the amount of target protein in the waste phase leaving the system should be minimised. To do this, stages should be added between the feed and the point at which the waste phase exits the system. The purity is more complicated because each contaminant may behave differently. As a result, while an extra step may be removing one contaminant, it may be concentrating another into the extract phase. Each contaminating protein may be influencing other proteins and the system behaviour. Proteins may partition at different rates and if the target protein is already in the extract phase, extra stages could reduce the purity by further concentrating contaminants into this phase. To remove a contaminant which is moving into the extract phase, a different system would then need to be selected. If only a single contaminant which is partitioning into the waste phase is considered alone, it can be seen there is a stepwise reduction of the contaminant between the feed and the extract collection.

For each additional step, there are trade-off's (aside from cost) that must be considered. For a system in which the waste phase is made up of part of the top

phase, the concentration of the target protein would be diluted for each step added between the feed and the extract collection point as fresh top phase or more dilute (in terms of target protein concentration) top phase is added to compensate for the loss of top phase in the waste. To offset the dilution, more of the top phase should be taken up in the extract, and to minimise the dilution, the entire top phase should be taken up. However, this would be very difficult to practically achieve, and may result in impurities in the horizontal interface being taken up with the extract. Even if all the top phase was taken up in the extract, protein is never 100% partitioned towards one phase, so there would still be a dilution effect. This means that no extra steps other than those required should be added, as it would reduce the performance of the process.

It can also be seen that the operating conditions make a difference to the results of the extraction. All three of the [MSEs](#) showed differences between the results when operated using the two methods: centrifuge operation, and gravity settling. The mechanisms behind these are complicated and require more experimentation to determine. In particular, the kinetics of the phase separation between the formation of the horizontal interface and true equilibrium, and material behaviour at the horizontal interface need to be studied in more detail to determine why this behaviour occurs. This is explored more in [Chapter 6](#).

From the specific extraction carried out, it can be seen that allophycocyanin favours the bottom phase, and C-phycocyanin and phycoerythrin favour the top phase. This could be a result of the isoelectric points of the protein shown in [Table 4.1](#); C-phycocyanin and phycoerythrin had lower isoelectric points than allophycocyanin and so are more readily partitioned into the extract phase. This suggests that it would be difficult to extract allophycocyanin and phycoerythrin from C-phycocyanin using a single system without the use of affinity ligands and [Aqueous Two-Phase Affinity Partitioning \(ATPAP\)](#) because C-phycocyanin's isoelectric point lies between that of allophycocyanin and phycoerythrin. As exact isoelectric points and [MWs](#) vary between different types of production methods / species used to produce the protein, it would be helpful to specifically characterise major components within a feed. The literature suggested that phycoerythrin may have a slightly higher [MW](#) than C-phycocyanin, so a higher [MW PEG](#) could be considered to discourage phycoerythrin from partitioning into the top phase. However, this may make both phases unfavourable to both phycoerythrin and C-phycocyanin as they are both large proteins and result in large amounts of material partitioning into the horizontal interface. It may be more sensible to carry a two-step extraction where the second step back-extracts the C-phycocyanin into the salt phase, while phycoerythrin still partitions into the [PEG](#) phase. If specific analysis of the protein shows difference in

the hydrophobic / hydrophilic amino acid ratios in the proteins, changing the **TLL** of the system could be used to alter protein partitioning.

In comparison with other purification methods, the **ATPS** used in this chapter was very good at separating C-phycoerythrin from allophycoerythrin. This is desirable as allophycoerythrin is commonly produced alongside C-phycoerythrin which pollutes the colour of the dye C-phycoerythrin. The purity ratio achieved sits in line with other literature for purification procedures of C-phycoerythrin; [da Silva Figueira et al. \(2018\)](#) achieved purity ratios of around 3 using a combination of ion exchange chromatography and diafiltration. Additional steps of diafiltration and precipitation allowed for a purity ratio of >4 to be achieved. While high purity ratios were achieved with these steps, global yields were between 58% (purity ratio = 3) and 42% (purity ratio = 4). A similar purity ratio (3) was achieved for the multi-stage centrifuge extraction of C-phycoerythrin stock 1, with a recovery of over 80%. These extractions are not directly comparable as the starting feed stock used in [da Silva Figueira et al. \(2018\)](#)'s work was cruder; however, it demonstrates that **ATPE** is in line with other purification procedures (including chromatography) in the literature. [Patil and Raghavarao \(2007\)](#) used single-stage **ATPE** to purify C-phycoerythrin and reported purity ratios of between 2 and 3.5 in a single step with recoveries of between 80% and 97%. Higher purity ratios were reported with salt buffers with a pH of around 6 which indicates that a more optimal system could have been selected for the **MSEs** carried out in this work. This is in line with the 'practical guidelines' published by [Benavides and Rito-Palomares \(2008\)](#) who state that setting the pH of the salt buffer too high encourages partitioning of contaminants into the extract phase. The very high yields reported by [Patil and Raghavarao \(2007\)](#) are theoretical and based upon the assumption that complete separation of the top and bottom phase could be achieved; in reality, this is very unlikely and these are likely to decrease as a result.

From the results, it can be seen that while the multi-stage configurations used improved the separation, they may not be optimal. The majority of the allophycoerythrin was removed within two steps, however, more of the C-phycoerythrin could be removed from the waste output. As a result, it would likely improve the results of the extraction to move the feed from stage three to stage two.

### 4.3 Conclusions

In conclusion, multi-stage **ATPE** is a tool which can be used to improve the yield and purity of a single-stage extraction; however, to do so effectively, the system and feed need to be properly characterised and controlled. It has been shown that

stages between a feed and extract collection can be used to improve the system purity, and stages between the feed and waste output can be used to improve the yield. Three different contaminant mixes were studied, evaluating single-stage vs multi-stage [ATPE](#) using two different modes of operation: centrifuge and gravity separation. All multi-stage operations had an improvement in yield when compared with the single-stage operation; however, the purity was not improved through extra stages. This was a result of the contaminant which favoured the salt-rich phase, allophycocyanin, being almost completely extracted in a single step making the additional steps unnecessary. If the feed contained a contaminant which was only partially removed in a single step additional stages could be utilised to improve the purity. The major finding of this chapter is that the two modes of operation, gravity and centrifuge settling, showed a difference in performance. In the [MSE](#), the centrifuge operation outperforming the gravity operation in both yield and purity. It is expected that this is a result of separation still taking place in the gravity system. This chapter shows that more work is required to understand both the behaviour of individual proteins and how they behave together with an [ATPS](#) to properly design and utilise multi-stage processes. In terms of system operation, the kinetics of the phase separation between the formation of the horizontal interface and true equilibrium need to be studied in more detail in order to understand the discrepancies between systems operated through the use of a centrifuge and with a gravity separation.

## Chapter 5

# Equilibrium Modelling of Multi-stage Aqueous Two-Phase Extraction

### 5.1 Introduction

The previous chapter demonstrated that [Multi-stage Extraction \(MSE\)](#) can be used to improve the resolution and performance of [Aqueous Two-Phase Extraction \(ATPE\)](#). It demonstrated that the systems need to be understood to a greater degree to enable multi-stage process design and optimisation. It also showed that there were a large number of mechanisms happening within the system. As a result, this chapter aims to evaluate multi-stage systems which have reached equilibrium at each stage, as defined by a clear phase rather than the formation of a horizontal interface and break down the component parts of the process in order to understand them more thoroughly. By gaining a better understanding of the system, the aim is to improve the accuracy of multi-stage modelling techniques enough to use them as a tool to aid in the design of multi-stage [ATPE](#). Consequently, the chapter looks at: evaluating the behaviour of a single model proteins, haemoglobin and C-phycoyanin, in a multi-stage system, building and validating a model to describe multi-stage [ATPE](#), and then using the model in this chapter for multi-stage [ATPE](#) process design.

As previously discussed, [ATPE](#) has two major drawbacks which need to be addressed in order for the process to be commercially viable: a low resolution, and a lack of understanding of the phase forming mechanisms ([Asenjo et al., 1994, 2002b; Rito-Palomares, 2004; Ruiz-Ruiz et al., 2012](#)). These drawbacks are inherently linked as the latter drawback has resulted in a lack of predictive models to describe the

partitioning of protein in systems (Torres-Acosta et al., 2019). This in turn has resulted in systems under performing in terms of process yield and purity.

Recent advances in modelling protein partitioning have involved using the physiochemical properties of both the system and the protein of interest to predict partitioning behaviour. Properties which have been considered in modelling protein partitioning include amino acid composition and structural features of the protein of interest as well as effects of salts (Salgado et al., 2008; Ferreira et al., 2015a,b). While establishing patterns of behaviour upon changing individual parameters is important, the ultimate goal would be to be able to predict and optimise the partitioning behaviour from a protein's characteristics. One attempt at this was made by Dismer et al. (2013) who predicted the binodal curve of a system and, from that, the partitioning of a particular protein through the use of molecular dynamic simulations.

While progress in this type of modelling has been made, there are still developments which need to be made to satisfactorily model protein partitioning in ATPE. This can be attributed to the large variety in different types of systems and the shifts in behaviour which, in some systems, can be a result of even small changes in conditions. Key process parameters which should be considered in system selection include:

- Type of phase forming components (i.e. polymer type(s), salt type)
- Use of additional constituents (i.e. NaCl, affinity ligands)
- Operating temperature
- Salt pH
- Polymer molecular weight
- System composition
- Flow rates for continuous operation
- Separation time and method

In order to speed up the development of predictive partitioning ATPE models, the use of high throughput screening and robotic-aided strategies has been suggested in order to maximise the amount and the consistency of the experimental data available (Torres-Acosta et al., 2019). Until robust and accurate models are available to optimise system selection so that systems are routinely capable of achieving high resolutions in a single step, alternative modelling strategies to improve the process should be explored.

One such area which can be explored is the modelling of multi-stage systems. The previous chapter showed this strategy can improve resolutions, but modelling tools still need to be developed to aid in multi-stage process design. Modelling strategies have been applied to both multi-stage [ATPE](#) as well in other two-phase extraction processes within the chemical processing industry. In an industrial setting, low-resolution two-phase extraction processes are routinely designed using multi-stage modelling to improve the performance of the process.

One method commonly used is the McCabe-Thiele method which has most extensively been applied to binary distillation, but has also been applied and modified for traditional [Liquid-Liquid Extraction \(LLE\)](#) and [ATPE](#) ([Richardson et al., 2002](#); [Seader et al., 2006](#); [Rosa et al., 2009b,a](#)). [Warade et al. \(2011\)](#), adapted McCabe-Thiele for traditional [LLE](#) and used this method to optimise the number of stages for a required purity. In binary distillation, there are only two components in the system: one is the target, and the other the contaminant. They each made up the dominant component in one of the two-phases of the system. As a result, by considering one component, the other component's concentration can be inferred. This is not possible in [ATPE](#) and traditional [LLE](#) as the material which determines the phase formation is mostly independent of the material to be partitioned. In [ATPE](#), the phase forming components (i.e. polymer(s), salt(s) and water) and system environmental conditions (i.e. temperature and salt pH) determine the partitioning of the target and contaminants (i.e. proteins, cells and solutes). While the concentration of other protein may influence the partitioning of another protein to some extent, the overriding driver behind protein partitioning is the phase forming components and environmental conditions. Consequently, one partitioned protein component cannot be used to infer the concentration of another partitioned protein component. While this can be problematic, it is advantageous as proteins to be partitioned can be evaluated separately assuming that the protein components are not significantly interacting, therefore simplifying the modelling required to evaluate the system.

The McCabe-Thiele method has been adapted for [ATPE](#) by [Rosa et al. \(2009a,b\)](#) and [Liu et al. \(2018\)](#). For the method to be adapted, equilibrium curves which evaluate the concentration of a component within each phase of the system were constructed. [Rosa et al. \(2009a\)](#) used the equilibrium curve of [Immunoglobulin G \(IgG\)](#) in a [Polyethylene Glycol \(PEG\)](#)-salt system to evaluate the number of steps required for the removal of [IgG](#) from the waste phase of the system. They also constructed an equilibrium curve for different fractions of [Chinese Hamster Ovary \(CHO\)](#) cell media, considering high and low molecular weight components separately, to predict the success of extracting [IgG](#) from [CHO](#) cell media using [ATPE](#). They did

not evaluate the number of steps required to remove the CHO cell media. Liu et al. (2018) used ionic liquid based ATPE to purify tetracycline, again only considering and optimising the yield of the system.

In these models, the concentration of the target component to be partitioned in each of the phases (top and bottom) is considered. However, it has been noted in ATPE that material can partition into the horizontal interface (Albertsson, 1971; Andrews and Asenjo, 1996). Figure 5.1 shows the two types of system described by Albertsson (1971): Liquid-Liquid (LL) distribution, and Liquid-Interface (LI) distribution, as well as a third theoretical Liquid-Interface-Liquid (LIL) distribution which is considered in this chapter. In a system with LL distribution, the material partitions between the top and bottom phase of the system, whereas, in a system with LI distribution, material partitions into only one of the liquid phases and the rest partitions into the horizontal interface. Systems with a LL distribution which become overloaded with protein have been observed to have protein aggregate and partition into the horizontal interface. This has been observed in systems with very high protein concentrations (Albertsson, 1971). This horizontal interface partitioning in overloaded systems was reported by Mündges et al. (2015) to affect the purity and yield of an ATPE of IgG from CHO cell media. Theoretically, most of the aggregated protein in the horizontal interface should redissolve in more favourable conditions, including lower protein concentrations, meaning that MSE could be used to overcome this issue. However, models will need to account for horizontal interface partitioning to accurately simulate system operation (Albertsson, 1971). Another component commonly found in ATPE is cell debris; this has also been shown to partition readily into the horizontal interface of a system Albertsson (1971). In ATPE where any material, contaminant, or target partitions into the horizontal interface of a system, models that only describe partitioning in terms of the two liquid phases will deviate from the true values. Andrews and Asenjo (1996) published work which indicated that true LL distribution did not occur in systems often and found protein partitioned into the horizontal interface even at low protein concentrations.

This chapter aims to build upon the multi-stage ATPE modelling work of Rosa et al. (2009b,a) and Liu et al. (2018) with the added consideration of partitioning of material into the horizontal interface of a system. The work firstly models the behaviour of a single protein, haemoglobin, in multi-stage systems using single-stage equilibrium data. Haemoglobin was used at this stage because it was easily obtained in isolation. Two models were compared: the first assuming a LL distribution, and the second assuming a LIL distribution. Predictions for three case study multi-stage ATPE were carried out and validated against experimental data. At this stage, experimental MSE and modelling predictions were carried out using both

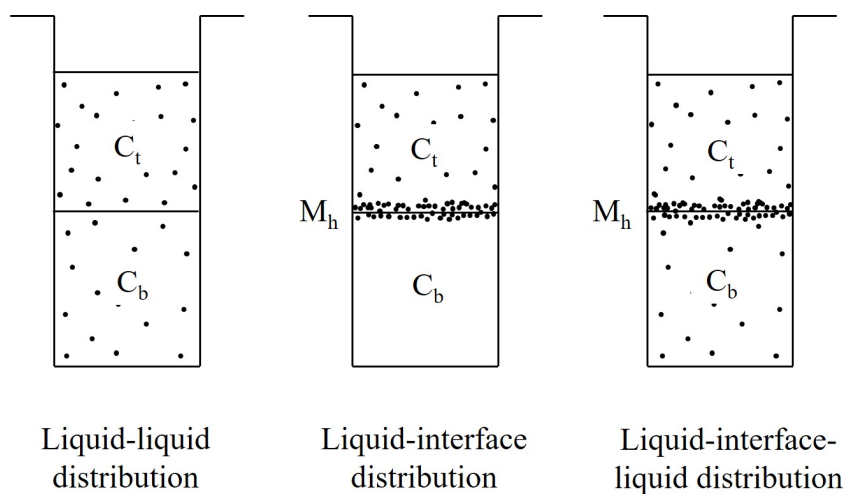


Figure 5.1: A diagram to show the different options for distribution of material in ATPE, adapted from Albertsson (1971).

haemoglobin and C-phycoyanin. Lastly, the work demonstrates how the model developed in this chapter can be used to build multi-stage, multi-step ATPE. A multi-stage ATPE was developed for an extraction of C-phycoyanin from model contaminant lysozyme, evaluating both purity and yield.

## 5.2 Results and Discussion

The aim of this chapter is to develop a model for multi-stage ATPE which is accurate enough to be used in process design. To do this, a more in depth understanding of protein behaviour in single-stage systems needs to be built. As such, this section is divided into three sections. In the first, the development of the model is discussed and results are presented. In the second, the model is validated against three MSEs. In the last section, the model is used to design a multi-stage ATPE of C-phycoyanin from lysozyme.

### 5.2.1 Model Development

Haemoglobin was chosen as the model protein to develop the MSE model. This was done so that a single protein could be studied in isolation away from contaminants and so that the model could be tested on more than one protein and system. Haemoglobin was chosen as a model protein because of its pigment, making it easy to analyse, and because there is literature surrounding extracting haemoglobin in ATPE.

The first step in developing an ATPE process is to screen for systems which

have desirable extraction conditions. In [ATPE](#), target proteins are often extracted into the top [PEG](#)-rich phase of a [PEG](#)-salt system. For single-stage extractions, the screening process may have to be extensive in order to find appropriate extraction conditions. By utilising [MSEs](#), this process can be drastically reduced because systems with lower resolutions can be accepted. The resolution of the entire process can then be improved by increasing the number of stages.

In [ATPE](#), there are many parameters which can be controlled in order to alter protein partitioning. As a result it can be advantageous to utilise [ATPE](#) literature surrounding a specific protein. In this case, as [ATPE](#) of haemoglobin had been studied before, starting conditions to evaluate were chosen from the literature ([Kan and Lee, 1994](#)). [Kan and Lee \(1994\)](#) found that very high partitioning coefficients for haemoglobin could be achieved using [ATPE](#) with lower molecular weights of [PEG](#), between 600 and 1500, paired with potassium phosphate buffers between 8 and 10.5. As the molecular weight of haemoglobin is around 64.5 kDa and its isoelectric point varies depending on type (but is around pH 7.1), these conditions follow the guidelines established by [Benavides and Rito-Palomares \(2008\)](#) ([Koepke and Miller, 1972](#); [Tame and Vallone, 2000](#)). For this system, an extraction with average partitioning conditions was required so it could easily be improved with [MSE](#). As a result, a [PEG](#) 1500 potassium phosphate with pH 8.0 system was chosen; the exact concentrations screened are shown in [Table 5.1](#).

The results of the screening are shown in [Table 5.1](#) and [Figure 5.2](#); [Table 5.1](#) shows the phase volumes of the systems screened and [Figure 5.2](#) shows the amount of haemoglobin in the top, bottom, and horizontal interface of the systems screened. [Table 5.1](#) shows that systems D, H, and I did not contain enough phase forming material to form two-phase systems. Systems A, B, C, and J partitioned so that one phase contained around 69% of the system, and the other around 31% of the system. For systems A, B, and C, the bottom phase consisted of the largest volume and for system J, the top phase made up the largest volume. While [LLE](#) with very large and small volume ratios are possible to run, it is preferable to set conditions so that the volume ratios are equal, as they are in systems E, K and L. The reason volume ratios equal to 1 are preferable is described later on in this section.

[Figure 5.2](#) shows the distribution of haemoglobin across the horizontal interface, top, and bottom phase of systems screened which formed two-phases. The first thing to note is that material was found in the horizontal interface of all systems screened as well as in both of the liquid phases. Because the majority of material partitioned into the top and horizontal interface phases in all cases, these systems would be classified as having a [LI](#) distribution. However, there is a large amount of protein in these systems so it is likely that the horizontal interface partitioning is exaggerated

Table 5.1: Position of the horizontal interface in a 1600  $\mu\text{L}$  sample of the PEG 1500 - potassium phosphate pH 8.0 systems screened

Label	PEG 1500 (% w/w)	Phosphate buffer (% w/w)	Horizontal interface position (Estimated) ( $\mu\text{L}$ )	Volume ratio $\frac{V_{Top}}{V_{Bottom}}$
A	9.7	12.6	1100	0.45
B	9.5	14.4	1100	0.45
C	9.4	16.2	1100	0.45
D	13.2	9.3	No Phase Formation	n/a
E	13.0	11.2	750	1.13
F	12.8	13.1	1000	0.6
G	12.6	15.0	1000	0.6
H	16.9	5.8	No Phase Formation	n/a
I	16.6	7.9	No Phase Formation	n/a
J	16.3	9.9	500	2.2
K	16.0	11.8	750	1.13
L	15.8	13.7	800	1

by the high protein loading and the top and bottom phases have become saturated.

When an ATPE is carried out, it is preferable that as much of the protein as possible is partitioned into the top and bottom phases, i.e. as suspended or dissolved protein rather than as precipitated protein at the horizontal interface. While Albertsson (1971) notes that precipitated protein in the horizontal interface should theoretically redissolve, in practice, the protein can become damaged, aggregate irreversibly, or be difficult to redissolve. In the literature, mostly the distribution of systems are considered to either be LL or LI; however, Figure 5.2 shows that in all the two-phase systems tested, material distributed across all three regions thereby following a LIL distribution. Relatively high concentrations, around 2 mg/mL, were used in these systems making phase saturation more likely. As higher protein concentrations are reached in a system, more material will partition towards the horizontal interface as the top and bottom regions of the system have become saturated. The point at which material will rapidly partition into the interface varies between systems and is dependent on system conditions and the protein being partitioned.

For further study, system E was chosen as it had a volume ratio close to one as well as a large amount of haemoglobin partitioning into the top PEG-rich phase of the system. While system J had more material partitioning into the top PEG-rich phase, it had a less suitable volume ratio. The volume ratio of the system is important to consider for three reasons. Firstly, there is a relationship between the volume ratio and kinetics of phase separation of a system. Secondly, systems with one large phase and one small phase are more likely to experience horizontal

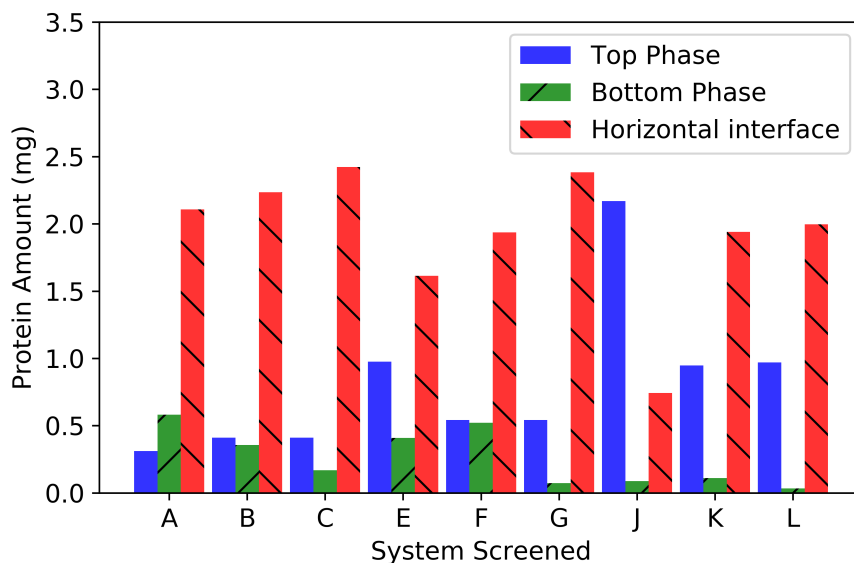


Figure 5.2: Distribution of 3 mg of haemoglobin in the different 1600  $\mu\text{L}$  PEG 1500 - potassium phosphate pH 8.0 systems screened.

interface partitioning as the small phase will quickly become saturated. Lastly, the separator design is dependent on volume ratios.

In terms of relating volume ratios to the phase separation kinetics in a PEG-salt system, systems which have a large top PEG-rich phase and a small salt-rich bottom phase will have a continuous PEG-rich phase. Continuous PEG-rich phases are associated with slower rates of separation due to the high viscosity of the phase (Albertsson, 1971; Kaul et al., 1995). Systems with the fastest phase separation kinetics are usually associated with continuous bottom phases and intermediate positions on the binodal curve where the volume ratios are approximately equal (Salamanca et al., 1998). Slow phase separation rates would cause scalability issues as phase separation is dictated by the system height, meaning slow separation rates at bench scale would be compounded on scale up and much less material could be processed as a result. For systems with a phase which has a small phase volume, even if the phase can handle large concentrations, it will still become saturated quickly because of its reduction in volume, meaning more material will partition into the horizontal interface. Lastly, separator designs are often dependant on the volume ratio of the system; a very large or small volume ratio may require a non-traditional settler design, increasing the complexity and cost of the equipment.

After the system used in the multi-stage ATPE was chosen, single-stage protein partitioning data in the chosen system was required. Firstly, calibration curves for haemoglobin in water, the top, bottom, waste, and extract phases were required; this

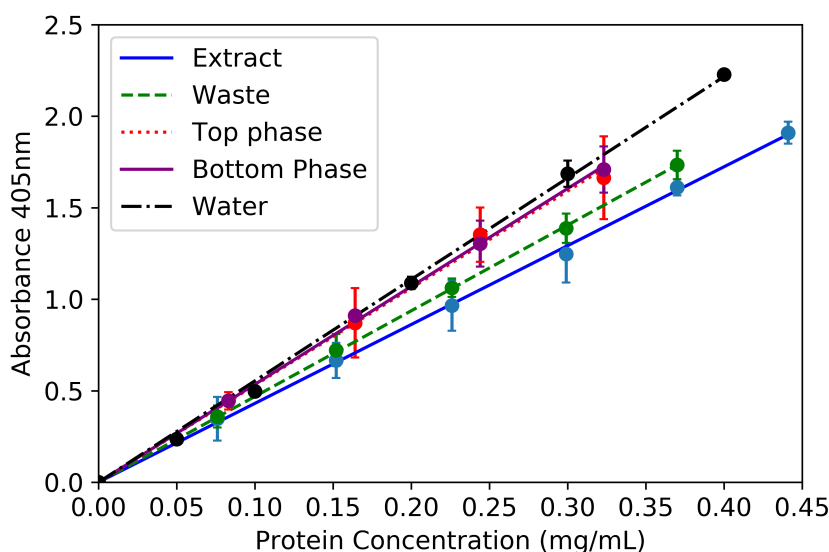


Figure 5.3: Calibration curves of haemoglobin in different concentrations of phase forming components, respective of concentrations used during experimentation.

is shown in Figure 5.3. The results from Figure 5.3 show that there is no statistical difference between calibrations in water, the top, and bottom phases used in the equilibrium curve. The top and bottom phases were diluted by around 1.5 times the sample volume, whereas the MSEs were diluted by 1 times the sample volume. The difference can be seen in the multi-stage calibration curves, which have a shallower slopes. The increase in PEG concentration in the extract and waste samples could be the reason for the difference in the calibration curves.

In order to model a multi-stage system, data on how a protein behaves in a single-stage system was required. As such, an equilibrium curve showing the partitioning of haemoglobin in the haemoglobin case study system to the top, bottom and horizontal interface of a system. Figure 5.4 displays this equilibrium curve in which the concentration of haemoglobin in the horizontal interface is displayed as a concentration relative to the total volume of the system. This is because the size of material in horizontal interface is too small to measure with the precision required to use it in the model and any inaccuracies would propagate through the model creating large amounts of error. The top and bottom phase concentrations are determined from their respective phase volumes. The first observation which can be made from Figure 5.4 is that haemoglobin favours the top phase, followed by partitioning into the bottom phase, and then the horizontal interface of the system of the system.

Haemoglobin is dissolved when it partitions into the top and bottom phases of

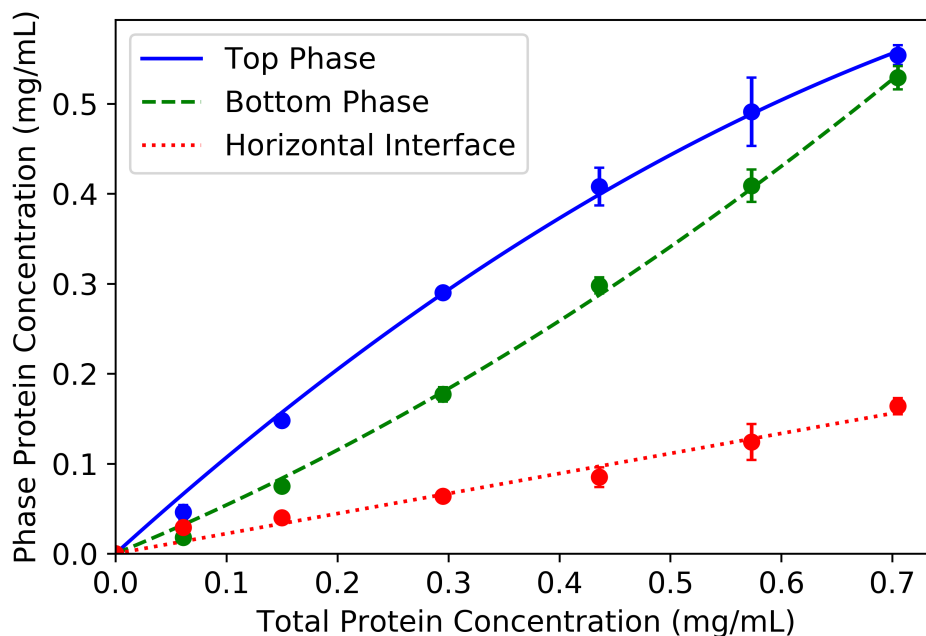


Figure 5.4: The partitioning of haemoglobin in the haemoglobin case study system.

the system; however, is precipitated in the horizontal interface. In the top and bottom phases, the colour of the phase increases in intensity as the concentration of haemoglobin increases. The precipitated material in the horizontal interface sits on top of the boundary between the phases, i.e., the mass in the interface was observed to encroach on the top phase. As the amount of material in the horizontal interface increases, the volume of the mass increases.

Figure 5.4 shows that the partitioning behaviour of the system in all three regions of the systems is fairly linear until a total system concentration of around 0.45 mg/mL was reached. At this point, the top phase begins to become saturated and more material begins to partition into the bottom phase of the system. Partitioning into the horizontal interface of the system follows a linear trend at the concentration range evaluated. If the system was loaded with a high enough concentration of protein, the bottom phase of the system would also become saturated and more material would partition into the horizontal interface, or possibly precipitate at the bottom of the system.

The equilibrium curve in Figure 5.4 also shows that material immediately partitions into all three regions: the top, bottom, and horizontal interface. This contradicts the assumption that the distribution of systems is either LL or LI until the system reaches protein concentrations at which it becomes saturated, and supports

the findings of [Andrews and Asenjo \(1996\)](#) who found partitioning across the top, bottom, and horizontal interface common in [Aqueous Two-Phase Systems \(ATPS\)](#).

Figure 5.5 shows the volume percentage of the horizontal interface against the total amount of haemoglobin in the system. In this system, the size of the horizontal interface got quite large; as a result, the horizontal interface would partition into the extract phase.

Along with Figure 5.4, Figure 5.5 was also used in the modelling. The equilibrium curve was used to predict the concentrations of the phases, and the volume curve was used to predict whether the material in the horizontal interface partitioned into the extract or the waste phase. Systems with a small horizontal interface would have material partition into the waste phase. This mechanism is only relevant in systems where large amounts of material partition into the horizontal interface, and is also dependant on the extraction method and extract volume taken. A volume curve is not required for systems where there is no visible build up of material in the horizontal interface. While the curve in Figure 5.5 is not accurate enough for phase concentrations, it is accurate enough to be used to predict when the volume at the horizontal interface is large enough to partition into the horizontal interface. If a very accurate method of determining the horizontal interface volume could be determined, the concentration of the horizontal interface material could be determined as a function of the horizontal interface volume.

The single-stage data required for the [MSE](#) consists of: equilibrium curves of protein to be evaluated in the system used in the extraction, a horizontal interface volume curve for systems with very large horizontal interface partitioning values, and calibration curves in the phase concentrations used in other analysis. This data is fairly simple to collect and is not extensive or time consuming. System screening can also be carried out in system selection. This may include different phase constituents and concentrations, phase separation rate data, and binodal curves.

### 5.2.2 Model Validation

Both a model using a [LL](#) distribution and one using a [LIL](#) distribution were tested against case study systems to test both the accuracy of the model and if the inclusion of material partitioning into the horizontal interface improved the performance of the model. The models were tested against a three stage counter-current multi-stage system which had haemoglobin fed into the system at stage one. This extraction used the haemoglobin case study system and required single-stage data on phase partitioning and data on the volume of the horizontal interface.

Figures 5.6a and 5.6b show the [Ultraviolet-visible \(UV-vis\)](#) analysis of the extract and waste phases, respectively, of each of the stages. Figure 5.7 shows the amount

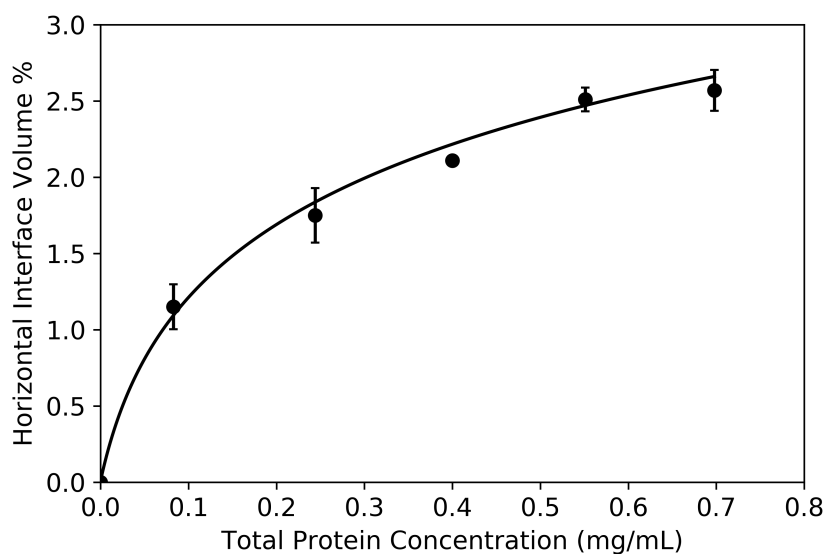


Figure 5.5: Volume of the horizontal interface as a percentage of the total volume in the haemoglobin case study system.

of haemoglobin in the extract and waste phases of each stage of the extraction. It can be seen that the recovery of haemoglobin improved from 61.8% in a single step to 85.3% in three stages which means that the use of MSE drastically improved the yield of the system.

The comparison of the LL and LIL distribution models with the experimental results is shown in Table 5.2. The table shows the amount (in mg) of haemoglobin found in each stage in the extract phases as well as the percentage difference between the experimental data and each of the models with respect to the feed. The feed

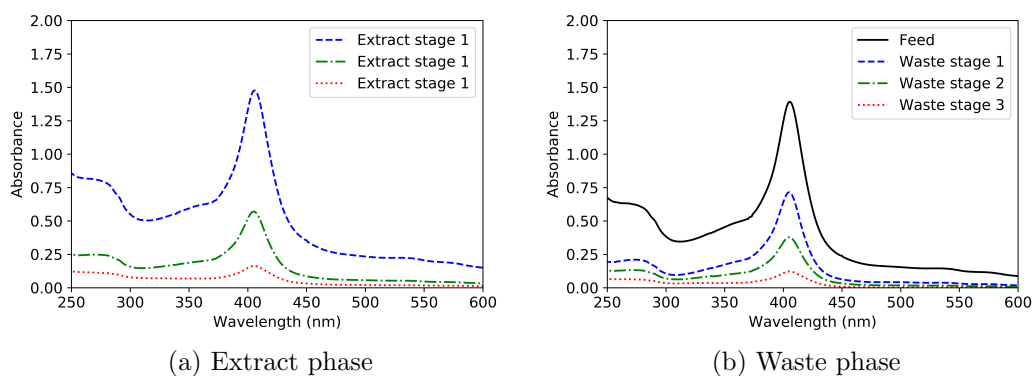


Figure 5.6: The UV-vis analysis of the extract and waste phases of a three-stage counter-current haemoglobin case study ATPE

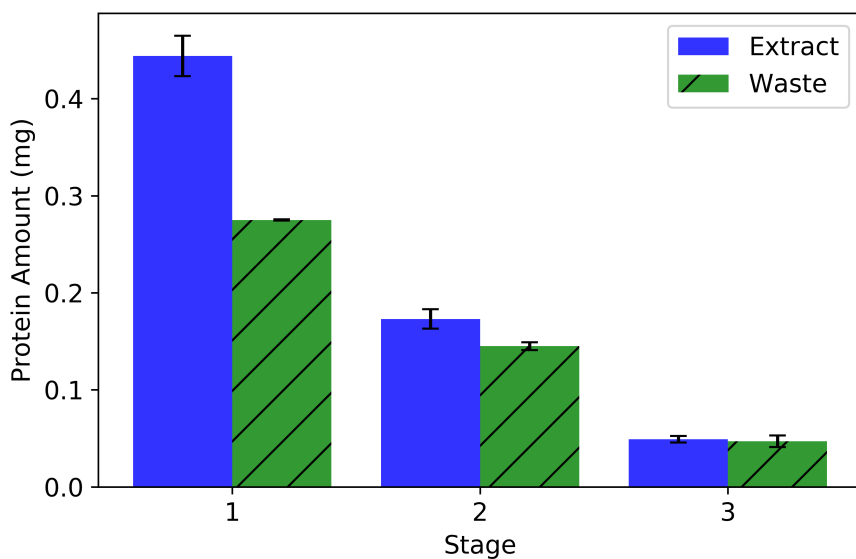


Figure 5.7: The amount of protein in the extract and waste phases of a three-stage counter-current haemoglobin case study [ATPE](#) with the feed in stage 1

for this system was 0.5 mg, 54  $\mu$ L of stock of haemoglobin in a 1.5 mL system. In the [LL](#) distribution model, there is an assumption that all material in the system partitions into the liquid phases of the system. This model is what has been used to previously describe the behaviour of multi-stage [ATPE](#) ([Rosa et al., 2009a,b](#); [Liu et al., 2018](#)). In the case study extraction with haemoglobin, the [LL](#) distribution model can be seen to adequately describe the stages with less material in the system, i.e. stages two and three. However, for the extract in stage one, the [LL](#) distribution model has a error of 40% less material than was observed in the experimental data.

While the model performs adequately at lower concentrations in isolation, any stages placed between the feed and the extract point would carry error forward, even if at a lower concentration which the [LL](#) distribution model could handle. There would also be problems if feeds at a higher concentration were used. In this system, a feed of 0.5 mg was used, which reflected a total concentration of around 0.322 mg/mL. The experimental data showed that after 15 runs, the total amount of protein in stage one is 0.719 mg amounting to a total concentration of 0.462 mg/mL. [Figure 5.4](#) showed that the system started becoming saturated at concentrations of  $>0.45$  mg/mL meaning that the system had only just started to reach the point at which it was becoming saturated. This means that the [LL](#) distribution model showed a 40% error in stage one, despite only just reaching concentrations at which the systems phases begin to become saturated. It is likely this model would deviate even more at higher concentrations. In comparison, [Table 5.2](#) shows that the [LIL](#)

distribution model adequately describes protein distribution in each stage. The highest error seen in the LIL distribution model is 11.0% (compared with 40% for the LL distribution) and mostly, the error is below 5%.

Table 5.2: Comparison of the amount of haemoglobin in each phase between the experimental data, the LL distribution model, and the LIL distribution model. The feed in this system was at stage 1.

Stage	Phase	Experiment	LL		LIL	
		Amount (mg)	Amount (mg)	Error (%)	Amount (mg)	Error (%)
1	Extract	0.444	0.244	-40.0	0.436	-1.6
	Waste	0.275	0.248	-5.4	0.295	4.0
2	Extract	0.173	0.127	-9.2	0.228	11.0
	Waste	0.145	0.107	-7.6	0.129	-3.2
3	Extract	0.049	0.048	-0.2	0.057	1.6
	Waste	0.047	0.037	-2.0	0.073	5.2

The models were also tested against a four-stage counter-current multi-stage system, with a feed in stage one, looking at the behaviour of C-phycoerythrin in the presence of contaminants including allophycocyanin and phycoerythrin. This extraction was carried out using the C-phycoerythrin case study system which was also used in the C-phycoerythrin extractions used in Chapter 4. C-phycoerythrin stock 1 was used as the protein feed. This allowed for the opportunity to test the models with a different system and target protein as well as in the presence of contaminants.

The C-phycoerythrin extractions only required single-stage data on the phase partitioning because the volume of the horizontal interface was not large enough to partition into the extract phase under the extraction conditions and concentrations of protein used. The equilibrium partitioning data for the C-phycoerythrin stock together with the equation lines used in the model is shown in Figure 5.8. This equilibrium curve is the same as the C-phycoerythrin equilibrium curve in Chapter 4.

The results for the four-stage MSE is shown in Figures 5.9a and 5.9b. The same patterns as seen in Chapter 4 are shown in this extraction: C-phycoerythrin favours the extract phase, and with each stage there is a decreasing amount of protein in the system. The total recovery of C-phycoerythrin was 84.0%; this represents a slight increase over the centrifuge operated ATPE carried out in the previous chapter with this feed. This achieved a 80.6% recovery of C-phycoerythrin using three stages between the point at which the feed was added to the system and the removal of the waste phase. The amount of protein added to the system in the extraction in the previous chapter was approximately 3 times less than the extraction carried out in this chapter which means that there is an improved yield with the extra stage as

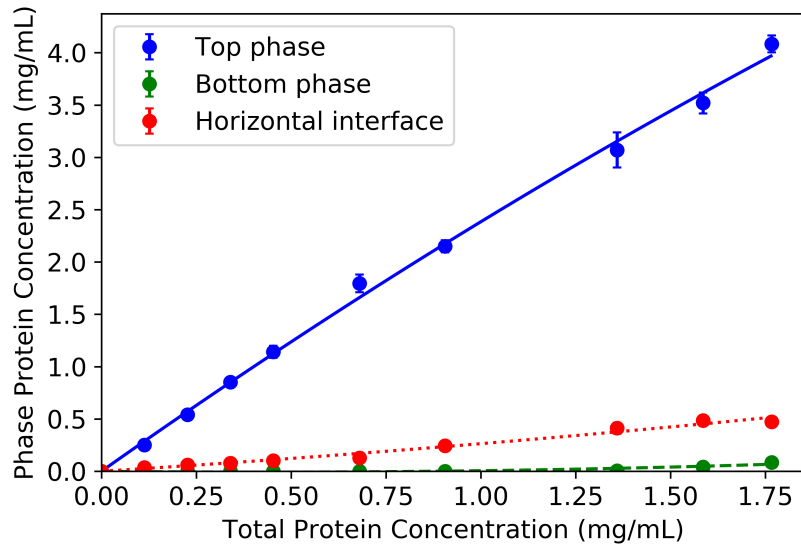


Figure 5.8: The partitioning of C-phycoerythrin in the top, bottom, and horizontal interface region with respect to the total C-phycoerythrin concentration in the C-phycoerythrin case study

well as increase in processing capacity.

Table 5.3 shows a comparison between the results of the experiment and the two models. As with the haemoglobin extraction, the results show that the **LIL** model described the system behaviour better than with the **LL** distribution model with the largest error being 15.2% compared with -33.8% error. Furthermore, the errors seen in the **LIL** distribution model are consistently much smaller, between -3 and 5%, whereas the **LL** distribution model errors are always more than -10% and are generally between 20 and 30% below the experimental value. This is likely a result of the **LL** distribution model not accounting for protein distributed into the horizontal interface. For the **LIL** distribution model, the earlier stages have been slightly over estimated, and the latter waste stages have been underestimated. This could be a result of protein in the horizontal interface not redissolving in the experimental study.

Lastly, the models were tested against the five-stage counter-current multi-stage system with a feed in stage three carried out with the C-phycoerythrin stock 1 used in the previous chapter. The results from this experimental **MSE** are shown in Section 4.2.4. The model looks at the behaviour of C-phycoerythrin between the feed and the waste removal. However, in this extraction there are additional stages between the feed and the extract removal which will increase the amount of C-phycoerythrin in the system. To account for this, the feed in the model was run with the feed

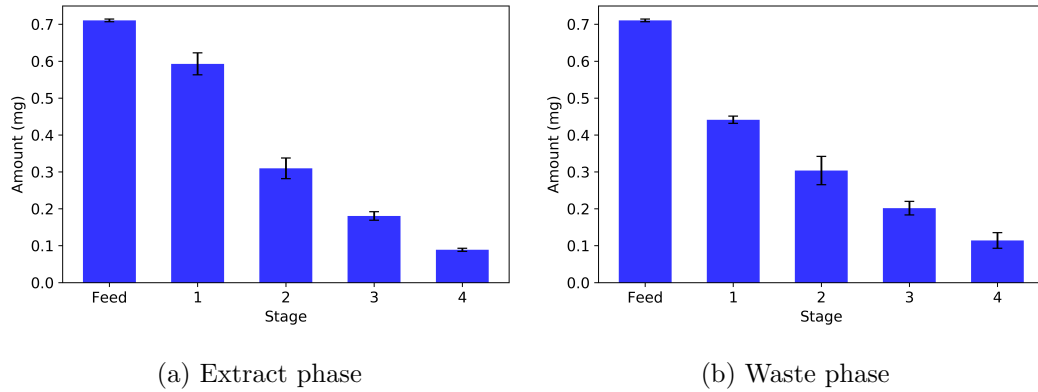


Figure 5.9: The amount of C-phycoerythrin in the extract and waste phases of a four-stage count-current ATPE with a feed at stage one the C-phycoerythrin case study system

Table 5.3: Comparison of the amount of C-phycoerythrin in each phase between the experimental data, the LL distribution model, and the LIL distribution model for the four-stage extraction with the feed at stage one.

Stage	Phase	Experiment	LL		LIL	
		Amount (mg)	Amount (mg)	Error (%)	Amount (mg)	Error (%)
1	Extract	0.593	0.494	-14.0	0.630	5.20
	Waste	0.441	0.259	-25.7	0.494	7.45
2	Extract	0.310	0.172	-19.4	0.417	15.2
	Waste	0.304	0.064	-33.8	0.320	2.22
3	Extract	0.181	0.041	-19.6	0.242	8.65
	Waste	0.202	0.014	-26.4	0.182	-2.81
4	Extract	0.089	0.008	-11.4	0.104	2.12
	Waste	0.114	0.003	-15.7	0.077	-5.27

plus the amount shown in the waste phase of stage two of the experimental study in Section 4.2.4. While extra experimental data was required to input this data, it provided an opportunity to see if the systems behaved consistently if a feed was not at the extract or waste entry points. The equilibrium curve shown in Figure 5.8 was used in the model. Table 5.4 shows the results from the experimental study and the LL and LIL distribution models. Shown are the stages from the feed entry point (stage three) to the point at which the waste phase exited the system (stage five). The LIL distribution model again outperformed the LL distribution model, with the largest error being -8.74% compared with -29.3%, respectively. The errors in the LIL distribution model were generally between -3 and 5% whereas the errors in the LL distribution model were always below -14% and largely around -28%. As a result, the LIL model can be seen to describe the behaviour of multi-stage ATPE

in a range of conditions more accurately than previous iterations of the model.

Table 5.4: Comparison of the amount of C-phycoyanin in each phase between the experimental data, the LL distribution model, and the LIL distribution model. The feed in this system was at stage 3

Stage	Phase	Experiment	LL		LIL	
		Amount (mg)	Amount (mg)	Error (%)	Amount (mg)	Error (%)
3	Extract	0.297	0.214	-28.2	0.271	-8.74
	Waste	0.153	0.066	-29.3	0.170	5.62
4	Extract	0.129	0.046	-28.0	0.141	3.86
	Waste	0.097	0.011	-28.9	0.086	-3.53
5	Extract	0.054	0.007	-16.0	0.054	0.05
	Waste	0.044	0.002	-14.3	0.033	-3.71

### 5.2.3 Process Design Using the Model

As the LIL model was shown to adequately describe the behaviour of protein in multi-stage ATPE, it was then utilised to predict the number of stages required in a model separation of C-phycoyanin from a model contaminant, lysozyme. In this extraction, the volume proportions of the extract and waste phases were changed to 28% and 72% of the system, respectively. It was expected that increasing the extract size from 24.8% to 28% would improve the theoretical performance of the system. The theoretical feed contained 8 mg/mL of C-phycoyanin and 10 mg/mL of lysozyme, and was spiked into the system at 4% of the total system volume.

To effectively model this, an equilibrium curve of lysozyme in the C-phycoyanin case study system was required; this is shown in Figure 5.10. The equilibrium shows that lysozyme overwhelmingly favours the bottom phase of the system which is not surprising considering it has an isoelectric point of 11.35. Again, lysozyme shows partitioning into the horizontal interface of the system and only very small amounts of lysozyme partition into the top phase of the system. Lysozyme could be reaching saturation in the bottom phase at around 0.65 mg/mL at which point more protein begins to partition into the horizontal interface; however, there are not enough data to know for sure.

To design the extraction process, firstly, the number of stages required to remove lysozyme from the extract phase was estimated. This was because the stages between the feed point and waste removal were unlikely to make much of a difference to lysozyme removal from the extract phases as only very small amounts of lysozyme were likely to be present in the extract phases. However, to ensure that no significant effect would occur to the yield if the extract stage before the feed contained lysozyme,

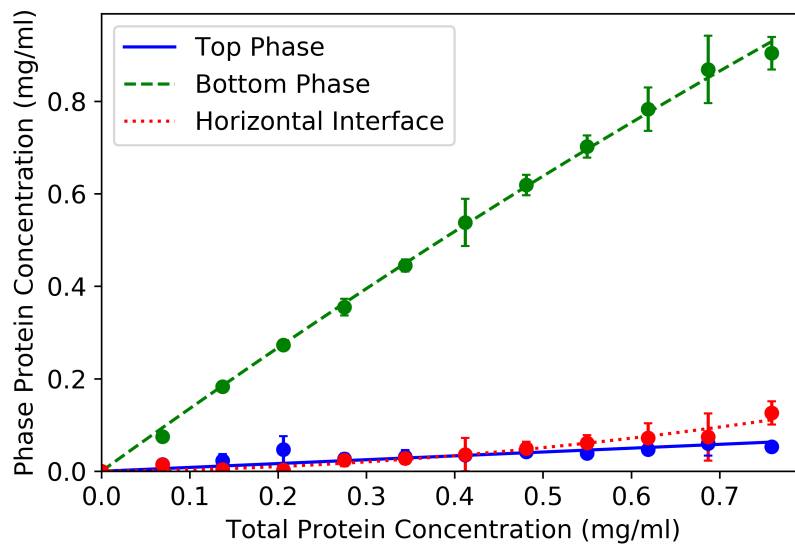


Figure 5.10: The partitioning of lysozyme in the top, bottom, and horizontal interface region with respect to the total lysozyme concentration in the C-phycoerythrin case study system

the model was run with the required feed added, and then with a 30% and 60% increase in feed. The percentage removal was worked out using the initial feed. This process was also carried out for C-phycoerythrin removal from the waste phase.

Table 5.5 shows the results for lysozyme removal from the extract phase of the system. It can be seen two stages are required to remove most of the lysozyme from the extract phase. The increase in feed had a small effect on a system with one extraction step but had a negligible effect on the system with two stages. More stages could be used, but no significant performance increase was seen.

The second step in designing the extraction process was to evaluate the number of stages for C-phycoerythrin recovery. Table 5.6 shows the results from the model for C-phycoerythrin recovery. It can be seen that drastic increases are seen in performance up to the addition of four stages and a negligible increase in performance on the system is seen after seven stages. Having fewer stages was also shown to result in having a process which was less capable of dealing with varying feeds and large variations in yield were seen when the feed was increased. Four stages would be required to achieve a recovery of >94% with this operational configuration. These results were then used to inform the extraction process shown in Figure 5.11. The number of stages required for an extraction would be dependant on the users requirements, but the model described in this chapter can be used to inform MSE process design.

Table 5.5: Predicted percentage removal of lysozyme from the C-phycoerythrin case study system.

Stages	Feed	Feed + 30 %	Feed + 60%
1	93.92	92.10	90.27
2	99.95	99.93	99.92
3	100.00	100.00	100.00
4	100.00	100.00	100.00

Table 5.6: Predicted percentage recovery of C-phycoerythrin from the C-phycoerythrin case study system.

Stages	Feed	Feed + 30 %	Feed + 60%
1	66.50	56.07	45.49
2	85.52	80.84	76.01
3	93.21	90.94	88.57
4	96.71	95.59	94.40
5	98.39	97.83	97.23
6	99.21	98.93	98.63
7	99.61	99.48	99.33
8	99.81	99.75	99.67
9	99.91	99.88	99.84
10	100.00	100.00	99.93

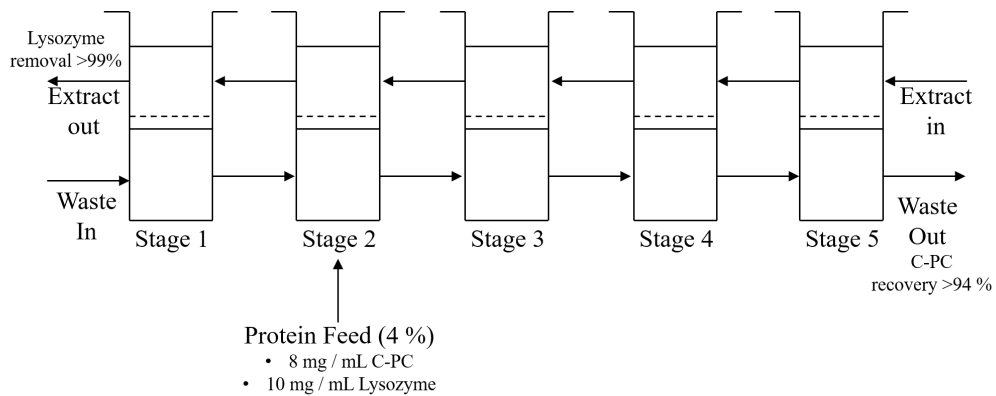


Figure 5.11: Schematic representing a MSE design of C-phycoerythrin from lysozyme in the C-phycoerythrin case study system.

### 5.2.4 Overview

In terms of process design, the material in the horizontal interface could be considered just as part of the extract or waste phase of a system, and the calibration curve could be constructed using the extract and waste phase concentrations. However, doing this would reduce the flexibility of the model as the extract and waste phases would have to remain at a set size. The extract and waste phases should be set in accordance with the amount and type of material in the horizontal interface, the total system size, and the equipment being used to carry out the extractions. The proportions of the extract and waste phase may change during the process design and scale up. Constructing equilibrium curves using the top, bottom, and horizontal interface concentrations (rather than the extract and waste phases) allows the user the flexibility to consider different extract and waste sizes.

This chapter has shown that considering horizontal interface behaviour in [ATPE](#) is very important in [MSE](#) design. The behaviour of the protein or material at the horizontal interface would be dependant on the volume of the mass at the horizontal interface and the way an extraction was carried out. For instance, systems which are centrifuged are likely to compact material in the horizontal interface more than systems allowed to separate via gravity, and systems with an extract phase which is very close to the size of the top phase or systems with large amounts of material in the horizontal interface are likely to pick up the material in the horizontal interface in the extract. When systems are screened, it is preferable to avoid selecting a system which precipitates a target protein or a significant amount of contaminant into the horizontal interface as it could affect the yield and purity of the process and could clog up equipment. [Mündges et al. \(2015\)](#) found that high loadings of [IgG](#) resulted in a decrease of the purity and yield of the process. The horizontal interface needs to be accounted for as it is common for things (particularly larger contaminants such as cells or cell debris) to partition to some extent into the horizontal interface. This is particularly important for [ATPE](#) as it can be used as a primary clarification step, therefore processing very crude (unpurified) material, for example, [CHO](#) cell media broth. Material straight from a bioreactor or homogeniser will contain a large variety of material, including cell debris. As a result, having models which account for horizontal interface behaviour are important for process design.

One way to minimise reductions in yields and purity as a result of horizontal interface partitioning is to avoid taking up the horizontal interface into the extract. This is because all material is likely to partition into the horizontal interface, including contaminants, making it difficult to achieve separation from the contaminants if the horizontal interface is taken up. There is also the possibility that target protein that partitions into the horizontal interface will become damaged. This could

render it a contaminant that may need to be separated out downstream. To avoid or minimise the loss of yield and purity without changing the feed characteristics, process design should look to:

- Reduce the volume of the extract
- Chose systems with larger top phases
- Lower the amount of feed added to the system
- Use equipment / or extraction techniques which avoid disturbing the horizontal interface
- Add extra stages.

These steps can all be used to reduce the amount of precipitated material in the extract; however, they all have a trade off. If the volume of the extract is reduced, extra stages will be required between the feed point and the waste removal to produce the same yield. If the amount of feed added to the system is reduced, more runs would be required to process the same amount of material thereby decreasing the productivity of the process. If systems with a larger top phase are chosen, more stages could be required to produce the same purity, the target protein concentration will be reduced which could increase the processing needs downstream, and, if the phase is large enough, the system may have a continuous top phase resulting in slower phase separation kinetics and reduced processing capacity. Using equipment and extraction methods which avoid disturbing the horizontal interface cannot reduce the size or amount of material in the horizontal interface. It is therefore limited by the system chosen and the partitioning behaviour of the protein. Lastly, adding extra steps will come with additional costs.

In the model, there will be some error generated because all of the horizontal interface material is assumed to go into the extract or the waste phase of the system. In the experimentation carried out, it was observed that the precipitated material tended to aggregate together and therefore most of the material partitioned into one phase or another. However, as there will be a small amount of material in the horizontal interface going into the opposing phase, error will be generated. Error may also be generated as it can be difficult to redissolve material which has precipitated at the horizontal interface. This may affect system behaviour when the [MSE](#) is carried out, and will not be detected with [UV-vis](#) analysis. Material could be less likely to redissolve in the [MSEs](#) than during analysis. This is because the samples for analysis are being diluted to a much greater degree in water rather than [ATPE](#)

phases. This could mean that the experimental readings for the waste phases are higher than expected, and the extract phases are lower than expected.

Evaluation of a single contaminant is carried out in this work. [Rosa et al. \(2009b,a\)](#) suggested that as contaminants make up a range of different materials, they could be grouped. Specifically, the work suggested grouping contaminants as high and low [Molecular Weight \(MW\)](#) components. There are other divisions possible, for instance, by isoelectric point, and a stubborn contaminant or contaminant present in high concentrations could be considered on its own.

The modelling in this chapter looks at evaluating a single protein at a time, evaluating target proteins and contaminants separately. The work considers that for extraction steps, the stages between the feed point and removal of the extract improve the purity of the system and the stages between the feed point and the waste removal improve the yield of the system. The model was used in this work to evaluate extraction steps; it could also be applied to back-extraction of the target protein from the polymer-rich phase into a salt-rich phase, or to washing steps for recycling of the polymer phase. The model could therefore be used as a basis to build up multi-stage, multi-step [ATPE](#) processes to improve the performance of [ATPE](#).

The number of contaminants present and variability of biological systems also mean that the models utilised to describe extraction processes need to be robust, and the systems need to be capable of handling complex and varying feeds. As a result, it would be necessary to carry out robustness testing on both systems selected and the models used. Robustness testing is evaluated in the next chapter.

### 5.3 Conclusions

In conclusion, multi-stage [ATPE](#) processes can be modelled more successfully when the model accounts for the behaviour in the horizontal interface of a system. Across multiple systems and with various proteins, protein was found to partition into the horizontal interface in all systems tested even at low concentrations.

The modelling requires single-stage data on the protein partitioning into the top, bottom, and horizontal interface regions of the system. In systems with significant amount of material partitioning into the horizontal interface of a system, two extra sets of data are required: data on the volume of horizontal interface region, and a threshold value for when the horizontal interface volume is large enough for horizontal interface material to partition into the extract phase. The modelling was tested against three case study [MSEs](#) using two different types of protein and systems. As the work builds upon the [LL](#) distribution modelling used by [Rosa et al. \(2009b,a\)](#) and [Liu et al. \(2018\)](#), the experimental data was compared against both the [LL](#) dis-

tribution modelling and the LIL modelling developed in this chapter. Considering the horizontal interface region in the modelling was found to drastically and consistently reduce the error between predicted and experimental values. The largest error seen in the LL modelling was -40.0% compared with +15.2% in LIL model. Furthermore, the error in the LL distribution modelling was consistently over -20%, whereas the error in the LIL model was very rarely greater than +10%.

As the modelling was now capable of accurately predicting protein behaviour, the model was used to design a MSE of C-phycoerythrin from a model contaminant, lysozyme, demonstrating how the model could be used in multi-stage, multi-step extraction processes for ATPE. The model was only used to consider yield and purity in extraction steps; however, could also be used to design back-extraction and washing steps.

The model requires very little experimental data and can be used to improve process design with reduced experimental work load. The model reiterated that multi-stage design is a valuable tool in improving yield and process purity. It also predicted that the robustness of the system would increase as the number of stages in the system.



## Chapter 6

# Variables Effecting Multi-Stage Aqueous Two-Phase Extraction

### 6.1 Introduction

This chapter aims to investigate the variables which were shown to affect the performance of multi-stage [Aqueous Two-Phase Extraction \(ATPE\)](#) in more detail. Two variables in particular were considered: phase separation after the formation of the horizontal interface, and partitioning of protein into the horizontal interface.

In terms of the first variable, Chapter 4 showed that there is a significant difference between systems operated through the use of a centrifuge and those operated through the use of gravity. Systems operated through the use of a centrifuge have significantly larger forces applied to them and, as a result, are at or very close to equilibrium. Systems which are operated through gravity are evaluated through the formation of a distinct horizontal interface. Currently, the separation of the phases of an [Aqueous Two-Phase Systems \(ATPS\)](#) is evaluated by eye through the dispersion and settling front; separation is considered complete at the formation of the horizontal interface ([Kaul et al., 1995](#); [Asenjo et al., 2002a](#)). However, it has been noted that small globules persist in each of these phases after the horizontal interface has formed when evaluating the system by eye. This means that the phases are still a turbid, cloudy colour ([Kaul et al., 1995](#)). This phase colour is used in the cloud point method in the determination of the binodal curve; it shows that a system is two-phase rather than a single-phase system ([Hatti-Kaul, 2000](#)). Therefore, it is reasonable to assume that an [ATPS](#) which has a distinct horizontal interface but still has turbid phases is still separating. The cloud point method uses clear, non-turbid phases to determine if a system is a single phase system; this is likely to also be an indication that equilibrium has been reached in a two-phase system and is seen in

systems which have been centrifuged under temperature-controlled conditions.

In the current literature, despite the turbid phases after the horizontal interface formation, the assumption is that the bulk separation has taken place and any separation after this point is unlikely to have a large impact of the performance of the process (Kaul et al., 1995). This may be the case for systems operated in a single-stage configuration. However, it has not been investigated (for either single or multi-stage systems) and the data in Chapter 4 showed that there was a significant difference in performance between gravity-operated and centrifuge-operated multi-stage ATPE. This chapter aims to investigate if separation after horizontal interface formation occurs and is significant enough to account for the differences between operational methods.

The second parameter investigated was protein partitioning into the horizontal interface of the system; this was also shown to have an impact on the behaviour of multi-stage ATPE. Andrews and Asenjo (1996) evaluated three different proteins across six ATPS and observed that protein partitioning into the horizontal interface of an ATPS was common. The data in the previous two chapters showed that both lysozyme and C-phycoerythrin partitioned into the horizontal interface of the C-phycoerythrin case study ATPS. Data from Chapter 5 demonstrated that haemoglobin partitioned into the horizontal interface of all nine Polyethylene Glycol (PEG) 1500 - phosphate systems screened and that large amounts of haemoglobin partitioned into the horizontal interface of the haemoglobin case study system even at very low concentrations.

Partitioning into the horizontal interface has been demonstrated to be a common occurrence which has an impact on system performance (Andrews and Asenjo, 1996; Mündges et al., 2015). Albertsson (1971) noted that the precipitated protein in the horizontal interface should redissolve under more favourable conditions; however, some of the protein may be permanently precipitated. This makes it difficult to accurately measure the protein in the horizontal interface. To analyse protein experimentally, a Ultraviolet-visible (UV-vis) can be used. For this, the protein needs to be in solution and so protein that has not redissolved will not be accounted for. Therefore, the most accurate way to determine the amount of protein in the horizontal interface of a single-stage system is to use a mass balance of the known amount of protein added to the system and the measured amounts of protein in the top and bottom phases. This method is not possible for Multi-stage Extraction (MSE)s as the total amount of protein in the system is not known. While every effort is made to redissolve the protein for analysis in the horizontal interface through dilution and vortexing, there is still uncertainty in the results for samples with horizontal interface material. Furthermore, the conditions in the multi-stage extraction may

not be favourable enough to result in protein redissolving when moved to another stage; this may affect the system's protein partitioning behaviour. In Chapter 4, stages which were far away from the feed point had more protein in the waste phase (containing the horizontal interface) than predicted from the equilibrium curve. One theory for this behaviour was that some of the protein in the horizontal interface had not redissolved when it was moved to another stage, therefore altering partitioning behaviour. This would further increase the uncertainty surrounding the results which include horizontal interface material.

One way to evaluate the impact of the uncertainty surrounding horizontal interface partitioning on results is to perform robustness testing on the model. Models need to be robust as the experimental data of [ATPS](#) are prone to errors which result in difficulties in its mathematical handling ([Selber et al., 2000](#)). Robustness testing has been utilised in [ATPE](#) before by [Patel et al. \(2018\)](#) to evaluate how variations in feeds affected multi-stage extraction performance. Practically speaking, while it is important to know the concentrations of the phases, it is more important to understand the number of stages required to meet a required yield or purity. Therefore, the model was extended from calculating the amount of protein in each phase to optimising the number of stages required in a [MSE](#) for a required yield or purity. This alteration allowed an assessment of how variations in horizontal interface partitioning impacted on the number of stages required. In terms of process optimisation of conditions, it has been estimated that there are over one billion possible systems to explore for any given separation problem ([Selber et al., 2000](#); [Torres-Acosta et al., 2019](#)). Therefore, employing optimisation strategies in [ATPE](#) is one method to overcome the low resolution without an extensive experimental workload.

This chapter is divided into two major sections with the aim of evaluating parameters which have a significant impact on the performance of multi-stage [ATPE](#). Firstly, the effect of the kinetics of the phase separation between the formation of the horizontal interface and true equilibrium is evaluated. To do this, systems had their kinetics evaluated by traditional dispersion height measurements, [UV-vis](#) analysis at 555 nm, microscopic observation of a separating system, and protein concentration analysis at various time points in a case study [ATPS](#). Secondly, the model built in Chapter 5 was modified to optimise the number of stages for a given yield or purity. The optimal number of stages of a case study [ATPS](#) was then calculated for a variety of required yields. To test the robustness of the system, the effect that varying the horizontal interface had on the optimal number of stages for a required yield was then tested over a number of runs.

## 6.2 Results and Discussion

### 6.2.1 The Kinetics of the Phase Separation

The first part of the experimental work in this chapter carries out a study of the kinetics of the phase separation on multiple systems. The systems chosen for the study were previously used in a kinetics study by [Asenjo et al. \(2002a\)](#). The first technique used to investigate the phase separation kinetics was the traditional dispersion height measurements. These measurements track the two fronts which are composed of visible globules that form in a settling system by eye. Studies which utilise these measurements assume that the bulk of the separation is over at the formation of a discrete horizontal interface ([Kaul et al., 1995](#); [Mistry et al., 1996](#); [Asenjo et al., 2002a](#)). However, it was indicated in Chapter 4 that there was appreciable separation taking place after the formation of the horizontal interface which affected the performance of a multi-stage [ATPE](#). As a result, [UV-vis](#) analysis at 555 nm of a system's bottom continuous phase was utilised to evaluate the separation of the phases as this could account for separation past the formation of the horizontal interface.

Separating systems are characterised as having a continuous phase and a dispersed phase. System conditions (specifically phase-forming salt concentration in a [PEG-salt](#) system) dictate which of the phases is continuous and which is dispersed ([Merchuk et al., 1998](#)). In a continuous phase, globules of the dispersed phase form and then rise or sink towards the horizontal interface. At the horizontal interface, globules queue until they coalesce and join their native phase. The dispersed phase is considered static and this can all be observed by eye. For separation which cannot be observed by eye, [UV-vis](#) analysis was used. As the separation is considered to take place in the continuous phase, this was carried out on the continuous bottom phases of the systems. For the [UV-vis](#) experimentation to track the separation, a fixed wavelength of 555 nm was chosen. At this wavelength, the phase forming constituents did not absorb strongly and changes seen in the absorbance were likely due to movement of globules which were still separating.

Figure 6.1 shows the dispersion height measurements for systems A, B, C, and D. Systems were [PEG 4000](#) - pH 7.0 ammonium phosphate [ATPS](#). All systems consisted of 10% w/w ammonium phosphate and systems A, B, C and D consisted of 14, 16, 18 and 20% w/w [PEG 4000](#), respectively. For these systems, the bottom phase was observed to be the continuous phase; as a result, the top line represents the settling front and the bottom line the coalescence front. The separation is considered complete when these two fronts meet and distinct horizontal interface is formed (with no globule queueing). For all systems tested by eye, Figure 6.1 shows

that the separation is rapid and can be considered complete 5 minutes after the separation began. Rapid eye level separation is to be expected as the bottom phase of the system is the continuous phase and the systems sit at intermediate positions on the binodal curve (Asenjo et al., 2002a). A general trend can be seen of the phase separation rate increasing as the concentration of PEG increases. While increasing the PEG concentration will increase the viscosity of the phases, particularly the top phase, it will also increase the density difference between the phases which increases the driving forces behind the phase separation. This mirrors the findings of Asenjo et al. (2002a) who found that phase separation rate increases as tie line length increases.

The systems evaluated in the dispersion height measurements were of different heights than those in the UV-vis separation experiment; the total height of the dispersion height experiments was 6.3 cm, whereas the total height of the UV-vis separation experiments was 3.5 cm. Taller systems were used for the dispersion height measurements because the rapid separation of the phases at eye level is difficult to measure, and are much more difficult at smaller heights. This difficulty is seen in Figure 6.1 by the large errors, especially at the second and third data points where the majority of the separation is taking place. Some of this error is due to the random nature of coalescing globules which means that the settling and coalescence fronts and the formation of the horizontal interface will naturally vary between repeats.

Shown in Figures 6.2 and 6.3 are the results of the UV-vis analysis at 555 nm of the continuous bottom phases of systems A, B, C, and D. Figure 6.2 shows the entire separation from when mixing ceased to the point that the phases were clear. Figure 6.3 shows the separation from the point at which mixing ceased to 20 minutes after it began. The red line in both Figures 6.2 and 6.3 is the point by which a distinct horizontal interface is known to have formed; this indicates complete separation according to the traditional measure of dispersion height.

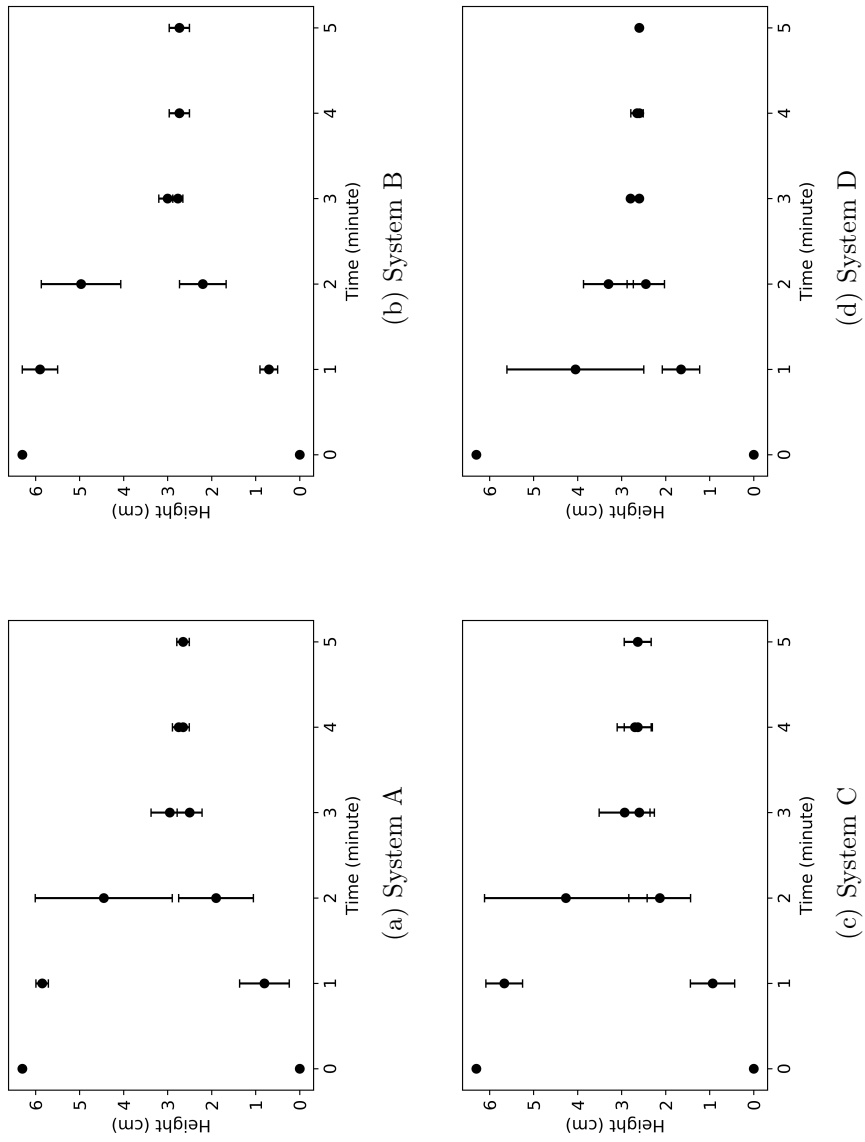


Figure 6.1: Dispersion height diagrams for systems A, B, C, and D.

The first conclusion that can be drawn from the [UV-vis](#) analysis is that the separation continues long after the formation of the horizontal interface. There are significant changes in the absorbance observed between the red line and the point at which a baseline is reached for each system. The systems that were used in the dispersion height experimentation had a greater total system height than those in the [UV-vis](#) experiments; it would therefore be expected that the [UV-vis](#) systems would separate more rapidly than the dispersion height diagrams. Even without taking this into account, an absorbance of around 0.75, 0.90, 1.0 and 1.15 is reached by the time the horizontal interface has formed for systems A, B, C, and D, respectively. These readings are significantly above the baseline for the systems (around 0.25) meaning that there is still a significant amount of separation to take place after the formation of the horizontal interface. The baseline for each system takes several hours after the formation of the horizontal interface to be reached for all systems tested.

Each curve follows a relaxation trend and the baseline was reached at *ca.* 150 minutes for system A, 200 minutes for system B, 250 minutes for system C, and *ca.* 300 minutes for system D. At eye level, system D (with the highest concentration of [PEG](#)) separated the most rapidly and system A (with the lowest concentration of [PEG](#)) separated most slowly. This is the opposite trend to that seen in the [UV-vis](#) measurements. It is likely that the bulk separation is over faster in systems with higher concentrations of [PEG](#); however, in this rapid time frame (first 5 minutes), a greater clarity (less turbid) of phases is achieved in systems with lower concentrations of [PEG](#). It can also be seen that it is likely that systems with a lower [PEG](#) concentration reach true equilibrium faster than systems with a higher concentration as the phases are much less viscous. Lastly, it can be seen from [Figure 6.2](#) that there are large amounts of error generated around the baseline reading. This is likely from globules of [PEG](#) attached to the sides of the cuvette moving.

### 6.2.2 C-phycoerythrin System Study

The previous section showed that it is likely that the separation of the continuous phase continues long after the formation of horizontal interface. Microscopic observation was used to determine if this is the case. It would also be useful to investigate how this phase separation after the formation of the horizontal interface affects the partitioning of protein within the system. In order to do this, a single system was evaluated in more detail; the C-phycoerythrin case study system was used so that the differences in operational method seen in [Chapter 4](#) could be investigated. In this section, the C-phycoerythrin system was evaluated with a number of methods: the traditional dispersion height measurements, the [UV-vis](#) analysis at 555 nm, the

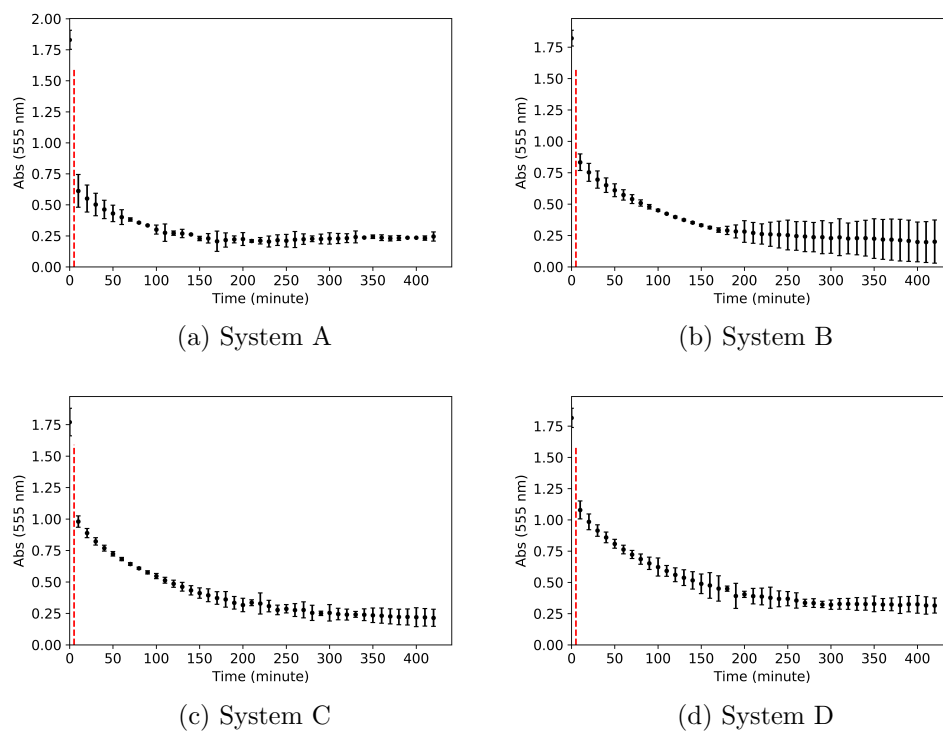


Figure 6.2: Turbidity measurements at 555 nm through the bottom, continuous phases of systems A, B, C, and D. The readings shown are from the start to the end of separation, the dotted red line indicates the point at which a distinct horizontal interface had formed.

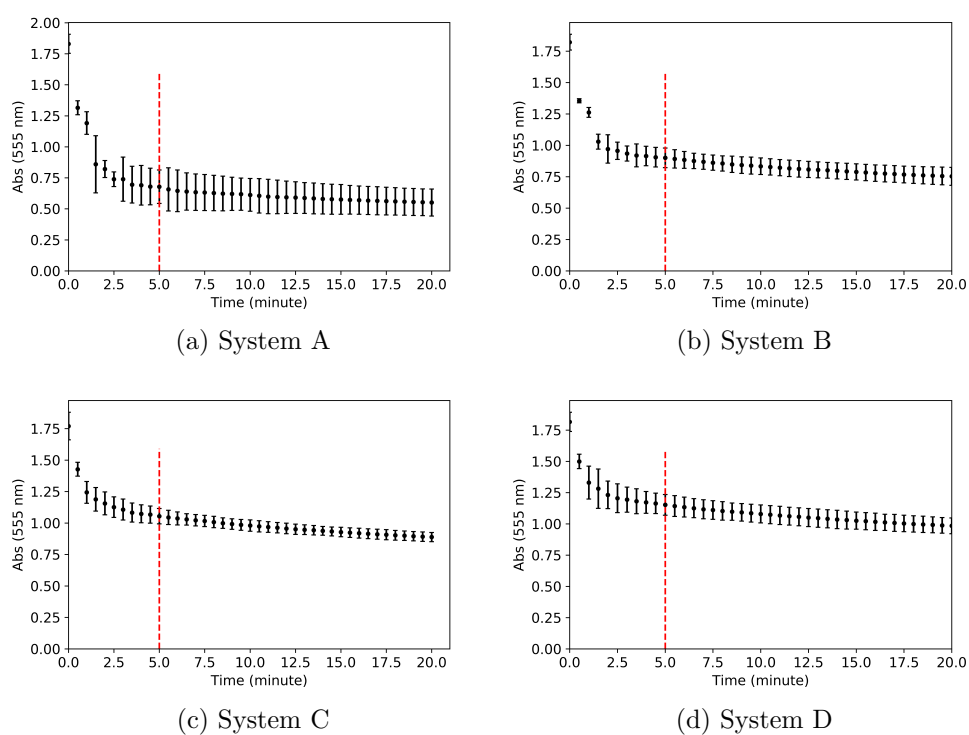


Figure 6.3: Turbidity measurements at 555 nm through the bottom, continuous phases of systems A, B, C, and D. The readings shown are from the start of separation to 20 minutes after separation began, the dotted red line indicates the point at which a distinct horizontal interface had formed.

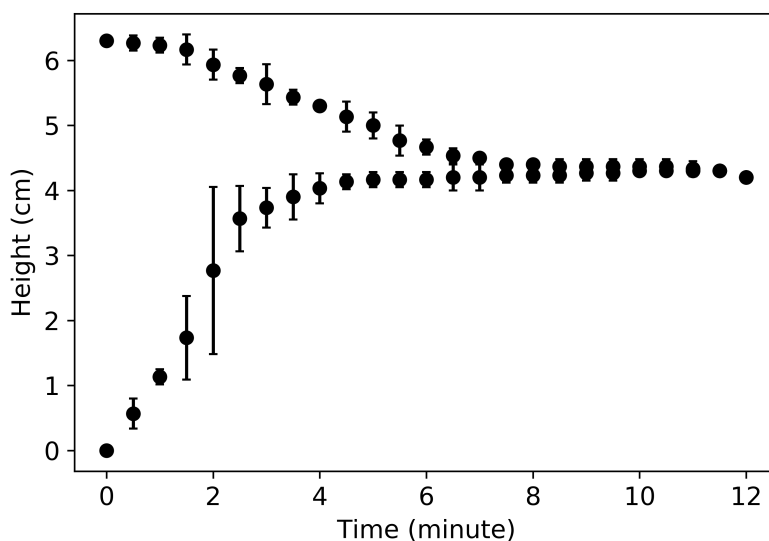


Figure 6.4: Dispersion height diagram for the C-phycoerythrin system.

phases were observed separating under a microscope, and analysis was carried out on the concentration of C-phycoerythrin in the phases at different time points. Investigating the C-phycoerythrin system allowed for data to be collected which could be directly correlated to the multi-stage extractions carried out in previous chapters.

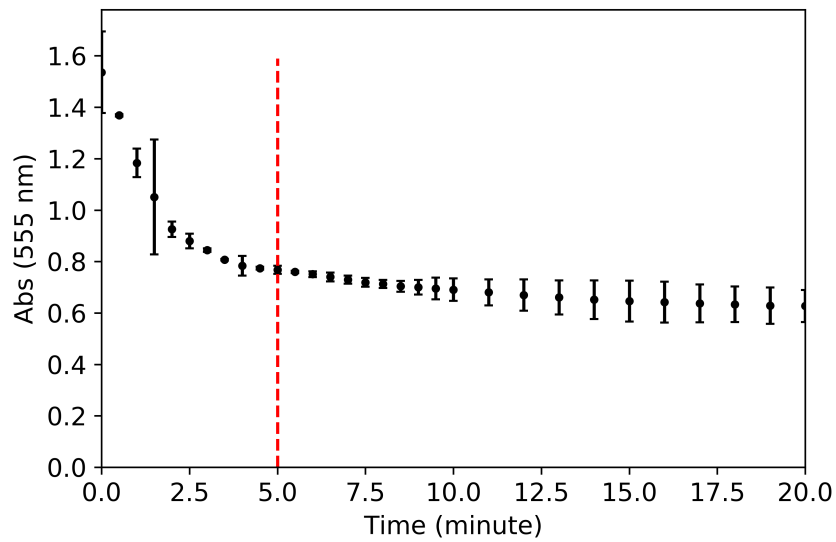
The first experiment carried on the C-phycoerythrin system was the dispersion height measurements; this is shown in Figure 6.4. This experimentation showed similar results to the systems in the previous section. At eye level, the system separated rapidly forming a horizontal interface within 12 minutes for a system with a total height of 6.3 cm. The system was observed to have a continuous bottom phase, so the bottom line shown in Figure 6.4 represents the coalescence front, and the top line represents the settling front. With the experimentation, a large amount of error was shown in the readings, particularly in the time regions of 1.5 - 4 minutes where the bulk of the separation was taking place. This separation was slower than the separations in the previous section. While the concentration of PEG was lower than systems B, C, and D, and the same as system A, the molecular weight of the PEG was higher. The higher molecular weight PEG is more viscous which increases the viscosity of the phases, especially the top PEG-rich phase, and slows separation.

The second experiment carried out on the C-phycoerythrin system was the UV-vis analysis at 555 nm of the continuous bottom phase of the system; this is shown in Figure 6.5. Figure 6.5a shows the beginning of separation (from the point at which mixing of the phases ceased) until 20 minutes after the separation began and Figure 6.5b shows the entire separation (to the point at which phases were clear). In both

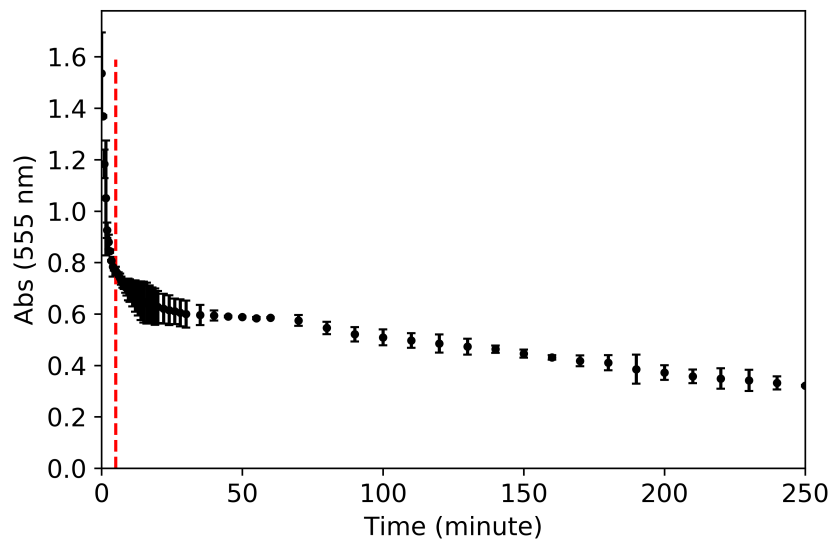
of these figures, the point at which a distinct horizontal interface is formed is shown by the red dotted line in a system which is the height of the cuvette; this was shown through experimentation to take 5 minutes in Chapter 4. This experimentation also shows similar results as seen in the previous section. Firstly, the UV-vis analysis indicates that it is likely that separation continues long after the formation of the horizontal interface. Figures 6.5a and b show that the most rapid separation is achieved in the first five minutes of separation; however, between five minutes and 250 minutes after separation began, the absorbance shifted from around 0.8 to 0.4. This change in absorbance was less than seen in systems A, B, C, and D. This experimentation cannot establish the effect of separation past the formation of the horizontal interface, and to be sure that separation is still taking place, auxiliary experimentation was used.

In order to further study the separation of the phases, the separation of the C-phycoerythrin system was observed under a microscope. Shown in Figures 6.6 and 6.7 are images of the system separating at various time points throughout the separation. Figure 6.6 shows the separation for the first 15 minutes and Figure 6.7 shows the remaining separation. For this system, the height of the separation would have been around the same as the systems used in the UV-vis analysis of the C-phycoerythrin system. As a result, the formation of a distinct horizontal interface would be achieved after 5 minutes of separation.

Figures 6.6 and 6.7 show that globules of phases form very rapidly, with globules being shown in the time it took to take the first image (<10 seconds). It can also be seen that the most rapid separation of the phases occurs before the formation of the horizontal interface, with the largest number and size of globules being shown in the images before the horizontal interface forms (<5 minutes). The figures also show that the separation of the phases continues to take place after the formation of the horizontal interface. In the initial few minutes after the formation of the horizontal interface, there appears to be some of the queuing at the horizontal interface at the microscopic level; this is characteristic of the phase separation of ATPS (Salamanca et al., 1998; Asenjo et al., 2002a). The globules persisting in the bottom phase that show this characteristic queuing behaviour are significantly larger than those which are observed in the bulk of the phase. These larger globules that remain in the bottom phase after the horizontal interface formation rapidly clear out of the bottom phase and are not seen in the microscopic observation 15 minutes after separation began. The characteristic queuing of globules at the horizontal interface of a system is used within the literature to indicate that the rate controlling process for the phase separation of most ATPS is globule coalescence (Salamanca et al., 1998; Asenjo et al., 2002a). While this has been routinely observed at eye level, Figures



(a) 0-20 minutes



(b) Entire separation

Figure 6.5: Turbidity measurements at 555 nm through the bottom, continuous phases of the C-phycoerythrin system. The dotted red line indicates the point at which a distinct horizontal interface had formed for a system of this height.

6.6 and 6.7 shows that there is a population of smaller globules which persist in the bottom continuous phase after horizontal interface formation that do not queue at the horizontal interface. Due to their much smaller size, it is likely that the rate controlling process for these globules is the rise to the horizontal interface. Therefore, this part of the separation is likely to take place at a much slower rate than the initial separation. This is also seen in the UV-vis analysis of the C-phycoerythrin system; Figure 6.5 shows that the initial separation taking place before horizontal interface formation is much more rapid than the separation taking place after this point. It is likely there is a period where both processes are seen and the dominance of the rate controlling process of globule coalescence is transferred to globule rise.

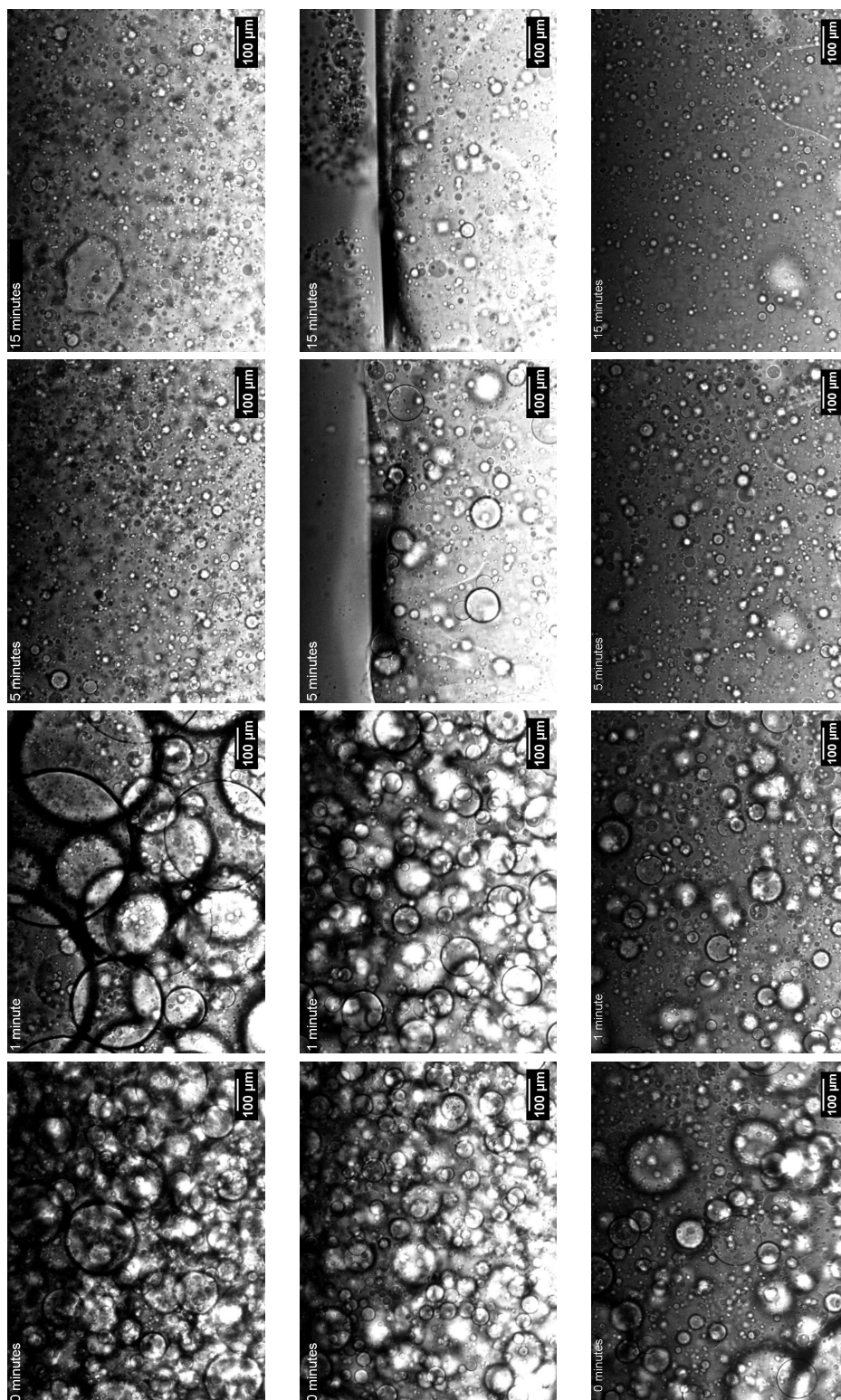


Figure 6.6: Microscope images taken of the C-phycocyanin system separating. The top row represents the top PEG-rich phase of the system, the second row represents the horizontal interface images and the bottom row represents the bottom phosphate-rich phase of the system. In a system of this height, the horizontal interface has formed after 5 minutes of separation

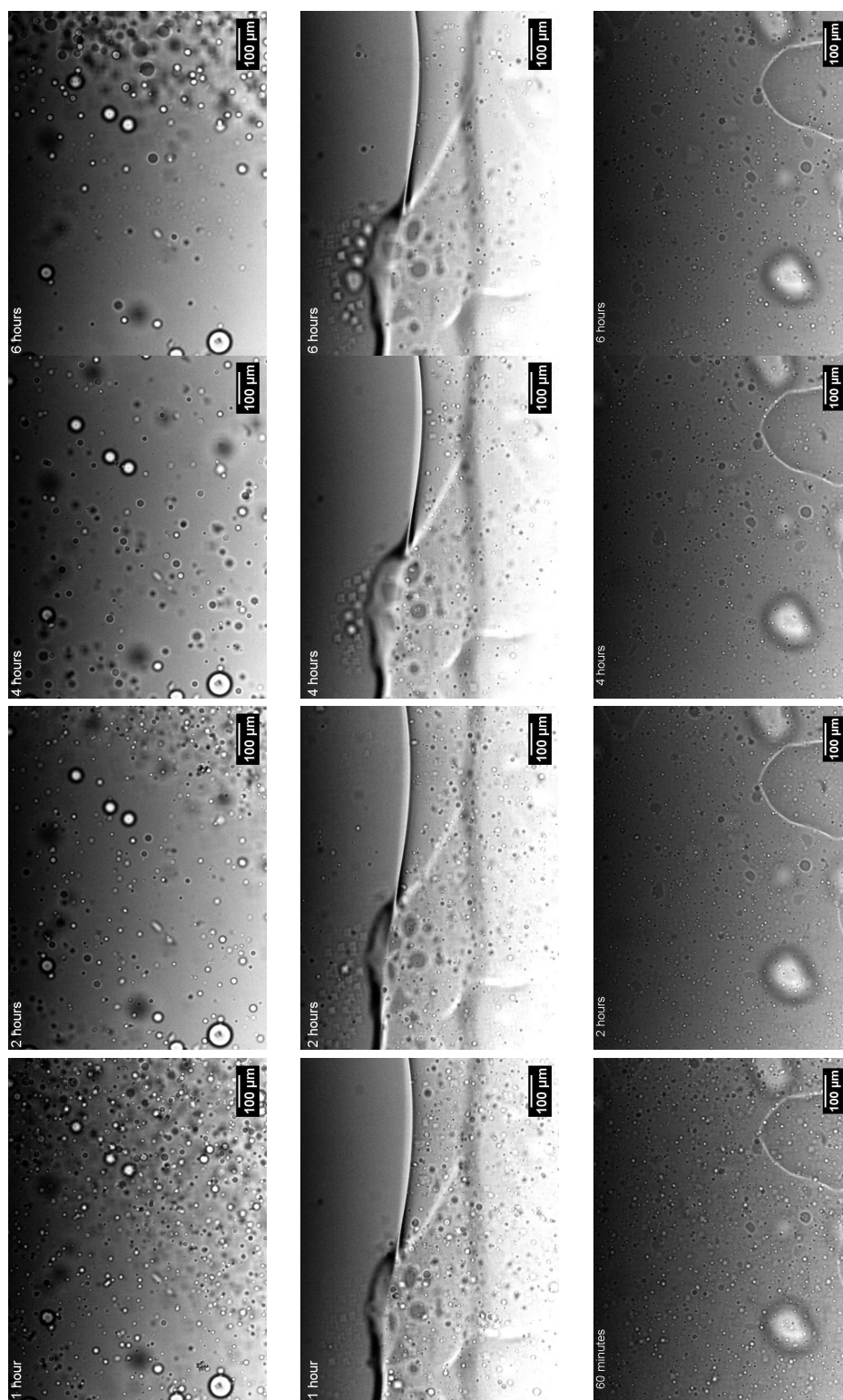


Figure 6.7: Microscope images taken of the C-phycocyanin system separating. The top row represents the top PEG-rich phase of the system, the second row represents the horizontal interface images and the bottom row represents the bottom phosphate-rich phase of the system.

The separation of the top, dispersed phase under a microscope is shown in the top rows of Figures 6.6 and 6.7. Generally, the separation of APTS are evaluated in terms of the continuous phase; however, the figures show that there are very small globules remaining in the dispersed phase of the C-phycoerythrin system. These globules slowly clear out of the top phase over a few hours. This settling of globules in the top PEG-rich phase is much slower than the settling in the bottom salt-rich phase; this is likely due to the increased viscosity of the top PEG rich phase.

The microscopic observation has confirmed that the separation continues after the formation of the horizontal interface and that there is separation taking place at the microscopic level in both the continuous and dispersed phase of the C-phycoerythrin system. However, it cannot show how it affects the separation of protein within the system. As a result, a fixed concentration of C-phycoerythrin in the C-phycoerythrin system was analysed at different time points after the formation of the horizontal interface; this is shown in Table 6.1.

The first observation which can be made from Table 6.1 is that the separation of the C-phycoerythrin system after the formation of the horizontal interface does have an effect on the partitioning of C-phycoerythrin. While it can be seen that the movement of C-phycoerythrin from the bottom phase is very small and within error, the amount of protein in the top phase increases from 0.109 mg immediately after the formation of the horizontal interface at 5 minutes to 0.150 mg 15 minutes after separation began; this 0.041 mg difference is around 24% of the total C-phycoerythrin in the system. By 6 hours after separation, 0.150 mg can still be found in the top phase and between 15 minutes and 6 hours 89% of the C-phycoerythrin in the system can be found in the top phase. However, 24 hours after the separation began and at equilibrium, the top phase only contained 0.122 mg of C-phycoerythrin which accounts for 72% of the total C-phycoerythrin in the system. This relates to a 22% reduction of C-phycoerythrin in the top phase between 6 and 24 hours. The equilibrium curve for C-phycoerythrin matches with the last data point generated for the C-phycoerythrin kinetics curve and cannot be correlated with the data immediately after horizontal interface formation. The data immediately after horizontal interface formation shows that the experimental top phase concentration is higher than the model prediction, and the amount of material in the horizontal interface is too low. As a result, this material clearing out of the top phase between 6 and 24 hours is most likely settling into the horizontal interface.

In this experimentation, the bottom phase sample taken was 500  $\mu\text{L}$  (out of a possible 1.057 mL) and the top phase sample was 200  $\mu\text{L}$  (out of a possible 457  $\mu\text{L}$ ). The amount of phase remaining was in the 557  $\mu\text{L}$  of the bottom phase, the 257  $\mu\text{L}$  of the top phase or the horizontal interface. For the systems at equilibrium, each

Table 6.1: The amount of C-phycoyanin measured in each of the top and bottom phases of the C-phycoyanin system at various time points after the separation began up until equilibrium had been reached. Also shown is the amount of material not accounted for; this is listed under ‘Remaining’.

Time (min)	Phase amount (mg)		
	Top	Bottom	Remaining
0			0.169
5 (horizontal interface formation)	0.109	0.007	0.053
15	0.150	0.006	0.012
30	0.154	0.005	0.009
60	0.150	0.006	0.012
360	0.159	0.004	0.005
1440	0.122	0.003	0.044

of the phases were assumed to have the same concentration throughout, and for the multi-stage extraction, all of the system was analysed. However, in these separating systems, it is likely that there is a concentration gradient across the phases, particularly the bottom continuous phase, with protein concentration increasing as distance from the horizontal interface decreases. In this experimentation, material around the horizontal interface was avoided when extractions of samples were made in order to avoid disturbing the horizontal interface and collecting material from the wrong phase. Therefore, it is possible that the concentration of the top half of the bottom phase is much higher than the bottom half (where the sample in this experimentation was taken) and the increase in concentration of the top phase is from material moving from the bottom phase to the top phase.

Table 6.1 shows that there is a rapid increase in the amount of C-phycoyanin in the top phase between the formation of the horizontal interface and 15 minutes after separation began. Then, between 15 minutes and 6 hours, there is a very small change in protein amount. It is likely the rapid change is accounted for in C-phycoyanin movement from the bottom phase to the top phase and this is reflected in the microscope images in Figure 6.6 and in the UV-vis analysis in Figure 6.5. While the separation was shown to carry on for around 6 hours after separation began, there appears to be a settling mechanism occurring between 6 hours and 24 hours which cannot be accounted for. Table 6.1 shows that between 6 hours and 24 hours the amount of C-phycoyanin in the top phase of the system dropped from 0.159 mg to 0.122 mg.

C-phycoyanin was shown in Chapters 4 and 5 to partition most readily into the top phase followed by the horizontal interface of the system with very little protein partitioning into the bottom phase. It was shown that separation after horizontal interface formation was important for this system; this chapter shows that there

were two mechanisms which should be considered. Firstly, movement of material into the dispersed phase from the continuous phase. This occurs from the beginning of separation until the larger globules of the dispersed phase in the continuous phase have been depleted. Secondly, the much slower mechanism of smaller globules of the continuous phase in the dispersed phase bringing material into the horizontal interface of the system. In this system the first mechanism dominated the separation for the first 15 minutes, and then second mechanism dominated the separation until equilibrium.

While it is unlikely that a gravity separation would be allowed to separate for hours, it is often assumed that the optimum time to allow a system to separate coincides with the horizontal interface formation or to use a centrifuge and operate systems to equilibrium. The data shown in this chapter indicated that the optimum time for separation does not coincide with either the formation of the horizontal interface or equilibrium. In terms of maximising the yield of C-phycoerythrin using the system, the greatest clarity was achieved at around 6 hours. This is not a practical separation time, but a large increase of 24.3% in amount of C-phycoerythrin in the top phase was achieved between the horizontal interface formation and 15 minutes after separation began (with respect to total protein amount). More data points are required to determine the exact time this rapid separation ends, but it is possible that a much higher yield could be achieved by allowing systems to separate for a few minutes after horizontal interface formation. It is likely that the optimal separation for purity and yield will differ in separations containing more than one contaminant. This is because any contaminant which separates into a separating dispersed phase, which also contains the target protein, could experience an increase in purity as the contaminant settles into the horizontal interface. This could occur as the target protein also settles into the horizontal interface, thereby reducing the yield.

### 6.2.3 Horizontal Interface Variation

Along with the kinetics of the phase separation, the partitioning of material into the horizontal interface was shown to be a variable which is important consideration in the design and modelling of multi-stage-ATPE. Previous work within this thesis has shown that partitioning into the horizontal interface is more important than previously considered. Firstly, in most of the literature, partitioning of material is generally considered to be between the two liquid top and bottom phases of a system. However, data in Chapter 5 demonstrated across multiple systems using different proteins and protein concentrations that protein partitioned into the horizontal interface of the system. This horizontal interface partitioning was shown

to be vital to accurately model multi-stage extraction of [ATPS](#). Secondly, previous literature considers that the bulk of the separation was complete at the formation of a horizontal interface and that, while there may be very small amounts of separation taking place, the important separation in terms of protein partitioning was complete. The data in the previous section of this chapter showed that partitioning of protein, particularly into the horizontal interface, was linked to the kinetics of the phase separation and significant partitioning of protein into a horizontal interface occurred after horizontal interface formation. This data demonstrated that the separation past the formation of the horizontal interface played a significant role in process performance even in a single-stage extraction.

Due to the importance of horizontal interface partitioning, this last section focuses on evaluating how variation of material in the horizontal interface affects the stage-wise results of multi-stage extraction. As previously discussed, it is difficult to measure partitioning of material into the horizontal interface experimentally in multi-stage extractions. This is because to measure protein concentration using a [UV-vis](#), it needs to be dissolved. However, protein precipitated in the horizontal interface of an [ATPS](#) can be difficult to redissolve or even irreversibly precipitated. As a result of this, the most experimentally accurate way to determine the amount of material is using a mass balance to calculate the material from the total known amount of protein added to a system and the experimentally determined amounts from the top and bottom phase. However, this is only possible in a single-stage system. There is also a limit to the number of experimental systems which can be processed using experimental methods due to the time-consuming nature of experimentation. As a result of these factors, a modelling approach was used to evaluate material in the horizontal interface. Variations in material at the horizontal interface was used to test the robustness of the model. As the experimental data for the horizontal interface material is less accurate than the data for the top and bottom phases, the greatest uncertainty for the results surrounds the horizontal interface partitioning behaviour. As the greatest amount of horizontal interface partitioning was experienced in the haemoglobin case study system, this system was chosen for study. The stage-wise optimisation is only useful if robust results are obtained, and small changes in the horizontal interface behaviour or small errors in data analysis do not impact the stage wise optimisation.

To evaluate the effect of horizontal interface partitioning on the outcome of multi-stage [ATPE](#) and the robustness of this outcome, the model was firstly altered to allow for a stage-wise optimisation. This allowed the model to evaluate the number of stages needed to accommodate different yield requirements as opposed to shifts in yield at a set number of stages. Then, to determine variation in the horizontal

interface partitioning, Deming regression was used to determine the variance of the equation describing the horizontal interface partitioning. Deming regression assumes that there are errors across both the x and y axis, that these errors have a constant and known error ratio,  $\lambda$ , and that the errors are normally distributed (NCSS, 2020). It was important to assume errors across both axis in the horizontal interface partitioning as with multi-stage ATPE there is no way to accurately determine either total protein concentration or horizontal interface concentration experimentally. The error ratio used in the Deming regression can be used to increase and decrease the confidence in the data; as  $\lambda$  gets smaller, larger errors are expected in the independent variable (the total protein concentration). Therefore, three different  $\lambda$  values across a wide range were tested so as to test the reliability of the model: 1, 1.63 (a calculated value from experimental data using Equation 3.38), and 7. The  $\lambda$  values and single-stage experimental data were used to calculate the distribution of the partition coefficient,  $\beta$ , describing horizontal interface partitioning in the model. This was then used to vary horizontal interface partitioning and test the stage-wise outcome of the model.

The haemoglobin system was evaluated for a number of reasons: it had been previously used in Chapter 5 with the Liquid-Interface-Liquid (LIL) distribution model, it was a stock solution with a single protein in it which partitioned into the PEG-rich phase of the system, and it had significant partitioning of protein into the horizontal interface. Using a system with significant partitioning of protein into the horizontal interface gave the most extreme conditions with which to test the robustness of the model. A probability function for the horizontal interface equation slope (based on a t distribution) was generated for each value of  $\lambda$ . Using this probability function, 1000 random values for the equation describing horizontal interface partitioning were generated. These values were then each used in the stage-wise optimisation to calculate an optimal number of stages for various yield requirements.

Table 6.2 shows the calculated values for  $\beta$  and the standard errors for  $\beta$  for each value of  $\lambda$  (1, 1.63, and 7) and linear regression (which is equivalent to  $\lambda = \infty$ ). It can be seen that the calculated values for  $\beta$  and standard errors vary little across each value; this gives confidence in the data gathered and the model generated to describe the horizontal interface. The standard errors are not large and the 95% confidence region for  $\beta$  for all data points lies between 0.21 and 0.234.

Shown in Table 6.3 is the calculated yields from the experimentally determined data and LIL distribution model from Chapter 5 for haemoglobin in the haemoglobin system. It can be seen from the calculated values that the largest increase in yield is from 63.93% to 80.57% using one to a two-stage system, respectively. The table also

Table 6.2: The calculated values for  $\beta$  and  $SE(\beta)$  from Deming regression using  $\lambda$  values of 1, 1.62 and 7 and linear regression.

$\lambda$	$\beta$	$SE(\beta)$
1	0.22276	0.00583
1.62	0.22271	0.00583
7	0.22266	0.00584
$\infty$ (Linear regression)	0.22269	0.00563

Table 6.3: The calculated yield of haemoglobin for a varying number of stages in a counter-current multi-stage operation using the haemoglobin system, using the same feed and extract and waste sizes as used in the experimentation. Shown is the stage-wise results for  $\beta - 2SE(\beta)$ ,  $\beta - SE(\beta)$ ,  $\beta$ ,  $\beta + SE(\beta)$  and  $\beta + 2SE(\beta)$  as calculated when  $\lambda = 7$ .

Stages	Yield				
	$\beta - 2SE(\beta)$	$\beta - SE(\beta)$	$\beta$	$\beta + SE(\beta)$	$\beta + 2SE(\beta)$
1	63.93	63.93	63.93	63.93	63.93
2	80.73	80.65	80.57	80.49	80.41
3	85.78	85.54	85.31	85.07	84.83
4	92.10	91.89	91.66	91.43	91.19
5	93.34	93.03	92.71	92.36	92.00
6	94.01	93.59	93.13	92.64	92.11
7	94.39	93.83	93.21	92.52	91.75
8	94.59	93.87	93.04	94.23	95.10

shows that significant increases in yield are shown up to the addition of four stages in a counter-current system. However, additional stages after this point do not have a significant impact on yield, and from 8+ stages, the yield begins to decrease (not shown). The decrease in yield will be a result of more of the protein partitioning into the horizontal interface and the size of the extract and waste phases. For this decrease to occur, the later stages reach a point where more protein is partitioning into the waste phase rather than the extract phase. This will not occur in all systems, or for all extract and waste volumes of this system. If the extract volume of this system was increased, the concentration range where more material partitions into the waste phase would decrease until it disappeared. As it stands, this concentration range is very small and only at very dilute concentration. Also shown in Table 6.3 is the stage-wise results at different confidence intervals surrounding  $\beta$ . These results reiterate that there is very little variation up until more than four stages are used and there is a high confidence in results until this point. After this point, the variation in results increases and the confidence in results decreases.

The results for the randomised equation for the horizontal interface partitioning are shown in Figures 6.8, 6.9, 6.10 and 6.11. The results are grouped around the

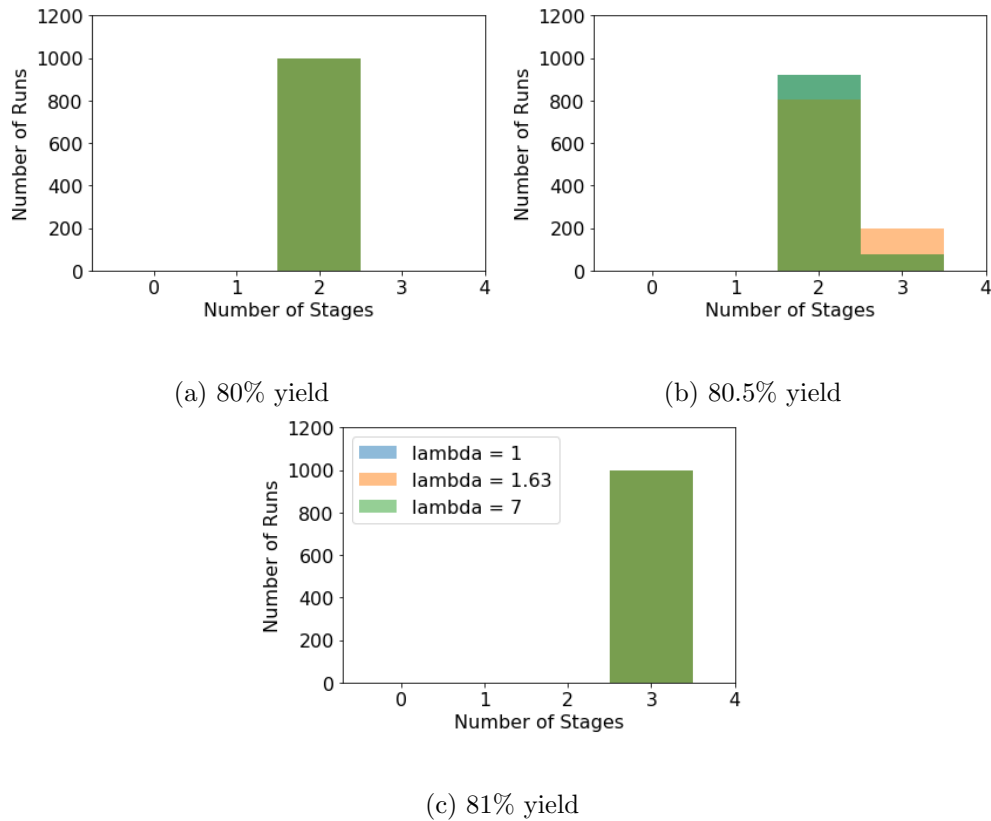


Figure 6.8: The number of stages required to reach varying yields around that which is achieved in a two-stage process. Shown are the results for  $\lambda = 1, 1.63, \text{ and } 7$ . The number of runs refers to the number of different  $\beta$  values tested within the model.

output for the calculated yields shown in Table 6.3 to see how the stage-wise optimisation changed around changes in stage numbers. Not shown are results around a single-stage process as the calculated yields did not change with varying horizontal interface slope. This is because a concentration high enough to result in horizontal interface partitioning into the extract phase was not reached and there was no variance in the amount of material entering the stage as there was no material entering from other stages.

Shown in Figure 6.8 is the robustness testing surrounding a two-stage process. The LIL model predicts that a yield of 80.6% would be achieved using a two-stage process which means that anything above this value would require a three-stage process. As a result, the stage-wise optimisation across varying horizontal interface slopes was run for a required yield of 80%, 80.5% and 81% for the three  $\lambda$  values tested. It can be seen from the results in Figure 6.8 that there is very little variation in results between the yields. Figure 6.8a shows that every run predicted a two-stage system for a yield of 80% and Figure 6.8c shows that a every run predicted a three-

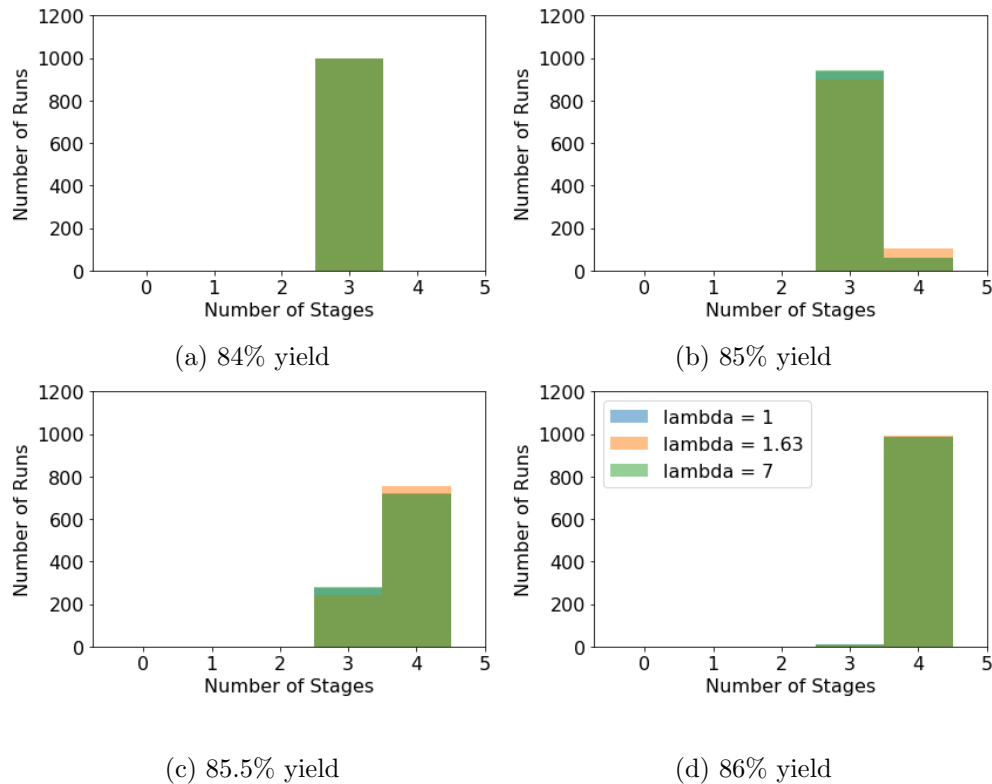


Figure 6.9: The number of stages required to reach varying yields around that which is achieved in a three-stage process. Shown are the results for  $\lambda = 1, 1.63, \text{ and } 7$ .

stage system for a yield of 81%. Figure 6.8b shows the results for a predicted yield of 80.5%, which shows that there is very little difference between the different lambda results meaning a user can be confident in the results and around 90% of results predict a two-stage system. The results for a two-stage system are robust, with a 0.5 - 1% interval where there is some uncertainty with the required number of stage. In system design, if a yield of over 80.5% is required, either operational parameters such as the extract and waste phase sizes would be adjusted or a three-stage system would be used.

Shown in Figure 6.9 is the robustness testing surrounding a three-stage process. The LIL model predicts that a yield of 85.4% would be achieved using a three-stage process, anything above this value would require more stages. As a result, the stage-wise optimisation across varying horizontal interface slopes was run for a required yield of 84%, 85%, 85.5% and 86% for the three  $\lambda$  values tested. Figure 6.9a shows that for all variations of the horizontal interface equation, a three-stage process was required to achieve a 84% yield and Figure 6.9d shows that almost all runs required a four-stage system to achieve an 86% yield. Figure 6.9b shows that around 90% of runs required a three-stage process to achieve a 85% yield and Figure 6.9c shows

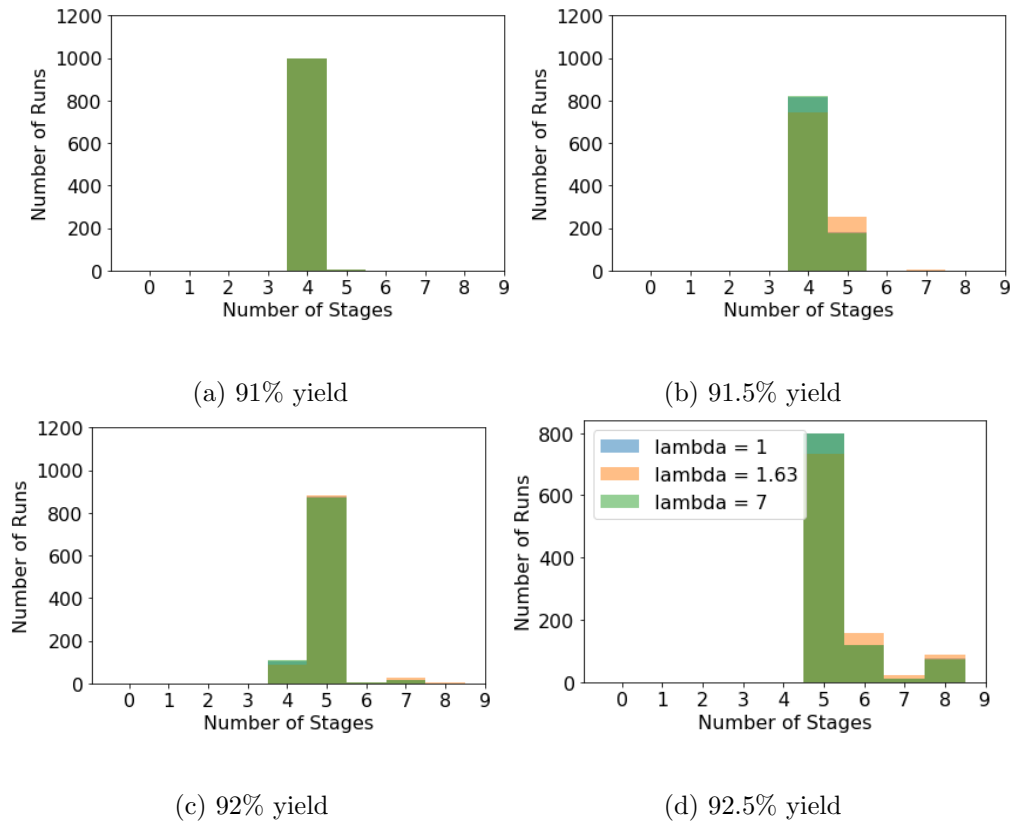


Figure 6.10: The number of stages required to reach varying yields around that which is achieved in a four-stage process. Shown are the results for  $\lambda = 1, 1.63,$  and  $7$ .

that around 70% of runs required a four-stage process to achieve a 85.5 % yield. Again, in all four sub figures,  $\lambda$  does not change the results significantly. The region in which there is uncertainty in the stage-wise results is between 85 and 86% which is slightly larger than that seen in the two-stage process, but that would be expected as the number of stages increases (thereby increasing the complexity of the system and model) and the region is still small. As both  $\lambda$  and the region in which there is an uncertainty in the stage-wise optimisation is small, a user can be confident in the model.

Shown in Figure 6.10 is the robustness testing surrounding a four-stage process. The LIL model predicts that a yield of 91.7% would be achieved using a four-stage process and yields above this value would require more stages. As a result, the stage-wise optimisation across varying horizontal interface slopes was run for a required yield of 91%, 91.5%, 92% and 92.5% for the three  $\lambda$  values tested. Figure 6.10a shows that almost all variations of the horizontal interface equation a four-stage process was required to achieve a 91% yield and Figure 6.10d shows that all runs

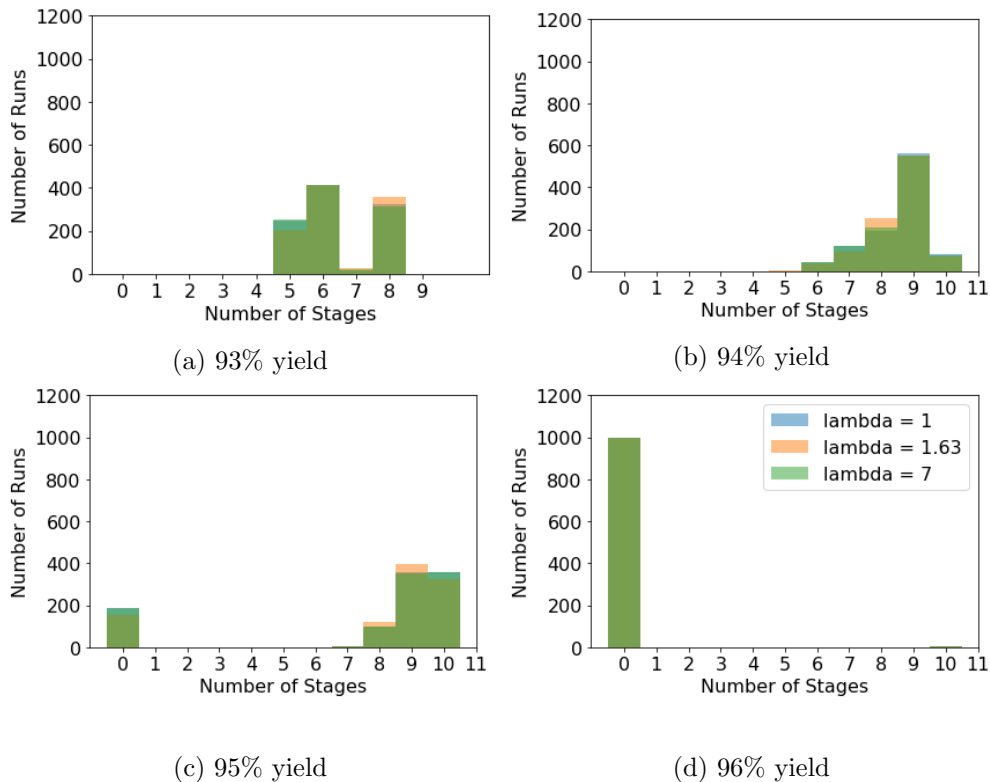


Figure 6.11: The number of stages required to reach varying yields around that which is achieved in a >four-stage process. Shown are the results for  $\lambda = 1, 1.63,$  and  $7.$

required at least a five-stage system to achieve an 92.5% yield. Figure 6.10b shows that around 80% of runs required a four-stage process to achieve a 85% yield and Figure 6.10c shows that around 90% of runs required a four-stage process to achieve a 92% yield. For Figure 6.10a,  $\lambda$  does not change the results significantly and a user could be confident in the results up to a four-stage process.

Shown in Figure 6.11 is the stage wise optimisation with varying horizontal interface for yields which require more than four stages. This is because above four stages, the stepwise improvement in yield is not significant; as a result, the improvement in yield is less than the uncertainty in the modelling. Figure 6.11 shows that there is a general trend of requiring more stages to reach a higher yield. However, there is a large spread of results across four or more optimal stage requirements. Figure 6.11d shows that it is not possible to achieve a yield of 96% under the operating conditions implemented by the model. Interestingly, there is little variation between the results, meaning that uncertainty in results is likely a result of process limitations rather than confidence in the horizontal interface equation. After four stages, the model is not accurate enough to predict robust conditions. This could

be because the model is not accurate enough for a large number of stages, but it is more likely that it is due to the very close results in yield achieved when more than four stages are used.

### 6.3 Conclusions

In this chapter, two variables which were known to affect the performance of multi-stage ATPE were investigated: the kinetics of the phase separation, and partitioning of protein into the horizontal interface of a system. The first was evaluated experimentally and the second through a modelling approach. The experimentation surrounding the phase separation applied the non-traditional techniques of using a UV-vis and microscopic observation alongside traditional dispersion height measurements to evaluate the separation of the phases. It was found that the separation continued long after the formation of the horizontal interface, and that separation occurred in both the continuous and dispersed phase. Concentration analysis of C-phycoerythrin demonstrated that this separation past horizontal interface formation had a large effect on protein partitioning even in single-stage extractions. Material continued to move into the top phase rapidly for around 15 minutes after separation started; this did not coincide with horizontal interface formation for a system of this size which took around 5 minutes. After this, there was a slower separation period between 6 hours and 24 hours. During this period, it was found that for C-phycoerythrin, partitioning into the horizontal interface from the top phase was achieved mostly during this separation period. As a result of both these factors, the equilibrium concentrations differed vastly to concentrations achieved at the formation of an horizontal interface. For a system where the yield was being evaluated, the optimum point at which to extract the phases did not coincide with either the horizontal interface formation or equilibrium.

Varying  $\lambda$  within the Deming regression had very little impact on both the value for  $\beta$  and its confidence intervals which were used to describe the partitioning of protein into the horizontal interface. This meant that there was a high degree of confidence in the data gathered and modelling used to describe horizontal interface partitioning despite difficulties presented in experimentally measuring precipitated protein. The modelling surrounding the robustness testing on the horizontal interface showed that stage-wise optimisation did not vary significantly while there was still a significant step-wise performance increase. After four stages, an increase in stages had little impact on process performance, at this point the model was shown to not be robust. It was thought that this was a result of the close results for the stages.

## Chapter 7

# Conclusions and Future Work

This chapter outlines the major conclusions and findings in this thesis followed by the future work to be carried out. The work in this thesis surrounds the use of [Aqueous Two-Phase Extraction \(ATPE\)](#); specifically, the work explores the use of multi-stage processing to improve the yield and purity achieved by the process. The literature review outlined the importance of investigating the use of [ATPE](#) as a continuous protein purification option in the biopharmaceutical industry. Moving towards continuous manufacturing options has become of increasing interest to the biopharmaceutical industry as it is a way to decrease costs, increase manufacturing capacity, and increase product consistency and quality.

Aside from being a process which is easily run continuously, [ATPE](#) is a developing process which is cheap in comparison with the more traditional batch purification processes such as chromatography. This is both a result of the cheap phase forming components (usually a citrate, phosphate, or sulphate salt, and [Polyethylene Glycol \(PEG\)](#) for protein purification) and the ability to more easily recycle the more expensive polymer phase. The ability to recycle the polymer phase is particularly important if expensive ligands are used to improve the process resolution as the ligands will also be recycled by recycling the polymer phase. Additional advantages of [ATPE](#) include that it is a gentle, low shear process which does not damage protein, and that it is capable of combining multiple steps in processing (for instance, primary clarification, purification and protein concentration). Lastly, [ATPE](#) has been shown to be a robust process capable of handling large, varying, and crude feeds. Robust processing has become of increasing importance as the upstream processes have moved to continuous processing as material coming from continuous bioreactors has been shown to vary.

Despite the many advantages to [ATPE](#), the process has two major challenges which must be overcome in order to be accepted as an industrial process: the low

resolution of the process, and the lack of understanding of the phase forming mechanisms. These two drawbacks are inherently linked as the lack of understanding of the phase forming mechanisms has resulted in a lack of predictive process design that leads to the low process resolution. Currently, process design is heavily reliant on both individual expertise and ‘trial and error’; this is not guaranteed to yield the desired results. These two drawbacks mean that there is an opportunity to research and develop the process to improve both process understanding and tools for process design. As such, this thesis aimed to improve process yield and design through the use of multi-stage [ATPE](#). Additionally, a deeper understanding behind the process behaviour and important process variables was developed through exploring the use of multi-stage [ATPE](#). This is because issues in single-stage [ATPE](#) were magnified and highlighted when multi-stage extraction was explored.

This thesis was divided into three results chapters. The first chapter experimentally explored the use of multi-stage [ATPE](#). The second chapter developed a model to describe multi-stage [ATPE](#) which was operated with each step at equilibrium. The third chapter explored two variables that were shown to be important in multi-stage [ATPE](#) in previous chapters: the kinetics of the phase separation after the formation of the horizontal interface, and horizontal interface partitioning.

## 7.1 Conclusions

Chapter 4 evaluated three different protein mixtures in case study multi-stage [ATPEs](#). Two different operational methods were considered: phase separation using a centrifuge, and phase separation using gravity. The chapter demonstrated that [Multi-stage Extraction \(MSE\)](#) is a valuable tool which could be applied to [ATPE](#) in order to improve the process performance. Generally speaking, it was found that target protein recovery could be improved through additional stages between the protein feed and the waste exit, and the removal of contaminants could be improved through additional stages between the protein feed and the extract exit. While this general rule could be followed and demonstrates that [MSE](#) is a valuable tool, the chapter also demonstrated that there were other parameters which need to be carefully considered and the multi-stage process needed to be carefully controlled. These parameters included: operational method, controlling the phase forming constituent concentrations in extract and waste feeds, the behaviour of individual contaminants in multi-contaminant mixtures, careful selection of appropriate [Aqueous Two-Phase Systems \(ATPS\)](#) conditions, and horizontal interface partitioning.

A parameter in Chapter 4 that was shown to be of particular importance was the operational method. It was shown that there was a vast difference between

systems which were separated through centrifugation versus gravitational settling. For each of the [MSE](#) extractions carried out, the target protein recovery and purity was greater for a system operated with a centrifuge operation. It was theorised that this was because the systems separated by gravity were still undergoing separation which impacted process performance, whereas the centrifuged systems were at true equilibrium due to the greater forces applied on them. This difference also meant that different stock solutions for the phase forming components had to be used because the position of the horizontal interface shifted. This meant that control over the [MSE](#) was lost if the concentrations used for the centrifuged systems were used for the gravity-operated systems.

In this first results chapter, for practical reasons, it was found that systems should be operated and considered using an ‘extract’ and a ‘waste’ phase rather than as a ‘top’ and ‘bottom’ phase. When using [ATPE](#), completely separating the top [PEG](#)-rich from the salt-rich bottom phase is difficult to achieve. Using extract and waste phases which can consist of parts of each of the phases can account for this. Another consideration was how different contaminants behaved in the extraction. In the case study [MSE](#), C-phycoerythrin was removed from contaminants, and the major contaminants identified were allophycoerythrin and phycoerythrin. In the [ATPS](#) used, allophycoerythrin was easily separated from C-phycoerythrin, however, phycoerythrin partitioned into the same phase as C-phycoerythrin. The result of this was that the yield of the process was much easier to consider than the purity of the extract in this multi-component mixture because additional steps to improve C-phycoerythrin purity in the extract could also concentrate contaminants into the extract phase. This highlighted the importance of careful process design in [ATPE](#).

The last observation was that protein was shown to partition into the horizontal interface of the system. Most of the previous literature considers protein to either be in the top or bottom phase of the system. It was observed that stages which were closest to the exit of the waste stream had different partitioning ratios than expected and had much more protein in the waste phase than expected. It was theorised that this was because protein was becoming trapped into the horizontal interface and not redissolving until dilution for analysis, thereby altering partitioning coefficient.

The second results chapter developed a model to describe a single protein’s behaviour in multi-stage [ATPE](#) when the stages were operated to equilibrium, i.e. operated using a centrifuge. This chapter developed a modified McCabe-Thiele method to describe the system and considered two different partitioning regimes: a [Liquid-Liquid \(LL\)](#), and a novel [Liquid-Interface-Liquid \(LIL\)](#) distribution. Previous work in this area is based upon a [LL](#) distribution and assumes all protein partitioned into the top and bottom phase of the system. The [LIL](#) distribution considered

partitioning into the horizontal interface of the system as well as the top and bottom phases. Both of these models required equilibrium curves to describe a protein partitioning between each of the phases. The [LIL](#) model also required data on the volume of protein at the horizontal interface of a system, which can result in visual build ups of material in systems with significant partitioning of protein into the horizontal interface. In systems with large visual build-ups the protein in the horizontal interface, this material can be taken up into the extract phase which was accounted for in the [LIL](#) model. Both of these models were validated against experimental case study [MSEs](#), one using a single protein target (haemoglobin), and others considering C-phycoerythrin in multi-component mixture. In all validations carried out, the [LIL](#) model was shown to significantly outperform the [LL](#) model that shows that partitioning of protein into the horizontal interface of a system was an important variable to consider.

As a result of the consideration of protein partitioning into the horizontal interface of a system, the [LIL](#) multi-stage model describing [ATPE](#) was considered accurate enough to be used in multi-stage [ATPE](#) process design. The previous results chapter showed that one side of the feed considered protein yield and the other contaminant removal. As a single protein can be considered at a time, the [LIL](#) model was utilised to predict an appropriate [MSE](#) configuration of a separation of a model target protein, C-phycoerythrin, from a model contaminant, lysozyme. The [LIL](#) model was capable of predicting the number of stages required for target protein recovery. The yield can be predicted from this and would remain the same in multi-component mixtures provided other proteins do not alter the target protein's partitioning. In terms of contaminants, the model is only currently capable of predicting the number of stages required to remove a single contaminant at a time. While the removal of this single contaminant would remain the same in multi-component mixtures (provided it's partitioning is not altered), the model cannot necessarily be used to predict a process purity as it cannot consider other contaminants which may behave differently. In a multi-component purification with multiple contaminants that behave similarly, it is probable that a single equilibrium curve could be used to describe the grouped contaminants and the model can be used as an approximation of the contaminant's behaviour. However, a single equilibrium curve cannot be used to describe the partitioning of contaminants that have drastically different behaviour such as phycoerythrin and allophycoerythrin in the C-phycoerythrin case study [ATPE](#). In this case, equilibrium curves for each of these components would need to be constructed for them to be considered in any capacity.

The final results chapter explored in more detail the two variables which were shown in the previous results chapters to have a significant impact on multi-stage

**ATPE**: the phase separation after the formation of the horizontal interface, and protein partitioning into the horizontal interface. The former was considered to be important due the differences observed between separating a system through the use of a centrifuge versus gravity. Systems operated through the use of a centrifuge have large forces applied to them and so rapidly reach equilibrium. Conversely, systems operated through gravity are judged by eye to have completed separation at the formation of a distinct horizontal interface; any separation after this point is assumed to have no significant effect on phase separation. To investigate phase separation, four techniques were used: traditional dispersion height measurements, **Ultraviolet-visible (UV-vis)** spectrophotometer analysis at 555 nm, microscopic observation, and protein concentration analysis of the phases at various time points. In all systems evaluated, phase separation was observed to continue after the formation of the horizontal interface. Furthermore, while in previous literature systems are considered to have a ‘continuous phase’ and a ‘dispersed phase’, microscopic observation showed separation in both phases as well as protein concentration changes after the horizontal interface formation.

From all data gathered, it appeared that there were two mechanisms in the phase separation. The first was the rapid initial separation of the larger globules within the system, and the second was a much slower settling of the smaller globules. In terms of protein partitioning, the model protein, C-phycoerythrin, rapidly separated into the liquid phases during the first stage which took around 15 minutes and then settled into the horizontal interface between 6 and 24 hours after separation began. For a system of the size used in **UV-vis**, microscopic and protein concentration analysis, horizontal interface formation took around 5 minutes. However, the movement of C-phycoerythrin into the top (extract) phase continued until 15 minutes and significantly improved between 5 and 15 minutes (24.3 % increase with respect to the total protein amount). The recovery of C-phycoerythrin in the top phase was reduced between 6 and 24 hours as C-phycoerythrin settled into the horizontal interface (21.9% of the total protein). Therefore, this data demonstrated that optimal separation time for **ATPE** does not necessarily coincide with either the horizontal interface formation or equilibrium because of horizontal interface settling.

The second variable investigated in the third results chapter was horizontal interface partitioning. As protein within the horizontal interface has precipitated, the accuracy of the experimental data generated around this was thought to be less than other experimental data. The data surrounding the horizontal interface was thought to be of key concern to the **LIL** model, and the model needed to be robust enough to handle variations and inaccuracies in the single-stage equilibrium data for horizontal interface partitioning. As such, robustness testing was carried out on

the model to determine if variation in horizontal interface partitioning impacted the stage-wise optimisation results. To do this, the model was adjusted to determine an optimal number of stages for a required protein recovery or removal depending on if a target protein or contaminant was being considered. Deming regression was then utilised to determine the variance of the equation describing the horizontal interface partitioning of a model protein, haemoglobin, in the haemoglobin case study system. This protein was used as it had the most drastic partitioning of all the system evaluated. The [LIL](#) model was then run using different variables for the horizontal interface partitioning to determine if the stage-wise results remained consistent. It was found that results remained consistent while additional stages had a significant impact on resolution. However, once there was little improvement from additional steps, the results became less robust.

Overall, the most important contribution of this thesis is the work in showing how crucial it is to consider partitioning of protein into the horizontal interface of an [ATPS](#). Previous literature considers that protein partitions only between the bulk phases and that the bulk separation takes place before the formation of a horizontal interface. This work has demonstrated that a significant amount of protein partitions into the interface, particularly between the horizontal interface formation and the point at which phases are clear and non-turbid. To utilise [ATPE](#) as a protein purification technique industrially both an accurate understanding of system behaviour and accurate models to describe system behaviour will be needed. This thesis shows that to do that both horizontal interface partitioning and separation after horizontal interface formation need to be considered.

## 7.2 Future Work

In Chapters [4](#) and [5](#) it was found that there was more protein in the waste phases close to the waste exit point. It was theorised that this was because protein was becoming trapped in the horizontal interface thereby altering partitioning. To determine if this is the case in future work, Native-PAGE samples could be ran on samples of the horizontal interface to detect aggregated protein in the horizontal interface. Measurements of the phase forming components at stage five and the feed could be determined to see if they have been altered by stage five, thereby altering partitioning. Full characterisation of the feed stock could be carried out using various techniques such as mass spectrometry analysis for all components and SDS-PAGE for protein components. Equilibrium curves of C-phycoyanin in the case study system could then be constructed in the presence of each of these contaminants to see if it alters the partitioning of C-phycoyanin, thereby altering partitioning across

the stages.

To develop the model further, work could be done on estimating how much of the protein does not redissolve in each step of the process, as well as looking at the best methods and conditions to redissolve the protein in the horizontal interface. To further reduce experimental workloads in [ATPE](#), multi-stage models could be utilised with single-stage predictive protein partitioning models. Together, these models could evaluate a large number of systems and operational procedures to pick optimal conditions. Until such models are developed with enough accuracy, high throughput robotic-aided strategies could be used to consider a large number of systems. The effectiveness of additional steps was found to decrease as more stages were added. Therefore, future work could also include investigating the cost-effectiveness of extra steps.

One area of future work is considering how multi-component protein mixtures impacts the behaviour of a single protein within that system. Within this, how much other proteins impact partitioning of a target protein at equilibrium needs to be established. This could be established through determining equilibrium curves of different proteins in different protein mixtures to see if the same proteins follow the same partitioning patterns. It would be expected that there would be some impact on behaviour, particularly for systems which are reaching phase saturation concentrations. Depending on the results of this experimentation, the modelling of multi-component mixtures in multi-stage [ATPE](#) operated at equilibrium should be explored in future work. This work could involve utilising a multi-component feed approach as is used in distillation and in traditional [Liquid-Liquid Extraction \(LLE\)](#). For processes where the component partitioning is strongly dependent on the phase forming components, as is the case in [ATPE](#), a Rachford-Rice algorithm could be applied to the system ([Seader et al., 2006](#)).

In terms of future work surrounding the kinetics of the phase separation, the first thing that needs to be established is a more in depth understanding of each step of separation. For this, analysis of different, much smaller fractions of a system across various time points should be carried out. This could be for protein concentration, phase constituent concentration or [UV-vis](#) analysis at 555 nm. Taking fractions at different time points would give an idea of how concentration gradients across the phases play a part in the phase separation, particularly in the first rapid stage of separation. Concentration gradients are unlikely to play a part in the slow settling, however, a more in depth analysis of the slow separation when material settles into the horizontal interface could be carried out using this method. Once this has been established, different settling regimes for proteins with different types of partitioning should be explored. In this study, a model protein which favoured the top phase and

horizontal interface of a system with a continuous top phase was investigated. In further work, a wider study which covers proteins that favour different phases as well as systems with continuous top and systems with continuous bottom phases should be considered. Future work could also see if different proteins settle at different rates in systems, and if settling can be linked to phase constituent concentration or distance to equilibrium. Lastly, multi-component mixtures should be considered to see if different proteins impact settling behaviour and if different proteins separate at different rates. Ideally, models should be built to accurately describe the phase separation and protein partitioning of the systems.

Ideally, future work should include both modelling to describe the kinetics of the phase separation as well as to optimise the settling time for gravity settling. Optimising settling time is an important consideration due to the fact that the optimal time does not coincide with either horizontal interface formation or equilibrium. This is even more important because significant differences in partitioning coefficient are seen in the minutes after horizontal interface formation, and between this point and equilibrium. To carry out settling time optimisation when considering a single protein, separation time (rather than stages) could be minimised. This would allow the model to account for separation after the formation of the horizontal interface. However, the model would not be capable of accounting for the additional cost of extra stages. One way round this is to optimise for cost; this can balance the amount of material which can be processed (increased settling time decreases this) with the cost of additional stages. Once multi-component mixtures are used, it is possible that the yield and purity requirements for minimum settling time will conflict. More work is required to fully understand how these requirements will conflict.

In future work, robustness testing could be expanded in order to consider other variables which could affect the system behaviour. The robustness testing should be carried out on more systems and proteins to test if the model is still reasonably robust under other conditions. Conditions which should be tested include horizontal interface behaviour with multiple proteins within the system, and for systems with different distribution and separation profiles. Other future work could look at evaluating the uncertainty surrounding other variables within the model, particularly how variations in the phase separation kinetics affect the extraction process. Another variable which could be evaluated is the variation surrounding the feed which is known to be changeable in bioprocessing. To make the model more useful to a user, the output of the model could be varied to determine regions of certainty and uncertainty in a stage-wise output for a required yield. This would make it much easier to compare results in testing different variables.

In terms of more extensive future work, there are several other areas which need

---

to be considered. Firstly, the different components of this thesis could be joined together. In particular, the more extensive understanding of the phase separation should be built into the equilibrium model to describe systems which are not operating at equilibrium. As there will be variance surrounding the phase separation, the robustness testing should be utilised to test this. Another place the model should be tested is upon scale up; scale up is largely based on phase separation to the point of horizontal interface formation. As such, the impact of separation of phases after horizontal interface formation should be considered in scale up. While this separation may take too long to be practical, it may influence the choice to operate systems with either gravity or centrifuge operation. Lastly, protein partitioning in the horizontal interface is not widely considered within the literature or within the current modelling of *ATPE*. Models such as [Mistry et al. \(1996\)](#) could be more accurate if horizontal interface partitioning is considered within in them. Once this is done, to even further expand the model built within this thesis, the multi-stage modelling could be linked to the predictive partitioning models described in the literature.



# References

- A. Ahmad, C. Derek, and M. Zulkali. Optimization of thaumatin extraction by aqueous two-phase system (ATPS) using response surface methodology (RSM). *Separation and Purification Technology*, 62(3):702–708, Sep. 2008. ISSN 1383-5866. doi: 10.1016/J.SEPPUR.2008.03.028.
- E. Akardere, B. Özer, E. B. Çelem, and S. Önal. Three-phase partitioning of invertase from Baker’s yeast. *Separation and Purification Technology*, 72(3):335–339, May. 2010. ISSN 13835866. doi: 10.1016/j.seppur.2010.02.025.
- P.-Å. Albertsson. Partition of Proteins in Liquid Polymer–Polymer Two-Phase Systems. *Nature*, 182(4637):709–711, Sep. 1958. ISSN 0028-0836.
- P.-Å. Albertsson. *Partition of cell particles and macromolecules in polymer two-phase systems*. Wiley, USA, second edition, 1971.
- P. A. Albertsson. *Partition of cell particles and macromolecules*. Wiley, New York, third edition, 1986. ISBN 0471828203. doi: doi.org/10.1002/cbf.290050311.
- A. M. Alhelli, M. Yazid, A. Manap, A. S. Mohammed, H. Mirhosseini, E. Suliman, Z. Shad, N. K. Mohammed, A. Shobirin, and M. Hussin. Response Surface Methodology Modelling of an Aqueous Two-Phase System for Purification of Protease from *Penicillium candidum* (PCA 1/TT031) under Solid State Fermentation and Its Biochemical Characterization. *International Journal of Molecular Sciences Article*, 2016. doi: 10.3390/ijms17111872.
- K. P. Ananthapadmanabhan and E. D. Goddard. Aqueous Biphasic Formation in Polyethylene Oxide-Inorganic Salt Systems. *Langmuir*, 3:25–31, 1987.
- Anaspec. R-PE (R-Phycocerythrin), 2020a. URL <https://www.anaspec.com/products/product.asp?id=29041>. Accessed: 2015-12-04.
- Anaspec. C-PC (C-Phycocyanin), 2020b. URL <https://www.anaspec.com/products/product.asp?id=48159>. Accessed: 2020-05-11.

- N. G. Anderson. Practical Use of Continuous Processing in Developing and Scaling Up Laboratory Processes. *Organic Process Research & Development*, 5(6):613–621, Nov. 2001. ISSN 1083-6160.
- B. Andrews and J. Asenjo. Protein partitioning equilibrium between the aqueous poly(ethylene glycol) and salt phases and the solid protein phase in poly(ethylene glycol)-salt two-phase systems. *Journal of Chromatography B*, 685(11):15–20, 1996. doi: 10.1016/0378-4347(96)00134-X.
- B. A. Andrews and J. A. Asenjo. Theoretical and Experimental Evaluation of Hydrophobicity of Proteins to Predict their Partitioning Behavior in Aqueous Two Phase Systems: A Review. *Separation Science and Technology*, 45(15):2165–2170, 2010.
- B. A. Andrews, D. M. Head, P. Dunthorne, and J. A. Asenjo. PEG Activation and Ligand Binding for the Affinity Partitioning of Proteins in Aqueous Two-Phase Systems. *Biotechnology Techniques*, 4(1):49–54, 1990.
- B. A. Andrews, S. Nielsen, and J. A. Asenjo. Partitioning and purification of monoclonal antibodies in aqueous two-phase systems. *Bioseparation*, 6(5):303–13, 1996. ISSN 0923-179X.
- B. A. Andrews, A. S. Schmidt, and J. A. Asenjo. Correlation for the partition behavior of proteins in aqueous two-phase systems: Effect of surface hydrophobicity and charge. *Biotechnology and Bioengineering*, 90(3):380–390, 2005. ISSN 00063592. doi: 10.1002/bit.20495.
- F. S. Antelo, J. A. V. Costa, and S. J. Kalil. Purification of C-phycoerythrin from *Spirulina platensis* in aqueous two-phase systems using an experimental design. *Brazilian Archives of Biology and Technology*, 58(1):1–11, 2015. ISSN 16784324. doi: 10.1590/S1516-8913201502621.
- J. a. Asenjo and B. a. Andrews. Aqueous two-phase systems for protein separation: A perspective. *Journal of Chromatography A*, 1218(49):8826–8835, 2011a. ISSN 00219673.
- J. A. Asenjo and B. A. Andrews. Aqueous two-phase systems for protein separation: A perspective. *Journal of Chromatography A*, 1218(49):8826–8835, 2011b. ISSN 00219673. doi: 10.1016/j.chroma.2011.06.051.
- J. A. Asenjo, A. S. Schmidt, F. Hachem, and B. A. Andrews. Model for predicting the partition behaviour of proteins in aqueous two-phase systems. *Journal of Chro-*

- matography A*, 668(1):47–54, 1994. ISSN 00219673. doi: 10.1016/0021-9673(94)80090-1.
- J. a. Asenjo, S. L. Mistry, B. a. Andrews, and J. C. Merchuk. Phase separation rates of aqueous two-phase systems: Correlation with system properties. *Biotechnology and Bioengineering*, 79(2):217–223, 2002a. ISSN 00063592. doi: 10.1002/bit.10273.
- J. A. Asenjo, S. L. Mistry, B. A. Andrews, and J. C. Merchuk. Phase separation rates of aqueous two-phase systems: Correlation with system properties. *Biotechnology and Bioengineering*, 79(2):217–223, 2002b. doi: 10.1002/bit.10273.
- A. M. Azevedo, P. A. Rosa, I. F. Ferreira, and M. R. Aires-Barros. Optimisation of aqueous two-phase extraction of human antibodies. *Journal of Biotechnology*, 132(2):209–217, Oct. 2007. ISSN 01681656. doi: 10.1016/j.jbiotec.2007.04.002.
- A. M. Azevedo, P. A. Rosa, I. F. Ferreira, and M. R. Aires-Barros. Chromatography-free recovery of biopharmaceuticals through aqueous two-phase processing. *Trends in Biotechnology*, 27(4):240–247, Apr. 2009a. ISSN 01677799. doi: 10.1016/j.tibtech.2009.01.004.
- A. M. Azevedo, P. A. Rosa, I. F. Ferreira, J. de Vries, T. Visser, and M. R. Aires-Barros. Downstream processing of human antibodies integrating an extraction capture step and cation exchange chromatography. *Journal of Chromatography B*, 877(1-2):50–58, Jan. 2009b. ISSN 1570-0232. doi: 10.1016/J.JCHROMB.2008.11.014.
- A. Bateman. UniProt: A worldwide hub of protein knowledge. *Nucleic Acids Research*, 47:D506–D515, Jan. 2019. ISSN 13624962. doi: 10.1093/nar/gky1049. URL <https://www.ebi.ac.uk/proteins/api/doc/>. Accessed: 2020-10-13.
- M. Beijerinck. Über eine Eigentümlichkeit der löslichen Stärke. *Journal für praktische Chemie*, 36:378, 1886.
- J. Benavides and M. Rito-Palomares. Practical experiences from the development of aqueous two-phase processes for the recovery of high value biological products. *Journal of Chemical Technology & Biotechnology*, 83(2):133–142, Feb. 2008. ISSN 02682575. doi: 10.1002/jctb.1844.
- J. Benavides, M. Rito-Palomares, and J. Asenjo. *Aqueous Two-Phase Systems*. Elsevier, 2011.

- A. Bennett and L. Bograd. COMPLEMENTARY CHROMATIC ADAPTATION IN A FILAMENTOUS BLUE-GREEN ALGA. *The Journal of Cell Biology*, 58: 419–435, 1973.
- M. Bensch, B. Selbach, and J. Hubbuch. High throughput screening techniques in downstream processing: Preparation, characterization and optimization of aqueous two-phase systems. *Chemical Engineering Science*, 62(7):2011–2021, 2007. doi: 10.1016/j.ces.2006.12.053.
- Bio-Rad. Chromatography in Food Production —, 2020. URL <https://www.bio-rad.com/en-uk/applications-technologies/chromatography-food-production?ID=MA7JLH15>. Accessed: 2020-07-09.
- E. A. Blackstone and P. F. Joseph. The economics of biosimilars. *American health & drug benefits*, 6(8):469–78, Sep. 2013.
- G. Blomquist and P.-A. Albertsson. A study of extraction columns for aqueous polymer two phase systems. *Journal of Chromatography*, 73:125–133, 1972.
- E. J. Bras, R. R. Soares, A. M. Azevedo, P. Fernandes, M. Arévalo-Rodríguez, V. Chu, J. P. Conde, and M. R. Aires-Barros. A multiplexed microfluidic toolbox for the rapid optimization of affinity-driven partition in aqueous two phase systems. *Journal of Chromatography A*, 1515:252–259, Sep. 2017. doi: 10.1016/j.chroma.2017.07.094.
- H. Cabezas. Theory of phase formation in aqueous two-phase systems. *Journal of Chromatography B: Biomedical Sciences and Applications*, 680(1-2):3–30, May. 1996.
- R. Carle and R. M. Schweiggert. *Handbook on Natural Pigments in Food and Beverages: Industrial Applications for Improving Food Color*. Elsevier Inc., Apr. 2016. ISBN 9780081003923. doi: 10.1016/C2014-0-03842-7.
- ClevelandDx. Clevelanddx: Our technology, 2021. URL <https://clevelanddx.com/our-technology>. Accessed:2021-07-21.
- M.-F. Clincke, C. Mölleryd, Y. Zhang, E. Lindskog, K. Walsh, and V. Chotteau. Very high density of CHO cells in perfusion by ATF or TFF in WAVE bioreactor™. Part I. Effect of the cell density on the process. *Biotechnology progress*, 29(3):754–67, Jan. 2013.
- E. J. Close, J. R. Salm, T. Iskra, E. Sørensen, and D. G. Bracewell. Fouling of an anion exchange chromatography operation in a monoclonal antibody process:

- Visualization and kinetic studies. *Biotechnology and Bioengineering*, 110(9):2425–2435, Sep. 2013.
- F. da Silva Figueira, C. C. Moraes, and S. J. Kalil. C-phycoerythrin purification: Multiple processes for different applications. *Brazilian Journal of Chemical Engineering*, 35(3):1117–1128, Jul. 2018. ISSN 01046632. doi: 10.1590/0104-6632.20180353s20170160.
- D. P. de Barros, S. R. Campos, A. M. Azevedo, A. M. Baptista, and M. R. Aires-Barros. Predicting protein partition coefficients in aqueous two phase system. *Journal of Chromatography A*, 1470:50–58, Oct. 2016. ISSN 18733778. doi: 10.1016/j.chroma.2016.09.072.
- S. de Belval, B. le Breton, J. Huddleston, and A. Lyddiatt. Influence of temperature upon protein partitioning in poly(ethylene glycol)–salt aqueous two-phase systems close to the critical point with some observations relevant to the partitioning of particles. *Journal of Chromatography B: Biomedical Sciences and Applications*, 711(1-2):19–29, Jun. 1998. ISSN 0378-4347. doi: 10.1016/S0378-4347(97)00561-6.
- R. Dembczyński, W. Białas, K. Regulski, and T. Jankowski. Lysozyme extraction from hen egg white in an aqueous two-phase system composed of ethylene oxide-propylene oxide thermoseparating copolymer and potassium phosphate. *Process Biochemistry*, 45(3):369–374, Mar. 2010. ISSN 13595113. doi: 10.1016/j.procbio.2009.10.011.
- R. Dembczyński, W. Białas, and T. Jankowski. Partitioning of lysozyme in aqueous two-phase systems containing ethylene oxide-propylene oxide copolymer and potassium phosphates. *Food and Bioproducts Processing*, 91(3):292–302, Jul. 2013. ISSN 09603085. doi: 10.1016/j.fbp.2012.11.001.
- F. Dimer, S. Alexander Oelmeier, and J. Hubbuch. Molecular dynamics simulations of aqueous two-phase systems: Understanding phase formation and protein partitioning. *Chemical Engineering Science*, 96:142–151, Jun. 2013. ISSN 00092509. doi: 10.1016/j.ces.2013.03.020.
- A. Dobry and F. Boyer-Kawenoki. Phase separation in polymer solution. *Journal of Polymer Science*, 2(1):90–100, Feb. 1947.
- P. M. Doran. *Bioprocess Engineering Principles*, Second Edition:, 2013.
- A. K. Dutta, T. Tran, B. Napadensky, A. Teella, G. Brookhart, P. A. Ropp, A. W. Zhang, A. D. Tustian, A. L. Zydney, and A. L. Shinkazh. Purification of monoclonal antibodies from clarified cell culture fluid using Protein A capture contin-

- uous countercurrent tangential chromatography. *Journal of Biotechnology*, 213: 54–64, Nov. 2015.
- E. Espitia-Saloma, P. Vázquez-Villegas, O. Aguilar, and M. Rito-Palomares. Continuous aqueous two-phase systems devices for the recovery of biological products. *Food and Bioproducts Processing*, 92(2):101–112, Apr. 2014.
- P.-F. Fauquex, H. Hustedt, and M.-R. Kula. Phase equilibration in agitated vessels during extractive enzyme recovery. *Journal of Chemical Technology and Biotechnology. Biotechnology*, 35(1):51–59, Mar. 1985. ISSN 02643421. doi: 10.1002/jctb.280350110.
- B. Fernández-Rojas, J. Hernández-Juárez, and J. Pedraza-Chaverri. Nutraceutical properties of phycocyanin. *Journal of Functional Foods*, 11:375–392, Nov. 2014. ISSN 17564646. doi: 10.1016/j.jff.2014.10.011.
- I. F. Ferreira, A. M. Azevedo, P. A. Rosa, and M. R. Aires-Barros. Purification of human immunoglobulin G by thermoseparating aqueous two-phase systems. *Journal of Chromatography A*, 1195(1-2):94–100, Jun. 2008.
- L. A. Ferreira, O. Fedotoff, V. N. Uversky, and B. Y. Zaslavsky. Effects of osmolytes on protein-solvent interactions in crowded environments: Study of sucrose and trehalose effects on different proteins by solvent interaction analysis. *RSC Advances*, 5(34):27154–27162, 2015a. ISSN 20462069. doi: 10.1039/c5ra02997j.
- L. A. Ferreira, P. P. Madeira, V. N. Uversky, and B. Y. Zaslavsky. Analyzing the effects of protecting osmolytes on solute-water interactions by solvatochromic comparison method: I. Small organic compounds. *RSC Advances*, 5(74):59812–59822, Jul. 2015b. ISSN 20462069. doi: 10.1039/c5ra08610h.
- FiercePharma. Top 20 drugs by global sales 2019: Avastin, 2020. URL <https://www.fiercepharma.com/special-report/top-20-drugs-by-global-sales-2019-avastin>. Accessed:2021-07-19.
- GE Healthcare. Continuous chromatography in downstream processing of a monoclonal antibody, 2015.
- Genentech. Avastin prescribing information, 2021. URL [https://www.gene.com/download/pdf/avastin\\_prescribing.pdf](https://www.gene.com/download/pdf/avastin_prescribing.pdf). Accessed:2021-07-19.
- R. Godawat, K. Brower, S. Jain, K. Konstantinov, F. Riske, and V. Warikoo. Periodic counter-current chromatography - design and operational considerations for integrated and continuous purification of proteins. *Biotechnology Journal*, 7(12): 1496–1508, Dec. 2012.

- J. Golob and R. Modic. Coalescence of Liquid-Liquid Dispersions in Gravity Settlers. *Transactions of the institutions of the institution of chemical engineers*, 55(3):207–211, 1977.
- A. L. Grilo, M. Raquel Aires-Barros, and A. M. Azevedo. Partitioning in Aqueous Two-Phase Systems: Fundamentals, Applications and Trends. *Separation & Purification Reviews*, 45(1):68–80, Jan. 2016.
- M. Hall, D. Hill, and G. Pave. Global Pharmaceuticals 2016 industry statistics. Technical report, Hardman and Co, 2017. URL <http://www.hardmanandco.com/docs/default-source/sector-docs/life-sciences-documents/02.03.17-global-pharmaceutical-industry-2016-statistics.pdf>. Accessed: 2018-03-25.
- N. Hammerschmidt, A. Tscheliessnig, R. Sommer, B. Helk, and A. Jungbauer. Economics of recombinant antibody production processes at various scales: Industry-standard compared to continuous precipitation. *Biotechnology Journal*, 9(6):766–775, Jun. 2014.
- D. P. Harris, A. T. Andrews, G. Wright, D. L. Pyle, and J. A. Asenjo. The application of aqueous two-phase systems to the purification of pharmaceutical proteins from transgenic sheep milk. *Bioseparation*, 7(1):31–7, 1997. doi: 10.1023/A:1007908703773.
- E. Harris. *Protein purification methods : a practical approach*. IRL Press at Oxford University Press, Oxford ;;New York, 1989. ISBN 9780199630028.
- R. A. Hart, P. M. Lester, D. H. Reifsnyder, J. R. Ogez, and S. E. Builder. Large scale, in situ isolation of periplasmic IGF-I from E. coli. *Bio/technology (Nature Publishing Company)*, 12:1113–1117, 1994.
- Harvard. A summary of error propagation, 2007. URL [http://ipl.physics.harvard.edu/wp-uploads/2013/03/PS3\\_Error\\_Propagation\\_sp13.pdf](http://ipl.physics.harvard.edu/wp-uploads/2013/03/PS3_Error_Propagation_sp13.pdf). Accessed:2021-07-18.
- R. Hatti-Kaul. *Aqueous Two-Phase Systems*, volume 11. Humana Press, New Jersey, Feb. 2000.
- M. Helfrich, M. El-Kouedi, M. . Etherton, and C. Keating\*. Partitioning and Assembly of Metal Particles and Their Bioconjugates in Aqueous Two-Phase Systems. 2005. doi: 10.1021/LA051220Z.

- L. R. Herron, C. Pridans, M. L. Turnbull, N. Smith, S. Lillico, A. Sherman, H. J. Gilhooley, M. Wear, D. Kurian, G. Papadakos, P. Digard, D. A. Hume, A. C. Gill, and H. M. Sang. A chicken bioreactor for efficient production of functional cytokines. *BMC Biotechnology*, 18(1):82, Dec. 2018. ISSN 14726750. doi: 10.1186/s12896-018-0495-1.
- F. Hilbrig and R. Freitag. Continuous annular chromatography. *Journal of Chromatography B*, 790(1-2):1–15, Jun. 2003.
- G. Hodge. Media development for mammalian cell culture. *Biopharm International*, 18(5), 2005.
- J. Huddleston, A. Veide, K. K6hler, J. Flanagan, S.-O. Enfors, A. Lyddiatt, J. Huddleston, J. Fianagan, and A. Lyddiatt. The molecular basis of partitioning in aqueous two-phase systems. *Tibtech*, 9:381–388, 1991.
- E. Huenupi, A. Gomez, B. A. Andrews, and J. A. Asenjo. Optimization and design considerations of two-phase continuous protein separation. *Journal of Chemical Technology & Biotechnology*, 74(3):256–263, Mar. 1999.
- W. Hummel, H. Schfitte, and M.-R. Kula. Microbiology and Biotechnology Large Scale Production of D-Lactate Dehydrogenase for the Stereospecific Reduction of Pyruvate and Phenylpyruvate. Technical report, 1983.
- IndustryArc. Biopharmaceutical market -forecast (2021-2026), 2019. URL <https://www.industryarc.com/Report/9586/biopharmaceutical-market.html>. Accessed:2021-07-19.
- H. Indyk, J. Williams, and H. Patel. Analysis of denaturation of bovine IgG by heat and high pressure using an optical biosensor. *International Dairy Journal*, 18(4): 359–366, Apr. 2008.
- G. V. Jeffreys and J. L. Hawksley. Coalescence of liquid droplets in two-component–two-phase systems: Part I. Effect of physical properties on the rate of coalescence. *AIChE Journal*, 11(3):413–417, 1965.
- L. Jiang, Y. Wang, G. Liu, H. Liu, F. Zhu, H. Ji, and B. Li. C-Phycocyanin exerts anti-cancer effects via the MAPK signaling pathway in MDA-MB-231 cells. *Cancer Cell International*, 18(1), Jan. 2018. ISSN 14752867. doi: 10.1186/s12935-018-0511-5.
- Y. Jiang, H. Xia, J. Yu, C. Guo, and H. Liu. Hydrophobic ionic liquids-assisted polymer recovery during penicillin extraction in aqueous two-phase system.

- Chemical Engineering Journal*, 147(1):22–26, Apr. 2009. ISSN 1385-8947. doi: 10.1016/J.CEJ.2008.11.012.
- J. Jin, S. Chhatre, N. J. Titchener-Hooker, and D. G. Bracewell. Evaluation of the impact of lipid fouling during the chromatographic purification of virus-like particles from *Saccharomyces cerevisiae*. *Journal of Chemical Technology & Biotechnology*, 85(2):pp. 209–215, 2010.
- H. O. Johansson, G. Karlström, F. Tjerneld, and C. A. Haynes. Driving forces for phase separation and partitioning in aqueous two-phase systems. *Journal of Chromatography B: Biomedical Applications*, 711(1-2):3–17, Jun. 1998. ISSN 15726495. doi: 10.1016/S0378-4347(97)00585-9.
- P. Kan and C. J. Lee. Application of aqueous two-phase systems in separation/purification of stroma free hemoglobin from animal blood. *Artificial cells, blood substitutes, and immobilization biotechnology*, 22(3):641–9, 1994. ISSN 1073-1199. doi: 10.3109/10731199409117894.
- T. Karkas, K. Karkas, and S. İl Önal. Characteristics of invertase partitioned in poly(ethylene glycol)/magnesium sulfate aqueous two-phase system. *Biochemical Engineering Journal*, 60:142–150, 2012. doi: 10.1016/j.bej.2011.11.005.
- A. Kaul, R. A. M. Pereira, J. A. Asenjo, and J. C. Merchuk. Kinetics of phase separation for polyethylene glycol-phosphate two-phase systems. *Biotechnology and Bioengineering*, 48(3):246–256, 1995.
- P. U. Kenkare and C. K. Hall. Modeling of phase separation in PEG–salt aqueous two-phase systems. *AIChE Journal*, 42(12):3508–3522, Dec. 1996.
- C. Kepka, J. Rhodin, R. Lemmens, F. Tjerneld, and P.-E. Gustavsson. Extraction of plasmid DNA from *Escherichia coli* cell lysate in a thermoseparating aqueous two-phase system. *Journal of Chromatography A*, 1024(1-2):95–104, Jan. 2004.
- J. A. Koepke and L. Miller. Fractionation of Human Hemoglobins Using Isoelectric Focusing. Technical report, 1972.
- K. B. Konstantinov and C. L. Cooney. White Paper on Continuous Bioprocessing. May 20–21, 2014 Manufacturing Continuous Symposium. *Journal of pharmaceutical sciences*, 104(3):813–820, 2015. doi: 10.1002/jps.24268.
- L. P. Kozłowski. IPC - Isoelectric Point Calculator. *Biology Direct*, 11(1), Oct. 2016. ISSN 17456150. doi: 10.1186/s13062-016-0159-9.

- K. H. Kroner, H. Schuette, W. Stach, and M. R. Kula. SCALE-UP OF FORMATE DEHYDROGENASE BY PARTITION. In *Journal of chemical technology and biotechnology*, volume 32, pages 130–137, 1982. doi: 10.1002/jctb.5030320117.
- T. Kruse, A. Schmidt, M. Kampmann, and J. Strube. Integrated clarification and purification of monoclonal antibodies by membrane based separation of aqueous two-phase systems. *Antibodies*, 8, 2019. doi: 10.3390/antib8030040.
- M. Kuddus, P. Singh, G. Thomas, and A. Ali. Production of C-Phycocyanin and its potential applications. In V. Kumar Gupta, M. G. Tuohy, A. O'Donovan, and M. Lohani, editors, *Biotechnology of Bioactive Compounds: Sources and Applications*, chapter 12, pages 283–303. Wiley Blackwell, 2015.
- M.-R. Kula, K. Kroner, and H. Hustedt. Purification of enzymes by liquid-liquid extraction. *Reaction Engineering*, pages 73–118, 1982. doi: 10.1007/3-540-11699-0\_11.
- B. Lain. Protein A, 2009. URL <http://www.bioprocessintl.com/upstream-processing/biochemicals-raw-materials/protein-a-346304/{#}CIT0004>. Accessed: 2017-11-07.
- M. C. Lay, C. J. Fee, and J. E. Swan. Continuous Radial Flow Chromatography of Proteins. *Food and Bioproducts Processing*, 84:78–83, 2006.
- M. Li, Z.-Q. Zhu, and L.-H. Mei. Partitioning of Amino Acids by Aqueous Two-Phase Systems Combined with Temperature-Induced Phase Formation. *Biotechnology Progress*, 13(1):105–108, Feb. 1997.
- K. Linnet. Estimation of the linear relationship between the measurements of two methods with proportional errors. *Statistics in Medicine*, 9(12):1463–1473, Dec. 1990. ISSN 02776715. doi: 10.1002/sim.4780091210.
- C. Liu and J. Morrow. *Biosimilars of monoclonal antibodies : a practical guide to manufacturing, preclinical, and clinical development*. 2017. ISBN 9781118940631.
- Y. Liu, L. Chen, J. Zhou, and Z. Yan. Extraction of Tetracycline using the Ionic Liquid-Based Aqueous Two-Phase Systems:Single-Stage Versus Multi-Stage. *Chemical Industry and Chemical Engineering Quarterly*, 24(4):387–397, 2018. doi: 10.2298/CICEQ170904011L.
- Y. Lu, W. Lu, W. Wang, Q. Guo, and Y. Yang. The optimization of aqueous two-phase extraction of lysozyme from crude hen egg white using response surface methodology. *Journal of Chemical Technology and Biotechnology*, 88(3):415–421, Mar. 2013. ISSN 02682575. doi: 10.1002/jctb.3868.

- F. Luechau, T. C. Ling, and A. Lyddiatt. Selective partition of plasmid DNA and RNA in aqueous two-phase systems by the addition of neutral salt. *Separation and Purification Technology*, 68(1):114–118, Jun. 2009.
- L. N. Mao, J. K. Rogers, M. Westoby, L. Conley, and J. Pieracci. Downstream antibody purification using aqueous two-phase extraction. *Biotechnology Progress*, 26(6):1662–1670, Nov. 2010.
- A. J. Marengo-Rowe. Structure-function relations of human hemoglobins. *Baylor University Medical Center Proceedings*, 19, 2006.
- L. McQueen and D. Lai. Ionic liquid aqueous two-phase systems from a pharmaceutical perspective. *Frontiers in Chemistry*, (7):135, 2019. doi: 10.3389/fchem.2019.00135.
- N. Mekaoui, K. Faure, and A. Berthod. Advances in countercurrent chromatography for protein separations. *Bioanalysis*, 4(7):833–844, Apr. 2012.
- J. C. Merchuk, B. a. Andrews, and J. a. Asenjo. Aqueous two-phase systems for protein separation. Studies on phase inversion. *Journal of chromatography. B, Biomedical sciences and applications*, 711(1-2):285–293, 1998.
- S. L. Mistry, A. Kaul, J. C. Merchuk, and J. A. Asenjo. Mathematical modelling and computer simulation of aqueous two-phase continuous protein extraction. *Journal of Chromatography A*, 741(2):151–163, 1996. doi: 10.1016/0021-9673(96)00179-3.
- MordorIntelligence. Biopharmaceuticals market - growth, trends, covid-19 impact and forecasts (2021-2026), 2021. URL <https://www.mordorintelligence.com/industry-reports/global-biopharmaceuticals-market-industry>. Accessed:2021-07-19.
- T. Müller-Späth, L. Aumann, L. Melter, G. Ströhlein, and M. Morbidelli. Chromatographic separation of three monoclonal antibody variants using multicolumn countercurrent solvent gradient purification (MCSGP). *Biotechnology and Bioengineering*, 100(6):1166–1177, Aug. 2008.
- J. Mündges, J. Zierow, and T. Zeiner. Experiment and simulation of an aqueous two-phase extraction process for the purification of a monoclonal antibody. *Chemical Engineering and Processing: Process Intensification*, 95:31–42, Sep. 2015. doi: 10.1016/j.cep.2015.04.013.
- NCSS. Deming Regression. In *NCSS Statistical software documentation*, chapter Deming Reg. 2020.

- A. Orta-Ramirez, J. Merrill, and D. Smith. pH Affects the Thermal Inactivation Parameters of R-Phycocerythrin from *Porphyra yezoensis*. *Journal of Food Science*, 65(6):1046–1050, Sep. 2000. ISSN 0022-1147. doi: 10.1111/j.1365-2621.2000.tb09415.x.
- E. Pacis, M. Yu, J. Autsen, R. Bayer, and F. Li. Effects of cell culture conditions on antibody N-linked glycosylation-what affects high mannose 5 glycoform. *Biotechnology and Bioengineering*, 108(10):2348–2358, Oct. 2011.
- PALL Biopharmaceuticals. Cadence™ BioSMB Process 80 System and Cadence BioSMB Process 350 System - Chromatography, 2017. URL [https://shop.pall.com/us/en/biopharmaceuticals/continuous-processing/chromatography/cadence-biosmb-process-80-system-and-cadence-biosmb-process-350-system-zidiqdr519?\[\\_\]ga=2.196492580.901929289.1508767162-1017270807.1507824847](https://shop.pall.com/us/en/biopharmaceuticals/continuous-processing/chromatography/cadence-biosmb-process-80-system-and-cadence-biosmb-process-350-system-zidiqdr519?[_]ga=2.196492580.901929289.1508767162-1017270807.1507824847). Accessed: 2017-10-24.
- N. Patel, D. G. Bracewell, and E. Sorensen. Dynamic modelling of aqueous two-phase systems to quantify the impact of bioprocess design, operation and variability. *Food and Bioprocess Processing*, 107:10–24, Jan. 2018.
- G. Patil and K. S. Raghavarao. Aqueous two phase extraction for purification of C-phycocyanin. *Biochemical Engineering Journal*, 34(2):156–164, May. 2007. ISSN 1369703X. doi: 10.1016/j.bej.2006.11.026.
- D. Petrides, D. Carmichael, C. Siletti, and A. Koulouris. Biopharmaceutical Process Optimization with Simulation and Scheduling Tools. *Bioengineering*, 1(4):154–187, Sep. 2014.
- A. Prinz, K. Koch, A. Górak, and T. Zeiner. Multi-stage laccase extraction and separation using aqueous two-phase systems: Experiment and model. *Process Biochemistry*, 49(6):1020–1031, Jun. 2014.
- Prozyme. C-Phycocyanin Technical Data Sheet. Technical report, 2019. URL [www.prozyme.com](http://www.prozyme.com). Accessed: 2020-05-1.
- S. Raja, V. R. Murty, V. Thivaharan, V. Rajasekar, and V. Ramesh. Aqueous Two Phase Systems for the Recovery of Biomolecules – A Review. *Science and Technology*, 1(1):7–16, 2011.
- A. Rathore, N. Kateja, H. Agarwal, and A. K. Sharma. Continuous Processing for the Production of Biopharmaceuticals. *Biopharm International*, 29(4):14–19, 2016.

- D. Reay, C. Ramshaw, and A. Harvey. *Process Intensification: Engineering for Efficiency, Sustainability and Flexibility*. Second edition, 2013.
- J. F. J. F. Richardson, J. H. J. H. Harker, J. R. Backhurst, and J. M. J. M. Coulson. *Coulson and Richardson's chemical engineering. Vol. 2, Particle technology and separation processes*. Butterworth-Heinemann, 2002. ISBN 9780080490649.
- M. Rito-Palomares. Practical application of aqueous two-phase partition to process development for the recovery of biological products. *Journal of Chromatography B: Analytical Technologies in the Biomedical and Life Sciences*, 807(1):3–11, 2004. doi: 10.1016/j.jchromb.2004.01.008.
- D. K. Robinson, C. P. Chan, C. Yu Lp, P. K. Tsai, J. Tung, T. C. Seamans, A. B. Lenny, D. K. Lee, J. Irwin, and M. Silberklang. Characterization of a recombinant antibody produced in the course of a high yield fed-batch process. *Biotechnology and Bioengineering*, 44(6):727–735, Sep. 1994.
- M. V. Rocha and B. B. Nerli. Molecular features determining different partitioning patterns of papain and bromelain in aqueous two-phase systems. *International Journal of Biological Macromolecules*, 61:204–211, Oct. 2013. ISSN 01418130. doi: 10.1016/j.ijbiomac.2013.06.055.
- R. D. Rogers and C. B. Bauer. Partitioning behavior of group 1 and 2 cations in poly(ethylene glycol)-based aqueous biphasic systems. *Journal of Chromatography B: Biomedical Sciences and Applications*, 680(1-2):237–241, May. 1996. ISSN 0378-4347. doi: 10.1016/0378-4347(95)00319-3.
- a. C. a. Roque, C. R. Lowe, and M. Â. Taipa. Antibodies and genetically engineered related molecules: Production and purification. *Biotechnology Progress*, 20(3): 639–654, 2004.
- P. Rosa, A. Azevedo, I. Ferreira, S. Sommerfeld, W. Bäcker, and M. Aires-Barros. Downstream processing of antibodies: Single-stage versus multi-stage aqueous two-phase extraction. *Journal of Chromatography A*, 1216(50):8741–8749, Dec. 2009a. doi: 10.1016/j.chroma.2009.02.024.
- P. A. J. Rosa, A. M. Azevedo, and M. R. Aires-Barros. Application of central composite design to the optimisation of aqueous two-phase extraction of human antibodies. *Journal of Chromatography A*, 1141(1):50–60, Feb. 2007.
- P. A. J. Rosa, A. M. Azevedo, S. Sommerfeld, A. Mutter, M. R. Aires-Barros, and W. Bäcker. Application of aqueous two-phase systems to antibody purification: a

- multi-stage approach. *Journal of biotechnology*, 139(4):306–13, Feb. 2009b. doi: 10.1016/j.jbiotec.2009.01.001.
- P. A. J. Rosa, A. M. Azevedo, S. Sommerfeld, W. Bäcker, and M. R. Aires-Barros. Continuous aqueous two-phase extraction of human antibodies using a packed column. *Journal of Chromatography B*, 880:148–156, 2011.
- P. A. J. Rosa, A. M. Azevedo, S. Sommerfeld, M. Mutter, W. Bäcker, and M. R. Aires-Barros. Continuous purification of antibodies from cell culture supernatant with aqueous two-phase systems: From concept to process. *Biotechnology Journal*, 8:352–362, Mar. 2013. ISSN 18606768. doi: 10.1002/biot.201200031.
- M. J. Ruiz-Angel, V. Pino, S. Carda-Broch, and A. Berthod. Solvent systems for countercurrent chromatography: An aqueous two phase liquid system based on a room temperature ionic liquid. *Journal of Chromatography A*, 1151(1-2):65–73, Jun. 2007.
- F. Ruiz-Ruiz, J. Benavides, O. Aguilar, and M. Rito-Palomares. Aqueous two-phase affinity partitioning systems: Current applications and trends. *Journal of Chromatography A*, 1244:1–13, 2012. doi: 10.1016/j.chroma.2012.04.077.
- P. Sá Gomes and A. E. Rodrigues. Simulated Moving Bed Chromatography: From Concept to Proof-of-Concept. *Chemical Engineering & Technology*, 35(1):17–34, Jan. 2012.
- M. Salamanca, J. Merchuk, B. Andrews, and J. Asenjo. On the kinetics of phase separation in aqueous two-phase systems. *Journal of Chromatography B: Biomedical Sciences and Applications*, 711(1-2):319–329, 1998. doi: 10.1016/S0378-4347(98)00173-X.
- J. C. Salgado, B. A. Andrews, M. F. Ortuzar, and J. A. Asenjo. Prediction of the partitioning behaviour of proteins in aqueous two-phase systems using only their amino acid composition. *Journal of Chromatography A*, 1178(1-2):134–144, Jan. 2008. ISSN 00219673. doi: 10.1016/j.chroma.2007.11.064.
- S. B. Sawant, S. K. Sikdar, and J. B. Joshi. Hydrodynamics and mass transfer in two-phase aqueous extraction using spray columns. *Biotechnology and bioengineering*, 36(2):109–115, 1990.
- T. Schirmer, W. Bode, R. Huber, W. Sidler, and H. Zuber. Xray crystallographic structure of the light-harvesting biliprotein c-phycoerythrin from the thermophilic cyanobacterium *Mastigocladus laminosus* and its resemblance to globin structures. *J Mol Biol*, 184:257–277, 1985.

- F.-X. Schmid. Biological Macromolecules: UV-visible Spectrophotometry, 2001. URL [www.els.net](http://www.els.net). Accessed: 2020-06-09.
- C. A. Schneider, W. S. Rasband, and K. W. Eliceiri. Nih image to imagej: 25 years of image analysis. *Nature Methods*, 9:671–675, 2012.
- K. Schügerl and J. Hubbuch. Integrated bioprocesses. *Current Opinion in Microbiology*, 8:294–300, 2005.
- J. D. Seader, E. J. Henley, and Roper. *Separation process principles: Chemical and Biochemical operations*. Wiley, 2006. ISBN 9780470481837.
- K. Selber, F. Nellen, B. Steffen, J. Thömmes, and M. R. Kula. Investigation of mathematical methods for efficient optimisation of aqueous two-phase extraction. *Journal of Chromatography B: Biomedical Sciences and Applications*, 743(1-2): 21–30, Jun. 2000. ISSN 13872273. doi: 10.1016/S0378-4347(00)00045-1.
- Sigma-Aldrich. C-Phycocyanin — Sigma-Aldrich. URL <https://www.sigmaaldrich.com/catalog/product/sigma/52468?lang=en&region=GB>. Accessed: 2020-04-29.
- Sigma-Aldrich. Simulated Moving Bed (SMB) Chromatography — Sigma-Aldrich, 2017. URL <http://www.sigmaaldrich.com/safc/contract-manufacturing-services-and-solutions/api-and-key-intermediates/smb-chromatography.html>. Accessed: 2017-10-23.
- L. Simon and S. Gautam. Modeling continuous aqueous two-phase systems for control purposes. *Journal of Chromatography A*, 1043(2):135–147, Jul. 2004.
- R. R. G. Soares, A. M. Azevedo, J. M. Van Alstine, and M. R. Aires-Barros. Partitioning in aqueous two-phase systems: Analysis of strengths, weaknesses, opportunities and threats. *Biotechnology Journal*, 10(8):1158–1169, Aug. 2015. doi: 0.1002/biot.201400532.
- R. R. Sonani. Recent advances in production, purification and applications of phycobiliproteins. *World Journal of Biological Chemistry*, 7(1):100, 2016. ISSN 1949-8454. doi: 10.4331/wjbc.v7.i1.100.
- A. Staby, N. Johansen, H. Wahlstrøm, and I. Møllerup. Comparison of loading capacities of various proteins and peptides in culture medium and in pure state. *Journal of Chromatography A*, 827(2):311–318, Dec. 1998.

- I. Sutherland, P. Hewitson, R. Siebers, R. van den Heuvel, L. Arbenz, J. Kinkel, and D. Fisher. Scale-up of protein purifications using aqueous two-phase systems: Comparing multilayer toroidal coil chromatography with centrifugal partition chromatography. *Journal of Chromatography A*, 1218(32):5527–5530, Aug. 2011.
- D. Swinehart. The Beer-Lambert Law. *The Journal of Chemical Education*, 39(7):333, 1962. doi: 10.1021/ed039p333.
- J. R. Tame and B. Vallone. The structures of deoxy human haemoglobin and the mutant Hb Tyr $\alpha$ 42His at 120 K. *Acta Crystallographica Section D: Biological Crystallography*, 56(7):805–811, 2000. ISSN 09074449. doi: 10.1107/S0907444900006387.
- M. Tidhar, J. C. Merchuk, A. N. Sembira, and D. Wolf. Characteristics of a motionless mixer for dispersion of immiscible fluids—II. Phase inversion of liquid-liquid systems. *Chemical Engineering Science*, 41(3):457–462, 1986.
- M. A. Torres-Acosta, K. Mayolo-Deloisa, J. González-Valdez, and M. Rito-Palomares. Aqueous Two-Phase Systems at Large Scale: Challenges and Opportunities. *Biotechnology Journal*, 14(1):1800117, Jan. 2019. ISSN 18606768. doi: 10.1002/biot.201800117.
- J. M. Utterback. *Mastering the dynamics of innovation : how companies can seize opportunities in the face of technological change*. Harvard Business School Press, 1994. ISBN 0875843425.
- A. W. P. Vermeer and W. Norde. The Thermal Stability of Immunoglobulin: Unfolding and Aggregation of a Multi-Domain Protein. *Biophysical Journal*, 78(1):pp. 394–404, 2000.
- H. Walter. *Partitioning in aqueous two-phase systems theory, methods, uses, and application to biotechnology*, 1985.
- H. Walter, F. D. Raymond, and D. Fisher. Erythrocyte partitioning in dextran—poly(ethylene glycol) aqueous phase systems: Events in phase and cell separation. *Journal of Chromatography A*, 609(1):219–227, 1992. ISSN 00219673.
- H. Walter, G. Johansson, J. N. Abelson, and M. I. Simon. *Aqueous Two-Phase Systems: 228 (Methods in Enzymology):*. San Diego; London: Academic Press, 1994. ISBN 0121821293.
- M. Wan, H. Zhao, J. Guo, L. Yan, D. Zhang, W. Bai, and Y. Li. Comparison of c-phycoerythrin from extremophilic *Galdieria sulphuraria* and *Spirulina platensis* on stability and antioxidant capacity. *Algal Research*, 58, 2021.

- A. Warade, R. Gaikwad, R. Sapkal, and V. Sapkal. Simulation of Multistage Countercurrent Liquid-Liquid Extraction. *Leonardo Journal of Sciences*, (20):79–94, 2011.
- H. Willauer, J. Huddleston, and R. Rogers\*. Solute Partitioning in Aqueous Biphasic Systems Composed of Polyethylene Glycol and Salt: The Partitioning of Small Neutral Organic Species. 2002. doi: 10.1021/IE010598Z.
- H.-L. Wu, G.-H. Wang, W.-Z. Xiang, T. Li, and H. He. Stability and antioxidant activity of food-grade phycocyanin isolated from spirulina platensis. *International Journal of Food Properties*, 19(10):2349–2362, 2016a. doi: 10.1080/10942912.2015.1038564.
- H.-L. Wu, G.-H. Wang, W.-Z. Xiang, T. Li, and H. He. Stability and Antioxidant Activity of Food-Grade Phycocyanin Isolated from Spirulina platensis. *International Journal of Food Properties*, 19(10):2349 – 2362, 2016b. ISSN 1532-2386. doi: 10.1080/10942912.2015.1038564.
- Y. Zang, B. Kammerer, M. Eisenkolb, K. Lohr, and H. Kiefer. Towards Protein Crystallization as a Process Step in Downstream Processing of Therapeutic Antibodies: Screening and Optimization at Microbatch Scale. *PLoS ONE*, 6(9): e25282, Sep. 2011.
- B. Zaslavsky, V. N. Uversky, and A. Chait. doi: 10.1016/j.bbapap.2016.02.017journal={BiochimicaetBiophysicaActa(BBA)-Proteins&Proteomics},title={Analyticalapplicationsofpartitioninginaqueoustwo-phasesystems: Exploringproteinstructuralchangesandprotein-partnerinteractionsinvitroandinvivobysolventinteracti},volume={1864},issue={5},year={2019}.
- B. Y. Zaslavsky. Aqueous Two-Phase Partitioning. In *Aqueous Two-Phase Partitioning*, chapter 3, pages 75–152. Marcel Dekker, Inc, New York, first edition, 1995.
- A. L. Zydney. Continuous downstream processing for high value biological products: A Review. *Biotechnology and Bioengineering*, 113(3):465–475, Mar. 2016.



# Appendix A

This appendix shows the calibration curves of the model protein C-phycoyanin in the extract and waste phases of the model case study system. This data correlates to the determination of C-phycoyanin content in an [Aqueous Two-Phase Systems \(ATPS\)](#) as shown in Chapter 3. The data in this section looks to determine if there are differences in the calibration curves. This could be as a result of differences in phase forming constituent concentration because of operational method, or because of errors generated in pipetting due to the high viscosity of the [Polyethylene Glycol \(PEG\)](#)-rich phase.

A concern addressed was that large errors would be generated when using volumes to evaluate the more viscous [PEG](#)-rich phase of the system. As a result, it was important to evaluate if there were differences between absorbance of protein in the extract and waste phases, and also between each phase when operated using a centrifuge and when operated through gravity. It was expected that there would be a difference between the absorbance of protein in the extract and waste phases because of the viscosity of the [PEG](#) creating error when pipetting. It was also considered that there could be a difference between systems operated under gravity and through the use of a centrifuge, as while the bulk of the systems have separated at the formation of the horizontal interface, the phases are still turbid which indicates that a system is still separating ([Hatti-Kaul, 2000](#)). From Figure 7.1 it can be seen that there is no difference between the same phases if they are operated differently, i.e. under gravity or through the use of a centrifuge. However, there is a difference between the extract and waste phase calibration phases. It was found that the relationship between each extract and waste phase calibration curves was:

For a curve of:

$$A_{WL} = k_{phase} \left( \frac{V_{stock}}{V_{Total}} \right) \quad (7.1)$$

$$k_W = 1.14k_E \quad (7.2)$$

Where  $A_{WL}$  is the absorbance value at wavelength  $WL$  nm,  $WL$  values of 280, 562, 615 and 652 nm were analysed,  $V_{stock}$  is the volume of feed stock added to the

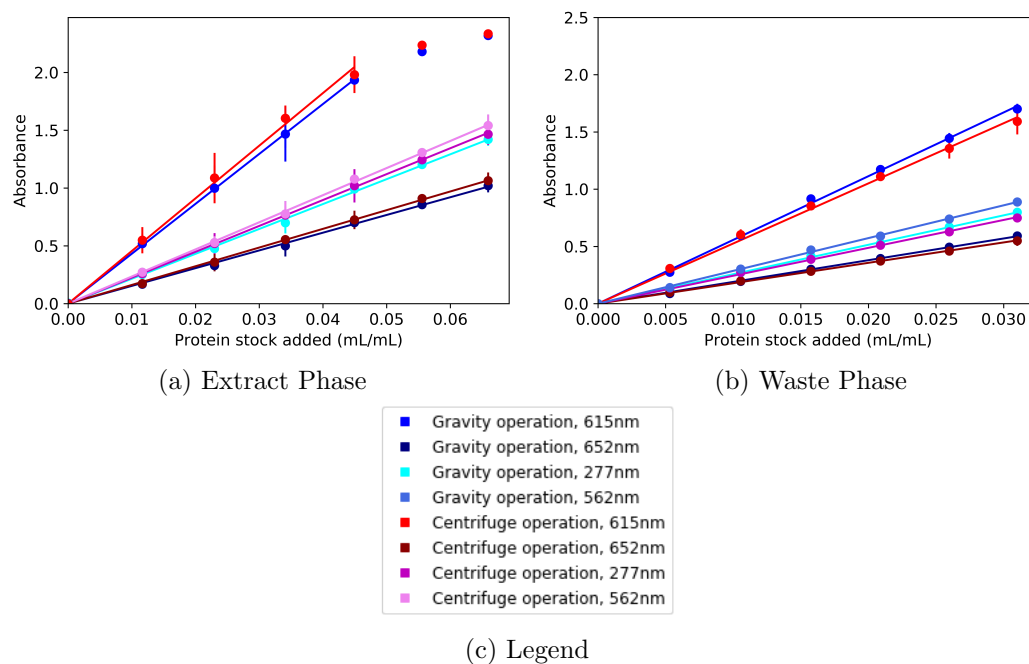


Figure 7.1: Calibration curves of C-phycoerythrin stock 1 in the extract and waste phases of a C-phycoerythrin case study system. As operated using gravity separation and centrifuge operation.

sample,  $V_{Total}$  is the total volume of the sample and  $k_{phase}$  is the gradient determined from the extract and waste phase calibrations. As this relationship was found for all values analysed, any sample in the top phase was adjusted by a factor of 1.14, with a standard deviation of 0.057, when the equations 3.2, 3.3 and 3.4 were applied. To calculate stock concentrations, the gradients on the calibrations were applied to equations 3.2, 3.3 and 3.4.

Figure 7.1a also shows that Beers law is followed until around 0.045 mL/mL of C-phycoerythrin stock 1 in the extract phase for the 619 nm calibration curve. As C-phycoerythrin is mostly responsible for this peak, this would correspond to a C-phycoerythrin concentration of around 0.33 mg/mL, at which point the calibration curve begins to flatten and Beers law can no longer be applied meaning samples above this concentration would have to be diluted for analysis.